`

INVOLVEMENT OF MICROGLIA ACTIVATION IN THE DEVELOPMENT OF CNS DISEASES

GIOVANNI PIETROGRANDE

MSc.

Thesis submitted for the degree of

Doctor of Anatomy

School of Biomedical Sciences and Pharmacy

Faculty of Health and Medicine

University of Newcastle

April 2018

`

`

Statement

I, Giovanni Pietrogrande, hereby certify that the work embodied in the thesis is my own work, conducted under normal supervision.

The thesis contains published scholarly work of which I am a co-author. For each such work a written statement, endorsed by the other authors, attesting to my contribution to the joint work has been included.

The thesis contains no material which has been accepted, or is being examined, for the award of any other degree or diploma in any university or other tertiary institution and, to the best of my knowledge and belief, contains no material previously published or written by another person, except where due reference has been made in the text. I give consent to the final version of my thesis being made available worldwide when deposited in the University's Digital Repository, subject to the provisions of the Copyright Act 1968 and any approved embargo.

The thesis contains no material which has been accepted for the award of any other degree or diploma in any university or other tertiary institution and, to the best of my knowledge and belief, contains no material previously published or written by another person, except where due reference has been made in the text.

`

Publications

- Chronic stress induced disturbances in Laminin: A significant contributor to modulating microglial pro-inflammatory tone?
  Pietrogrande G, Mabotuwana N, Zhao Z, Abdolhoseini M, Johnson SJ, Nilsson M, Walker FR.
  Brain Behav Immun. 2018 Feb;68:23-33. doi: 10.1016/j.bbi.2017.09.012. Epub 2017 Sep 22.

- Low Oxygen Post Conditioning as an efficient non-pharmacological strategy to promote motor function after stroke.
  Pietrogrande G, Zalewska K, Zhao Z, Abdolhoseini M, Johnson SJ, Nilsson M, Walker FR.
  Submitted to Translational Stroke Research

- Low Oxygen Post Conditioning prevents thalamic secondary neuronal loss caused by excitotoxicity in a murine model of cortical stroke.
  Pietrogrande G, Zalewska K, Zhao Z, Abdolhoseini M, Johnson SJ, Nilsson M, Walker FR.
  To be submitted to Scientific reports after approval from all the authors

Additional publications

- Sustained administration of corticosterone at stress-like levels after stroke suppressed glial reactivity at sites of thalamic secondary neurodegeneration.
  Zalewska K, **Pietrogrande G**, Ong LK, Abdolhoseini M, Kluge M, Johnson SJ, Walker FR, Nilsson M.
  Brain Behav Immun. 2017 Nov 21. pii: S0889-1591(17)30515-9. doi: 10.1016/j.bbi.2017.11.014.

- Growth hormone improves cognitive function after experimental stroke
  Ong LK, Chow WZ, TeBay C, Kluge M**, Pietrogrande G**, Zalewska Z, Crock P, Åberg ND, Bivard A, Johnson SJ, Walker FW, Nilsson M, Isgaard J.
  Stroke, manustript accepted

- Normobaric post-conditioning hypoxia improves stroke-induced cognitive impairment through improved glymphatic flow

  Zhao Z, Ong LK, **Pietrogrande G**, Ottersen O, Johnson SJ, Nilsson M, Walker FR.
  Stroke, manuscript under review

`

- Delayed normobaric hypoxic exposure rescued neuron loss and reduced Amyloid beta accumulation at thalamic secondary neurodegeneration post-stroke
  Zhao Z, Ong LK, **Pietrogrande G**, Johnson SJ, Nilsson M, Walker FR
  Stroke, in preparation

`

Table of Contents

`

`

List of figures

Abbreviations

CNS: central nervous system

MS: multiple sclerosis

DAMP: damage associated molecular pattern

TLR: toll-like receptor

HOSC: organotipic hippocampal slice culture

NMDA: N-methyl-D-aspartate

ROS: reactive oxygen species

LPS: lipopolysaccharides

IL1β: interleukin 1 beta

TNF-α: tumor necrosis factor -α

SND: secondary neurodegeneration

Iba1: ionized calcium-binding adapter molecule 1

iNOS: inducible nitric oxide synthase

`

IFN-γ: interferon gamma

IRF: Interferon regulatory factor

ISRE: interferon (IFN)-stimulated response element

GTP: guanosine-5'-triphosphate

ECM: extracellular matrix

FAK: focal adhesion kinase

HPA: hypothalamic–pituitary–adrenal

GC: glucocorticoid

MCAO: middle cerebral artery occlusion

LOPC: low oxygen post conditioning

tPA: tissue plasminogen activator

WD: wallerian degeneration

SND: secondary neurodegeneration

NMDAR: N-methyl-D-aspartate receptor

PSD95: post synaptic density protein 95

`

Abstract

Microglia are the resident immune cells within the brain, however, in the last 20 years it has become clearer that their function is more complex than ordinary macrophages and goes well beyond guarding CNS from pathogens. In fact microglia are also responsible for maintaining the homeostatic balance within the brain. Factors that can modulate this balance can be of differing natures: for instance they can include subtle and prolonged factors like hormonal changes driven by stress; alternatively they can be dramatic like an ischemic injury; or prolonged and sustained as during the processes of secondary neurodegeneration associated with stroke. During my PhD I focused my attention on all these aspects, which can be considered at the opposite poles in the spectrum of events threatening homeostasis. In this thesis I describe the current knowledge about these CNS pathologies and how they are linked to inflammation in general and microglia activation in particular. Only by analysing microglia in such different conditions it is possible to fully appreciate the different shades that characterize microglia activation, and especially how different tuning of inflammation can have very different consequences for the CNS.

There is already quite an extensive literature that describes the role of microglia in chronic stress and in stroke. These studies show the pivotal importance of microglia in these pathologies and especially the importance of microglia activation as modulator of inflammation. Thus, I decided to take an innovative approach and investigate aspects that are crucial to fully understand the role of microglia but that have not been yet characterised

More specifically, in the first study I investigated the status of microglia activation in a murine model of chronic stress. Higher levels of basal inflammation correlate in a unique

`

way with development of depression in humans but the leading mechanism is still largely uncharacterised. Using *in vivo* and *in vitro* models, I found that the extracellular matrix (ECM) is dysregulated after chronic stress and influences microglia activation. This finding makes ECM a potential key player in the development of mood disorders.

The focus of the second study was the role of microglia activation in the post-acute phase after stroke, which is a leading cause of disability worldwide (1). In this context, the reports about microglia activation are mixed, since they can have both a positive and a negative influence on the outcome. Using a novel intervention, low oxygen post conditioning (LOPC), I analysed the correlation between its neuroprotective effect and microglia activation, and I validated LOPC therapeutic potential in improving motor function.

In the third study, I extended my previous findings to the stroke-associated neurodegenerative event called secondary neurodegeneration (SND). SND develops in areas distal but connected to the infarct site and is characterised by progressive neuronal loss concomitant to glial activation. Microglia activation is inextricably linked to SND; however microglial involvement in SND and its contribution are still largely not understood. Using LOPC as intervention and analysing the temporal evolution of microglia activation in the site of SND, I concluded that LOPC can ameliorate neuronal loss and promote the return of microglia to a basal state in later stages.

In conclusion, in this thesis I present novel observations into microglia involvement in the development of CNS pathologies and provide useful insights in the mechanism leading to microglia activation, with important implications for future research.

`

`

CHAPTER 1 – Introduction

Overview

In this introduction I will begin describing the role and features of the brain's resident immune cells, microglia. In particular, I will focus on microglial morphology and its relationship to neuroprotection and neurotoxicity in different contexts. This description will be supported by analysis of the current literature on studies performed *in vivo* and *in vitro*, with particular emphasis on the molecular mechanisms defining microglia morphology and activation, and the connection between the two. In this context I will introduce the extracellular matrix (ECM) and its relationship with both microglia morphology and activation. Then I will explain the importance of inflammation and microglia activation in the development of psychological pathologies, providing a rationale for a potential link with alterations in the ECM composition; the aim being considering a psychological and a physical modulator of microglial disturbances. Finally, I will highlight the data concerning microglia activation in stroke and stroke induced secondary neurodegeneration, while introducing the concept of low oxygen post conditioning and its validity as a therapeutic intervention. Considering the complexity and variety of topics, the reader will find a supplementary introduction before each paper to integrate the general introduction.

Microglia

Microglia are the resident immune cells of the central nervous system (CNS) and account for around 10% of the total cell population of the brain (2). Microglia were first described

`

around 100 years ago in the 1919 by two Spanish researchers: Nicolás Achúcarro and Pío del Río-Hortega (3). Using a labelling method based on silver ions combined with other metals, they managed to visualise microglia and postulated correctly about microglial plasticity (called "nomadic nature") and function. The two researchers described microglia as cells possessing numerous processes with extensive branching, terminating with fine tapered tips and capable of phagocytosis. In the following decades many studies showed that microglia indeed possessed macrophage-like characteristics and readily responded to tissue injury by both phagocytosing necrotic tissue and initiating and regulating the inflammatory response by releasing proteins capable of transducing pro- or anti-inflammatory actions. However, more recently it has become clear that microglia are not just simply CNS macrophages that respond to damage or pathogens.

Microglia are also involved in pathologies that are not caused by direct damage to the brain but still present neuronal death. Among neurodegenerative diseases microglia have been shown to be involved in: Alzheimer's disease (4), Parkinson's disease (5), multiple sclerosis (MS)(6) and Huntington disease (7). Additionally, the role of neuroinflammation in psychological and psychiatric disorders has recently started to attract considerable attention, highlighting the need for studies specifically aimed to investigate immune activation in the field of psychopathology (8). The role of microglia as the main modulators of inflammation seems to be the key to explain their involvement in such different pathologies but the exact mechanisms linking microglia to the development of CNS disorders is still in need of further investigations.

The first aim of my PhD was to expand understanding of the relationship between the inflammatory status of microglia and psychological disorders like chronic stress. A second aim was to investigate the involvement of activated microglia in stroke and stroke

`

related neuronal loss. Microglia in the development of mood disorders and stroke-induced neurodegeneration will be extensively discussed later in this introduction. However, to fully understand how immune cells can be involved in different pathologies, it is necessary to first grasp the pivotal role of microglia in maintaining brain homeostasis.

Role of microglia in healthy brain

Most of what we know about microglia function in the embryonic phase and in adult individuals come from studies performed in rodents. Microglia are involved in many of the key processes that happen both during and after embryonic development. During the development phase, microglia originate from myeloid progenitors in the embryonic yolk sack and start populating the brain from embryonic day E9.5 (9, 10) . It has been shown that this mechanism is necessary for the normal brain development during the embryonic stage (11) and that microglia contribute to the fundamental reorganization of neuronal connections (Fig 1). Indeed, both excess production of neurons and neuronal loss by apoptosis are evident in most regions of the developing CNS, and microglia are responsible for the removal of apoptotic cellular debris (12). Additionally, during late CNS development, selective synapse elimination and axon pruning by microglia are required for mature neural circuit formation (13, 14). In the adult brain microglia compose the first line of immune defence. To effect this function, microglial cells display extensive ramifications, covering the entire CNS parenchyma to detect potential threats to the homeostasis of the brain. In accordance with their immunological role microglia migrate to sites of damage, undergo structural changes that effect their morphology, release cytotoxic mediators against invading microbes and clear dead cells debris by phagocytosis.

`

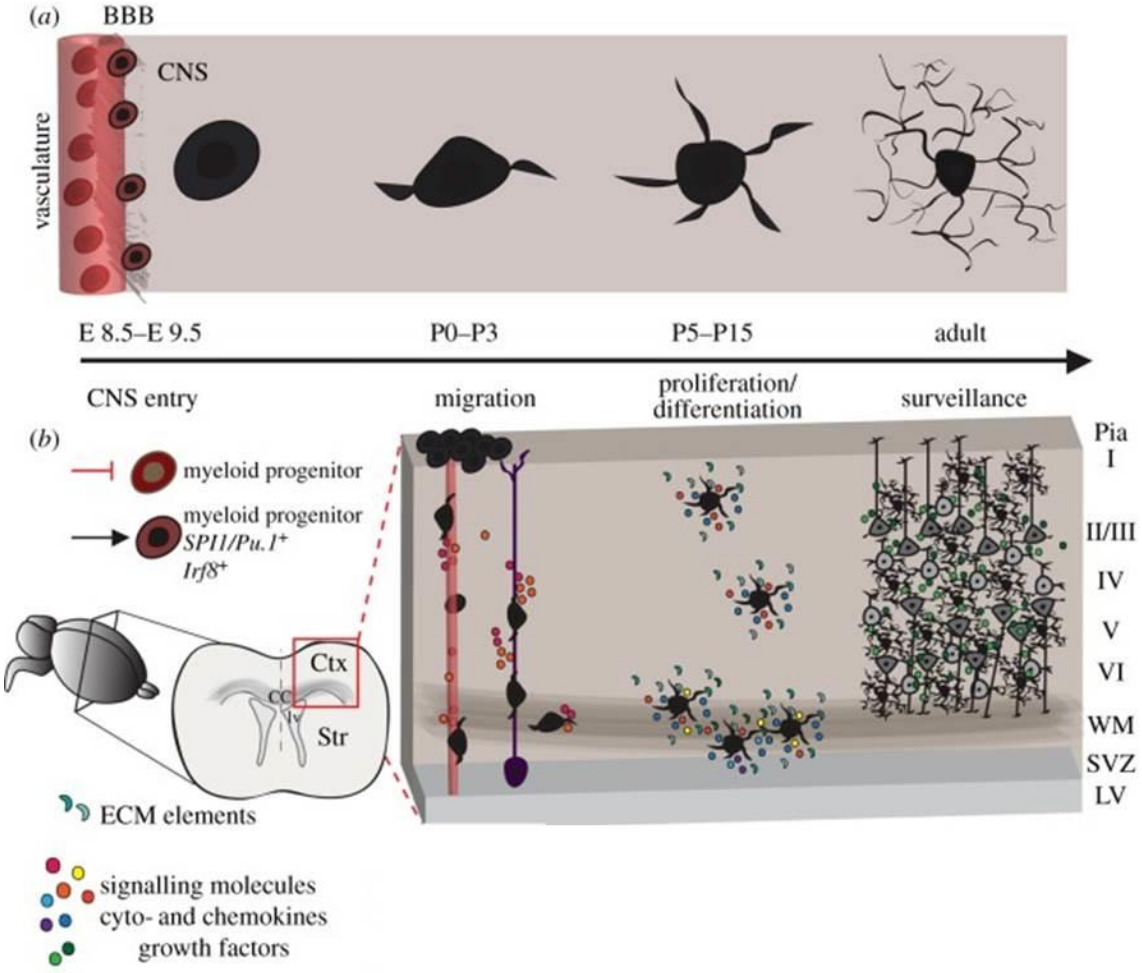

Figure 1. Origin and establishment of microglia in the CNS. (a) Microglia morphological changings during development, from amoeboid to the typical ramified. (b) Microglia cells are exposed to several signalling molecules (extracellular matrix proteins, chemokines and growt). Microglia derived from the yolk sac (SPI1/Pu.1+ and Irf8+) enter the CNS during embryonic stages E8.5–E9.5. At neonatal stages (P0–P3), amoeboid microglia populate the parenchyma. Once established, microglia undergo proliferation and spread in the cerebral cortex parenchyma and acquire their fully ramified morphology. Adapted from (2).

`

It was presumed for many years that under normal physiological conditions microglial cells are quiescent and in a resting state. Surprisingly, two-photon microscopy studies showed that microglial processes in the healthy brain/ absence of disease or damage are substantially motile and survey their local surroundings through formation of random filopodia-like protrusions (15). This state of high motility facilitates microglial processes to perceive the status of their immediate microenvironment and dynamically assess surrounding synapses, regulating growth or elimination of small spines (16, 17) and shaping neuroplasticity in physiological and pathological conditions in both rodents and humans (18, 19). Therefore their ramified morphology is fundamental for microglial proper function.

Relationship between morphology and function in microglia

From a morphological point of view, microglia transit from an amoeboid to a ramified phenotype during the postnatal phase, as they gradually enter an inactivated state (20). Indeed in the postnatal brain microglia are initially mitotic, rounded in shape (amoeboid), and phagocytic. During this phase microglia participate in important developmental functions including cell debris phagocytosis, guidance of axons in white matter tracts and synapse elimination (21, 22). As brain development proceeds, microglia transit from an amoeboid to a ramified phenotype during the postnatal phase as they gradually enter a deactivated state. During this process amoeboid microglia become gradually less abundant while the number of ramified microglia increases as they acquire a surveillance role. Even though this ramified state is usually considered a resting phenotype, it has been shown that microglia are not actually “resting”. In fact their processes actively scan the

`

environment for endogenous signals of unbalanced homeostasis, like damage associated molecular patterns (DAMPs) (15, 23). Intriguingly, the ramification process that begins after birth is almost the reverse of what happens during microglia activation in the adult brain. In response to injury or immune challenge, surveillant microglia undergo a ramified-to-amoeboid morphological transformation and become phagocytic (Fig 2).

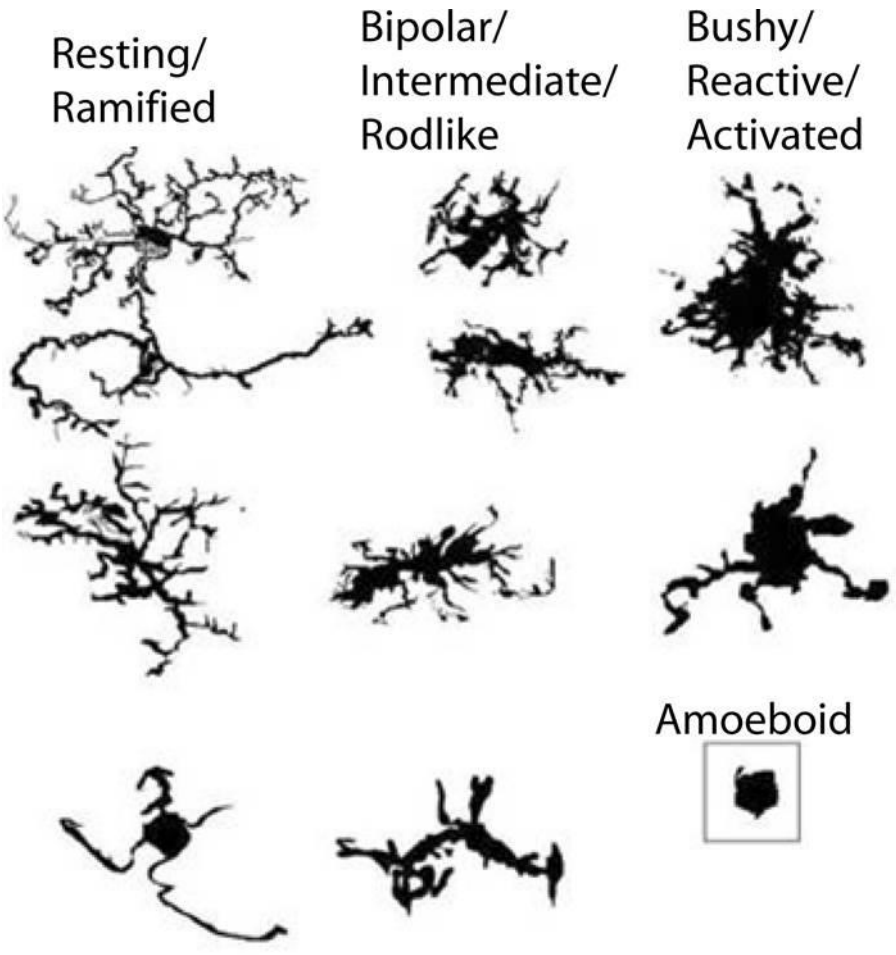

Figure 2. Morphological characteristics of microglia. Example of reconstructed *in vivo* microglia from post mortem human tissue showing different adopted morphologies (24).

`

Two complementary roles for microglia have been described. In their canonical role, as a member of the innate immune system, microglia detect invading pathogens and control the innate /initial defence response, mainly through the Toll-like receptors (TLRs) signalling cascade (25, 26). Secondly, microglia are also the in charge of preserve the CNS homeostasis and they exert this function through their scanning activity. Alterations of homeostasis, for example caused by neuronal death, induce the activation of microglia and a consequent sterile inflammation state. During their continuous surveillance of the environment using their processes, microglia also dynamically form new cell to cell interaction with other brain populating cells, like neurons (27) and astrocytes (15). For example, activation of the neuronal NMDA receptor can trigger the release of ATP and promote neuron-microglia interaction (28, 29). As result, a third role has been recently proposed for microglia, as monitor of other cells functional status and, more importantly, as guardians of synaptic activity and plasticity. In fact ramified microglia actively interact with neurons at the synaptic level also during adulthood, for example with selective partial phagocytosis of pre-synaptic structures (30); for an exhaustive review see Salter and Beggs 2014 (31).

Neuroprotective role of microglia

In vitro, a neuroprotective function, both direct and indirect, has been attributed to ramified microglia using organotypic hippocampal slices (HOSC). The HOSC method allows investigators to simulate an *in vivo* system, with all the components and cell types present in the hippocampus, but in a controlled environment. An example of the direct role has been described in the 2012, when Vinet et al. showed that ramified microglia prevent excitotoxic neuronal cell death caused by n-methyl-D-aspartic acid (NMDA) treatment (32). An indirect role was described in a study in 2014, where authors showed

`

how microglia trigger astrocytes to protect neurons from death caused by neurotoxic methylmercury treatment (33). However many factors can influence the behaviour of cells in vitro, hindering researchers in their effort to model perfectly *in vivo* responses. For example resident cells of the intact CNS are not exposed to serum, which is commonly added to cell medium and contains components that are known to be modulators of microglial activation (34). Still, organotypic hippocampal slice cultures have proven extremely valuable in uncovering microglia involvement in neuroprotection, and now *in vivo* investigation is required to sort out the physiological relevance of ramification status to mediate this role. The general neuroprotective role of microglia *in vivo,* by promoting neurogenesis or clearing debris (35), is discussed later in specific sections about microglia in brain injuries.

Microglia as mediators of neurotoxicity

In addition to their neuroprotective effects microglia can also be neurotoxic in their activated amoeboid shape. In fact activated microglia release neurotoxic factors like pro-inflammatory cytokines or reactive oxygen species (ROS)(36). This neurotoxic phenotype is, at least in part, regulated by the fracktaline receptor signalling cascade as suggested by Cardona et al. (37). In this paper the authors, using three separate models of CNS damage, identified that the absence of functional CX_3CR1 leads to increased neuronal loss due to microglial toxicity, indicating that fracktaline signalling facilitates neuroprotection. Specifically, when systemic inflammation was induced by intraperitoneal injection of lipopolysaccharide (LPS), $CX_3CR1^{-/-}$ mice displayed increased microglial activation and significantly higher levels of neuronal apoptosis. This effect is likely to be mediated at least in part by IL-1β, as LPS-stimulated $CX_3CR1^{-/-}$ microglia expressed increased levels of IL-1β and microglial transplant into IL-1β

`

receptor null mice failed to cause neuronal cell death. Since the chemokine fracktaline is mainly expressed by neurons, this was one of the first examples of cross-talk between microglia and neurons.

Prolonged microglial activation exacerbates neurotoxicity in two stages. In the first phase, microglia can initiate neuron damage when they recognize pro-inflammatory stimuli, such as LPS, become activated and produce neurotoxic pro-inflammatory factors. In the second phase, microglia can become over-activated by reacting to this neuronal damage, giving rise to an event called reactive microgliosis. This over-activation amplifies the toxic effect to neighbouring neurons, resulting in a perpetuating cycle of neuronal death (38). Reactive microgliosis could be an underlying mechanism of progressive neuron damage across numerous neurodegenerative diseases, regardless of the instigating stimuli. In an interesting study, (39) a singular, very strong LPS challenge is enough to induce prolonged microglial activation lasting months after the challenge. The authors suggest that the prolonged microglia activation with consequent high expression of the pro-inflammatory cytokine TNF-α can potentially promote neuronal loss, illustrating an important link between high activation levels of microglia and neurotoxicity. I will discuss later the important involvement of this process in the development of neurodegeneration after stroke.

Modelling microglia morphology

In order to fully describe and understand the mechanisms contributing to changes in microglia morphology, in my studies I used both *in vivo* and *in vitro* methods. From an experimental point of view, microglia have been most closely studied using *in vitro* preparations, typically utilising cells lines or microglia derived from neonatal rodents (40). Despite the many advances made by using *in vitro* approaches, it is important to

`

recognise that microglia are quite different *in vitro* and *in vivo*. Most significantly for this review and my doctoral investigations, microglia in culture can differ in morphology to what is observed in vivo. For example in mixed glia culture, microglia identified immunohistochemically using ionized calcium-binding adapter molecule (Iba-1) or CD11b antibodies present two different morphologies: one is round and loosely attached; the other is flat and tightly attached. Usually, only round cells are identified as microglia since it is difficult to recognize microglia without staining or unless they express a fluorescent marker since they are tightly attached to astrocytes. Further, in my studies I observed that primary microglia *in vitro* alone present fewer processes (branches) with a significantly lower level of branching complexity and tortuosity than *in vivo* (41, 42). Despite the intrinsic limits, the *in vitro* approach is sufficient for proof-of-concept studies, and can provide clues about the mechanisms inducing profound changes in microglia morphology. I will describe first few studies *in vivo* models used to investigate microglia morphology, followed by short overview on the limitations of the *in vitro* approach.

Microglia in vivo

Changes of microglia morphology can be triggered by many factors. *In vivo*, it has been observed that upon damage or insult microglia display an activated profile, and this phenotype has been validated using many different models. The presence of an insult like moderate midline fluid percussion (FPI) causes 7 days after the injury an increase on the Iba-1 staining, a marker of microglial activation (43). Moreover, microglia show swollen cell bodies and fewer processes (44). Similar transition to a less ramified morphology have been shown also in the acute phase after stroke, up to 24 hours (45). In particular, Morrison HW et al. showed in their study that microglia in the region proximal to the injury start to transition to a more de-ramified morphology at 8 hours after ischemic

`

stroke, and at 24 hours microglia in all the ipsilateral regions display a marked de-ramified morphology. As discussed later, this finding prompted us to investigate the morphology changes after stroke in a wider temporal window up to 4 weeks after stroke (Chapters 4 and 5).

Similarly with what has been reported after brain injury, after immune challenge (like LPS injection) microglia acquire an amoeboid morphology (46), switching from resting ramified with extensive branching to larger cell body and reduction of ramified processes. But exogenous causes are not the only ones that can influence microglia morphology *in vivo*; another crucial factor is cross-talk with other brain cells and in particular neurons. For example CD200, a membrane glycoprotein expressed by neurons, regulates microglia activation. Moreover in CD200 knock out mice microglia look less ramified with shorter glial processes (47). But the cross-talk between microglia and neurons is quite broad. Indeed it has been shown in retinal explant that microglia morphology can be modulated by endogenous neurotransmission, and in particular that different modes of neurotransmission differentially regulate morphological parameters (48). Finally neurons can also modulate microglial behaviour after LPS challenge, as it has been observed in vitro (49). Later in this introduction I will discuss more in detail about the role of microglia and microglia morphology in vivo, specifically in the context of chronic stress and stroke pathobiology.

Microglia in vitro

BV-2 cells are the mostly widely used microglial cell line within the scientific literature (50). Driving the widespread usage of the BV-2 line is the fact that they are widely available, readily grown, and tolerate most culture based interventions very well. While these practical advantages are important, it is also worth noting that the molecular

`

phenotype of the BV-2 line has been extensively compared to primary cells derived from neonate and adult microglia. From these studies it became clear that while BV-2 cells possess many typical microglial features, they do not perfectly recapture the features of primary microglia (51). Besides the differences between using a cell line and primary cells, it is also important to be aware that the *in vitro* approach is limited in recapitulating the in vivo behaviour of microglia (Fig 3). For example a recent study clearly highlights the difference between *in vitro* and *in vivo*, as the authors showed that the tissue environment substantially influences both gene expression and epigenetic profiles of human microglia (52). Another example can be found in the difference in the transcriptome of microglia between in vivo and in vitro profile after LPS stimulation described in a study by S. Lund et al.(53). However, the correlation found between the two methods in this study suggests that in vitro culture is still a viable option to study the behaviour of microglia. The situation of cells *in vitro* is very simplified but controlled compared to *in vivo*, where microglia receive inputs from other cells and from soluble and insoluble factors. For the purposes of my studies this is a critical difference. Various elements can induce a microglial morphological transformation besides molecules strictly related to the immune response, like LPS or cytokines. Indeed, it has been shown that both soluble (54-58) and non-soluble factors (57, 59-61) can alter microglial morphology, activation or proliferation. Therefore, the innate immunity cascade is likely not to be the only factor that influences morphology. The molecular pattern that mediates the effect of these non-soluble factors is still unknown, but it is likely to involve systems that are deeply related to cellular morphology, like cytoskeleton organization and composition of/adhesion to the extracellular matrix. Therefore *in vitro* methods are a valuable asset to dissect the nature of different factors influencing microglia morphology and they are a critical part of my first study (Chapter 3).

`

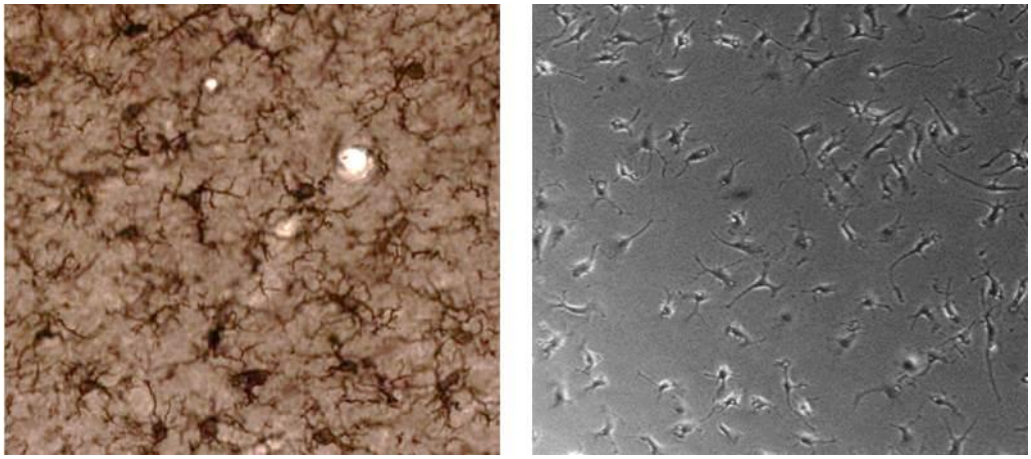

Figure 3. Microglia *in vivo* and *in vitro*. Morphology of microglia identified by Iba-1 staining (left) and primary microglia cultured *in vitro* on uncoated surface (right). The in vitro approach can only partially recapitulate the complexity of microglia branching.

Mechanisms driving changes in microglial morphology

Molecularly many studies have aimed to investigate microglia morphology by considering signalling cascades triggered by cytokines, which are known to induce morphological modifications. The response to LPS is mediated by the toll like receptor 4 (TLR4) (62) and blocking the TLR4 signalling impairs the classical change in morphology characteristic of activated microglia (63). Also IFN-γ treatment triggers an inflammatory response that causes an increase in iNOS production and glutamate uptake (64), as well as microglial morphology changes (65). The signalling cascade that mediates IFN-γ-induced morphological changes includes Interferon regulatory factor 8 (IRF8), a transcription factor that binds to the interferon (IFN)-stimulated response element (ISRE) and is constitutively expressed in microglia. IRF8 binds to other transcription factors and, by doing so, it regulates expression of genes stimulated by type I IFNs (66). Intriguingly, in the cortex of IRF8 knock-out mice, microglia are less ramified, and when cultured they

`

maintain an amoeboid morphology that is very different from WT microglia (67), suggesting a pathway through which IFN-γ may affect microglia morphology regardless of its pro-inflammatory activity.

All the morphological variations described are mediated by changes in the cytoskeleton, which defines the cellular shape and structure of all types of cells.

Cytoskeleton

Changes in morphology are correlated with changes in the composition and organization of the cytoskeleton (68, 69) as well as cellular function and cellular migration capability (70). Rho GTPases have a pivotal role in managing the changes in of cytoskeleton and are responsible for the formation of f-actin rich protrusions like lamellipodia and filopodia. The importance of the branch structures during microglia activation is supported by studies showing that the inactivation of Rho GTPases results in morphological de-ramification and activation (71). Additionally, microtubules are important for the ramification of primary microglia (72). During microglia activation, the microtubule organization is altered profoundly and their polarization is correlated to different microglia activation states (73). Iba-1 is specifically expressed by microglia in the brain and macrophages. On top of that, Iba-1 cooperates with Rac, a small G protein of the Rho GTPases family. The Iba1-Rac tandem has been identified as a mediator between activation and regulation of the reorganization of actin cytoskeleton, which is a peculiar event of microglia activation (74). This link between activation and morphology would put activation as the upstream event that leads to a change in microglia morphology but, as explained later, other studies suggest that the morphology and relative cytoskeleton reorganization could itself promote an activated phenotype. Thus, elements that are not considered pro-inflammatory *per se* could induce changes in microglia

`

morphology, and doing so influence microglia activation state. However, this kind of signalling needs the mediation of receptors.

One of the best examples of mechanisms inducing cytoskeleton reorganization is given by the signalling mediated by integrins. These cellular receptors provide a physical link between the cytoskeleton and extracellular structural elements, like extracellular matrix (ECM). Indeed integrins are named as such for their role in integrating the intracellular cytoskeleton with the ECM (75). Thus, in my first study I investigated whether different ECM elements can induce morphological changes and modulate microglia activation status. I will now first describe the integrin signalling mechanisms and then I will present a brief overview of the ECM components.

Integrin mediated signalling

Adhesive interactions between cells and ECM proteins play a vital role in a vast array of biological processes, including but not limited to: cell survival, differentiation, migration, growth, tissue repair, tumor invasion and inflammatory responses (75, 76). The major group of proteins mediating these interactions belongs to a family of cell surface receptors known as integrins. Integrins represent a family of proteins consisting of alpha and beta subunits, which form transmembrane heterodimers (77). Integrins function as adhesion receptors for extracellular ligands and transduce a variety of biochemical signals into the cell through downstream effector proteins (78). For example the interaction of integrins with their ligand induces the activation of the focal adhesion kinases (FAK) after co-localization with integrins themselves (79), and FAK signalling regulates cell motility and actin polymerization (80). In particular, FAK regulates the activation status of the aforementioned Rac GTPase by activating GRAF, the relative GTPase activating protein (GAP). Moreover, FAK can also regulate gene expression by impairing the transcription

`

of p53 dependent genes (81) or supporting p53 degradation (82). Thus interaction of ECM proteins with integrins can result in a large number of different biological changes. ECM proteins can also induce cells to further modify the types of integrins expressed on their surface, so that alternative ECM -intergrin interactions are possible.

But the role of integrins in microglia goes beyond their function as ECM receptors. Indeed LPS treatment on in vitro microglia upregulates a number of different integrins (83) and the DAMP ATP can stimulate integrin beta1 activation through one of its receptors p2y12 (84). Furthermore also cytokines can modulate the activation state of integrins (85). Altogether, these studies suggest that inflammatory stimuli modulate integrin function. Therefore integrins, and possibly the ECM /cell interaction they mediate, can modulate the activation process of immune cells (86). Finally, integrins are also involved in the crosstalk between microglia and other cell types. For instance, the signal cascade that regulates microglial morphology can be activated by the α-synuclein released by neurons, and integrin beta-1 is essential for the reception of this signal (87). In my first study I determined a relationship between microglia morphology and one of the most important elements constituting ECM, Laminin. However the ECM composition and associated signalling cascade is very complex.

The extracellular matrix

The extracellular matrix (ECM) forms a three-dimensional network surrounding cells that defines the structure of tissues. The ECM is produced and secreted by neurons and glia to generate a framework formed by a wide range of proteins and glycans (88). This complex structure constitutes between the 10 to 20% of the total brain volume (89, 90), but surprisingly relatively few studies focused on the ECM compared to the vast literature on the other cellular components of CNS. Recently, it has become

`

increasingly evident that the ECM is more than just a structural frame between cells and that it can actually regulate physiological responses in the brain. Thus, we can identify two main roles exerted by ECM. The first one is structural, as ECM provides neurons with anchorage points and defines their organization in the different CNS regions. Moreover, differences in composition of this matrix are the main feature that grant different biomechanical properties to these regions. The second highly complex role of ECM resides in its involvement in signalling cascades. Depending on the composition, ECM can be a source of signalling since it can guide cellular growth (91) and survival (92), but can also function as a controller of the diffusion of signalling molecules in cell-to-cell communication. I will now introduce some of the main components of ECM and their importance in the CNS.

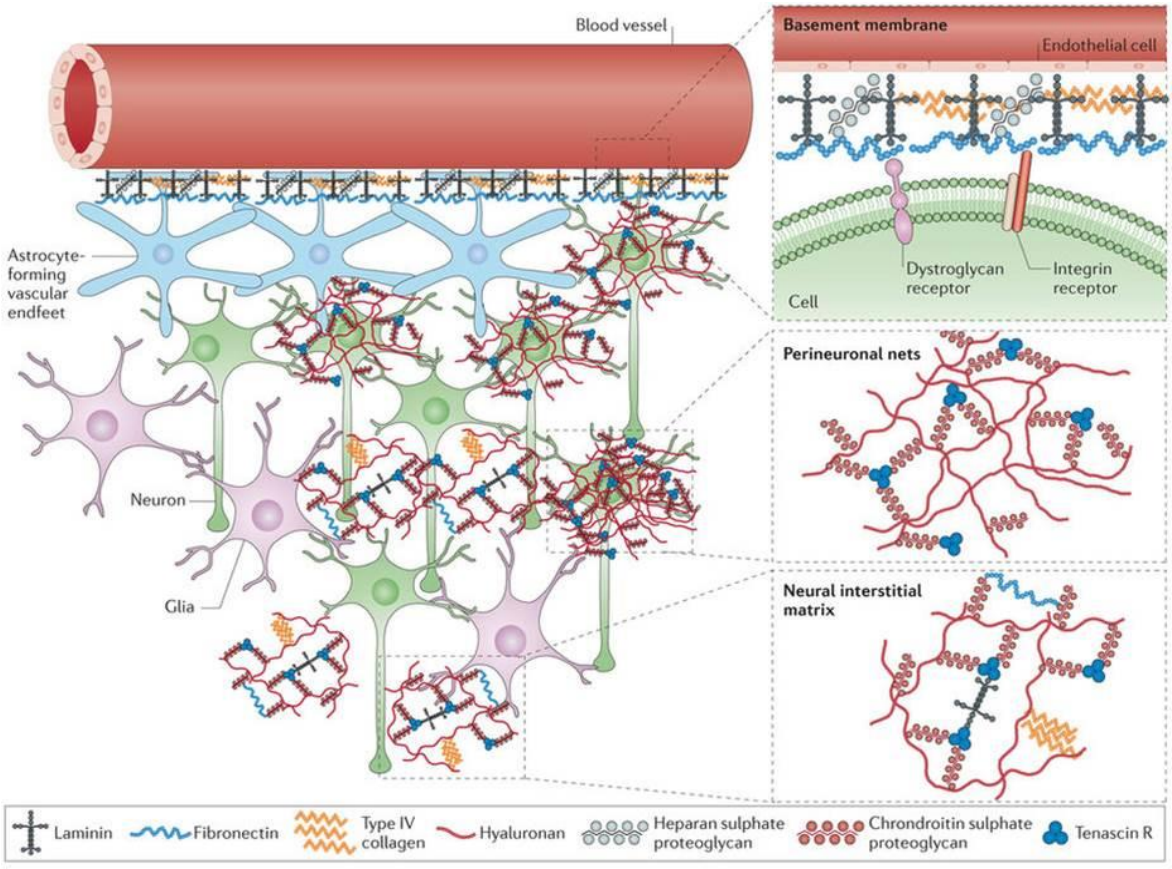

`

Figure 4. ECM components localization and structural organization in the CNS. Extracellular matrix (ECM) components are distributed in the basement membrane, the perineuronal nets around neurons or in the interstitial matrix between cells of the CNS. Different proteins interact together and contribute to form the ECM. Adapted from (93).

Main components of the extra cellular matrix and involvement in CNS pathologies

Chondroitin Sulfate Proteoglycans. Chondroitin Sulfate Proteoglycans (CSPGs) are a family of molecules composed by a number of elements (neurocan, brevican, aggrecan, versican among others) present in a variety of tissues. CSPGs are involved in several processes within the CNS; they influence dendritic spines formation (94), are important components of peri neural nets (95) and even modulate inflammation, for example by regulating inflammatory cells migration or sequestering cytokines (96). CSPGs are also one of the main components released by astrocytes to form the glial scar (97, 98). The glial scar is a protective mechanism that aims to isolate the area of damage to prevent its spreading (99, 100), but it has also been shown to restrict axonal regeneration after damage, and following injury a dramatic increase in expression of CSPG in the area surrounding the damage can be observed (101, 102). However the model that proposes negative control of axonal regrowth by CSPGs has been challenged recently (103) suggesting that their role is still not completely understood.

Collagen. The collagen family is composed of 28 members and together the collagen protein family are the most abundant proteins in mammals, accounting for an astonishing 30% of total protein mass (104). Different members are found in different tissues like connective tissue, cartilage, bones, ligaments and finally brain. In particular great interest

`

arose for the role of Collagen VI in the brain as a neuroprotectant from Amyloid beta neurotoxicity (105), a mechanism possibly involved in Alzheimer's disease development.

Fibronectin. Fibronectin is the product of a single gene but alternative splicing results in 20 different variants in humans (106). Fibronectin also plays a very important role in cellular processes like migration, differentiation, growth and can interact with as many as 12 different integrin receptors (107, 108). Fibronectin has two forms: a soluble one called plasma fibronectin and an insoluble one called cellular fibronectin which is assembled in the ECM. Surprisingly, the soluble form is important in preserving neurons after cerebral ischemia since knock-out mice lacking this form show increased ischemic area (109), while one particular isoform soluble fibronectin can instead exacerbate brain injury and inflammation after stroke (110). Moreover in multiple sclerosis the soluble form has also been shown to form aggregates that prevent remyelination (111) while the insoluble form is a pro-inflammatory modulator of microglia (86). These studies give a good example of how different isoforms of ECM proteins can have very different impact on CNS pathologies.

Laminin. Laminins are heterotrimers composed by three different chains: α, β and γ. Currently, 5α, 3β and 3γ chains have been identified that can assemble into 45 heterotrimers, but up to now only a total of 17 isoforms have been observed (112). These various isoforms are expressed in different tissues (kidney, muscles, skin) and can interact with a wide range of integrin receptors and other ECM proteins. We can define two main roles for Laminin in the brain that are expressed by specific cell types, although some elements overlap. Firstly, Laminins that are expressed by pericytes, astrocytes and endothelial cells are important for vascular and blood brain barrier integrity. Secondly, isoforms of Laminin deposited mainly by neurons are important for neuronal function.

`

These isoforms have been shown to stabilize synapses (113), trigger axonal formation (114) and promote neuronal survival (115).

Laminin adhesion to the ECM can be modulated by the activation of microglia (85) and in turn ECM components can tune microglia activation (116). ECM components like Laminin can also influence microglia morphology (117) suggesting a potential connection between microglia activation, morphology and extracellular matrix. However all these studies have been performed in vitro. Prompted by previous results in our lab (118) and literature supporting this hypothesis, in Chapter 3 I investigated this connection in the context of psychological disorders and specifically chronic stress. As detailed in the next paragraph and following, chronic stress is an environmental factor that can lead to psychological disorders like major depression (MD). Numerous studies have indicated that microglia morphology is profoundly altered in various brain regions in animal models of chronic stress. Further, both preclinical and clinical studies found a deregulation of inflammatory status in chronically stressed/ depressed subjects. However, the causes leading these phenotypes are still largely not characterised. The concept itself of stress is quite elusive, so I will now proceed illustrating what stress is, the signalling cascades triggered by this response and their association with inflammation.

Aetiology of Stress

The formulation of a comprehensive definition of stress has been subject of debate for decades. Back in the 1938 one the pioneers of the stress field, Hans Selye, defined stress as ‘the non-specific response of the body to any demand’ (119). This debate is still ongoing (120), but in the modern days it is general consensus that the word “stress” describes the response that is activated when the subject perceives an uncontrollable

`

danger, which is termed as ‘stressor’. While the stressor causes a perturbation in the systemic homeostasis, the stress response is the mechanism in charge of restoring the lost homeostasis. Repeated activation of the stress response is highly detrimental to a range of systems essential to physiological functioning (121, 122). In fact stress is considered a major risk factor in the development of psychopathological (123, 124) and pathological (125) conditions. Given these associations, it is not surprising that the effects of stress are a substantial economic and psychological burden.

The induction of the stress response by a stressor involves the initiation of a number of physiological changes. Particularly relevant among these changes is the activation of the autonomic nervous system, with a consequent release of catecholamines (epinephrine, also known as adrenaline, and norepinephrine). These hormones are known to induce rapid physiological changes within seconds to a few minutes and set the body in a “reactive state” in order to be immediately prepared for the imminent challenge. However, the activation of this pathway is only the first part of the stress response. The second part, necessary to give the body the resources to cope with the stressor, is the activation of the hypothalamic-pituitary-adrenal (HPA) axis and the release of adrenal steroid glucocorticoids (GCs). These two pathways cooperate together for a concerted response. While epinephrine induces fast changes to cope with the challenge, glucocorticoids have a slower dynamic aimed at the mobilization of resources for the body, for example by regulating the metabolism of glucose with subsequent prolonged modulation of glucose concentration in the blood stream (hence the name gluco-corticoids). However the function of GCs is much more complex since they can have both preparative or suppressive effects (126).

`

The systemic effects of chronic stress involve a coordinated response by the cellular components of all activated systems. These responses are facilitated either by cell-to-cell interactions or by cell-to-matrix interactions (93, 127). In particular, one of the most well-characterised response to chronic stress involves the overproduction of GCs via the hypothalamic-pituitary-adrenal (HPA) axis .Stress activates the HPA axis that can lead in the upregulation of the levels of circulating glucocorticoids (GC). It has been hypothesized that prolonged activation status can lead to glucocorticoid receptor resistance (GCR) (122), which interferes with appropriate regulation of inflammation. In fact GCs are hormones that are known for their anti-inflammatory properties. Not all the stress related disorders cause an imbalance in the immune response, nonetheless recent studies have shown that stress or high concentrations of GCs can aggravate the immune response in different brain regions (128). In line with these observations, studies from our and other labs performed in rats suggest that microglia are affected by chronic stress at various extent and that, in pathological stress conditions, microglia change their ramified state (129) . Therefore the activation state and reactivity of microglia are altered by chronic stress, but the mechanism that leads microglia to this altered phenotype is still unclear. Moreover it is still unclear if this is correlated with stress driven inflammation.

The relationship between chronic stress and inflammation

Both pre-clinical studies performed in animal models and clinical studies in humans suggest that there is a close relationship between stress and inflammation. On the one hand, activation of the immune system in rodent models has been shown to induce depressive like behaviour, with changes in eating and drinking, sleeping, and social behaviour (130-132). However, probably the most compelling evidence of the involvement of inflammation in the development of depression comes from observations

`

in humans. Continuous activation of immune signalling has been shown to lead to the development of depression-like symptoms in vulnerable subjects (133, 134). There are numerous findings in support of this concept obtained in patients undergoing cytokine therapy. A good example can be found in the therapeutic delivery of Interferon-α (IFN-α) for treatment of infections or as cancer therapy, since a significant psychiatric morbidity has been shown following this treatment with up to 45% of patients developing major depression (135, 136). Even more relevant, the emergence of depression was validated by findings obtained in a malignant melanoma clinical study, where these symptoms were prevented by standard antidepressant therapy (137). On the other hand, a number of studies suggest that depression can induce an inflammatory status. Indeed, it has been observed that patients with major depression have activated inflammation even if they are otherwise medically healthy. In these studies, inflammatory status is assessed by measurement of inflammatory cytokines in the serum, providing a marker of systemic inflammation. Most notably, three inflammatory cytokines have been consistently reported to be increased in patients with major depression: Intereukine-6 (IL-6) (138-140), Interleukin-1β (IL-β) (141, 142) and tumor necrosis factor –α (TNF-α) (140, 143, 144). Beside the systemic inflammation it is not surprising that that pathological stress has been associated also with inflammation in other specific tissues, like lungs (145), heart (146) and gut (147). While this finding are extremely intriguing and suggest some level of overlap as deregulation of the immune system, the neurobiology and temporal dynamics of sickness behaviour and mood disorders are significantly different. It is not very clear, however, how disturbances in the HPA axis can induce this inflammatory phenotype. A possible explanation has been found in the dysfunction of the glucocorticoid receptor (GR), that leads to a state of glucocorticoid resistance (148, 149). GR is a transcriptional regulator that resides in the cytosol and, upon binding with the

`

ligand, translocates in the nucleus acting as a transcriptional activator or repressor. Structurally, GR proteins contain two zinc-finger domains that mediate the binding to specific DNA sequences called glucocorticoid responsive elements (GRE), while the N-terminal transactivation domain of GR has a powerful function that regulates the transcriptional machinery (150). Glucocorticoids are widely used to suppress inflammation and they exert this function by activating GR. Activated GR can bind to and inhibit the transcriptional activity of NF-kB, one the main transcription factors responsible for the expression of pro-inflammatory cytokines (151). In the GCR paradigm, GR dysfunction can be explained by reduced expression, alteration of the binding affinity to its ligand, binding to DNA or interaction with other proteins or transcription factors (152, 153), ultimately leading to dysregulation of the inflammatory response. However this paradigm is still debated and the context-dependent actions of the steroid hormone contribute to complicate the whole picture.

Few studies have already shown that stress can alter microglia morphology in animals. For example, Diz-Chaves et al. (2012) exposed pregnant mice to stress throughout gestation and identified disruption of microglia morphology in the offspring. Hinwood et al. (2012b) used a detailed method of digital reconstructions and showed changes in the microglia morphology in rats exposed to chronic stress. Intriguingly, these changes could be prevented by delivery of the microglial inhibitor minocycline. In my first study I validated the inflammatory status after chronic stress and dissect its relationship with microglia morphology and, potentially, changes in ECM composition (Chapter 3).

In addition to examining how microglia respond to an environmental challenge like chronic stress, I was also interested in how they respond to a physical challenge. One of the best models of brain injury is the photothrombotic stroke because of its precision and

`

high reproducibility. Moreover, as detailed later, this model induces secondary lesions in specific regions and this mechanism will be the focus of the third report. So in my following studies I focused on microglia activation following stroke, where the presence of inflammatory response is very well verified but the role of microglia is still not completely characterised. Now I will briefly describe the clinical relevance of stroke and current treatments.

Stroke

Stroke is one of the major causes of death and disability in developed counties, especially among the elderly. Stroke occurs when the blood supply to a part of the brain is cut-off so that the tissue does not receive enough oxygen and nutrients. This can be caused by vessel occlusion due to a clot (ischemic) or by a vessel rupture (haemorrhagic). Within minutes, the consequent disruption of cerebral blood circulation rapidly induces neuronal death in the primarily affected area, which is known as infarct core. The area surrounding the core, called penumbra or peri-infarct area, displays a blood flow below normal but sufficient enough to not cause immediate neuronal loss and can be rescued when the normal blood flow is restored and, in doing so, prevent permanent damage (154). In the case of ischemic stroke, the blood flow can be restored by delicate microsurgery. The physician uses very thin tubes called catheters guiding them along the blood vessels of the brain and performs mechanical thrombectomy, deploying a stent to keep the blood flowing (155). In conjunction with surgery the patient can qualify for treatment with thrombolytics, which are compounds that help dissolve blood clots. In particular tPA is currently the gold standard treatment but the time limit for its benefits is 4.5 hours post-stroke (156).

`

During the past decades a huge effort has been made in finding new treatments to prevent neuronal death after stroke. However, despite promising results in pre-clinical studies (more than 1000 studies have identified potential compounds), the identified compounds fail during clinical trials (out of 100 trials, none gave consistent benefits to patients)(157). These numbers clearly called for a drastic change in our approach to investigate new interventions. It has been proposed that other targets often neglected should be pursued, because the interaction between neurons, microglia, astrocytes and vasculature has actually a pivotal role in stroke recovery and focusing only on neurons seemed not sufficient (158). During my studies I used Phototrombotic stroke as model for brain stroke induction. As every other model, PT stroke has both advantages and disadvantages.

Since it seems vital to broaden our view when investigating neuroprotective mechanisms, in my studies I did not focus only on neurons but also on microglia. I will now briefly describe the importance of microglia and microglia activation in the pathology of stroke.

Microglia in stroke

It has been shown that microglia in the region adjacent to the infarction become activated in response to stroke. Specifically, they undergo a morphological transition progressively retracting their branches and adopting a more rounded morphology that is described as amoeboid shape. As previously mentioned amoeboid microglia are the activated pro-inflammatory form, they can phagocytose debris and release high levels of pro-inflammatory cytokines and free radicals (41). It is still debated whether microglia activation is detrimental or beneficial for recovery after injury, as a number of studies support both these views (159). I will highlight studies supporting the general importance of microglia, their pro-inflammatory status and the prevention of their pro-inflammatory phenotype.

`

There is compelling evidence supporting a neuroprotective role of microglia after stroke. A proof of concept comes from a study of Gergely Szalay, who showed in 2016 that microglia protect the brain from ischemic damage using a model of pharmacological microglia depletion (160). Within the brain microglia are self-renewing and this mechanism requires a colony-stimulating factor 1 receptor (CSF1R)-dependent signalling (161). Using a high-dose treatment of a CSF1R kinase inhibitor that can permeate the blood brain barrier, it is possible to reversibly deplete microglia (162). The authors showed that in rats depleted of microglia, stroke by middle cerebral artery occlusion (MCAO) induces a marked increase in neuronal death caused by increased excitotoxic injury, which correlated with a dysregulation of neuronal responses. Intriguingly, giving enough time for microglia to repopulate the brain before the stroke reversed the effects of microglia depletion, resulting in an infarct size similar to controls.

Activation and proliferation of microglia are an important component of the physiological response after injury. In a similar study, Lalancette-Hébert et al (163) ablated the proliferating microglia after stroke by MCAO using a transgenic mouse model where a mutant of the herpes simplex virus type 1 thymidine kinase is expressed under the control of the promoter for CD11b, whose expression is specific of the myeloid lineage. Therefore, treatment with Ganciclovir specifically ablates proliferating CD11b-positive like microglia and macrophages but it doesn't affect the quiescent cell population (164). The ablation of proliferating microglia greatly changes the temporal dynamics of inflammation after stroke, with increased expression of pro-inflammatory cytokines at 72 hours, and induces a wider area of infarction.

Microglia phagocytic activity after injury alters the removal cellular debris; however there are conflicting describing both a positive and a detrimental effect on active

`

phagocytosis. On the one hand, the activity of microglia to phagocytize and ingest damaging components contributes to the re-establishment of homeostasis after injury, and this is considered a key component of tissue repair (165). On the other hand, prolonged induction of phagocytic activity can be highly detrimental, as shown by Neher et al. in a model of endothelin-1 induced stroke in rats (166). In this study the knock-out of either one of two proteins mediating phagocytosis, Mer receptor tyrosine kinase (MerTK) or Milk fat globule EGF-like factor 8 (MFG-E8), lead to decreased neuronal death at 3, 7, and 28 days post-stroke and prevented long-term functional motor deficits. As the authors suggest, this is likely to be the consequence of the inhibition of viable neurons phagocytosis, thus preventing delayed neuronal death. In another study Lui et al. (167) inhibited microglia activation at 4 days after MCAO using minocycline, a tetracyclic antibiotic whose anti-inflammatory effect has been extensively reported (168-171). Intriguingly, the treatment resulted in a reduction of activated microglia, an increase in number of new neurons and most importantly an improved functional recovery.

All together, these studies and others suggest that the temporal dynamic of microglia activation and the timing of intervention are very important in determining the severity of neuronal loss and associated functional outcome after stroke. It is considering these reports that in Chapters 4 and 5 I aimed to investigate the progression of microglia activation in the weeks following stroke. Very promising preliminary data in our lab showed low oxygen post conditioning (LOPC) can be a valuable intervention to promote neuroprotection after stroke (Appendix 1). I decided to use LOPC as a tool to help me understand how modulating stroke severity alters microglia and what the relationship between stroke severity and microglia activation is.

Low oxygen post conditioning

`

For a long time athletes have exploited the benefits of training at high altitude to improve physical performance. For example, this peculiar training has been shown to improve aerobic performance and endurance in professional runners or swimmers (172-174). These improvements have been mostly attributed to the pronounced benefits for the cardiovascular function associated with the intervention (175), suggesting potential applications of low oxygen exposure in cardiovascular pathologies. In fact numerous experimental and clinical studies have now investigated the benefits of hypoxic training in the treatment of cardiovascular diseases (176). In particular, it has been recently proposed that hypoxic training can effectively enhance cardiovascular function in pathological conditions like hypertension, coronary heart disease, and heart failure (177).

The best and most studied example of the benefits of low oxygen exposure in CNS injury is given by studies that investigated this treatment following spinal cord injury. The first preclinical reports, suggesting that low oxygen exposure could improve synaptic plasticity in a rat model of cervical spinal injury, date back more than a decade ago (178, 179). These findings were followed by small but indicative clinical studies that aimed to translate this treatment to humans. Intriguingly, these studies proved the translatability of low oxygen exposure and confirmed that it is beneficial in patients with spinal cord injury (180-182). In particular were reported improvements in ankle strength (183), walking speed and endurance (184, 185), and finally hand function (186). Therefore, it is not surprising that hypoxic exposure has been proposed as a low risk and therapeutically valuable treatment in humans (187).

Interest in the potential of low oxygen exposure in stroke as a therapeutic intervention originated by clinical observations. Some reports suggested that few minutes of sub-lethal cerebral ischemia grants transient tolerance to a subsequent, prolonged stroke event. For

`

example, prodromal transit ischemic attacks were found to attenuate stroke severity in numerous clinical studies (188-191), opening the doors to the concept of ischemic tolerance, also known as hypoxic/low oxygen pre-conditioning. This phenomenon has been demonstrated in pre-clinical studies of cerebral ischemia (192, 193), and it has also been observed in humans with reduced cerebral blood flow (190, 194-196)

Preclinical studies had very promising results, showing that moderate hypoxic pre-conditioning (8-10% Oxygen) could indeed give protection against brain and cardiac ischemia (197). However from a practical point of view the finding was hard to put into practice as ischemic attack is very difficult to prospectively predict. In 2009, Leconte et al. showed that neuroprotection could be achieved also by hypoxic or low oxygen post-conditioning (LOPC) using a rat model of MCAO and exposing the animals to 8% oxygen 5 days after stroke (198). Later pre-clinical studies confirmed these results and reported that delayed LOPC strongly promotes neurogenesis, BDNF expression and functional synaptogenesis with concomitant improvements in cognitive-function (199-201). Many different mechanisms of neuroprotection have been proposed for LOPC, like post-translational modification of neuroprotective heat shock protein (202), inactivation of the ERK pathway (203) or promotion of VEGF signalling (204). Stroke is a catastrophic event that disrupts countless pathways in the brain. On the other hand, LOPC stimulates a concerted physiological response with multiple effects, so these studies suggest that LOPC ameliorates stroke induced neuronal death acting on multiple levels.

As discussed above, microglia activation can be deleterious for neuronal survival after stroke. In the animal models of stroke, a few studies have shown that LOPC can effectively suppress microglia activation and decrease the release of pro-inflammatory factors like IL-1β and iNOS (205-207). Based on these results and others obtained in the

`

lab (Appendix 1) in Chapter 4 I investigated the effectiveness of LOPC on stroke induced motor deficits and the correlation between neuroprotection in the peri-infarct area and microglia activation. Instead in Chapter 5 I focused on LOPC neuro-protection and inflammation in a pathological event subsequent but closely related to stroke: secondary neurodegeneration.

`

Stroke and induced secondary neurodegeneration

Stroke is caused by a sudden interruption of the blood supply to the CNS that leads to neuronal loss in a matter of minutes. Additionally, it has been recognised for a long time that in the weeks to months following stroke dramatic changes can be identified in regions remote from the infarct site. We can identify three different but closely related events that affect areas distal from the infarct site: diaschisis, Wallerian degeneration (WD) and secondary neuronal death (SND).

The term 'diaschisis' was first introduced one century ago by the German neuropathologist Constantin von Monakow to describe neurophysiological changes (i.e. in metabolism or neuronal activity) in regions distal from the focal brain region (208, 209). This definition is quite vague, and for decades clinical patterns that were not directly explained by the lesion were generally ascribed to diaschisis. Only recently, with the development of advanced imaging techniques, it has been possible to validate the characteristics and clinical relevance of diaschisis (210).

Regions connected to the area where the focal damage occurs not only can display neurophysiological dysfunctions, but can also present signs of degeneration of fibre tracts within white matter. This process is called Wallerian degeneration (WD) or axonal degeneration, and is primed by a lesion to the axonal body that can result from the neuronal loss due to ischemic infarction. For example, WD has been observed both in the corpus callosum and in the pyramidal tract in longitudinal clinical studies on patients with large middle cerebral arterial stroke, using diffusion tensor imaging (211, 212). The progressive axonal disintegration triggers a series of events: macrophages infiltration, myelin degradation, microglia activation, and finally atrophy of the fibre tract (213-216). These structural changes evolve with time and have been detected in both the acute and chronic phases after stroke (212, 217, 218) and more importantly can correlate with the

`

motor-function (219). This has been reported in patients with subcortical ischemia, where WD affected the pyramidal tract both proximal and distal to the site on injury, and highly correlated with motor function (220, 221). However, it is important to notice that WD does not necessarily lead to neuronal death (222).

Neuronal death in grey matter areas distant from the primary injury is described as secondary neurodegeneration (SND). SND is characterised by a unique dynamic that unfolds in a time scale of months to years after the primary injury. This process has been observed in patients using a number of different imaging approaches like CT (223), MRI (224, 225) and DTI (226, 227) and it is independent of the type of occlusion. But at present, few studies have been aimed to specifically investigate the SND associated with stroke (228, 229). In fact only recently SND has been proposed as a potential therapeutic target (230), despite being identified more than 30 years ago and being associated with impaired functional recovery (231-233). In particular, SND has been shown in the thalamus. The thalamus is a very complex system of somatosensory relay nuclei that processes somatosensory input to the somatosensory area of the ipsilateral cortex. Thalamo-cortical projections have been deeply characterised in mice (234) and highlight the intimate relationship between the two systems.

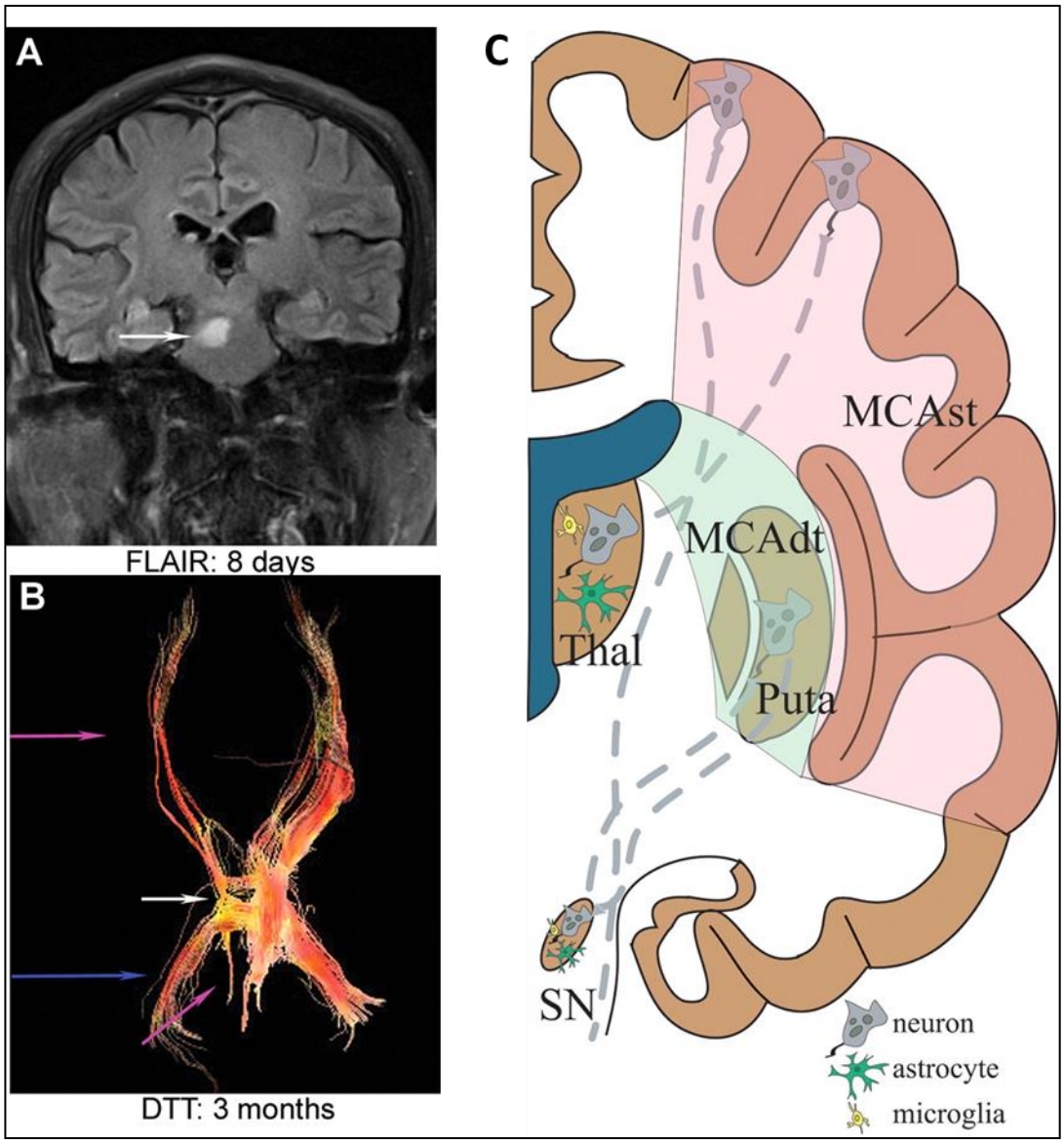

Figure 5. Imaging of MCA infarction and SND development. (A) Infarction site (white arrow) at 8 days after stroke imaged by fluid-attenuated inversion recovery (FLAIR, a form of MR image processing). (B) Imaging by diffusion tensor tractography (DTT) after 3 months post stroke. The white arrow indicates the primary infarction site, while the purple ones indicate the degeneration of pyramidal tract superior and inferior to the infarction. The blue arrow indicates the secondary degeneration of the ipsilateral middle cerebellar peduncle. (C) Schematic of the SND pathway after MCA stroke. Remote non-ischemic regions

`

synaptically connected to the primary lesion, such as the ipsilateral thalamus, the substantia nigra (SN), and the distal pyramidal tract, present pathological changes including neuronal death and gliosis.. MCAdt, middle cerebral artery deep territory; MCAst, middle cerebral artery superficial. Adapted from (230).

Tamura et al in the 1991 first reported ipsilateral thalamic atrophy after MCA stroke in a small clinical study (223). Intriguingly, the area of the thalamus gradually decreased during one year of observation. Previous studies in our lab using a mouse model of cortical stroke have shown a marked neuronal loss associated with extensive microgliosys in the thalamus (Appendix 1). The extensive connections between cortex and thalamic nuclei make the cortical stroke model an excellent tool to investigate SND in remote but connected areas. Therefore in Chapter 5 I aimed to investigate the mechanism that leads to SND using this model. In particular, I focused on the temporal dynamic of microglia activation and the association with neuronal death and I evaluated the direct involvement of the excitotoxic pathway. I will now discuss more in detail these two mechanisms possibly behind SND.

Mechanisms of SND

The mechanisms that lead to neuronal death in remote areas from the infarct are still not completely understood (235) but inflammation has been shown to play a major role. In a rat model of MCAO investigating SND and inflammation in the thalamic area, increased expression of the pro-inflammatory cytokine TNF-α has been reported after one day, while microgliosis appeared after 3 days and SND was clearly evident only after 14 days (236). Another example of the importance of microglia activation in the development of

`

SND can be found in a study from 2006 from Schroeter et.al (229). The authors induced cortical stroke in a murine genetic model knock-out for osteopontin, a glycoprotein abundantly secreted by activated macrophages that can modulate the inflammatory response (237-239). Knock-out mice presented an infarct area similar to the wild type and a strikingly increased thalamic SND, associated with increased microglia activation. Nevertheless, it still needs to be elucidated whether the inflammatory response is cause or consequence of neuronal death, especially considering that other pathways can lead the development of SND. For example, inhibition of the autophagy pathway by Beclin-1 knock down decreased thalamic SND after stroke, as shown by decreased number of autophagic and of apoptotic neurons and increased number of intact neurons (240). Intriguingly, the authors also observed reduced microgliosis and admitted that inflammation could contribute to induce of autophagy, suggesting that different mechanisms are involved in the development of SND.

Another hypothesis to explain remote neuronal after stroke loss postulates a retrograde neurodegeneration process of the thalamocortical projections caused by excitotoxicity (241). Briefly, in this model, Ca^{2+} influx through N-methyl-D-aspartate glutamate receptors (NMDARs) activates, through the post synaptic density protein PSD-95, the neuronal nitric oxide synthase (nNOS) and stimulates NO production (242). In turn, the increase in NO and associated production of peroxynitrile damages the cellular components (243). Attempts to block NMDARs to avoid excitotoxicity and brain damage failed as clinical therapy (244), since directly targeting NMDARs and nNOS can have severe consequences by interfering with physiological functions in the CNS (245). These side effects may be circumvented by blocking specifically the neurotoxic NMDAR signalling mediated by PSD-95/nNOS without inhibiting NMDARs (246, 247). However, very few studies have investigated this model specifically in the context of SND.

`

Moreover, also the choice of the stroke model adopted has an important impact on the development of SND. Indeed the process of distal neurodegeneration is gaining increasing attention and more studies are needed to investigate this pathology closely associated with stroke and, within this context, many studies showed that the choice of model is crucial. Phototrombotic (PT) ischemia targeting the motor-cortex area provides a unique, clean model to study stroke-induced retrograde degeneration, without major interference by penumbra (248, 249) and edema (250). In support of this concept, as shown in (251), middle cerebral artery occlusion (MCAO) and PT ischemia in rat induce SND by different mechanisms. While the MCAO delayed neuronal loss can be caused also by edema or by the globus pallidus damage, the SND caused by PT ischemia is most likely attributed to retrograde degeneration from the cortex.

`

CHAPTER 2

Aims and hypotheses

Study 1: Chronic stress induced disturbances in Laminin: A significant contributor to modulating microglial pro-inflammatory tone?

Hypothesis: Many studies suggested that chronic stress is accompanied with a chronic status of mild inflammation. The relationship seems to be bidirectional, as higher expression of pro inflammatory cytokines is found in individual with depression and the activation of the immune system can induce behaviour consistent with a mental disorder. To examine how stress induces inflammation, in my first study I considered a phenomena that has been largely neglected up to now, the composition of the ECM. Chronic stress is known to increase the basal activation level of microglia, but the mechanism has not been fully elucidated. It is well described in the literature that ECM can influence a number a key cellular processes like growth, survival and differentiation. However the influence of ECM composition on the inflammatory response, particularly in the context of chronic stress, has not been deeply characterised. By screening a number of microarrays performed on chronic stressed mice and rats we found that mRNA levels of some ECM components, in particular Laminins, are significantly deregulated. At the present time, there are no studies that specifically associate chronic stress with increased levels of Laminin. Moreover our lab recently showed that chronic stress alters the morphology of microglia and their degree of ramification in rats. As ramification is considered a measure of microglia activation, this data indicates a state of microglia activation associated with chronic stress exposure. Previous studies have shown that ECM proteins can induce

`

morphological changes in microglia, supporting a potential role of ECM in microglia altered ramification and hemce activation during chronic stress. Based on preliminary experiments, I hypothesised that Laminin presence can alter microglia morphology and inflammatory tone.

Aims: The first aim was to verify that chronic stress alters the expression of the ECM component Laminin. In particular, we focused on Lamininα-1 expression in the hippocampus. We sourced tissue specifically from the hippocampus as microglial disturbances have consistently been reported in this structure following chronic stress (252). The second aim was to investigate if changes in Laminin correlated with changes in the degree of microglial ramifications. The third aim was to assess an increase of the levels of pro-inflammatory cytokines expression in mice after chronic stress exposure and verify using an in-vitro approach whether Laminin can directly alter the inflammatory status of microglia.

Study 2: Low Oxygen Post Conditioning promotes persistent motor recovery after stroke

Hypothesis: As discussed above, inflammation appears to have an important role in the pathogenesis of stroke. Approaches directed to specifically target inflammation have shown promising results in pre-clinical studies (253, 254). However these results have yet to translate in clinical efficacy. For example a small clinical trial recently showed no clinical effect of treatment with minocycline, a tetracycline that inhibits microglia activation (255). Nevertheless many studies suggest that acute inflammation is detrimental for the outcome after stroke, so the role of microglia activation is unclear. Our lab has recently identified a very promising intervention capable of ameliorating neuronal loss after stroke: low oxygen post conditioning (LOPC), which consists of

`

prolonged exposure days after stroke to atmospheric air with a low content of oxygen. However the role of microglia activation in this neuroprotective mechanism is not known. Preliminary data showed that LOPC can prevent neuronal loss in the area close to the ischemic infarction, and I therefore hypothesised that the observed neuroprotection could translate into functional outcome. Considering that prolonged activation of microglia can exacerbate neuronal death, I also speculated that a decrease in inflammation could be one of the mediators of LOPC induced neuroprotection.

Aims: The first aim was to verify the clinical relevance of LOPC as potential treatment after stroke. To this end I used different behavioural tests to estimate the motor deficit induced by stroke and evaluate the effect of LOPC treatment in ameliorating the motor impairment. LOPC is a very complex treatment since it likely does not affect just one pathway, but induces a concerted physiological response. Previous studies have already shown that LOPC can induce a number of different neuroprotective mechanisms. Based on the literature, I also evaluated two potential mechanisms though which LOPC can exert neuroprotection: microglia activation/inflammation and BDNF expression.

Study 3: Low Oxygen Post Conditioning ameliorates thalamic secondary neurodegeneration induced by excitotoxicity

Hypothesis: Secondary neurodegeneration (SND) describes the process of neuronal death in areas distal from but connected to the primary injury. Our lab and others have previously reported the occurrence of neuronal death by SND in the thalamus after cortical ischemia. Preliminary data generated in our lab showed that LOPC after 15 days can reduce thalamic SND specifically, but did not affect the level of microglia activation. For a long time it has been debated whether activation of microglia in the thalamus is a cause or consequence of SND. I hypothesised that assessing the time line of microglia

`

activation will shed light on a possible contribution of microglia and their role and or response to SND. Additionally, this study also investigated the potential neuroprotective effect of LOPC on the potential underlying mechanism driving SND. Many studies, using models of stroke and traumatic brain injury (TBI), have shown that damage in the cortex leads to neuronal death in the thalamus. One intriguing explanation involves retrograde degeneration of the thalamic projections after the cortical damage through an excitotoxic mechanism. As detailed later, excitotoxicity is mediated by the NMDA receptor that, once activated, promotes the activation of nNOS and generation of free radicals, toxic for neurons. I hypothesised that LOPC could disrupt this signalling pathway and prevent secondary neuronal death.

Aims: Previous results generated in our lab showed that microglia in the thalamus have an activated phenotype at 30 days after stroke. The first aim of this study was to compare microglia activation in the thalamus at 15 and 30 days after stroke between LOPC and control (atmospheric air) group. The second aim directly associated with the first was to verify that the effect of the LOPC protocol was not temporary and SND wouldn't progress once the treatment ended at 15 days. The third aim was to investigate the excitotoxic process in the thalamus after LOPC.

`

CHAPTER 3

Chronic stress induced disturbances in Laminin: A significant contributor to modulating microglial pro-inflammatory tone?

Introduction

The main aim of my first study was to investigate microglial morphological alterations in a murine model of chronic stress and determine how these modification correlate with microglial inflammatory status and composition of the extracellular matrix. There is extensive evidence showing that chronic stress induces an inflammatory status and structural remodelling in microglia, but the mechanism leading to these changes is largely unknown.

In homeostatic conditions, the innate immune system is triggered by the occurrence of an injury or invasion of pathogens and initiates a molecular cascade of inflammatory processes mediated by the expression and release of cytokines (256). The aim of this process is in first instance to help contain infection, and secondly to promote healing and recovery after damage. It has been also shown that immune response can be triggered by mental health status. Specifically, it has been shown in both pre-clinical and clinical studies that the expression of inflammatory markers is increased in subject with depression but otherwise healthy. In particular, many studies report an increased expression of two particular pro-inflammatory cytokines: Intereukine-1β (IL-1β) (141, 142) and tumor necrosis factor –α (TNF-α) (143, 144). Chronic inflammation in patients is often associated with early signs of depression (257), while patients diagnosed with depression show increased levels of systemic inflammation (258). Furthermore, studies revealed that the activation of microglia was exacerbated in individuals that committed suicide, indicating a crucial role for neuroinflammation in depression pathogenesis (259).

`

In light of these reports, in this study we focused on these two cytokines and inducible nitric oxide synthase (iNOS), a very well characterised marker of microglial activation (260).

For many years it has been reported that microglia undergo morphological changes following activation caused by a pro-inflammatory stimulus but, until recently, microglial morphological status was categorised either as resting-ramified or as activated-amoeboid. Only a few years ago it was discovered that microglia can undergo structural remodelling in response to environmental challenges as well, like after exposure to chronic stress (118, 261, 262). However, the mechanism leading to these morphological changes was largely uncharacterised. Here I contemplated an intriguing hypothesis, the involvement of the ECM in modulating microglia remodelling and activity. ECM components are capable of transducing both intracellular signalling and morphological remodelling in different cell types, especially in correlation with different adhesive properties (263-267). Thus, I expected that ECM composition can potentially affect microglia.

Increasing evidence has built up in the past decades about the importance of microglia not only in response to treats of different nature, but also to changes in the homeostatic balance within the CNS. This study proposes that changes in the ECM composition can be a pivotal element among the mediators that can induce alterations in microglia function. As a proof of concept I used the chronic stress model of depression, a model in which microglia profile is profoundly affected. I identified differential expression of one particular ECM component, Laminin-1, and I showed that this isoform has the potential to induce microglia structural remodelling and an activated phenotype.

`

Contribution

As coauthors of the paper: Pietrogrande G, Mabotuwana N, Zhao Z, Abdolhoseini M, Johnson SJ, Nilsson M, Walker FR *(2018).*
Chronic stress induced disturbances in Laminin: A significant contributor to modulating microglial pro-inflammatory tone?
Published in Brain, Behavior, and Immunity, we confirm that **Giovanni Pietrogrande** has made the following contribution;
75% conception and design of research;
75% experimental procedures;
75% analysis and interpretation of the findings;
80% writing of the paper and critical appraisal of content

Mabotuwana Nishani		*27.03.2018*
Name of Co-author	*Signature*	*Date*
Zhao Zidan		*27.03.2018*
Name of Co-author	*Signature*	*Date*
Mahmoud Abdolhoseini		*27/03/18*
Name of Co-author	*Signature*	*Date*
Sarah J. Johnson		*27/03/2018*
Name of Co-author	*Signature*	*Date*

`

Michael Nilsson		*27/03/2018*
Name of Co-author	*Signature*	*Date*
Frederick Rohan Walker		*27/03/2018*
Name of Co-author	*Signature*	*Date*

`

PAPER 1

Brain, Behavior, and Immunity 68 (2018) 23–33

Contents lists available at ScienceDirect

Brain, Behavior, and Immunity

journal homepage: www.elsevier.com/locate/ybrbi

Full-length Article

Chronic stress induced disturbances in Laminin: A significant contributor to modulating microglial pro-inflammatory tone?

Giovanni Pietrogrande [a,b], Nishani Mabotuwana [b], Zidan Zhao [a,b], Mahmoud Abdolhoseini [c], Sarah J. Johnson [c], Michael Nilsson [a,b], Frederick R. Walker [a,b,*]

[a] School of Biomedical Sciences and Pharmacy and the Priority Research Centre for Stroke and Brain Injury, University of Newcastle, Callaghan 2308, NSW, Australia
[b] Hunter Medical Research Institute, Newcastle 2305, NSW, Australia
[c] School of Electrical Engineering and Computer Science, University of Newcastle Callaghan 2308, NSW, Australia

ARTICLE INFO

Article history:
Received 7 June 2017
Received in revised form 10 September 2017
Accepted 21 September 2017
Available online 22 September 2017

Keywords:
Microglia
Inflammation
Extracellular matrix
Laminin
Chronic stress

ABSTRACT

Over the last decade, evidence supporting a link between microglia enhanced neuro-inflammatory signalling and mood disturbance has continued to build. One issue that has not been well addressed yet are the factors that drive microglia to enter into a higher pro-inflammatory state. The current study addressed the potential role of the extracellular matrix protein Laminin. C57BL6 adult mice were either exposed to chronic stress or handled for 6 consecutive weeks. Changes in Laminin, microglial morphology and pro-inflammatory cytokine expression were examined in tissue obtained from mice exposed to a chronic restraint stress procedure. These in vivo investigations were complemented by an extensive set of in vitro experiments utilising both a primary microglia and BV2 cell line to examine how Laminin influenced microglial pro-inflammatory tone. Chronic stress enhanced the expression of Laminin, microglial de-ramification and pro-inflammatory cytokine signalling. We further identified that microglia when cultured in the presence of Laminin produced and released significantly greater levels of pro-inflammatory cytokines; took longer to return to baseline following stimulation and exhibited enhanced phagocytic activity. These results suggest that chronic restraint stress is capable of modulating Laminin within the CNS, an effect that has implications for understanding environmental mediated disturbances of microglial function.

1. Introduction

For some time now there has been interest in examining the effects of chronic stress on microglia. This motivation has stemmed largely from clinical studies that have identified a probable association between depression and inflammatory disturbances within the CNS (Dwyer and Ross, 2016; Krishnan and Nestler, 2008; Wohleb et al., 2016). It has now been shown that microglia are both structurally and functionally altered in rodents exposed to persistently stressful situations (Walker et al., 2013; de Pablos et al., 2014; Sugama et al., 2007; Sugama et al., 2011; Kreisel et al., 2014). Further, pharmacologically modulating the responsiveness of microglia during exposure to stressful experiences can limit the severity of stress induced impairments in cognition and mood-like behaviour (Hinwood et al., 2012; Nair and Bonneau, 2006; Wohleb et al., 2011; Hwang et al., 2008; Ramirez et al., 2015; McKim et al., 2016). Despite these advances, still much remains to be understood about the specific mechanisms involved.

Research undertaken by our own group has been interested in chronic stress-induced changes in microglial morphology. Specifically, we have identified that rats exposed to chronic restraint stress undergo significant morphological remodelling, with pronounced changes in their branching structure (Tynan et al., 2010). While multiple signals could be involved, one intriguing possibility is the extracellular matrix (ECM). ECM proteins are recognised for their wide ranging biological actions (Vegh et al., 2014), are a highly stable, potentially allowing them to influence microglial actions over significant time scales (Lu et al., 2011). Although not extensively examined, stress induced disturbances of the ECM have been reported (Lussier et al., 2011). For instance, several microarray studies have identified stress-induced changes within the ECM. Closer examination of these studies indicates that disturbances in expression of Laminins are particularly common (Jungke et al., 2011; Andrus et al., 2012; Santha et al., 2012; Li et al., 2013; Lisowski et al., 2013).

* Corresponding author at: Hunter Medical Research Institute, Level 3 East, Kookaburra Circuit, New Lambton Heights, NSW 2305, Australia.
E-mail address: rohan.walker@newcastle.edu.au (F.R. Walker).

https://doi.org/10.1016/j.bbi.2017.09.012
0889-1591/

Laminin is an interesting ECM component, as it is known to play a key role in modulating vascular function (Yao et al., 2014), neurogenesis and synaptic structure (Luckenbill-Edds, 1997; Flanagan et al., 2006; Plantman et al., 2008), all of which are disrupted in mood disturbance. Laminin is also increased in response to CNS trauma (Tate et al., 2007); and microglia bind more vigorously to Laminin in the presence of pro-inflammatory cytokines, suggesting a dynamic coupling during neuro-inflammation (Milner and Campbell, 2002).

While microarray expression based studies have indicated the ability of chronic stress to alter the expression of Laminin, one of our initial study goals was to confirm this effect at the protein level. We then wished to determine, whether there was an association between altered levels of Laminin and changes in pro-inflammatory signalling and microglial morphology. To induce chronic stress, we used restraint stress as it is the most widely used and extensively characterised model of chronic stress in rodents (Campos et al., 2013; Buynitsky and Mostofsky, 2009; Pare and Glavin, 1986). We sourced tissue from analysis specifically from the hippocampus as microglial disturbances have consistently been reported in this structure following chronic stress (Calcia et al., 2016). Having confirmed that Laminin is elevated after chronic stress we next turned to more detailed cell cultured based investigation of how Laminin influences microglial function and morphology. Our intent here was not to consider the effects of stress, rather we wished to investigate, if Laminin was elevated, how that would alter the activity of microglia. As such with our cell culture experiments, which made use of both primary microglia and BV-2, we assessed pro-inflammatory tone and phagocytic capacity of microglia grown in the presence or absence of Laminin-1 and in the presence or absence of pro-inflammatory stimuli. Collectively, the results from these studies are the first to suggest that stress induced changes in the deposition of Laminin within the CNS may act as a potent cue to stimulate and maintain microglial pro-inflammatory tone in response to chronically stressful situations.

2. Materials and methods

2.1. Experimental design

In-vivo: In the in vivo studies we initially screened the expression of 8 Laminin subunits (Fig. 1a and Supp. Fig. 1a). We followed this using targeted confirmation using western blotting and immunohistochemistry. Additionally, we assessed levels of TNF, IL-1 and iNOS mRNA expression and assessed changes in microglial morphology using Iba-1 immunolabelling.

In-vitro: In the in vitro studies we investigated whether the corticosterone was sufficient to alter the neuronal production of Laminin-α1. We next examined the influence of Laminin on the expression and release of pro-inflammatory cytokines from primary microglia and from the BV-2 cell line. We further examined the influence of Laminin on the phagocytic capacity of microglia, using flow cytometry. Finally, we examined whether microglia pre-stimulated with LPS and then replated either in the presence or absence of Laminin, influenced the speed at which the cells changed the pro-inflammatory cytokine output. It is important to note that we only used BV-2 cells for the phagocytosis and replating experiments and the primary cells did not tolerate the replating process well.

2.2. Repeated restraint stress protocol

As per (Jones et al., 2015), 32 8-week-old C57BL/6 male mice (WT) from the ARC were randomly allocated to control and chronic restraint stress groups (16 for protein and transcriptional analysis and 16 for fixed tissue processing), 5 days per week for a total of 20 h per week over 6 consecutive weeks. Stress was induced using a restraint stress model where animals were placed in ventilated conical tubes. All experimental procedures were approved by the Animal Care and Ethics Committee (ACEC) of the University of Newcastle. Controls access to food and water was restricted for the same time period as the stress animals and were handled for 2 min twice daily, 5 days per week.

2.3. Tissue processing

For all in vivo experiments mice were deeply anesthetized via intraperitoneal injection of sodium pentobarbital and transcardially perfused. For fresh tissue collection mice were perfused with 12–13 mL ice cold 0.9% saline, prior to being frozen. Whereas for fixed tissue collection saline perfusion was followed by the delivery of 55 mL ice cold 4% paraformaldehyde (PFA, pH 7.4). Brains were removed and postfixed for 4 h in 4% PFA before being transferred to a 12.5% sucrose solution in 0.1 M PBS for storage and cryoprotection. 30 μm thick serial coronal sections were sliced on a freezing microtome (SM2000R, Leica) at −25 °C.

2.4. Immunohistochemistical labelling of Laminin and Iba-1

To assess the expression of Laminin-111 in the hippocampus, brain sections from control and CRS mice and were generated and immunolabelled for Laminin-α1 (Sigma-Aldrich, Cat#L9393), a subunit unique to Laminin-111 (Gawlik et al., 2011), or Iba-1 (Wako, Cat# 016-20001) as previously described (Jones et al., 2015). Cresyl violet staining was performed on immunolabelled sections as described (Tynan et al., 2013). High definition images of the mounted section were obtained using Aperio AT2 (Leica) and Aperio ScanScope Console software (V102.0.2.44).

2.5. Cell lines

BV2 cells were maintained as previously described (Tynan et al., 2012) in DMEM medium (HyClone, Cat# SH30081.01) supplemented with 10% heat inactivated foetal bovine serum (FBS) (Bovogen Biologicals, Cat# SFBS-F), 2 mM L-glutamine (HyClone, Cat# AZM197541) and Pen/Strep (Gibco, Cat# 15070-063) in a humidified incubator at 37 C with 5% CO_2.

2.6. Primary microglia cultures

C57BL/6 WT males were bred with C57BL/6 *Cx3cr1*$^{GFP/GFP}$ (Jung et al., 2000) females to obtain heterozygotes *Cx*$_3$*cr1*$^{GFP/+}$ pups. Primary mixed glia culture was derived as previously described (Shieh et al., 2014). Briefly whole brains were extracted from p1/p2 neonatal mice, cortices were isolated and meninges removed under a stereoscope. Cortical homogenate was filtered through a 70 μm cell strainer and washed twice. Finally, cells derived from each brain were resuspended in DMEM, 10% heat inactivated FBS with Sodium Pyruvate 1 mM (Invitrogen) and plated on two T75 flasks. Cells were kept at 37 °C in a humidified incubator with 5% CO_2 and half of the medium was replaced with fresh medium twice a week. After 3–4 weeks GFP positive microglia cells were FACS sorted (FACSAriaIII) and used for experiments. Although FBS could have an effect on microglia behaviour, we reasoned that using mixed glia conditioned medium in all the primary microglia experiments would actually better mimic physiological conditions.

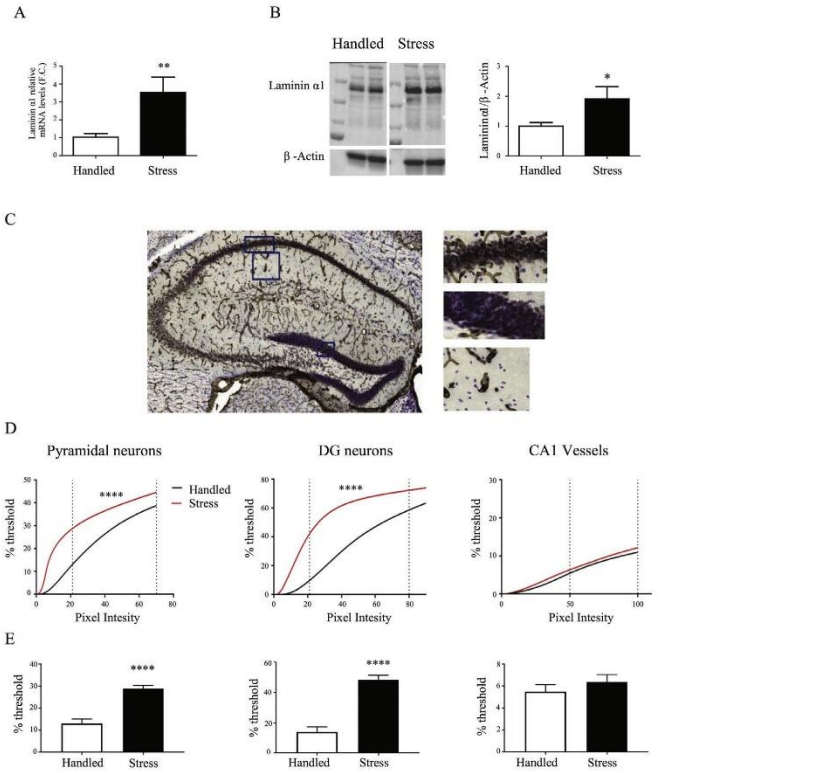

Fig. 1. Chronic stress increases the hippocampal expression of Laminin. (A) Quantification by real time qPCR shows significant increase of Laminin-α1 in the hippocampus ($^{*}p < 0.05$). (B) Western blot of the protein level of Laminin-α1 in the hippocampus normalised to beta actin. Stress increases the levels of Laminin-α1 by 2 fold ($^{*}p < 0.05$, Student's *t*-test). (C) Laminin-α1 IHC with Cresyl violet counterstaining. The Laminin signal co-localizes with Cresyl violet in both the pyramidal area and DG. (D) Cumulative thresholding spectra for Laminin-α1 immunostaining for neurons and vessels. Initially, separate images were acquired for the CA1 and DG neurons as well as the territory immediately adjacent to the neuronal layer, which was rich in blood vessels but contained no visible neuronal specific Laminin labelling. The analysis revealed that chronic stress exposure increased the expression of Laminin-α1 in both the pyramidal neurons and the dentate gyrus (DG) while the levels of Laminin-α1 expressed in the vessels are not affected (CA1 vessels). Analysis was performed on the pixel intensity interval up to the pixel intensity level that clearly contained all the labelled material (see Supp. Fig. 2). (E) Thresholding analysis of hippocampal immunolabeling at pixel intensity 21 selected out the pyramidal and DG neurons and a pixel intensity of 50 (CA1 vessels) ($^{****}p < 0.0001$, Mann-Whitney test, n = 10 both groups, mean and s.e.m. shown).

2.7. Coating experiments

Laminin from Engelbreth-Holm-Swarm murine sarcoma (Laminin-111) (Timpl et al., 1979) was purchased from Sigma Cat# L2020, Life Technologies Cat# 23017-015, In Vitro Technologies Cat#3400-010-01. For *in vitro* experiments on microglia the optimal concentration of Laminin was assessed. ELISA analysis for TNF-α release showed that using 4 μg of Laminin to coat each well (19 mm^2) of a 24 well plate (Cellstar) (2.1 μg/cm^2, concentration suggested by the manufacturers) was necessary and sufficient to induce higher release of TNF-α in BV2 cells (Supp. Fig. 3). Using Laminin from different suppliers did not influence the results. Collagen (20 μg/well) (Sigma, Cat# C0543) and Fibronectin (10 μg/well) (Sigma, Cat# F2006) were used as coating controls at the concentrations suggested by the manufacturer.

2.8. RNA isolation and quantitative RT-PCR

RNA was isolated using the Illustra RNAspin Kit (GE Healthcare, Cat# 25-0500-70) according to manufacturer's specifications from cultured cells or from hippocampal tissue punched from frozen brain slices. cDNA was generated using SuperScript™ III First Strand Synthesis System for RT-PCR (Invitrogen, Cat# 18080-044) according to manufacturer's instructions on a GeneAmp PCR System 9700 instrument (Applied Biosystems). Quantitative RT-PCR was performed on an Applied Biosystems® 7500 (Applied Biosystems) or ViiA7 (Thermofisher) instruments using SensiFAST SYBR® Lo-ROX Master Mix (Bioline, Cat# BIO-94020). Genes of interest (Supp. Table 1) were normalised on the housekeeping gene and data are expressed as $2^{-\Delta\Delta Ct}$ as fold change relative to control.

2.9. Enzyme linked immunosorbent assay (ELISA)

BV2 or primary microglia were plated on 24 multi-well coated or uncoated with Laminin and after 48 h incubated with LPS at the indicated concentration for 24 h. Cells were detached and counted using an automated cell counter (Countess, ThermoFisher). In all cases the collected medium was spun at 10000 g for 10 min at 4 °C to remove cell debris and frozen at −20 °C until analysed. ELISAs for both TNF-α (R&D Systems Mouse TNF-alpha DuoSet, Cat# RDSDY41005) and IL-1β (R&D Systems Mouse IL-1β/IL-1F2 DuoSet, Cat# RDSDY40105) were performed on supernatants according to manufacturer's protocol. Results are presented as cytokine concentration in the medium normalised on the number of cells.

2.10. Western blot

The hippocampal regions from frozen murine brain slices were processed for western blot as previously described (Ong et al., 2016). The hippocampal regions from frozen murine brain slices were punched and the tissue disrupted though two cycles of sonication in RIPA buffer. Protein concentration was assessed by Pierce BCA protein Assay Kit (Thermofisher) and 15 μg of proteins were loaded per line. After transfer on nitrocellulose membrane the blots were blocked by 5% BSA and incubated overnight at 4 °C with the primary antibody (Actin Cat# A3854, Laminin-α1 Cat#L9393, Sigma-Aldrich). Immunoblots were imaged with an Amersham Imager 600 (GE Healthcare) and bands quantified using the program ImageJ.

2.11. Phagocytosis assay

BV2 cells were plated on Laminin or uncoated for 48 h then incubated with different concentrations of a 2% solution of latex fluorescent beads (Life Technologies, Cat# F8826) and LPS 100 ng/ml for 24 h. Before been added, beads were pre-absorbed in DMEM 10% FBS for 1 h. After incubation cells were detached, washed 3 times with PBS and incubated for 5 min in PBS-trypan blue 0.04% for quenching (Simons, 2010). After 2 PBS washings cells were resuspended in PBS 1%FBS and analysed by FACS (FACSCantoII, BD Bioscience) on the PE channel. FlowJo V10 was used to analyse the data.

2.12. Image analysis

The thresholding quantification for Laminin was performed as previously described (Kongsui et al., 2014; Johnson and Walker, 2015). Optimal pixel intensity level was determined using ImageJ software. Microglia from brain slices reconstruction was performed using the cell reconstruction script 'MicroTrac' written in MatLab®. This program is based on multilevel thresholding to identify cell soma, followed by application of a minimum spanning tree algorithm to trace the cell processes (Johnson, 2016) (Fig. 2b). 'MicroTrac' calculates the number of cells per image and several morphological parameters for each single cell, specifically number of primary branches, total number of branch points, total branch length. Joined cells which were not separated by the script, were manually excluded from the analysis. The area of in vitro primary microglia was assessed as previously described (Kongsui et al., 2014). Fixed thresholding was used to segment soma and cell processes from 2D MIP images. Cells with soma area of less than 76 pixels and total area of less than 250 pixels were not included in the analysis. A watershed algorithm was used to separate joined cells.

2.13. Data analysis

All data for in vivo and in vitro groups are expressed as mean ± SEM and were analysed using Prism for Windows Version 7, GraphPad Software. Student *t*-test or Mann-Whitney test were used based on Gaussian distribution test. One way ANOVA was used to analyse the effect of different coating on microglia activation. 2-Way ANOVA was used to analyse the effects of time and laminin in the temporal persistence experiment. All differences were considered to be significant at $p < 0.05$.

3. Results

3.1. Chronic stress increases the Laminin-α1 levels in hippocampus

We evaluated the expression levels of Laminins in the hippocampus of mice after unpredictable chronic restraint stress by qPCR. Stress significantly increased the expression of Laminin-α1 (3.2-fold) ($p < 0.01$, Fig. 1a and Supp. Fig. 1a). The observed increase at the mRNA levels was confirmed at a protein level by western blot for Laminin-α1 (1.9-fold) ($p < 0.05$ Fig. 1b). To identify the cell type responsible for this increased production of Laminin, we quantified by IHC the levels of Laminin-α1 in control and stressed animals ($n = 10$/group) within the CA1 and dentate gyrus of the hippocampus (Supp. Fig. 2). Cresyl violet counterstaining suggested that Laminin-α1 in the hippocampus is produced in the blood vessels and in neurons residing in the neuronal layers (Fig. 1c). Cumulative thresholding analysis showed a highly significant (Fig. 1d, $p < 0.0001$) increase in Laminin-α1 immunolabelling in pyramidal neurons and DG. Instead, the expression of Laminin-α1 in the vessels of the CA1 wasn't affected (Supp. Fig. 2c). In particular we found that neurons present a 2.7-fold increase of Laminin-α1 immunoreactivity in the pyramidal layer (Pixel Intensity 21, $p < 0.0001$) and 4-fold increase in the DG (Pixel Intensity 21, $p < 0.0001$) (Fig. 1e and Supp. Fig. 2c).

3.2. Chronic stress increases the expression of pro-inflammatory markers in the hippocampus

We quantified by qPCR the expression of the pro-inflammatory cytokines TNF-α and IL-1β and of the inflammatory mediator iNOS in the hippocampus of chronically stressed mice. We observed a significant increase in the expression of TNF-α (4-fold) and iNOS (2-fold) ($p < 0.01$ and $p < 0.05$ respectively, Fig. 2a), while the expression of IL-1β was not significantly different.

3.3. Hippocampal microglia in stressed animals display a lower degree of branching

Brain slices were subjected to IHC for the microglial marker Iba1 as previously described. Pictures of microglia in the CA1 region were analysed using a Matlab® program aimed to identify the degree of branching in microglia (Fig. 2b). After stress, hippocampal microglia show a significant decrease in the total branch length (15%, $p < 0.05$), number of primary branches (47%, $p < 0.001$) and number of branching points (68%, $p < 0.001$) when compared to microglia from handled mice (Fig. 2c).

3.4. Microglial pro-inflammatory cytokine gene expression in the presence of Laminin

Unstimulated cells: expression of TNF-α, IL-1β and iNOS transcripts was found to be significantly higher in both BV2 and primary cells when incubated on Laminin after 48 h of culture. In BV2, TNF-α was increased 1.4-fold and IL-1β 2.4-fold ($p < 0.05$,

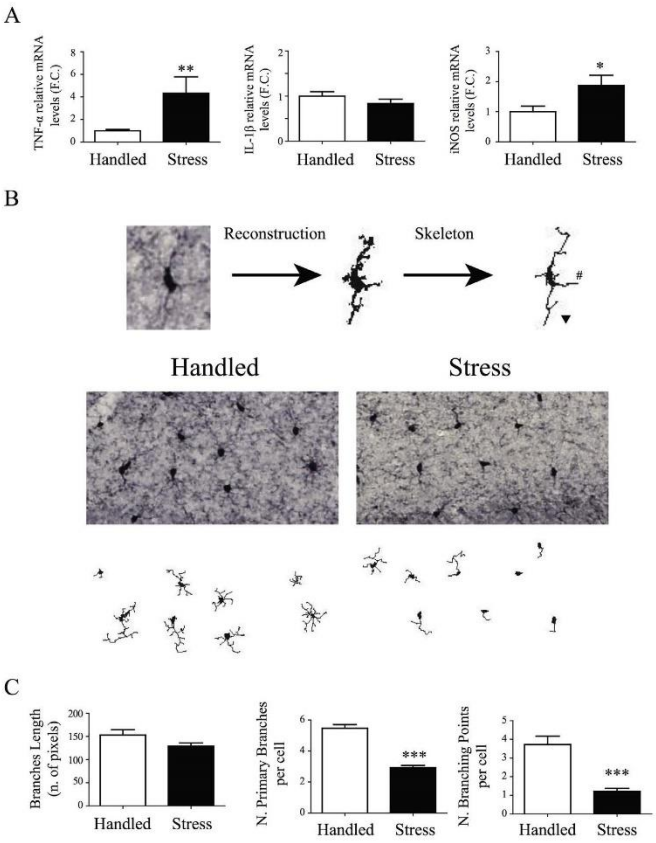

Fig. 2. Chronic stress increases the transcriptional level of pro-inflammatory cytokines and reduces microglia branching in hippocampus. (A) Quantification by real time qPCR of the expression within the hippocampus of the pro-inflammatory cytokines TNF-α, IL-1β and iNOS ($^{*}p < 0.01$, $^{**}p < 0.05$). All data shown as fold change to handled mice (Student's *t*-test, mean and s.e.m. shown). (B) Representative IHC of Iba1 in the CA1 region of hippocampus in handled and stressed mice. Microglia were digitally reconstructed using a Matlab® program previously developed and the degree of branching was quantified. (C) Microglia in stressed animals presented with a significant decrease of total branch length ($^{*}p < 0.05$), number of primary branches (#) ($^{***}p < 0.001$) and number of branching points (black triangle) ($^{***}p < 0.001$) (Student's *t*-test, mean and s.e.m. shown).

Supp. Fig. 4). In primary cells incubated on Laminin TNF-α was found to be increased 2.9-fold, IL-1β, 3.2-fold and iNOS 3.3-fold ($p < 0.05$, Fig. 3a, b and c respectively).

LPS Stimulated cells: In primary and BV2 cells we found that LPS (respectively 1 and 0.1 μg/ml) robustly stimulated the expression of both pro-inflammatory cytokines but, at the LPS concentrations used, we could not find any significant difference between cells grown on uncoated or Laminin at the mRNA level (not shown).

3.5. Microglial production of TNF-α protein production is increased in the presence of Laminin

Unstimulated cells: Our analysis indicated that 2 μg/cm^2 of Laminin coating induces an increase in the release of TNF-α protein both in BV2 (uncoated 18pg vs Laminin 61pg/ml/2 * 10^{5}cells, One way ANOVA $p < 0.01$) (Supp. Fig. 5a) and primary microglia (uncoated 40 pg vs Laminin 80 pg/ml/10^5 cells $p < 0.05$) (Fig. 4d). Using other ECM proteins for the coating like Collagen or Fibronectin did not show a significant effect (Supp. Fig. 5a and c).

LPS Stimulated cells: It was not possible to use the same concentration of LPS for BV2 and primary microglia, with primary microglia significantly more sensitive to LPS. Specifically, we identified that 100ng/mL of LPS resulted a significant increase in TNF-α release when BV2 cells were plated on Laminin (See Supp. Fig. 5b) (uncoated 200 pg vs Laminin 900 pg/ml/2 * 10^{5}cells, One way ANOVA $p < 0.005$). We initially found that primary microglia coated on Laminin and uncoated and stimulated with LPS 100 ng/ml produced very high and equivalent amounts of TNF-α. Accordingly, we reduced the stimulating concentration to 1ng/ml. We found that, at this concentration, cells grown on Laminin released significant more TNF-α than when grown on uncoated (uncoated 180 pg vs Laminin 600 pg/ml/10^{5}cells, $p < 0.005$)

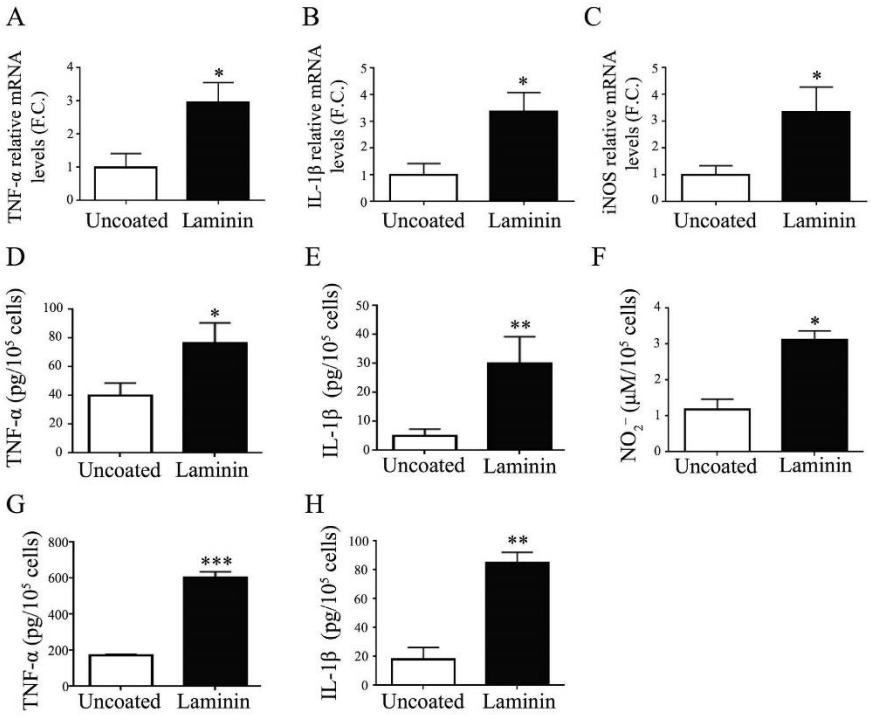

Fig. 3. Primary microglia grown on Laminin display a higher inflammatory tone. (A) Primary microglia were plated on uncoated or Laminin for 48 h and then assessed for pro-inflammatory markers expression, while the medium was collected to measure cytokines release. Expression analysis of TNFα, (B) IL-1β and (C) iNOS by qPCR shows increased mRNA levels in the group grown on Laminin. Real-time PCR analysis is presented as fold change to uncoated ($^{*}p < 0.05$, Student's *t*-test, mean and s.e.m. shown of n = 5). The medium was analysed for (D) TNF-α and (E) IL-1β presence by ELISA. (F) Primary microglia were treated with 1 ng/ml of LPS for TNF-α detection and with 1000 ng/ml of LPS for (G) IL-1β and (H) NO_2^- detection. NO_2^- concentration was measured using the Griess reagent system (Promega). LPS concentration was adapted to achieve the minimum detectable amount of target protein in the supernatant without reaching the saturation point per ml in all the samples. Optimal LPS concentrations were empirically assessed. ELISA results were normalised per cell number. ($^{*}p < 0.05$, $^{**}p < 0.01$ Student's *t*-test, mean and s.e.m. showed of n = 5).

(Fig. 3g). Again, Collagen or Fibronectin failed to induce a significant effect (Supp. Fig. 5b and d).

3.6. Microglial production of IL-1β protein production is increased in the presence of Laminin

Unstimulated cells: Primary microglia plated on Laminin produced significantly more IL-1β than cells coated on uncoated (uncoated 5 pg vs Laminin 28 pg/ml/10^5cells, $p < 0.01$) (Fig. 3e).

LPS Stimulated cells: Primary microglia plated on Laminin and stimulated with LPS (1μg/ml) produced significantly more IL-1β than cells coated on uncoated (uncoated 18 pg vs Laminin 85 pg/ml/10^5 cells, $p < 0.01$) (Fig. 3h).

3.7. Microglial nitrite release after incubation on Laminin and after stimulation with LPS

Unstimulated cells: preliminary experiments showed that primary unstimulated microglia fail to produce a detectable amount of nitrite in the medium at 24 h.

LPS Stimulated cells: We observed that media taken from cells grown on Laminin and stimulated with LPS (1 μg/ml) 24 h possessed higher levels of nitrite (uncoated 1.1 μM vs Laminin 3.1 μM, $p < 0.05$), indicating greater production of Nitric Oxide (Fig. 3f).

3.8. Laminin increases microglial phagocytic capacity after stimulation with LPS

Unstimulated cells: We observed that cell removal transfer and FACS for primary cells led to problematic changes in cellular viability, as such the phagocytosis assay were performed only using BV2 cells. We further determined that the levels of phagocytosis in BV2 were below measurable levels if the cells were not stimulated with LPS.

LPS Stimulated cells: $1.2 * 10^5$ BV2 cells plated on Laminin or uncoated were incubated with different concentrations of latex fluorescent beads and LPS 100 ng/ml for 24 h (Fig. 4c). Cells were analysed by FACS (Fig. 4a) for bead internalization. We observed that more cells are phagocytic when grown on Laminin after LPS challenge (Fig. 4b).

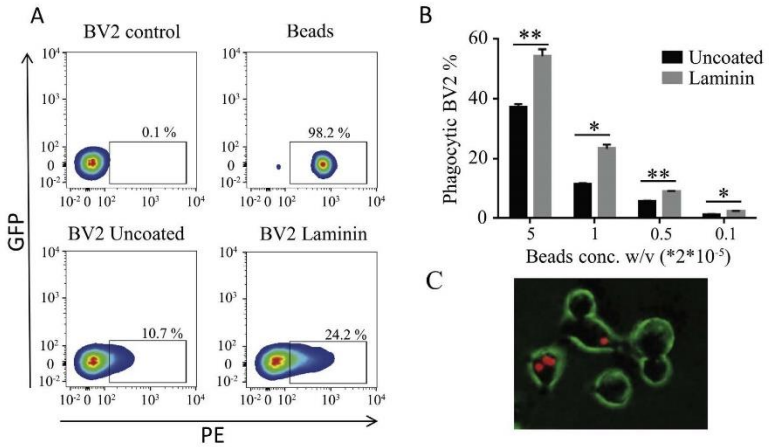

Fig. 4. BV2 cells on Laminin are more phagocytic. BV2 cells were plated on uncoated or Laminin. After 48 h LPS 100 ng/ml and fluorescent beads at scalar concentrations were added. After further 24 h, cells were analysed by FACS for beads phagocytosis. (A) An example of the flow cytometer based phagocytosis assay after appropriate gating. BV2 grown on uncoated and incubated with LPS but not beads were used as negative control (BV2 control). Beads alone were used as positive control (Beads). Cells that engulfed fluorescent beads are quantified as positive in the PE channel. (B) Data show that BV2 microglia grown on Laminin engulf more beads at all bead concentrations. (Beads conc. 5–35.8% ± 1.8% vs Laminin 53.5% ± 3.7 $p < 0.01$, Beads conc. 1–10.6% ± 0.8% vs Laminin 21.9% ± 2.4% $p < 0.05$, Beads conc. 0.5-uncoated 5.5% ± 0.6% vs Laminin 8.1% ± 0.5% $p < 0.01$, Beads conc. 0.1-uncoated 1.3% ± 0.2% vs Laminin 2.1% ± 0.2% $p < 0.05$, all Beads conc. meant as $^{*}2 * 10^{-5}$). (C) Phase contrast overlay to fluorescent image showing the internalization of beads inside BV2 cells. (mean and s.e.m. showed, Student *t*-test $^{*}p < 0.05$, $^{**}p < 0.01$ n = 3).

3.9. Laminin induces structural remodelling of microglia

We observed that primary cells grown on uncoated surfaces display quite a branched appearance (Supp. Fig. 6a). This branching, however, was abolished when microglia are plated on Laminin. We quantified the loss of ramification both as the area covered by cells ($p < 0.0001$) (Supp. Fig. 6b) and by direct count of processes ($p < 0.0001$) (Supp. Fig. 6c), defined as protrusions longer than 10 μm clearly distinguishable from the soma.

3.10. Temporal persistence of microglia pro-inflammatory status after incubation on Laminin

In order to discriminate the effect of Laminin only on the return to a basal state, in these experiments we grew microglia on a uncoated substrate and then stimulated them with LPS. We allowed these cells four hours to respond to the LPS prior to detaching them by gentle scraping and replating back onto either a Laminin or uncoated substrate. We used only the BV2 cells in these studies as we determined that the primary cells did not tolerate well the process of detachment and subsequent replating. We analysed the expression levels of TNF-α, IL-1β and iNOS after 24 h and then again 48h. After 4 h, LPS treatment greatly increased the expression of TNF-α, IL-1β and iNOS relative to non-stimulated cells (PBS).

TNF-α: After 24h there wasn't any significant difference identified for the expression TNF-α in all conditions. After 48 h TNF-α expression was significantly increased in both Laminin groups ($p < 0.05$) (Fig. 5a).

IL-1β: Both at 24 h and 48 h Laminin alone induces an increase of IL-1β mRNA level ($p < 0.01$) (Fig. 5b). In LPS pre-treated BV2 cells, the expression of IL-1β drastically drops after 24 h but in cells grown on Laminin the decrease of IL-1β is less pronounced (IL-1β uncoated 9 FC vs Laminin 28 FC, FC to untreated, $p < 0.001$). Moreover at 48h, cells on uncoated revert to an expression level of IL-1β similar to untreated ($p = 0.35$) while in cells grown on Laminin the expression of IL-1β is still sustained (IL-1β Laminin 22 FC to untreated, $p < 0.001$).*iNOS:* Both at 24 h and 48 h Laminin alone induces an increase of iNOS mRNA level (2.2 FC increase, $p < 0.05$) (Fig. 5c). At 24 h from LPS stimulation cells grown on Laminin still express five times more iNOS than the uncoated counterpart (uncoated 18 FC vs Laminin 101 FC, FC to untreated, $p < 0.005$). Similarly, at 48 h cells grown on Laminin still express about twice the level of iNOS (uncoated 14 FC vs Laminin 28 FC, FC to untreated, $p < 0.01$).

5. Discussion

We and several other groups (Sugama et al., 2007, Sugama et al., 2011; Hellwig et al., 2016) have now identified the ability of chronic stress to induce remarkable and often quite persistent changes in microglial morphology. One of the outstanding questions that has emerged from these observations is what may be some of the key factors involved in driving such substantial and persistent changes in microglia. The aim of the current of study was to explore a novel possibility, that a contributor to disturbances in microglia structure and function may be changes in the composition of the extracellular matrix (ECM) and in particular alterations in the ECM protein Laminin. While an extensive literature has charted the importance of Laminin for neuronal plasticity and dendritic spine stability (Flanagan et al., 2006; Plantman et al., 2008; Seil, 1998; Levy et al., 2014; Dansie and Ethell, 2011), only a handful of reports have addressed the relationship between Laminin and glial cells (Milner and Campbell, 2002; Summers et al., 2009).

In considering the impact of how chronic stress may alter expression of Laminin we utilised a model of chronic restraint stress. We employed this model as it has been the most extensively used model to induce stress in the rodent (Campos et al., 2013; Buynitsky and Mostofsky, 2009; Glavin et al., 1994). As impor-

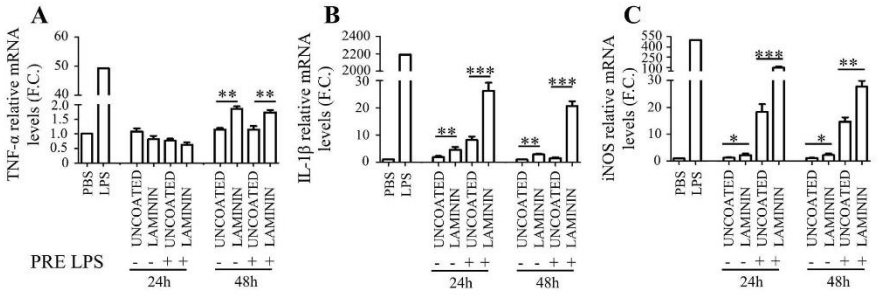

Fig. 5. Return to a resting state is delayed in BV2 microglia challenged with LPS when replated on Laminin. BV2 cells were incubated with LPS and re-plated on uncoated or Laminin-coated wells. After 24 and 48 h from replating, BV2 from n = 3 wells for each condition were analysed by real-time PCR analysis for the expression of (A) TNF-α, (B) IL-1β and (C) iNOS. qPCR results are presented as the fold change variation to PBS sample. (*p < 0.05, **p < 0.01, ***p < 0.001 Student's *t*-test, mean and s.e.m. shown n = 3). 2 way ANOVA analysis with Bonferroni post-test of cytokines expression in the 3 time points shown was performed on the LPS treated populations. For TNF-α only the variable time was found significant source of variation (p < 0.0001), while Laminin was found significant at 48 h (p < 0.001, Bonferroni post-test). For IL-1β both Laminin and Time were found very significant sources of variation (p < 0.0001), with Laminin found significant at both 24 and 48 h (0 < 0.001, Bonferroni Post-test). For iNOS both Laminin (p = 0.0023) and Time (p < 0.0001) were significant sources of variation, with Laminin found significant at 24 h (p < 0.001, Bonferroni post-test). In all cases analysis revealed a significant interaction between Laminin and Time variables.

tantly, our group have used the same model previously across a number of studies and have found it to consistently and robustly engage the hypothalamic pituitary adrenal axis, as well as a number of other classical stress metrics (Jones et al., 2015; Ong et al., 2017; Zhao et al., 2017). While not possessing the same level of face validity as some other models, such as social defeat (Beery and Stress, 2015), the restraint stress model is highly controllable, induces stress with minimum variance, and produces very similar results on a study to study basis making it an excellent choice for preclinical experimentation.

We were particularly interested in examining the effects of chronic stress on the expression within the hippocampus. While the choice of the hippocampus was somewhat arbitrary in the sense that we could have considered changes in any of several other forebrain known to be involved in the stress response, the hippocampus has effectively been used as a 'model' region to study the effects of chronic stress (Conrad, 2008). As such, how the hippocampus responds to chronic stress at a cellular level has been exquisitely described, thus the findings that we generated from the current study can be readily placed in context against a highly detailed set of pre-existing experimental results. Clearly, however, it is important to not generalise these findings to other brain regions at the current time.

Due to the inherent practical difficulties in quantitatively examining the impact of chronic stress on all ECM proteins, we decided at the outset to take a targeted approach. The strategy we decided upon was to consider the results from several previously published microarray studies (Jungke et al., 2011; Andrus et al., 2012; Santha et al., 2012; Li et al., 2013; Lisowski et al., 2013). Across these studies it was abundantly clear that the expression of Laminin was frequently altered as a result of exposure to stress. Having found what appeared as a promising candidate, we next considered the existing literature on impact of stress on the ECM. Here we could find remarkably few studies (Kavushansky et al., 2009; Laifenfeld et al., 2005) performed in rat. As such, we decided that one of the first goals of the study should be to directly confirm with at several complementary analytical approaches that Laminin was indeed altered in its expression after chronic stress in mouse. Here we specifically, chose to consider the expression of multiple Laminin subunits at the RNA level, and extending from this scan, focused particularly on the Laminin-α1 a key subunit of Laminin-1. We further characterised changes in Laminin-1 using both immunohistochemistry and western blotting.

Our screening of mRNA Laminin subunits revealed that Laminin-α1 expression was higher within the hippocampus of mice stressed by chronic restraint. No other Laminin's were found to substantially altered. We next confirmed this finding by using immunoperoxidase labelling and semi-quantitative western blotting. For analysis of our immunoperoxidase based labelling we used a cumulative threshold spectra analysis (Johnson and Walker, 2015), which provides complete information of the differences between treatment groups at all thresholding levels. This approach has a distinct advantage over classical thresholding as it provides much more complete and transparent information of the actual between group differences. Our analysis using this approach revealed very robust differences in the neuronal based expression of Laminin-α1. We further confirmed this effect with western blotting, on tissue homogenate obtained from the hippocampus, which confirmed that stress provoked a modest two fold change in the expression of Laminin-α1.

Extending from our observation that chronic stress elevated the expression of Laminin in the hippocampus we were next interested to consider microglial morphology. There already exists a compelling literature indicating the ability of chronic stress to alter microglial morphology (Hellwig et al., 2016; Bollinger et al., 2016). Specifically, it has been identified that the chronic stress in the mouse results in significant atrophy of microglia, with significant shortening of branch length (Kreisel et al., 2014). This phenotype is also typically considered transitioned from a non-inflammatory to a pro-inflammatory signalling phenotype (Kim and de Vellis, 2005). Consistent, with this concept we confirmed that stress resulted in microglial process shortening, as well as significantly higher expression of both TNF-α and iNOS within the hippocampus. In considering the most appropriate way to advance these results in the in vivo context we met some challenges, as there are no known systems to conditionally induce the overexpression of Laminin or pharmacological agents that can do the same. As such, we reasoned that the most appropriate course of action that would allow us to unequivocally examine the relationship between Laminin, microglial morphology and pro-inflammatory cytokine release was to take our investigations in vitro.

In undertaking in vitro experiments with microglia it was important to consider the culture models themselves. Briefly, BV-2 cells are the mostly widely used microglial cell line within the scientific literature (Stansley et al., 2012). Driving the widespread usage of the BV-2 line is the fact that they are widely available, readily grown, and tolerate most culture based interventions well. While these practical advantages are important, it is also worth noting that molecular phenotype of the BV-2 line has been extensively compared to primary cells derived from the neonate as well as adult microglia. From these studies it is clear that while BV-2 cells possess many typical microglial features, they also do not perfectly recapture the features of primary microglia (Henn et al., 2009; Butovsky et al., 2014). Primary cells, however, also have a number of disadvantages in that they take considerable time to establish, have limited growth potential, are very sensitive to handling, and are ultimately derived from the neonate rather than from the adult brain. Unfortunately, while procedures have been described (Ohtaki et al., 2013) it remains very challenging to derive stable primary cell cultures from the adult mouse. As such, we made use of primary cultures and BV2 cells, except for when primary cultures did not tolerate assay related handling (as was the case for the phagocytosis assay, in which we observed unacceptably high levels of mortality in the primary cells when detached for FACS analysis).

In turning to microglial cultures, the first issue that we wished to address was whether we would see a dose dependent increase in pro-inflammatory cytokine production as we increased the concentration of Laminin coating on culture plates. Our results here revealed that TNF-α release progressively rose as the concentration of Laminin coating increased. As we did not see any differences between coating concentrations above the one actually suggested by the manufacturer, we chose this concentration for all further studies. We next considered whether other ECM proteins (Fibronectin and Collagen) could induce a similar pro-inflammatory effect. Our results from these experiments indicated that microglia cultured on Fibronectin or Collagen did not exhibit any noticeable change in pro-inflammatory cytokine release. This later finding suggests that the stimulatory effect of Laminin was unlikely due to process of simply coating plates with ECM proteins.

The next question that we were interested in examining was how would growing microglia on Laminin influence their morphology Would it be consistent with what we observed in vivo? Here our analysis revealed robust structural alterations, with microglia grown on Laminin exhibiting a lower number of processes per cell and a decrease of total cell area, consistent with a lower degree of ramification. These findings are quite similar to those reported by Kreisel et al., in mice exposed to chronic unpredictable stress (Kreisel et al., 2014). We next considered how the pro-inflammatory status of microglia varied both in the presence and absence of lipopolysaccharide stimulation when the cells were plated in the presence or absence of Laminin. Here we identified that microglia when incubated on Laminin, irrespective of LPS stimulation, displayed enhanced expression of iNOS and release greater levels of the pro-inflammatory cytokines TNF-α and IL-1β. Within the limitations of an in vitro model, these findings are, to our knowledge, the first to demonstrate that Laminin by itself is a potent enhancer of microglial mediated pro-inflammatory function.

To complement the pro-inflammatory cytokine assessment we also examined microglial phagocytosis in the BV2 cell line. To examine phagocytosis we utilised a standard assay involving incubation of the cells with fluorescent beads. Following the incubation we determined the levels of fluorescent bead incorporation using flow cytometry. These investigations revealed that cells incubated on Laminin and stimulated with LPS consistently phagocytose a greater number of beads than cells grown on uncoated surface. Based on this result, we find it interesting to propose that sustained changes in Laminin may persistently influence microglial pro-inflammatory tone, as such may influence a variety of critical roles performed by microglia including modulating synaptic firing and stabilising new formed spines during learning.

In our final experiment we examined how Laminin influenced the return of LPS stimulated cells back to a baseline phenotype. Specifically, the results from this experiment indicated that expression levels for IL-1β or iNOS remained significantly elevated at both 24 and 48 h relative to cells that have been returned to a uncoated substrate. The results from this experiment suggest that an increased presence of Laminin within the extracellular matrix may contribute to a more persistent pro-inflammatory state of microglia once triggered.

The current study has a number of important limitations. Firstly, we recognise that the ability of chronic restraint stress to enhance the levels of Laminin within hippocampus does not preclude the possibility of other ECM proteins being altered by stress. The ECM consists of many dozens of proteins including collagens, vitronectin, fibronectin, chondroitin sulphate proteoglycans (GSPGs) (Lau et al., 2013). It is entirely possible that stress may influence the entire constellation of these proteins and their associated subunits. It was, however, well beyond the scope to systematically consider each of these proteins. Instead, we collapsed our attention onto Laminin as prior microarray studies had consistently identified it as being influenced by stress, as such it appeared to be a very attractive candidate further evaluation. Therefore, given their relative narrowness our results are probably best considered as providing proof-of-concept evidence that stress can disrupt specific components of the ECM. It is not, however, inconceivable that stress may exert more wide-ranging disruptive effects upon the composition of the ECM. We propose that this possibility, even though only modestly substantiated, is intriguing, as permanent disruption of the ECM composition has not been previously considered as a factor in provoking sustained changes in microglial function. A primary goal for future studies will be to consider not only the persistence of changes induced in Laminin expression but also to consider the correlation between changes in Laminin and changes in classical Depression-like behaviours. A second limitation of the current study was our focus on changes only within the hippocampus of the mouse after stress. Obviously, chronic stress has been shown to impact microglia across a variety of forebrain nuclei involved in the both the generation and control of stress responses (Tynan et al., 2010). Further, investigation is undoubtedly required to establish the permanency and breadth of the ECM changes induced by stress exposure.

6. Conclusions

Changes in the composition of the extracellular matrix are now only beginning to be examined as potential biological modifiers in the context of psychopathology. In the current study we have provided evidence for association between chronic restraint stress, Laminin, altered microglial plasticity and enhanced pro-inflammatory cytokine levels within the hippocampus. In-vitro we have further substantiated these associations determining for the first time that increased levels of Laminin are sufficient to persistently enhance microglial pro-inflammatory tone. This evidence joins a small but emerging literature highlighting a potentially very significant role for the ECM in stress-induced structural changes within the CNS (Greenbaum et al., 2011; Caruncho et al., 2016). At this stage, it is not clear why Laminin is increased after stress, or how in fact the elevated levels of Laminin influence other key cells types within the CNS. However, given that conditions such as major depression have now been linked to persistent distur-

bances in microglial function, the results from the current study suggest further attention could be given to potential contribution of the ECM in these disturbances.

Conflict of interest statement

All authors report no biomedical financial interests or potential conflicts of interest.

Acknowledgment

This work was supported by the NHMRC Project grant scheme (G1300330).

Appendix A. Supplementary data

Supplementary data associated with this article can be found, in the online version, at https://doi.org/10.1016/j.bbi.2017.09.012.

References

Dwyer, J.B., Ross, D.A., 2016. Modern microglia: novel targets in psychiatric neuroscience. Biol. Psychiatry 80 (7), e47–e49.
Krishnan, V., Nestler, E.J., 2008. The molecular neurobiology of depression. Nature 455 (7215), 894–902.
Wohleb, E.S., Franklin, T., Iwata, M., Duman, R.S., 2016. Integrating neuroimmune systems in the neurobiology of depression. Nat. Rev. Neurosci. 17 (8), 497–511.
Walker, F.R., Nilsson, M., Jones, K., 2013. Acute and chronic stress-induced disturbances of microglial plasticity, phenotype and function. Curr. Drug Targets 14 (11), 1262–1276.
de Pablos, R.M., Herrera, A.J., Espinosa-Oliva, A.M., Sarmiento, M., Munoz, M.F., Machado, A., et al., 2014. Chronic stress enhances microglia activation and exacerbates death of nigral dopaminergic neurons under conditions of inflammation. J. Neuroinflamm. 11, 34.
Sugama, S., Fujita, M., Hashimoto, M., Conti, B., 2007. Stress induced morphological microglial activation in the rodent brain: involvement of interleukin-18. Neuroscience 146 (3), 1388–1399.
Sugama, S., Takenouchi, T., Fujita, M., Kitani, H., Hashimoto, M., 2011. Cold stress induced morphological microglial activation and increased IL-1beta expression in astroglial cells in rat brain. J. Neuroimmunol. 233 (1–2), 29–36.
Kreisel, T., Frank, M.G., Licht, T., Reshef, R., Ben-Menachem-Zidon, O., Baratta, M.V., et al., 2014. Dynamic microglial alterations underlie stress-induced depressive-like behavior and suppressed neurogenesis. Mol. Psychiatry 19 (6), 699–709.
Hinwood, M., Morandini, J., Day, T.A., Walker, F.R., 2012. Evidence that microglia mediate the neurobiological effects of chronic psychological stress on the medial prefrontal cortex. Cereb. Cortex 22 (6), 1442–1454.
Nair, A., Bonneau, R.H., 2006. Stress-induced elevation of glucocorticoids increases microglia proliferation through NMDA receptor activation. J. Neuroimmunol. 171 (1–2), 72–85.
Wohleb, E.S., Hanke, M.L., Corona, A.W., Powell, N.D., Stiner, L.M., Bailey, M.T., et al., 2011. beta-Adrenergic receptor antagonism prevents anxiety-like behavior and microglial reactivity induced by repeated social defeat. J. Neurosci. 31 (17), 6277–6288.
Hwang, J., Zheng, L.T., Ock, J., Lee, M.G., Kim, S.H., Lee, H.W., et al., 2008. Inhibition of glial inflammatory activation and neurotoxicity by tricyclic antidepressants. Neuropharmacology 55 (5), 826–834.
Ramirez, K., Shea, D.T., McKim, D.B., Reader, B.F., Sheridan, J.F., 2015. Imipramine attenuates neuroinflammatory signaling and reverses stress-induced social avoidance. Brain Behav. Immun. 46, 212–220.
McKim, D.B., Niraula, A., Tarr, A.J., Wohleb, E.S., Sheridan, J.F., Godbout, J.P., 2016. Neuroinflammatory dynamics underlie memory impairments after repeated social defeat. J. Neurosci. 36 (9), 2590–2604.
Tynan, R.J., Naicker, S., Hinwood, M., Nalivaiko, E., Buller, K.M., Pow, D.V., et al., 2010. Chronic stress alters the density and morphology of microglia in a subset of stress-responsive brain regions. Brain Behav. Immun. 24 (7), 1058–1068.
Vegh, M.J., Heldring, C.M., Kamphuis, W., Hijazi, S., Timmerman, A.J., Li, K.W., et al., 2014. Reducing hippocampal extracellular matrix reverses early memory deficits in a mouse model of Alzheimer's disease. Acta Neuropathol. Commun. 2, 76.
Lu, P., Takai, K., Weaver, V.M., Werb, Z., 2011. Extracellular matrix degradation and remodeling in development and disease. Cold Spring Harb. Perspect. Biol. 3 (12).
Lussier, A.L., Romay-Tallon, R., Kalynchuk, L.E., Caruncho, H.J., 2011. Reelin as a putative vulnerability factor for depression: examining the depressogenic effects of repeated corticosterone in heterozygous reeler mice. Neuropharmacology 60 (7–8), 1064–1074.
Jungke, P., Ostrow, G., Li, J.L., Norton, S., Nieber, K., Kelber, O., et al., 2011. Profiling of hypothalamic and hippocampal gene expression in chronically stressed rats treated with St. John's wort extract (STW 3-VI) and fluoxetine. Psychopharmacology (Berl) 213 (4), 757–772.
Andrus, B.M., Blizinsky, K., Vedell, P.T., Dennis, K., Shukla, P.K., Schaffer, D.J., et al., 2012. Gene expression patterns in the hippocampus and amygdala of endogenous depression and chronic stress models. Mol. Psychiatry 17 (1), 49–61.
Santha, P., Pakaski, M., Fazekas, O.C., Fodor, E.K., Kalman, S., Kalman Jr, J., et al., 2012. Restraint stress in rats alters gene transcription and protein translation in the hippocampus. Neurochem Res. 37 (5), 958–964.
Li, X.H., Chen, J.X., Yue, G.X., Liu, Y.Y., Zhao, X., Guo, X.L., et al., 2013. Gene expression profile of the hippocampus of rats subjected to chronic immobilization stress. PLoS One 8 (3), e57621.
Lisowski, P., Wieczorek, M., Goscik, J., Juszczak, G.R., Stankiewicz, A.M., Zwierzchowski, L., et al., 2013. Effects of chronic stress on prefrontal cortex transcriptome in mice displaying different genetic backgrounds. J. Mol. Neurosci. 50 (1), 33–57.
Yao, Y., Chen, Z.L., Norris, E.H., Strickland, S., 2014. Astrocytic laminin regulates pericyte differentiation and maintains blood brain barrier integrity. Nat. Commun. 5, 3413.
Luckenbill-Edds, L., 1997. Laminin and the mechanism of neuronal outgrowth. Brain Res. Brain Res. Rev. 23 (1–2), 1–27.
Flanagan, L.A., Rebaza, L.M., Derzic, S., Schwartz, P.H., Monuki, E.S., 2006. Regulation of human neural precursor cells by laminin and integrins. J. Neurosci. Res. 83 (5), 845–856.
Plantman, S., Patarroyo, M., Fried, K., Domogatskaya, A., Tryggvason, K., Hammarberg, H., et al., 2008. Integrin-laminin interactions controlling neurite outgrowth from adult DRG neurons in vitro. Mol. Cell Neurosci. 39 (1), 50–62.
Tate, C.C., Tate, M.C., LaPlaca, M.C., 2007. Fibronectin and laminin increase in the mouse brain after controlled cortical impact injury. J. Neurotrauma 24 (1), 226–230.
Milner, R., Campbell, I.L., 2002. Cytokines regulate microglial adhesion to laminin and astrocyte extracellular matrix via protein kinase C-dependent activation of the alpha6beta1 integrin. J. Neurosci. 22 (5), 1562–1572.
Campos, A.C., Fogaca, M.V., Aguiar, D.C., Guimaraes, F.S., 2013. Animal models of anxiety disorders and stress. Rev. Bras. Psiquiatr. 35 (Suppl 2), S101–S111.
Buynitsky, T., Mostofsky, D.I., 2009. Restraint stress in biobehavioral research: Recent developments. Neurosci. Biobehav. Rev. 33 (7), 1089–1098.
Pare, W.P., Glavin, G.B., 1986. Restraint stress in biomedical research: a review. Neurosci. Biobehav. Rev. 10 (3), 339–370.
Calcia, M.A., Bonsall, D.R., Bloomfield, P.S., Selvaraj, S., Barichello, T., Howes, O.D., 2016. Stress and neuroinflammation: a systematic review of the effects of stress on microglia and the implications for mental illness. Psychopharmacology (Berl.) 233 (9), 1637–1650.
Jones, K.A., Zouikr, I., Patience, M., Clarkson, A.N., Isgaard, J., Johnson, S.J., et al., 2015. Chronic stress exacerbates neuronal loss associated with secondary neurodegeneration and suppresses microglial-like cells following focal motor cortex ischemia in the mouse. Brain Behav. Immun. 48, 57–67.
Gawlik, K.I., Oliveira, B.M., Durbeej, M., 2011. Transgenic expression of Laminin alpha1 chain does not prevent muscle disease in the mdx mouse model for Duchenne muscular dystrophy. Am. J. Pathol. 178 (4), 1728–1737.
Tynan, R.J., Beynon, S.B., Hinwood, M., Johnson, S.J., Nilsson, M., Woods, J.J., et al., 2013. Chronic stress-induced disruption of the astrocyte network is driven by structural atrophy and not loss of astrocytes. Acta Neuropathol. 126 (1), 75–91.
Tynan, R.J., Weidenhofer, J., Hinwood, M., Cairns, M.J., Day, T.A., Walker, F.R., 2012. A comparative examination of the anti-inflammatory effects of SSRI and SNRI antidepressants on LPS stimulated microglia. Brain Behav. Immun. 26 (3), 469–479.
Jung, S., Aliberti, J., Graemmel, P., Sunshine, M.J., Kreutzberg, G.W., Sher, A., et al., 2000. Analysis of fractalkine receptor CX(3)CR1 function by targeted deletion and green fluorescent protein reporter gene insertion. Mol. Cell Biol. 20 (11), 4106–4114.
Shieh, C.H., Heinrich, A., Serchov, T., van Calker, D., Biber, K., 2014. P2X7-dependent, but differentially regulated release of IL-6, CCL2, and TNF-alpha in cultured mouse microglia. Glia 62 (4), 592–607.
Timpl, R., Rohde, H., Robey, P.G., Rennard, S.I., Foidart, J.M., Martin, G.R., 1979. Laminin–a glycoprotein from basement membranes. J. Biol. Chem. 254 (19), 9933–9937.
Ong, L.K., Zhao, Z., Kluge, M., Walker, F.R., Nilsson, M., 2016. Chronic stress exposure following photothrombotic stroke is associated with increased levels of Amyloid beta accumulation and altered oligomerisation at sites of thalamic secondary neurodegeneration in mice. J. Cereb. Blood Flow Metab.
Simons, E.R., 2010. Measurement of phagocytosis and of the phagosomal environment in polymorphonuclear phagocytes by flow cytometry. Curr. Protoc. Cytom. Chapter 9. Unit9 31.
Kongsui, R., Beynon, S.B., Johnson, S.J., Walker, F.R., 2014. Quantitative assessment of microglial morphology and density reveals remarkable consistency in the distribution and morphology of cells within the healthy prefrontal cortex of the rat. J. Neuroinflamm. 11, 182.
Johnson, S.J., Walker, F.R., 2015. Strategies to improve quantitative assessment of immunohistochemical and immunofluorescent labelling. Sci. Rep. 5, 10607.
Johnson MAaFWaS. Automated tracing of microglia using multilevel thresholding and minimum spanning trees. In: 2016 38th Annual International Conference of the IEEE Engineering in Medicine and Biology Society (EMBC) 2016. p. 1208–1211.

Hellwig, S., Brioschi, S., Dieni, S., Frings, L., Masuch, A., Blank, T., et al., 2016. Altered microglia morphology and higher resilience to stress-induced depression-like behavior in CX3CR1-deficient mice. Brain Behav. Immun. 55, 126–137.
Seil, F.J., 1998. The extracellular matrix molecule, laminin, induces purkinje cell dendritic spine proliferation in granule cell depleted cerebellar cultures. Brain Res. 795 (1–2), 112–120.
Levy, A.D., Omar, M.H., Koleske, A.J., 2014. Extracellular matrix control of dendritic spine and synapse structure and plasticity in adulthood. Front. Neuroanat. 8, 116.
Dansie, L.E., Ethell, I.M., 2011. Casting a net on dendritic spines: the extracellular matrix and its receptors. Dev. Neurobiol. 71 (11), 956–981.
Summers, L., Kielty, C., Pinteaux, E., 2009. Adhesion to fibronectin regulates interleukin-1 beta expression in microglial cells. Mol. Cell Neurosci. 41 (2), 148–155.
Glavin, G.B., Pare, W.P., Sandbak, T., Bakke, H.K., Murison, R., 1994. Restraint stress in biomedical research: an update. Neurosci. Biobehav. Rev. 18 (2), 223–249.
Ong, L.K., Zhao, Z., Kluge, M., TeBay, C., Zalewska, K., Dickson, P.W., et al., 2017. Reconsidering the role of glial cells in chronic stress-induced dopaminergic neurons loss within the substantia nigra? Friend or foe? Brain. Behav. Immun. 60, 117–125.
Zhao, Z., Ong, L.K., Johnson, S., Nilsson, M., Walker, F.R., 2017. Chronic stress induced disruption of the peri-infarct neurovascular unit following experimentally induced photothrombotic stroke. J. Cereb. Blood Flow. Metab. 271678X17696100.
Beery, A.K., Kaufer, D., 2015. Stress, social behavior, and resilience: insights from rodents. Neurobiol. Stress 1, 116–127. 55.
Conrad, C.D., 2008. Chronic stress-induced hippocampal vulnerability: the glucocorticoid vulnerability hypothesis. Rev. Neurosci. 19 (6), 395–411.
Kavushansky, A., Ben-Shachar, D., Richter-Levin, G., Klein, E., 2009. Physical stress differs from psychosocial stress in the pattern and time-course of behavioral responses, serum corticosterone and expression of plasticity-related genes in the rat. Stress 12 (5), 412–425.
Laifenfeld, D., Karry, R., Grauer, E., Klein, E., Ben-Shachar, D., 2005. Antidepressants and prolonged stress in rats modulate CAM-L1, laminin, and pCREB, implicated in neuronal plasticity. Neurobiol. Dis. 20 (2), 432–441.
Bollinger, J.L., Bergeon Burns, C.M., Wellman, C.L., 2016. Differential effects of stress on microglial cell activation in male and female medial prefrontal cortex. Brain Behav. Immun. 52, 88–97.
Kim, S.U., de Vellis, J., 2005. Microglia in health and disease. J. Neurosci. Res. 81 (3), 302–313.
Stansley, B., Post, J., Hensley, K., 2012. A comparative review of cell culture systems for the study of microglial biology in Alzheimer's disease. J. Neuroinflamm. 9, 115.
Henn, A., Lund, S., Hedtjarn, M., Schrattenholz, A., Porzgen, P., Leist, M., 2009. The suitability of BV2 cells as alternative model system for primary microglia cultures or for animal experiments examining brain inflammation. ALTEX 26 (2), 83–94.
Butovsky, O., Jedrychowski, M.P., Moore, C.S., Cialic, R., Lanser, A.J., Gabriely, G., et al., 2014. Identification of a unique TGF-beta-dependent molecular and functional signature in microglia. Nat. Neurosci. 17 (1), 131–143.
Ohtaki, H., Tsumuraya, T., Song, D., Sato, A., Ohara, K., Miyamoto, K., et al., 2013. Establishment and characterization of primary adult microglial culture in mice. Acta Neurochir Suppl. 118, 49–54.
Lau, L.W., Cua, R., Keough, M.B., Haylock-Jacobs, S., Yong, V.W., 2013. Pathophysiology of the brain extracellular matrix: a new target for remyelination. Nat. Rev. Neurosci. 14 (10), 722–729.
Greenbaum, L., Levin, R., Lerer, E., Alkelai, A., Kohn, Y., Heresco-Levy, U., et al., 2011. Association of reelin (RELN) single nucleotide polymorphism rs7341475 with prepulse inhibition in the Jewish Israeli population. Biol. Psychiatry 69 (5), e17–e18. author reply e9.
Caruncho, H.J., Brymer, K., Romay-Tallon, R., Mitchell, M.A., Rivera-Baltanas, T., Botterill, J., et al., 2016. Reelin-related disturbances in depression: implications for translational studies. Front. Cell. Neurosci. 10, 48.

`

Supp. Figures

A

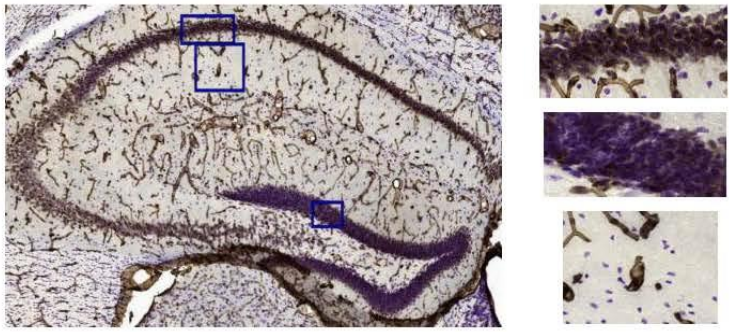

B

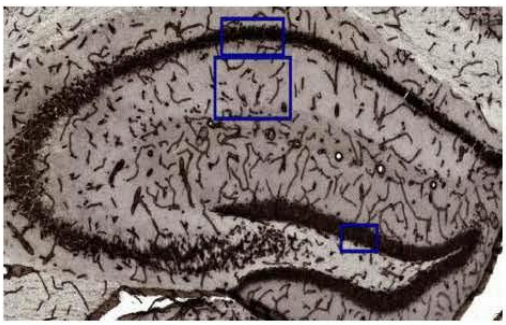

C

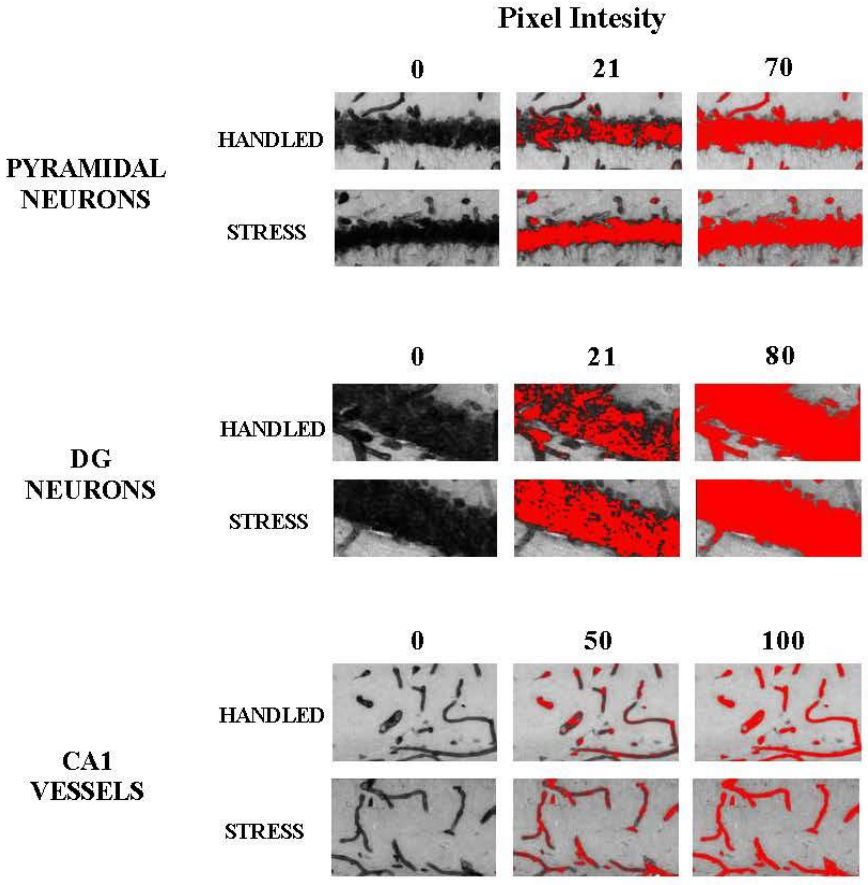
Pixel Intesity
0
21
70
HANDLED
STRESS
PYRAMIDAL NEURONS
0
21
80
HANDLED
STRESS
DG NEURONS
0
50
100
HANDLED
STRESS
CA1 VESSELS

`

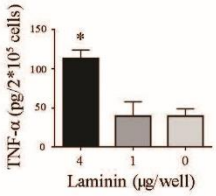
TNF-α (pg/2*10⁵ cells)
150
100
50
0
*
4
1
0
Laminin (μg/well)

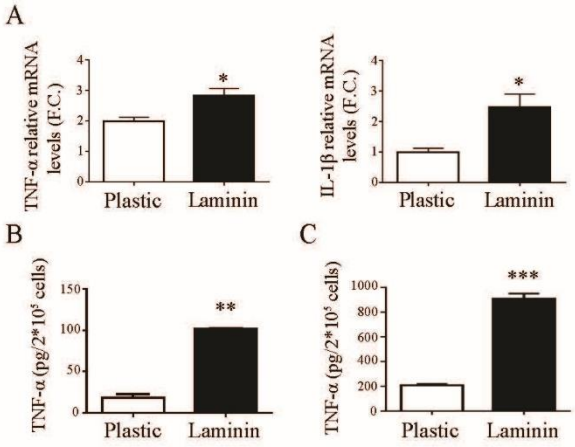
A
TNF-α relative mRNA levels (F.C.)
4
3
2
1
0
*
Plastic
Laminin
IL-1β relative mRNA levels (F.C.)
4
3
2
1
0
*
Plastic
Laminin
B
TNF-α (pg/2*10⁵ cells)
150
100
50
0
**
Plastic
Laminin
C
TNF-α (pg/2*10⁵ cells)
1000
800
600
400
200
0
***
Plastic
Laminin

`

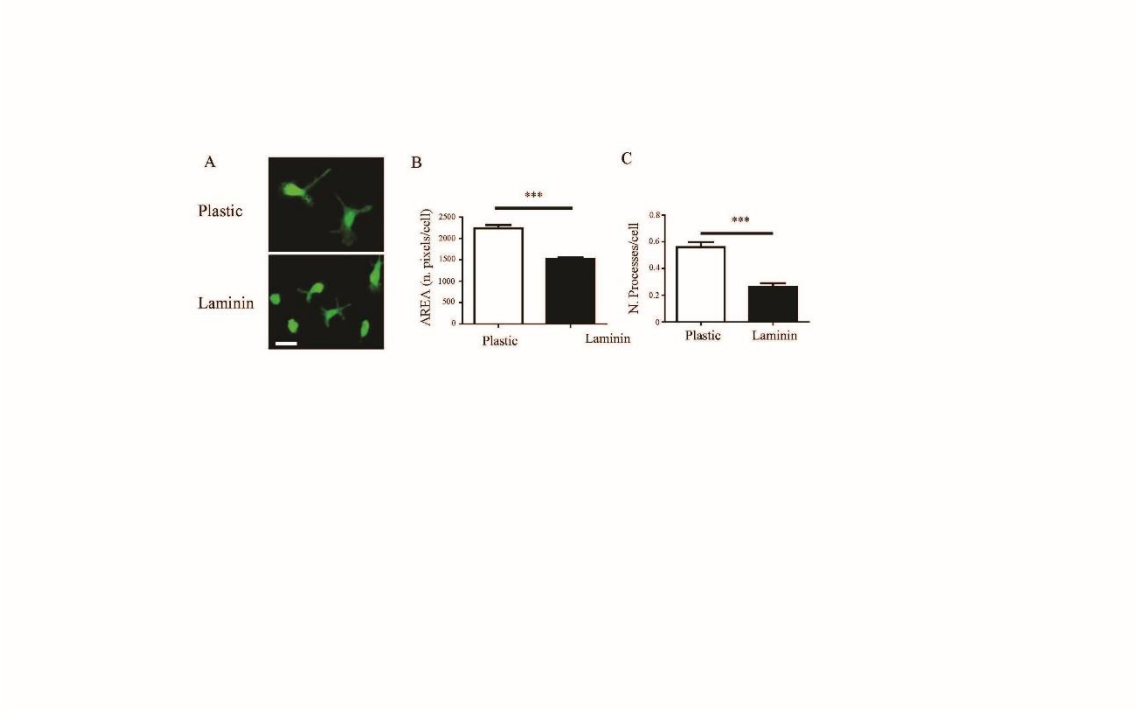

Supp. Fig.1 Laminins expression profile by qPCR in vivo and in vitro. (**A**) Quantification by real time qPCR of the expression of other Laminin subunits expressed in the hippocampus do not show significant variations. (**B**) Quantitative qPCR shows an increase in expression of Laminin-α1 in N2a cells after 24h of incubation corticosterone (50 μM). Data are shown as fold change to carrier alone (Ethanol 1:1000) (* $p<0.05$).

Supp. Fig.2 Laminin-α1 immunohistochemistry in the hippocampus. (**A**) Laminin-α1 IHC with Cresyl violet counterstaining. The Laminin signal co-localizes with Cresyl violet in both the pyramidal area and DG. (**B**) Example of the areas cropped for Laminin-α1cumulative thresholding. (**C**) Visual example of the difference in material thresholded, in the indicated hippocampal areas and at the shown pixel intensity, between samples derived from handled and stressed mice.

Supp. Fig.3 Laminin coating dose response. 24 wells plates were coated with increasing concentrations of Laminin, from 1 to 16 μg per well. BV2 cells were then plated on these substrates at an equal density and left for 48 hrs. After incubation supernatant was collected and assessed via ELISA for TNF-α release. Analysis revealed that the concentration suggested from the manufacturer (4 μg/1.9 cm^2 was sufficient to induce a robust biological effects on BV2 microglia (* $p<0.05$, ** $p<0.01$ one way ANOVA, n=4 mean and s.e.m. shown).

Supp. Fig.4 BV2 grown on Laminin express higher levels of pro-inflammatory cytokines. BV2 microglia were plated on Uncoated or Laminin for 48 hours and then assessed for pro-inflammatory expression markers. Expression of the pro-inflammatory cytokines TNF-α and IL-1β is increased in BV2 plated on Laminin as determined by qPCR. Real-time PCR analysis is presented as fold change to Uncoated. (* $p<0.05$, Student's t-test, mean and s.e.m. shown of n=5).

`

Supp. Fig.5 Laminin but not Collagen or Fibronectin induces higher TNF-α release in BV2 and primary microglia. (**A**) Medium was collected form BV2 plated on Uncoated, Laminin, Collagen or Fibronectin for 48 hours, and analysed for TNF-α presence by ELISA. (** $p<0.01$ One way ANOVA, mean and s.e.m. shown of n=5) (**B**) BV2 microglia were plated on Uncoated, Laminin, Collagen or Fibronectin for 48 hours, then cells were treated with 100ng/ml of LPS for 24 hours and medium collected for TNF-α detection (*** $p<0.001$ One way ANOVA, mean and s.e.m. shown of n=5). (**C**) Primary microglia were plated on Uncoated, Laminin or Collagen for 48 hours and then the medium was collected to measure TNF-α release. (* $p<0.05$ One way ANOVA, mean and s.e.m. shown of n=4). (**D**) After 48 h on Uncoated, Laminin or Collagen, primary microglia were challenged with 1ng/ml of LPS for 24 h and medium collected to quantify TNF-α release. (* $p<0.05$ One way ANOVA, mean and s.e.m. shown of n=4). ELISA results were normalised per cell number.

Supp. Fig.6 Laminin alters microglia morphology. (**A**) Detail of a representative images taken by fluorescent microscope of primary microglia $CX_3CR1^{GFP/+}$ grown for 48h on Uncoated or Laminin. Primary microglia grown on Laminin are smaller and present with fewer processes compared to those grown on Uncoated (Bar 10 μm) (GFP in green). (**B**) Quantification of primary cells area with Morphological analysis software. (**C**) Number of processes counted per cell (Mann-Whitney test, *** $p<0.0005$, fields n=15 mean and s.e.m. shown).

`

Discussion

The aim of this study was to investigate the mechanisms that lead to microglia structural remodelling and inflammatory status. In particular I focused on the role of extracellular matrix and its potential in inducing microglia disturbances. This is a very novel line of research since the ECM is mostly investigated for its structural properties and only recently we started to appreciate that the ECM has an active role in modulating cell function (268). I will now discuss these results in light of the existing literature and highlight some of the inevitable limitations of this study.

Major depressive disorder (MDD) has the third highest incidence worldwide. The most accepted hypothesis about the development of MDD is called the stress hypothesis, which identifies pathological alterations in the stress-responsive HPA axis as a cause of depression. While it is impossible to model all the aspects and shades of human depression using animal models, many paradigms using different stressor have been developed over the years, giving us the opportunity to efficiently induce depression-like behaviours in animals (269, 270). In this study I used restraint chronic stress paradigm. This model has been extensively used and validated in our and other labs, gives very consistent results, and is simple and less prone to be influenced by the examiner; all these elements made this model an excellent choice to induce chronic stress for my experiments (118, 270-276). Many studies show that chronic restraint stress induces the archetypal features of the stress response and physiological changes, including weight loss, a long lasting consequence of ongoing stress in rodents (277-279). The duration of the unpredicted stressor was varied between two and six hours/day. This is fundamental considering that varying the ratio between free time and restraint time maintains responsiveness to a homotypic stressor (280).

`

In this study we report several new findings that shed some light on how chronic stress can alter microglia morphology and inflammatory tone. The first part of this study was performed in vivo, and I focused on the hippocampus in particular. A conspicuous number of studies have shown that chronic stress induces morphological and molecular alterations in the hippocampus. For example, chronic stress causes changes in the hippocampal structure with consequent volume loss (281), in dendritic spine density and size (282, 283), and diminishes neurogenesis (284-286). More importantly, these changes are associated with a very robust functional outcome. Hippocampal function is important for spatial learning and memory (287) and many groups using different tests confirmed that chronic stress is associated with spatial learning and memory impairment in animal models (283, 288-291). Furthermore, chronic stress significantly elevates the expression of pro-inflammatory cytokines specifically within the hippocampus (292-294), supporting the involvement of neuro-inflammation in the development of impairments induced by chronic stress. Therefore, despite focusing exclusively on the hippocampus might seem somewhat arbitrary, existing literature supported this choice. Moreover the study design did not exclude further analysis in other brain regions and a project aimed in this direction and based on my results is currently been planned.

In this study, we analysed the expression of the pro-inflammatory mediators TNF-α, IL-1β and iNOS. While there was no detectable change in IL-1β expression, TNF-α and iNOS profiles confirmed a mild inflammatory status induced by chronic stress. Concomitantly, I found a profound alteration of microglia morphology. Microglia presented significant shortening of branch length and marked decrease in number of primary branches and number of branching points. These findings confirmed a general microglial deregulation but this is the first paper specifically reporting microglia atrophy in the hippocampus induced by chronic stress in the mouse model.

`

Additionally, I focused on Laminin among all the components of ECM. This choice was made after extensive analysis of microarray gene expression of brain tissue from chronically stressed animals published by other groups. In these data I found that the ECM component that most often resulted deregulated was Laminin. We then analysed the expression profile of Laminin using three different approaches. Firstly, I screened for the differential expression of Laminin subunits using qPCR, finding a valid candidate in Laminin-α1. Secondly, I validated the increase expression of this sub-unit using western blot, since mRNA expression is not always confirmed at protein level. Thirdly, I used immunohistochemistry to identify the origin of this increase in Laminin since, as discussed in the introduction, Laminins can be expressed by different cell types within the CNS. This analysis revealed that the increase in Laminin expression was restricted to the neuronal layers of the hippocampus, a finding particularly intriguing considering the importance of Laminin for neuronal plasticity and dendritic spine stability (295-299). Whereas these finding do not preclude the deregulation of other ECM proteins, this is the first report specifically aimed to investigate ECM disturbances after chronic stress, and makes a compelling case for the importance of future investigations.

The in vivo findings suggested a correlation between microglia morphology and Laminin alterations. However further validation in vivo was very difficult, since for example the knock-out of Laminin genes causes spontaneous intracerebral haemorrhage (300, 301). Therefore we used an in vitro approach to validate the potential effect of Laminin on microglia. The Laminin-α1 subunit drives the deposition of Laminin-1 (302), so in the in vitro experiments microglia were plated on surfaces coated with recombinant Laminin-1. Moreover control microglia were plated also on uncoated, as well as collagen and fibronectin coated surfaces. These controls allowed me to discriminate between a general effect due to coating and specific phenotypes induced by the substrate. Morphological

`

analysis on primary microglia plated on substrates showed that Laminin induced a decrease in ramifications after 48 hours form plating.

Using the in vitro approach I also investigated the inflammatory tone of the BV2 microglial cell line as well as primary microglia derived from newborn mice, when plated on Laminin or others substrates. This analysis was performed on three levels: gene expression profile of the pro-inflammatory cytokines TNF-α, IL-1β and inflammatory marker iNOS, release of TNF-α and IL-1β and production of nitrites (marker of iNOS activity), and phagocytic activity. All these data suggested that Laminin increases the global inflammatory status of microglia. Furthermore, we characterized the relationship between microglia inflammatory status and Laminin, showing that Laminin increases not only the basal expression of pro-inflammatory cytokines, but also enhances microglial response to a pro-inflammatory stimulus like LPS. Finally, I designed and set up a delicate experiment with the purpose of testing the effect of Laminin on the resolution of inflammation. This was a very innovative and really unique experiment that allowed us to precisely dissect the role of Laminin in this process. In this experiment cells were stimulated with LPS before being plated on different substrates. The expression of pro-inflammatory cytokines was then assessed after 24 and 48 hours from the stimulus. The overall result was were intriguing and suggested that the resolution of inflammation can be slowed down by the presence of Laminin.

Whereas other factors remain to be investigated, the findings presented in this paper suggest that the process of neuroinflammation that has been described in chronic stress models can also be mediated by the composition of the extracellular matrix. Taken together, the findings presented in this chapter provide fundamental new information about the process of neuroinflammation and microglia alterations after chronic stress.

`

Collectively, these observations build upon the foundations of the relatively under-researched area of ECM composition and further our understanding of the phenomenon of clinical depression. This information will provide future direction to research in the field.

`

CHAPTER 4

Low Oxygen Post Conditioning as an efficient non-pharmacological strategy to promote motor function after stroke.

Introduction

Stroke is caused by the sudden interruption of blood supply that leads to neuronal death within minutes after the event. While the formation of a thrombus or embolus is the responsible for the primary injury in ischemic stroke, many other mechanisms contribute to exacerbate the damage in the days following the ischemic attack. Inflammatory pathways in the acute phase are important pathophysiologic contributors to ischemic brain damage, and appear to be detrimental for the outcome post-stroke. Activated microglia can already be identified hours after the injury, and can release a variety of pro-inflammatory and cytotoxic mediators that can contribute to neuronal death (303, 304). A prolonged status of acute inflammation can promote neuronal death in a number of ways, and many preclinical studies over the years have shown that the reduction of inflammation after stroke is a promising target with the potential of salvaging brain tissue. For example, the inhibition of TNF-α or IL-1β by delivery of monoclonal antibodies has been shown to reduce the size of the infarct and promote neuroprotection (305, 306). Consistent with these findings, rats genetically ablated for the expression of IL-1 have smaller infarct compared to wild type in a MCAO model (307), whereas administration of recombinant IL1 leads to a worse outcome (306).

Suppressing microglia activation using treatment with specific compounds can protect brain tissue after ischemic damage (308, 309). In particular, microglia quickly become phagocytic after stroke, as indicated by their amoeboid shape and higher expression levels of CD68 (310, 311). This is an important activity aimed to re-establish homeostasis (165),

`

however inhibition of the pro-phagocytic (the ‘eat-me’ signalling) in neurons prevents neuronal death without affecting inflammation, implying that microglia phagocytosis may be detrimental after stroke (312). Therefore the inflammatory profile of microglia after stroke is very significant for the outcome and modulating inflammation can be a valuable therapeutic approach to reduce the impact of stroke.

Preliminary data generated in our lab showed that low oxygen post conditioning (LOPC) has a neuroprotective effect. In particular, LOPC decreases tissue loss and the presence of aggregates of β-amyloid. These aggregates can have a toxic effect on neurons promoting their death, so we investigated the process that lead to formation, degradation and transport of beta amyloid (Appendix 1). Whether this is a very intriguing hypothesis, I chose to focus on the role of microglia in the neuroprotective activity of LOPC and in particular, I investigated changes in microglia morphology, which is an important feature of microglia that defines their role, and the expression of activation markers CD11b, CD45 and CD68. As mentioned, activated and phagocytic microglia are less ramified and more amoeboid in shape and express higher levels of the marker CD68. Thus, in this study I evaluated by morphological and molecular criteria the differential status of microglia activation after LOPC and its correlation with neuronal death. Furthermore, I focused on the production of BDNF, an extremely important neurotrophic and neuroprotective factor that is also produced by microglia.

`

Contributions

As coauthors of the paper: **Pietrogrande G**, Zalewska K, Zhao Z, Johnson SJ, Nilsson M, Walker FR *(2018).*

Low Oxygen Post Conditioning as an efficient non-pharmacological strategy to promote motor function after stroke.

Submitted to Translational Stroke Research, we confirm that **Giovanni Pietrogrande** has made the following contribution;

75% conception and design of research;

75% experimental procedures;

75% analysis and interpretation of the findings;

80% writing of the paper and critical appraisal of content

Katarzyna Zalewska		*27.03.2018*
Name of Co-author	*Signature*	*Date*
Zhao Zidan		*27.03.2018*
Name of Co-author	*Signature*	*Date*
Sarah J. Johnson		*27/03/2018*
Name of Co-author	*Signature*	*Date*
Michael Nilsson		*27/03/2018*
Name of Co-author	*Signature*	*Date*
Frederick Rohan Walker		*27/03/2018*
Name of Co-author	*Signature*	*Date*

`

PAPER 2

Translational Stroke Research
https://doi.org/10.1007/s12975-018-0656-5

ORIGINAL ARTICLE

Low Oxygen Post Conditioning as an Efficient Non-pharmacological Strategy to Promote Motor Function After Stroke

Giovanni Pietrogrande[1,2] · Katarzyna Zalewska[1,2] · Zidan Zhao[1,2] · Sarah J. Johnson[3] · Michael Nilsson[2,4,5] · Frederick R. Walker[1,2,5]

Received: 30 March 2018 / Revised: 26 July 2018 / Accepted: 19 August 2018

Abstract
Low oxygen post conditioning (LOPC) has shown promising results in terms of neuroprotection after stroke, but the effects on motor function have not been considered. Cortical stroke targeting the motor and sensory cortex was induced by photothrombotic occlusion and after 48 h allocated to LOPC (11% O_2) for 2 weeks. Motor impairment was assessed using the cylinder and grid walk tests during the exposure period and for two further weeks upon completion of the intervention. Neuroprotection was evaluated by histological and molecular analysis at two time points. Two weeks of LOPC was sufficient to significantly reduce motor deficits and tissue loss after stroke. This functional improvement was associated with increased capillary density, enhanced levels of BDNF, decreased neuronal loss and decreased microglia activation. These improvements, in most instances, were maintained up to 2 weeks after the end of the treatment. To our knowledge, this is the first study to demonstrate that LOPC induces a persistent improvement in motor function and neuroprotection after stroke, and in doing so provides evidence to support a case for considering taking LOPC forward to early stage clinical research.

Keywords Stroke · Motor function · Neuroprotection · BDNF · Hypoxia · Angiogenesis · Inflammation

Introduction

For several decades, it has been recognised that reducing the concentration of inspired oxygen over the course of several weeks can robustly improve athletic performance at sea level [1–3]. Performance improvements have been largely attributed to the pronounced improvements in cardiovascular function associated with intervention [4]. The benefits in stimulating cardiovascular fitness in otherwise healthy individuals have started to attract interest from those working on promoting cardiovascular fitness and repair in the context of pathology. Notably, Nakada et al. have recently identified that exposing adult mice to a reduced oxygen environment exerts a pronounced regenerative effect when deployed after myocardial infarction [5].

Several preclinical studies have now begun to consider the therapeutic potential of exposure to low oxygen environments after stroke. Low oxygen post conditioning (LOPC), or intermittent hypoxic post conditioning, has been shown to robustly promote neurogenesis and vasculogenesis [6–8]. Extending from this, LOPC has been shown to improve cognitive function, an effect that appears to be associated with a reduction in neuroinflammation [9]. LOPC has also been found to limit thalamic atrophy after stroke, with a neuroprotective effect confirmed in vitro [10]. Another major advantage of LOPC is that the equipment necessary to deploy the intervention is already commercially available, has a recognised safety profile, is available from several manufactures and is moderately priced.

Although it has not yet been clinically considered in the context of stroke, LOPC has been shown to be beneficial in

✉ Frederick R. Walker
rohan.walker@newcastle.edu.au

1 School of Biomedical Sciences and Pharmacy and Priority Research Centre for Stroke and Brain Injury, University of Newcastle, Callaghan 2308, NSW, Australia

2 Hunter Medical Research Institute, New Lambton Heights 2305, NSW, Australia

3 School of Electrical Engineering and Computing, University of Newcastle, Callaghan 2308, NSW, Australia

4 Priority Research Centre for Stroke and Brain Injury, University of Newcastle, Callaghan 2308, NSW, Australia

5 NHMRC Centre of Research Excellence Stroke Rehabilitation and Brain Recovery, Heidelberg, VIC, Australia

Published online: 28 August 2018

patients with spinal cord injury [11–13], improving ankle strength [14], walking speed and endurance [15, 16] and hand function [17]. Given the promising results shown in improving motor function after spinal cord injury, it is somewhat surprising that the intervention has not been evaluated for its promotor effects after stroke, especially considering the ability of the intervention to promote vasculogenesis and neurogenesis. Given this situation, the primary aim of the current study was to examine the extent to which LOPC could promote motor function following exposure to LOPC.

LOPC involved exposure 48 h post stroke to normobaric 11% oxygen for 8 h/day for 14 days. To induce stroke in the motor and somatosensory cortex, we chose the photothrombotic (PT) model because it is well recognised to induce highly controllable vascular occlusion and, importantly, it produces only a modest penumbral area. Therefore, for longer term repair and rehabilitation studies that are concerned with cellular events long after penumbral conversion, the PT model represents an ideal model. To assess motor deficits, we used the cylinder test and the foot fault test (as per [18]). The behaviour of the mice was evaluated before, during and after intervention with a total follow-up period of 30 days. This allowed us to examine the immediate and persistent influence of LOPC on motor function. Prompted by the promising results, we investigated whether these improvements were associated with decreased level of tissue loss within the ipsilateral hemisphere along with improvements in the level of brain-derived neurotrophic factor, vasculogenesis and decreased microgliosis, all features that have been shown to be associated with a neuroprotective phenotype. This study itself involved four groups where we examined the impact of LOPC compared to controls in stroked animals at 2 weeks (immediately following the end of LOPC exposure) and then again at 4 weeks (2 weeks after the end of exposure).

Material and Methods

All the experimental groups were randomised and coded by an independent team member to blind the experimenter to the treatment condition.

Study Design

This study was planned and conducted according to the ARRIVE guidelines. In all experiments, mice were acclimatised to the environment and to the experimenter to avoid stress. Two to four mice were housed for cage. Mice were maintained in a temperature- (21 °C ± 1) and humidity-controlled environment with food and water available ad libitum. Lighting was on a 12:12 h reverse light–dark cycle (lights on 19:00 h) with all procedures conducted in the dark phase. Sample size was estimated using the following formula [19]:

$$SS = \frac{2SD^2\left(z_{1-\frac{\alpha}{2}} + z_{1-\beta}\right)^2}{d^2}$$

Using previous and preliminary data on hypoxic treatment, we estimated the effect size. We allowed a type-1 error $\alpha = 0.05$ with power of 0.8, and we calculated a sample size of six animals/group for immunohistology, eight for western blot and seven for motor test. A total of 80 male C57/BL6 8 weeks old were allocated into groups dedicated to different follow-up experiment (western blot, immunohistology and behavioural test) and underwent stroke surgery. After 48 h, mice were randomly assigned to the control (stroke) or treated (LOPC) groups and randomly sacrificed at 15 or 30 days for all experiments (Fig. 1a). A total of 16 mice were used for motor test (stroke $n = 7$, LOPC $n = 9$). A total of 35 mice were used for western blot (stroke 15 days $n = 8$, LOPC 15 days $n = 8$, stroke 30 days $n = 9$ and LOPC 30 days $n = 10$) (Fig. 2a). A total of 27 mice were used for immunohistology (stroke 15 days $n = 6$, LOPC 15 days $n = 6$, stroke 30 days $n = 7$ and LOPC 30 days $n = 8$) (Fig. 2a). As exclusion criteria, mice were removed from the study if the stroke was not identified by histological evaluation.

Photothrombotic Occlusion

On day 0, mice were anesthetised by using 2% of isoflurane and injected intraperitoneally with 0.2 mL of 10 mg/mL of rose bengal. After 8 min, a cold light source with a fibre optic end of 4.5 mm diameter was placed 2.2 mm left lateral of the bregma onto the exposed skull for 15 min [20].

Low Oxygen Post Conditioning

Forty-eight hours after stroke induction (day 2), cages of animals were randomly allocated to the control (atmospheric oxygen) and LOPC groups (11% oxygen, 8 h/day) for 14 days (Figs. 1a and 2a), after which half of each group was euthanised for tissue collection. A customised hypoxic environment consisting of an independently ventilated cage system provided 11% oxygen, at atmospheric CO_2 concentration (300 ± 50 ppm) and atmospheric pressure (100 kPa). The remaining half of both groups was exposed to atmospheric air for further 14 days before the endpoint at day 30.

Assessment of Motor Deficit

Motor function was evaluated by cylinder test and foot fault test as described [18, 21]. We assessed the baseline for these tests 2 days before stroke induction (Figs. 1a and 2a). The

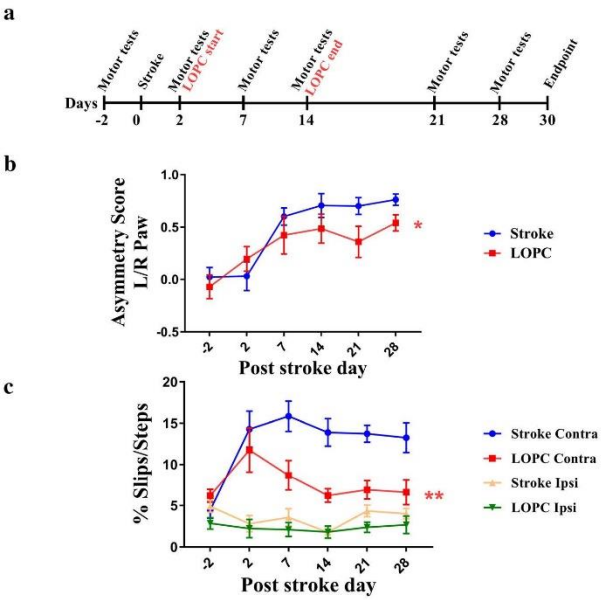

Fig. 1 LOPC prevents impaired motor function and tissue loss. **a** Experimental design for motor testing. Asymmetry score evaluated by cylinder test (**b**) and paw slips count in the grid walk test (**c**) show that mice that underwent LOPC significantly preserve their motor function. Ipsi, ipsilateral paw; Contra, contralateral paw. Results are shown as the mean ⊥ SEM. Results are shown as the mean ⊥ SD. $*p < 0.05$, $**p < 0.01$, two-way ANOVA

deficit was evaluated 2 days post stroke before the beginning of LOPC, during LOPC at days 7 and 14 and after the end of treatment at days 21 and 28. Control and LOPC groups underwent testing the same day and under the same conditions of light and noise.

Cylinder Test Two days before (day − 2) and days 2 (before the first LOPC session), 7, 14, 21 and 28 after stroke, each mouse was placed in a glass cylinder, and movements were recorded from both sides for 10 min. Afterwards, paw placement was determined by researcher blinded to the experimental condition. The first forelimb to contact the wall during a full rear determined one score for that side. The simultaneous contact of both the left and right forelimbs to the wall during a full rear was considered as one placement for both limbs. Up to 20 movements were scored, and mice below ten rears were excluded. A final asymmetry score was calculated as the ratio of non-impaired forelimb movement minus impaired forelimb movement to total forelimb movement. Total of $n = 16$ mice were used for this test.

Grid Walk This test determines sensorimotor function and motor coordination deficits during locomotion. Two days before (day − 2) and days 2 (before the first LOPC session), 7, 14, 21 and 28 after stroke, each mouse was placed on elevated grid of 2×2 cm^2. Healthy mice (− 2 days, before stroke) walk on the grid place paws precisely on the bars with a low percent of slips. After stroke, the mouse motor coordination of the contralateral paw is compromised while the ipsilateral paw is not affected. Each mouse was recorded for 5 min from below the grid and at an angle of − 20°, and a number of foot faults on each side, defined as limb crossing the grid, were calculated by a blinded researcher on a total of 50 steps after 30 s from the beginning of the test. Total of $n = 16$ mice were used for this test.

Tissue Processing

At the scheduled endpoint (day 15 or 30), mice were deeply anaesthetised with sodium pentabarbitol and perfused via the ascending aorta with ice cold PBS followed by ice cold 4% paraformaldehyde (pH 7.4) for immunohistochemical analysis or with cold PBS only for western blotting. For immunohistochemical analysis, the brains were dissected, post fixed in 4% paraformaldehyde (4 h) and transferred to sucrose 12.5% in PBS for storage for a maximum of 1 month. Coronal sections of the brains were sectioned at a thickness of 30 μm with a freezing microtome (Leica). For cohorts dedicated to western blot analysis, the brains were dissected and flash-frozen in − 80 °C isopentane. The frozen brains were sliced using the cryostat at a thickness of 200 μm. The tissue was then punched using 2-mm tissue punch in the peri-infarct region. Samples were stored frozen in − 80 °C until further analysis.

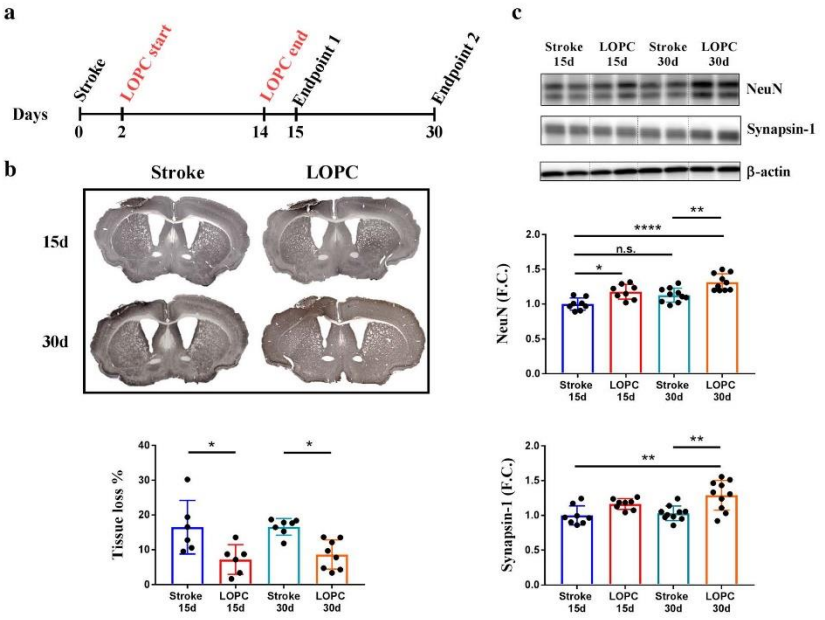

Fig. 2 LOPC is neuroprotective. **a** Experimental design of post condition and follow-up for histological and biochemical analysis. **b** NeuN staining at bregma 0. Evaluation of tissue loss as area (%) of the ipsilateral to the contralateral hemisphere shows decreased tissue loss in LOPC mice. **c** Representative blot shows increase of the neuronal marker NeuN and the presynaptic marker synapsin-1 after LOPC. Results are shown as the mean ± SD. $*p < 0.05$, $**p < 0.01$, $***p < 0.001$, $****p < 0.0001$, n.s., not significant. Two-way ANOVA and Turkey's multiple comparison test

Molecular Analysis by Western Blot and ELISA

Punched samples were sonicated in 150-µl lysis buffer (50-mM tris buffer pH 7.4, 1-mM EDTA, 1-mM DTT, 80-µM ammonium molybdate, 1-mM sodium pyrophosphate, 1-mM sodium vanadate, 5-mM β-glycerolphosphate, 1% SDS, 1 protease inhibitor cocktail tablet, 1 phosphatase inhibitor cocktail tablet, final concentration) and centrifuged for 20 min at 4 °C. Samples for ELISA were sonicated in 50-mM tris buffer pH 7.4, 150-mM NaCl and 1% Triton X-100 with protease inhibitor cocktail according to manufacturer instruction. Next, supernatants were collected and protein levels were estimated by Pierce BCA protein assay kit according to the manufacturer instructions. For western blot analysis, 15 µg of lysate was loaded per lane while 20 µg/well was used for ELISA (Fig. 3). After transferring and blocking, the membrane was incubated overnight with the appropriate antibody: CD11b (cat#ab75476, Abcam), CD45 (cat#ab208022, Abcam), CD68 (cat#ab76308, Abcam), NeuN (cat#MAB377, Millipore), BDNF (cat#SC-546, Santa-Cruz), Synapsin-1 (cat#5297, Cell Signalling) and β-actin (cat#A3854, Sigma-Aldrich). Analysis was performed with the Amersham Imager 600 analysis software.

Immunohistochemistry and Immunofluorescence

Free-floating sections were immunostained as described with minor modification [22]. All reactions for label markers were run at the same time, with the same reagents, at the same concentrations. Briefly, brain sections were incubated with 1-µg/ml pepsin in 0.01-M HCl for 2 min at 37 °C to retrieve antigen. Brain sections were then incubated with 1% hydrogen peroxidase for 30 min at RT followed by blocking with 3% horse serum for 30 min. Brain sections were incubated with primary antibodies: Iba1 (cat#019-19741, WAKO), NeuN (Millipore, cat#MAB377) and CD31 (cat#77699, Cell Signalling) for 72 h at 4 °C followed by appropriate secondary antibodies for 1 h at 25 °C. Next, brain sections were incubated for 2 h at 25 °C with avidin–biotin-peroxidase complex and finally developed using DAB peroxidase substrate. Brain sections were washed with PBS in between each incubation step. After the processing was complete, brain sections were mounted onto polylysine-coated slides and cover slipped. For lectin staining, after blocking as described above, brain sections were incubated in PBS-T with GFP labelled tomato-lectin (cat#L0401, Sigma) at 1:1000 for 2 h followed by repeated washings. Images were taken at × 20 with an Aperio

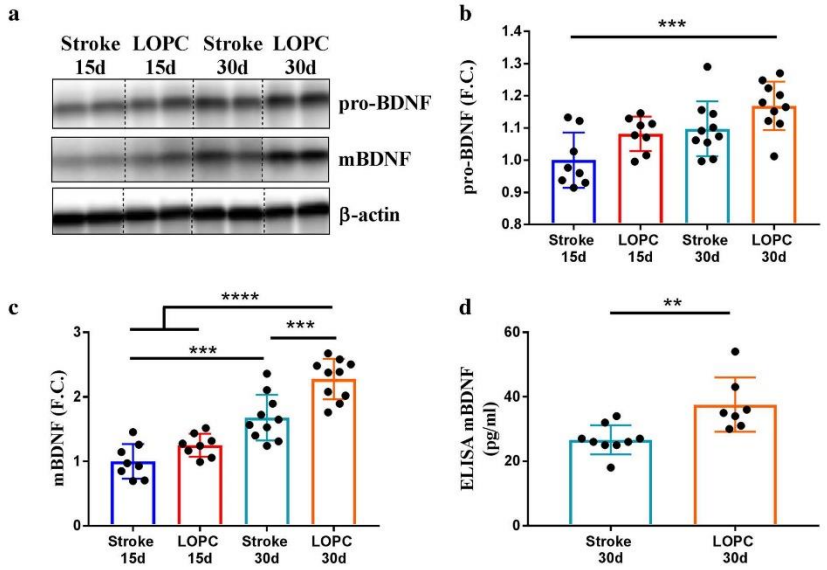

Fig. 3 LOPC increases proBDNF and mBDNF in the peri-infarct area. **a** Representative example of blot of proBDNF and BDNF at 15 and 30 days after LOPC. Quantification by western blot of proBDNF (**b**) and mBDNF (**c**). **d** Absolute quantification by ELISA of mBDNF. Results are shown as the mean ± SD. $^{**}p < 0.01$, $^{***}p < 0.001$, $^{****}p < 0.0001$. Two-way ANOVA, Turkey's multiple comparison test and Mann-Whitney test

AT2 (Leica), and fluorescent images were taken at confocal microscope (× 40). ImageJ software (1.50, NIH) or Matlab custom script (R2015a, MathWorks) was used to estimate tissue loss, area coverage of immunolabelling and microglia morphology [22]. Analysis of vessel density and microglia morphology was focused on the area near the edge of the injury, referred to as peri- infarct (Fig. 4a).

Biochemical Analysis

Protein homogenates from the peri-infarct samples were obtained as described [21, 23]. The peri-infarct supernatants were prepared for ELISA according to manufacturer instruction and measured for mBDNF using commercially available human/mouse/rat mature BDNF Rapid ELISA kit (cat#BEK-2211-1P, Biosensis). Western blotting was performed as described [21, 23].

Statistics

Data were analysed using the Prism for Windows Version 7 (GraphPad Software) with either Mann-Whitney test or two-way ANOVA followed by the Turkey multiple comparison post test. $P < 0.05$ was considered significant.

Results

Low Oxygen Post Conditioning Reduces the Severity of Motor Deficits

Mice ($n = 16$) were tested for motor deficits before (−2 days) and at 2, 7, 14, 21 and 28 days post stroke. Locomotor asymmetry was assessed using the cylinder test. Time had a significant effect on the development of the impairment (two-way ANOVA $F_{(5, 84)} = 12.26$, $p < 0.0001$). Overall, LOPC treatment significantly increased spontaneous use of the stroke-affected limb (Fig. 1b) (two-way ANOVA $F_{(1, 84)} = 5.172$, $p < 0.05$), showing that LOPC persistently improves post stroke function for at least 2 weeks after the end of the treatment. Motor impairment was also evaluated by the foot fault test. In this case, LOPC reduced motor function deterioration, and the effect was observed to persist for 2 weeks after the end of the treatment (Fig. 1c) (two-way ANOVA $F_{(1, 83)} = 9.456$, $p < 0.01$). As expected, the ipsilateral paw was not affected by either stroke or LOPC.

Low Oxygen Post Conditioning Decreases Ipsilateral Tissue Loss

The tissue loss was quantified as (contralateral hemisphere area − ipsilateral hemisphere area) / contralateral hemisphere

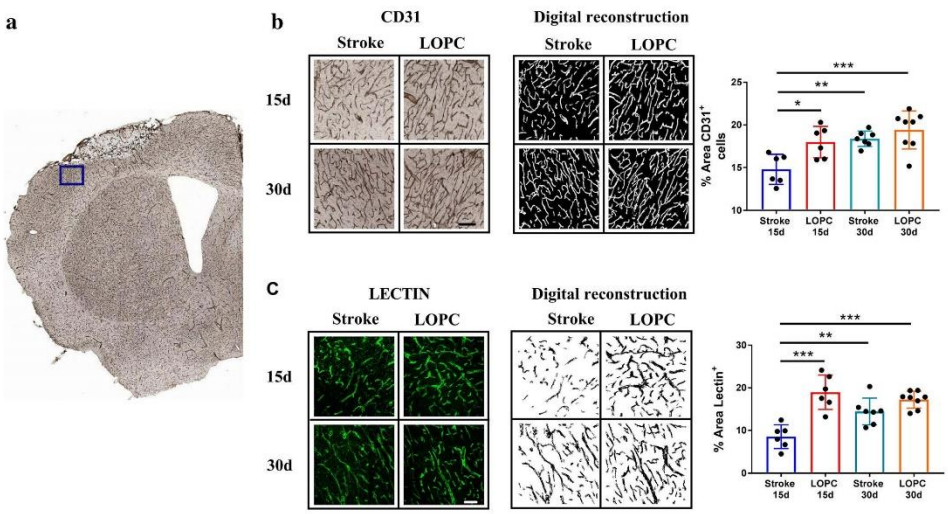

Fig. 4 LOPC increases vessel density in peri-infarct area. **a** Location of the peri-infarct region examined. Blood vessels were identified by immunolabelling targeting CD31 (scalebar = 100 μm) (**b**) or with fluorescent (GFP-conjugated) tomato-lectin (scalebar = 50 μm) (**c**). After digital reconstruction, the area covered by vessel was quantified as (%) of total area (right panels) showing a proangiogenetic effect of LOPC. Results are shown as the mean ± SD. $^{*}p < 0.05$, $^{**}p < 0.01$, $^{***}p < 0.001$. Two-way ANOVA and Turkey's multiple comparison test

area × 100 at bregma = 0, as per [24] in NeuN-stained sections at 15 ($n = 12$) and 30 ($n = 15$) days after stroke. Results expressed as fold change (FC). Analysis identified that LOPC prevents tissue loss at days 15 (Fig. 2b) (0.56 FC, $p < 0.05$) and 30 (0.47 FC, $p < 0.05$).

Low Oxygen Post Conditioning Prevents Neuronal Death Within the Peri-Infarct Area and Promotes Expression of Presynaptic Markers

To investigate the neuroprotective activity of LOPC, we evaluated the expression of the mature neuronal marker NeuN and the presynaptic protein synapsin-1 (Fig. 2c). Our analysis indicated that increased levels of NeuN in the LOPC groups were present at both 15 (1.17 FC, $p < 0.01$) and 30 (1.11 FC, $p < 0.01$) days, while the increase on synapsin-1 was significant at 30 days (1.26 FC, $p < 0.01$).

Increases Expression of Mature Brain-Derived Neurotrophic Factor

The improvement observed in the motor tests suggests that LOPC can have a neuroprotective effect. We decided to investigate this aspect by measuring the precursor and the mature form of BDNF, one of the most important neuroprotective and neurotropic factors. To investigate the effect of LOPC on BDNF expression, we considered the levels of proBDNF and mBDNF immediately after the treatment (15 days, $n = 16$) and 15 days later (i.e. day 30 of the study, $n = 19$) (Fig. 3a). Two-way ANOVA analysis revealed that for proBDNF (Fig. 3b), there was a main effect for time ($F_{(1,\ 32)} = 12.81$, $p < 0.005$) and LOPC ($F_{(1,\ 32)} = 8.864$, $p < 0.01$), with the LOPC group at 30 days showing a significant increase to the stroke group at 15 days (1.17 FC, $p < 0.0005$). Also for mBDNF (Fig. 3c), both time ($F_{(1,\ 32)} = 75.36$, $p < 0.0001$) and LOPC ($F_{(1,\ 32)} = 18.65$, $p = 0.0001$) were identified as significant. Multiple comparison analysis showed no difference among the groups at 15 days, while at 30 days, the increase in mBDNF was significant between groups (1.35 FC, $p < 0.0005$) and between time points (15 vs 30 days, stroke 1.67 FC, $p < 0.0005$; LOPC 1.82 FC, $p < 0.0001$). To validate this result, we used an ELISA kit specific for the mature form of BDNF with minimal cross reactivity with the precursor form to analyse homogenates from peri-infarct area in the cohorts that underwent the motor function test (30 days, $n = 16$). We confirmed that at 30 days, there is indeed a significant increase of mBDNF (Fig. 3d) in the LOPC group compared to the stroke group alone (1.36 FC, $p < 0.01$).

Low Oxygen Post Conditioning Increases Vessel Density in Peri-Infarct

Exposure to transiently reduced oxygen levels has been shown to have a proangiogenetic effect. To assess if our

LOPC protocol had a proangiogenetic effect, we analysed the changes in peri-infarct vessels with two independent approaches. First, we used immunohistochemistry targeting CD31 (Fig. 4b), a specific marker expressed on the membrane of endothelial cells. Second, we used immunofluorescent labelled tomato-lectin, which binds to carbohydrate components of the endothelial plasmalemma (Fig. 4c). In both cases, we observed a higher density of vessels at 15 days in the LOPC group (CD31 1.2 FC, $p < 0.05$, lectin 2.2 FC, $p < 0.005$) while at 30 days, it was similar between the groups.

Expression of Microglia Activation Markers Is Reduced After LOPC

We analysed the expression of microglial activation markers in the peri-infarct area (Fig. 5a). Our two-way ANOVA analysis revealed that both time and LOPC had a significant effect on CD11b levels (time $F_{(1, 32)} = 19.43$, $p < 0.001$; LOPC $F_{(1, 32)} = 4.835$, $p < 0.05$), CD45 (time $F_{(1, 32)} = 37.54$, $p < 0.0001$; LOPC $F_{(1, 32)} = 12.47$, $p < 0.001$) and CD68 (time $F_{(1, 32)} = 5.956$, $p < 0.05$; LOPC $F_{(1, 32)} = 10.64$, $p < 0.005$). In particular, LOPC induced a significant decrease in the expression of CD45 (0.8 FC, $p < 0.05$) at 15 days, while at 30 days, there is no difference among the groups. With our analysis of CD68, we identified a significant decrease following LOPC at 15 days (0.73 FC, $p < 0.05$). However, post hoc analysis did not show significant differences in the single time points for CD11b. We further consider microglial changes by examining the morphological reconfiguration, which is recognised to change under conditions of neuroinflammation (Fig. 5b, c). This analysis indicated that the number of primary branches in the LOPC group at 30 days was elevated relative to the stroke alone group both at

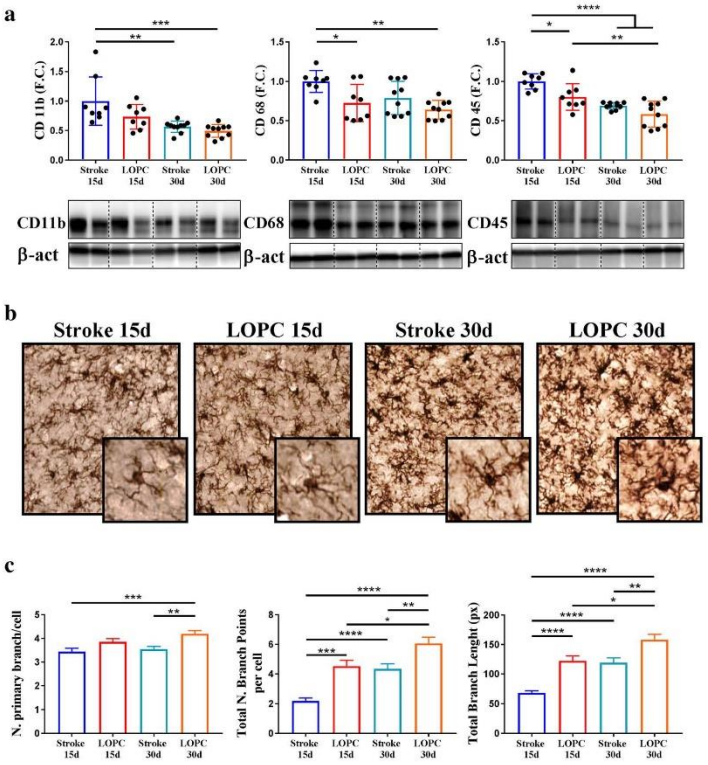

Fig. 5 LOPC decreases microglia activation in the peri-infarct area. **a** Quantification by western blot of activation markers CD11b, CD45 and CD68. **b** Representative images of Iba-1 immunostaining and high magnification detail (scalebar = 10 μm). **c** Parameters analysed to estimate microglia ramification. $*p < 0.05$, $**p < 0.01$, $***p < 0.001$, $****p < 0.0001$. Two-way ANOVA and Turkey's multiple comparison test

15 (1.22 FC, $p < 0.005$) and 30 days (1.18 FC, $p < 0.01$). The number of branch points was increased by LOPC at both 15 (2 FC, $p < 0.005$) and 30 days (1.39 FC, $p < 0.01$). Increased ramification was also noted to occur with time (15 vs 30 days, stroke 1.98 FC, $p < 0.001$; LOPC 1.33 FC, $p < 0.05$). The total branch length has a very similar pattern, being increased by LOPC (15 days 1.8FC, $p < 0.001$; 30 days 1.32 FC, $p < 0.01$) and with time (15 vs 30 days, stroke 1.75 FC, $p < 0.001$; LOPC 1.29 FC, $p < 0.05$). These morphological changes are consistent with microglia entering into a less inflamed phenotype.

Discussion

While LOPC has been shown to improve a number of deficits induced by stroke, the ability of the intervention to improve motor function had not, until now, been extensively investigated [10, 25]. As such, the primary aim or our study was to investigate whether LOPC could ameliorate motor impairment after stroke. Motor function was assessed using two different tests [18]; and in both tasks, we observed that mice exposed to LOPC demonstrated less severe motor deficits. To our knowledge, this is the first report to describe the ability LOPC to promote a sustained improvement in motor function after stroke in adult mice.

Specifically, in the current study, we utilised two separate tasks to consider the impact of LOPC on motor function, the cylinder task and the grid walk task. Both of the tasks were chosen because of the fact that they have been extensively used and validated in preclinical studies interested in considering motor impairments. The cylinder task considers the preference given to one forepaw over the other while stabilising the trunk during spontaneous rearing. Post stroke mice typically demonstrate a preference to bear weight on the paw that is ipsilateral to the brain injury (i.e. the paw not connected to the damaged hemisphere). We have previously reported that deficits following photo thrombotic occlusion directed to the motor cortex induce an asymmetry score of 0.5 after 2 weeks from stroke. Our data were completely consistent with these prior findings [21]; and at 7 days, the deficit is established. LOPC had a small but significant overall effect, ameliorating the preferential use of the non-affected limb. In terms of the animals' grid walk performance, we identified clear evidence of a stroke-induced increase in foot faults, as per our expectations. We further observed that LOPC was associated with a significant reduction in overall foot fault errors. Together, these results indicate that LOPC improves stroke-induced motor impairments, and the benefits persist for at least 2 weeks following the cessation of the intervention.

The positive effect of LOPC on motor function was directly supported by our examination of tissue loss from the peri-infarct territory. Specifically, we examined tissue loss using two separate and complementary approaches. Firstly, we used and examined the total area of tissue loss by measuring the hemispheric area (taking into consideration the negative area representative by the ventricular cavities). This analysis indicated that stroke produced a loss of approximately 15% of tissue from the infarcted hemisphere relative to the contralateral hemisphere, a finding consistent with prior work [21, 23]. We further identified that LOPC was associated with an improvement, exhibiting only an 8% loss of area. Interestingly, there were no identifiable differences in the amount of tissue loss in the LOPC group seen at day 15 and day 30; a result that suggests that most of the neuroprotective effect is attributable to benefits obtained during the primary treatment window. Secondly, we considered the abundance of NeuN and synapsin-1 using semi-quantitative western blotting. NeuN is marker for mature neurons, and syanpsin-1 is found with the membrane of synaptic vesicles. Our analysis indicated that LOPC increased NeuN levels at both 15 and 28 days post stroke and synapsin-1 levels at 30 days post stroke. These results in combination with the area measurements indicate that LOPC is robustly neuroprotective.

In terms of considering the mechanisms involved in mediating the neuroprotective effects conferred by LOPC, we considered several factors. An extensive literature has shown the importance of the neurotrophin brain-derived neurotrophic factor (BDNF) after stroke. Specifically, in preclinical studies, the intravenous delivery of BDNF has shown to improve the motor outcome after photothrombotic ischaemia [26], while blocking BDNF expression prevents improvement associated with rehabilitation [27]. Moreover, lower levels of circulating BDNF are associated with poorer long-term functional outcomes in patients after stroke [28]. BDNF is synthetised as a precursor (proBDNF) which is cleaved to generate mature BDNF (mBDNF). Using western blot, we investigated changes in both proBDNF and mBDNF. For both the precursor and the mature BDNF, we observed a trend to increase with time, which was enhanced by LOPC treatment. Only after the end of the treatment at 30 days did the LOPC group display a higher level mBDNF, whereas no effect on proBDNF was noted. To validate this result, we performed mBDNF absolute quantification by ELISA in samples at 30 days. Using this alternative approach, we confirmed that mBDNF was significantly increased in the LOPC group. BDNF delivery is a very promising treatment to promote motor function and neuroplasticity after stroke, but an efficient method of delivery in patients is yet to be found. Here, we show that LOPC can boost physiological expression of BDNF, circumventing problems associated with invasive delivery or blood brain barrier permeability. Future studies with a longer time horizon are needed to analyse how this increase translates in functional outcomes.

BDNF has been shown to be proangiogenetic, and in turn endothelial cells can secrete BDNF; therefore, these two factors are intertwined. Angiogenesis is considered to be central to promoting recovery [29]; and after stroke, both apoptosis and proliferation of capillary endothelial cells are observed, with a neuroprotective role of the latter [30]. In addition, LOPC has been shown to have a robust proangiogenetic effect in the brain [31]. Given these findings, we analysed vessel density in the peri-infarct area using the two different markers for endothelial cells that are commonly used to identify blood vessels, CD31 and lectin. Our results indicated that LOPC-treated animals exhibited greater vessel density at day 15 indicating that 2 weeks of LOPC strongly induces angiogenesis in the peri-infarct area. At day 30, the stroke group displays a higher vessel density than at 15 days, reflecting the endogenous activation of proangiogenetic signals after stroke. However, we did not observe significant difference at 30 days between the stroke and the LOPC group. The results show that 2 weeks of exposition to LOPC stimulates angiogenesis, and this stimulus fades after the end of treatment. The formation of new vessels provides oxygen and nutrients to the tissue and might have a supportive role for surviving neurons; thus, LOPC could exert its neuroprotective role by promoting neo-vascularisation. It will be the object of future studies whether prolonging the protocol of LOPC translates in a further enhancement of angiogenesis and neuroprotection.

The final mechanism that we explored, with a view to improving our understanding of the neuroprotective effects of LOPC, was neuroinflammation and especially microgliosis. Excessive microglial-mediated neuroinflammatory responses have been shown to be detrimental for the outcome after stroke, and approaches directed to specifically target inflammation have shown promising results in preclinical studies [32, 33] . In this study, we estimated neuroinflammatory status by assessing expression levels of microglia activation markers. We found that LOPC reduced the expression of CD68 and CD45 at 15 days post stroke, but no differences were observed in CD11b. We take this result to indicate that LOPC moderately dampens neuroinflammatory tone rather than suppressing it. As expected, the expression of these markers also decreased with time independently of the treatment, indicating the natural progression and resolution of neuroinflammation.

A second index often used to investigate changes in neuroinflammatory status is changes in microglial morphology and in particular changes in branching status (otherwise referred to as process ramification) [22, 34]. Several studies have now identified that ramified microglia is typically associated with neuroprotection [35]. Here, we show that LOPC induces an intriguing phenotype that to our knowledge has not been previously described. Specifically, we identify that stroke induces a typically activated morphology characterised by short ramifications with low complexity. Against this background, it appears that LOPC promotes ramification. Therefore, stroked mice treated with LOPC exhibit feature of activation and enhanced ramification. This effect was noted at both 15 and 30 days post stroke and was confirmed by analysis indicating that microglia post stroke and LOPC had longer processes with a greater number of branches. This result suggests that LOPC promotes microglia shift towards a less inflammatory state; however, further investigation of this unusual phenotype is required.

In conclusion, here, we describe for the first time the ability of LOPC to improve motor function post stroke. This observation is also robustly supported by a constellation of complementary mechanistic markers that collectively all point to the ability of LOPC in inducing a neuroprotective phenotype. Second, and an important finding from the current study is that LOPC not only produced positive effects during the delivery of the treatment but many persisted for 2 weeks following cessation. While this is only a modest window for persistence, it is certainly encouraging and it would be very worthwhile to further consider both how long the benefits last for as well as to consider how late the treatment could be started. Another promising angle has been suggested by several reports showing that exposure to low oxygen in hypobaric conditions can improve anxiety and depression-like symptoms in rats [36, 37]. We have previously shown that chronic stress inducing depression-like symptoms in mice is detrimental for their recovery after stroke. In particular, chronic stress promotes neuronal loss and reduction in vascular density in the peri-infarct area, accompanied by an exacerbation of motor impairment [23, 38]. Notably, in the current study, all these parameters were significantly improved by LOPC. Future studies are now needed to verify if LOPC can effectively prevent the deleterious effects associated with chronic stress after stroke, potentially adding translational value to LOPC treatment [39]. While our results are promising and support earlier promising results from other groups, further research should consider undertaking a full multi-organ safety audit as well as identifying the minimum length of exposure required to produce therapeutic effects. Despite the requirement for additional research, it is now important to recognise that LOPC is one of the first non-pharmacological interventions that can be deployed days after the initial stroke and still reduce tissue loss, promote neurogenesis, angiogenesis and cognitive and motor functions. Moreover, the technology to translate this intervention to the clinic already exists [13]. Therefore, we propose that LOPC appears to represent an excellent therapeutic intervention and should soon be considered for translation into early stage clinical research.

Authors' Contributions Experiments were designed by GP, MN and FRW and performed by GP, KZ and ZZ. Manuscript was written by GP and FRW and edited by GP, SJ, MN and FRW.

Funding This study was supported by the Hunter Medical Research Institute, Faculty of Health and Medicine Pilot Grant and The University of Newcastle, Australia.

Compliance with Ethical Standards

All experiments were conducted in accordance with the New South Wales Animals Research Act (1985) and the Australian Code of Practice for the use of animals for scientific purposes.

Conflict of Interest The authors declare that they have no conflicts of interest.

Ethical Approval All experiments were approved by the University of Newcastle Animal Care and Ethics Committee.

References

1. Brugniaux JV, Schmitt L, Robach P, Nicolet G, Fouillot JP, Moutereau S, et al. Eighteen days of "living high, training low" stimulate erythropoiesis and enhance aerobic performance in elite middle-distance runners. J Appl Physiol (1985). 2006;100(1):203–11.
2. Wehrlin JP, Zuest P, Hallén J, Marti B. Live high-train low for 24 days increases hemoglobin mass and red cell volume in elite endurance athletes. J Appl Physiol (1985). 2006;100(6):1938–45.
3. Rodriguez FA, et al. Performance of runners and swimmers after four weeks of intermittent hypobaric hypoxic exposure plus sea level training. J Appl Physiol (1985). 2007;103(5):1523–35.
4. Faiss R, Girard O, Millet GP. Advancing hypoxic training in team sports: from intermittent hypoxic training to repeated sprint training in hypoxia. Br J Sports Med. 2013;47(Suppl 1):i45–50.
5. Nakada Y, Canseco DC, Thet SW, Abdisalaam S, Asaithamby A, Santos CX, et al. Hypoxia induces heart regeneration in adult mice. Nature. 2017;541(7636):222–7.
6. Zhu LL, Zhao T, Li HS, Zhao H, Wu LY, Ding AS, et al. Neurogenesis in the adult rat brain after intermittent hypoxia. Brain Res. 2005;1055(1–2):1–6.
7. Tsai YW, Yang YR, Sun SH, Liang KC, Wang RY. Post ischemia intermittent hypoxia induces hippocampal neurogenesis and synaptic alterations and alleviates long-term memory impairment. J Cereb Blood Flow Metab. 2013;33(5):764–73.
8. Tsai YW, Yang YR, Wang PS, Wang RY. Intermittent hypoxia after transient focal ischemia induces hippocampal neurogenesis and c-Fos expression and reverses spatial memory deficits in rats. PLoS One. 2011;6(8):e24001.
9. Qiao Y, Liu Z, Yan X, Luo C. Effect of intermittent hypoxia on neuro-functional recovery post brain ischemia in mice. J Mol Neurosci. 2015;55(4):923–30.
10. Leconte C, Tixier E, Freret T, Toutain J, Saulnier R, Boulouard M, et al. Delayed hypoxic postconditioning protects against cerebral ischemia in the mouse. Stroke. 2009;40(10):3349–55.
11. Astorino TA, Harness ET, White AC. Efficacy of acute intermittent hypoxia on physical function and health status in humans with spinal cord injury: a brief review. Neural Plast. 2015;2015:409625.
12. Dale EA, Ben Mabrouk F, Mitchell GS. Unexpected benefits of intermittent hypoxia: enhanced respiratory and nonrespiratory motor function. Physiology (Bethesda). 2014;29(1):39–48.
13. Baillieul S, Chacaroun S, Doutreleau S, Detante O, Pépin JL, Verges S. Hypoxic conditioning and the central nervous system: a new therapeutic opportunity for brain and spinal cord injuries? Exp Biol Med (Maywood). 2017;242(11):1198–206.
14. Trumbower RD, Jayaraman A, Mitchell GS, Rymer WZ. Exposure to acute intermittent hypoxia augments somatic motor function in humans with incomplete spinal cord injury. Neurorehabil Neural Repair. 2012;26(2):163–72.
15. Hayes HB, Jayaraman A, Herrmann M, Mitchell GS, Rymer WZ, Trumbower RD. Daily intermittent hypoxia enhances walking after chronic spinal cord injury: a randomized trial. Neurology. 2014;82(2):104–13.
16. Navarrete-Opazo A, Alcayaga J, Sepúlveda O, Rojas E, Astudillo C. Repetitive intermittent hypoxia and locomotor training enhances walking function in incomplete spinal cord injury subjects: a randomized, triple-blind, placebo-controlled clinical trial. J Neurotrauma. 2017;34(9):1803–12.
17. Trumbower RD, Hayes HB, Mitchell GS, Wolf SL, Stahl VA. Effects of acute intermittent hypoxia on hand use after spinal cord trauma: a preliminary study. Neurology. 2017;89(18):1904–7.
18. Schaar KL, Brenneman MM, Savitz SI. Functional assessments in the rodent stroke model. Exp Transl Stroke Med. 2010;2(1):13.
19. Charan J, Kantharia ND. How to calculate sample size in animal studies? J Pharmacol Pharmacother. 2013;4(4):303–6.
20. Zalewska K, Pietrogrande G, Ong LK, Abdolhoseini M, Kluge M, Johnson SJ, et al. Sustained administration of corticosterone at stress-like levels after stroke suppressed glial reactivity at sites of thalamic secondary neurodegeneration. Brain Behav Immun. 2018;69:210–22.
21. Zalewska K, Ong LK, Johnson SJ, Nilsson M, Walker FR. Oral administration of corticosterone at stress-like levels drives microglial but not vascular disturbances post-stroke. Neuroscience. 2017;352:30–8.
22. Pietrogrande G, Mabotuwana N, Zhao Z, Abdolhoseini M, Johnson SJ, Nilsson M, et al. Chronic stress induced disturbances in Laminin: A significant contributor to modulating microglial pro-inflammatory tone? Brain Behav Immun. 2018;68:23–3.
23. Zhao Z, Ong LK, Johnson S, Nilsson M, Walker FR. Chronic stress induced disruption of the peri-infarct neurovascular unit following experimentally induced photothrombotic stroke. J Cereb Blood Flow Metab. 2017;37(12):3709–24.
24. Paxinos G, Franklin KBJ, editors. The mouse brain in stereotaxic coordinates. Compact. 2nd ed. Amsterdam: Elsevier Academic Press; 2004.
25. Joo SP, Xie W, Xiong X, Xu B, Zhao H. Ischemic postconditioning protects against focal cerebral ischemia by inhibiting brain inflammation while attenuating peripheral lymphopenia in mice. Neuroscience. 2013;243:149–57.
26. Schabitz WR, Steigleder T, Cooper-Kuhn CM, Schwab S, Sommer C, Schneider A, et al. Intravenous brain-derived neurotrophic factor enhances poststroke sensorimotor recovery and stimulates neurogenesis. Stroke. 2007;38(7):2165–72.
27. Ploughman M, Windle V, MacLellan CL, White N, Dore JJ, Corbett D. Brain-derived neurotrophic factor contributes to recovery of skilled reaching after focal ischemia in rats. Stroke. 2009;40(4):1490–5.
28. Stanne TM, et al. Low circulating acute brain-derived neurotrophic factor levels are associated with poor long-term functional outcome after ischemic stroke. Stroke. 2016;47(7):1943–5.
29. Ergul A, Alhusban A, Fagan SC. Angiogenesis: a harmonized target for recovery after stroke. Stroke. 2012;43(8):2270–4.
30. Li Y, Lu Z, Keogh CL, Yu SP, Wei L. Erythropoietin-induced neurovascular protection, angiogenesis, and cerebral blood flow restoration after focal ischemia in mice. J Cereb Blood Flow Metab. 2007;27(5):1043–54.

31. Harb R, Whiteus C, Freitas C, Grutzendler J. In vivo imaging of cerebral microvascular plasticity from birth to death. J Cereb Blood Flow Metab. 2013;33(1):146–56.
32. Zhang L, Zhang ZG, Zhang RL, Lu M, Krams M, Chopp M. Effects of a selective CD11b/CD18 antagonist and recombinant human tissue plasminogen activator treatment alone and in combination in a rat embolic model of stroke. Stroke. 2003;34(7):1790–5.
33. Prestigiacomo CJ, Kim SC, Connolly ES, Liao H, Yan SF, Pinsky DJ, et al. CD18-mediated neutrophil recruitment contributes to the pathogenesis of reperfused but not nonreperfused stroke. Stroke. 1999;30(5):1110–7.
34. Karperien A, Ahammer H, Jelinek HF. Quantitating the subtleties of microglial morphology with fractal analysis. Front Cell Neurosci. 2013;7:3.
35. Vinet J, et al. Neuroprotective function for ramified microglia in hippocampal excitotoxicity. J Neuroinflammation. 2012;9:27.
36. Zhu XH, Yan HC, Zhang J, Qu HD, Qiu XS, Chen L, et al. Intermittent hypoxia promotes hippocampal neurogenesis and produces antidepressant-like effects in adult rats. J Neurosci. 2010;30(38):12653–63.
37. Kushwah N, Jain V, Deep S, Prasad D, Singh SB, Khan N. Neuroprotective role of intermittent hypobaric hypoxia in unpredictable chronic mild stress induced depression in rats. PLoS One. 2016;11(2):e0149309.
38. Jones KA, Zouikr I, Patience M, Clarkson AN, Isgaard J, Johnson SJ, et al. Chronic stress exacerbates neuronal loss associated with secondary neurodegeneration and suppresses microglial-like cells following focal motor cortex ischemia in the mouse. Brain Behav Immun. 2015;48:57–67.
39. Walker FR, Jones KA, Patience MJ, Zhao Z, Nilsson M. Stress as necessary component of realistic recovery in animal models of experimental stroke. J Cereb Blood Flow Metab. 2014;34(2):208–14.

`

Discussion

The aim of this study was to explore the neuroprotective potential of low oxygen post conditioning (LOPC) as modulator of microglia activation after stroke in the peri-infarct area. The application of LOPC in the context of stroke is inspired by the numerous benefits that have been reported in athletes training at high altitude. LOPC has been suggested as a potential non-pharmacological therapeutic intervention for a number of pathologies; including cardiovascular diseases (177, 313), spinal cord injury (181, 185, 186), and ischemic stroke (198, 200, 201, 314, 315). Furthermore, it has been suggested that LOPC can induce decreased microglia activation after stroke, as indicated by diminished expression of the pro-inflammatory mediators iNOS (205), and IL-1β (207), and partial prevention of the shifting of microglia towards an amoeboid morphology observed in the early phase after hypoxic injury. However most of these studies focus on the outcome right after the end of treatment, while in a translational perspective it is pivotal to assess the effects of an intervention like LOPC also in the mid and long term. Thus, in the current study, I was interested to investigate whether our LOPC following stroke could improve outcome after stroke and if the positive effects were sustained over time.

In the experiments for this project included 2 different groups, stroke alone and stroke with LOPC, assessed at 2 timepoints, 15 and 30 days after stroke. The LOPC protocol consisted of 2 weeks of exposure to normobaric 11% oxygen for 8h/day starting 48 hours after stroke. I used this protocol since preliminary data showed that intermittent post conditioning had results similar to continuous exposure (Appendix 1) but in a translational view it has a higher value and is technically more feasible. It is important to consider that there is plenty of room to optimize this treatment, since protocols consisting

`

in shorter exposure, e.g. fewer hours per day or less days of treatment, might still retain therapeutic effects. However this kind of investigation was beyond the scope of this project, and considering the data available, I deemed more valuable for now to verify whether the effects were transient and explore the potential mechanisms of neuroprotection.

A first important aspect that I investigated, and that is sometimes neglected in pre-clinical studies, was to verify that the neuroprotection observed in our previous study was associated with a functional outcome. Our lab and others have previously verified using different tests that LOPC can ameliorate cognitive impairment after stroke. However, the effect of LOPC on motor function has not been object of investigations. The target of the photo-thrombotic ischemia that I induced was the motor sensory area of the cortex, therefore the motor functional outcome is particularly relevant. To evaluate motor function I choose two tests: the grid walk and the cylinder test. In the grid walk, each mouse is placed on an elevated grid of 2x2 cm squares and recorded for 5 minutes while exploring the surroundings. Healthy mice walk on the grid by placing their paws precisely on the grid. After stroke, the mouse motor-coordination of the affected paw is compromised causing the mouse to slip when walking with that limb. The opposite paw instead is not affected by the stroke and the frequency of slipping does not change after surgery. The number of foot faults, identified as a slip that causes the limb to cross the grid, was counted on a total of 50 steps. In the cylinder test the mouse is placed in a glass cylinder and recorder for 10 minutes. Afterward, paw placement was evaluated and the first forelimb to contact the wall during a full rear determined one score for that side. A final asymmetry score was calculated as the ratio of non-impaired forelimb movement minus impaired forelimb movement to total forelimb movements. Mice were tested before stroke, during the LOPC treatment and up to14 days after the end of LOPC. The

`

analysis of these two tests showed the effectiveness of LOPC to enhance motor performance following stroke and suggest an improvement long lasting after the end of the treatment.

To explore the potential underlying mechanisms contributing to the improved motor function following LOPC, I first examined tissue and neuronal loss in the peri-infarct regions. As predicted, stroke animals exposed to LOPC showed an overall improvement relative to the stroke only animals. Strikingly, the neuronal loss was constant between 15 and 30 days, showing that 15 days of LOPC was enough to partially prevent neuronal death on long term after the end of the treatment.

Furthermore, I observed that vessel growth was also increased by LOPC, a finding in line with our previous study (Appendix 1). Stroke itself triggers pro-angiogenic signals to promote repair over time, as shown by the increase in vessel density between 15 and 30 days in untreated mice. These findings show that LOPC can enhance the endogenous pro-angiogenetic signalling, resulting in increased vessel density at 15 days. At 30 days I could not observe a significant difference in vessel growth between LOPC and stroke alone, suggesting that the pro-angiogenetic stimulus of LOPC fades with the end of the treatment. A future direction will be to extend the LOPC exposure for a longer period, to confirm this observation and verify if prolonged pro-angiogenetic stimuli can also promote a better functional outcome.

Brain derived neurotrophic factor (BDNF) belongs to a family of neurotrophins that promotes neuronal proliferation, survival and differentiation (316). Treatment with BDNF in the acute phase after stroke reduces the infarct volume and neuronal loss (317), while a delayed delivery can improve motor recovery in rats (318, 319). BDNF is synthetised as a precursor (proBDNF) which undergoes N-terminal is cleavage to

`

generate mature BDNF (mBDNF). mBDNF is the biologically active form and is crucial for brain protection after ischemic injury (320). Prompter by the decrease of neuronal loss observed after LOPC, I investigated the expression of BDNF as a potential mediator of neuroprotection. Protein analysis showed that mice underwent LOPC significantly present higher levels of the mature form of BDNF at 30 days, while the increase at day 15 was not significant. Based on these results, I conclude that the neuroprotective activity of LOPC is unlikely to be mediated by BDNF. However, this is still a very promising result considering the importance of BDNF for stroke recovery, and shows that LOPC can induce beneficial effects after the end of the treatment. This particular finding has important limitations. Indeed the mechanism that triggers mBDNF increase is unclear. The increased BDNF that I observed by western blot analysis is likely to be caused by enhanced production, since the level of total BDNF is normalized to overall protein levels. However neurons are an important source of BDNF, so it is possible that this increase just reflects the higher number of surviving neurons after LOPC. This would imply that, in this model, the increase in BDNF is a consequence and not a cause of neuroprotection. Further studies are now needed to clarify the origin and the effects of mBDNF increase and elucidate the relationship with LOPC.

Modulation of inflammation is a particularly interesting therapeutic approach after stroke, and extensive literature describes the importance of inflammation in the development of brain damage after injury. As mentioned in the introduction, LOPC has the potential to attenuate the expression of proinflammatory markers after stroke. Building on these observations, I investigated the expression of microglia activation markers by western blot, and I found that the expression levels of CD68 and CD45 were decreased in the peri-infarct region of LOPC treated mice, suggesting decreased microglia activation. As expected, the expression of these markers also decreases with time, consistently with the

`

progression of inflammation resolution over time. These conclusions were also supported by the morphological analysis of microglia. At 15 days microglia in LOPC mice are extensively more branched, as pointed out by the significant increase in branch points and total branch length, and the degree of ramification increases with time. Altogether, these data suggest that LOPC can induce a decrease in microglia activation that progresses also after the end of the treatment. As discussed in the introduction, inflammation is a complex mechanism consisting in an acute phase, aimed in first instance to respond to harmful stimuli, and a second phase aimed to promote angiogenesis, regeneration and repair. Future studies are needed to specifically investigate whether LOPC can shift the balance from the harmful, acute phase in favour of the second, pro-regenerative phase, and doing so promote a globally neuroprotective environment.

In conclusion, the results from the current study are an important addition to literature investigating the modulation of microglia activation and LOPC treatment after stroke. LOPC has a significant effect on improving motor function and promotes many different mechanisms that can contribute to neuroprotection: tissue loss reduction, neurogenesis, angiogenesis, expression of neurotrophic factors, with concomitant promotion of cognitive and motor function. While the exact mechanisms need to be further investigated, this study helped to build a strong rationale supporting the validity of LOPC as a therapeutic intervention, mature for translational studies in patients.

`

CHAPTER 5

Low Oxygen Post Conditioning prevents thalamic secondary neuronal loss caused by excitotoxicity in a murine model of cortical stroke.

Introduction

Ischemic stroke is characterized by dramatic cell death and sustained inflammatory response at the lesion site. As explained above, the rapid activation of microglia in this region has a pivotal role for the biological response to injury. In addition to the damage surrounding the vascular occlusion, stroke triggers neuronal death and an associated inflammation also in regions distal from the primary damage but structurally connected to the infarct. This phenomenon is referred to as secondary neurodegeneration (SND) and develops in a timeframe of weeks to months after the insult, making this damage and its consequences an insidious problem difficult to evaluate. Recently, more attention has been dedicated to SND and an increasing number of studies suggest that the severity of SND has clinical relevance (230). The exact cause for this neuronal degeneration is not fully understood, thus in this study I investigated the potential involvement of the excitotoxic mechanism and its relationship with microglia activation.

Neuronal death following injury triggers anterograde and retrograde degeneration of neuronal axons, and may induce excitotoxicity and oxidative stress leading to further neuronal death in remote brain areas. Briefly, glutamate is the major excitatory neurotransmitter in mammalian CNS and its extracellular levels have been shown to be dramatically elevated after injuries like ischemia and TBI (321). Glutamate activates Ca^{2+} permeable ion channels like NMDARs to transmit post synaptic excitatory signals and, in homeostatic conditions, this process is important for neuronal communication and

`

learning. However, excessive release of glutamate and subsequent over-stimulation of targeted receptors triggers excessive influx of Ca^{2+} into cells in a process known as "excitotoxicity". The high concentration of intracellular free calcium activates a variety of enzymes, beginning a series of signalling cascades that ultimately lead to cell death. The alteration of Ca^{2+} homeostasis hereby described is considered to be one of the key mechanisms that cause secondary neurodegeneration following brain injury. As such, in this study I investigated the potential role of LOPC as a treatment to interfere with this excitotoxic process.

Another mechanism that is considered to be involved in the development of SND is inflammation. While the dynamics of immune cells activation in the peri-infarct area during the acute phase post-stroke are well characterized, much less is known about the role of the inflammatory process during SND. In rodents, microglial activation have been consistently reported in the thalamus across different models of stroke, and is usually identified by increased expression of activation markers (CD68, CD11b and MHCII) (272, 322). First signs of activation in the SND area can be observed around the third day after ischemia, and persist for at least 4 weeks. (251, 272, 323). Intriguingly, this intense microgliosis occurs in the same areas affected by neuronal loss. The close spatial and temporal correlation between microglial activation and neuronal loss strongly suggests a detrimental role of inflammation for the development of SND. Changes in microglial activation markers have been shown to precede neuronal death in the thalamus, thus supporting an active contribution of microglia to SND (236, 251). Studies using different approaches (drug compounds or knock-out models) to modulate the extent of SND often show effects for both neuronal loss and microglial activation (229, 324). However recent studies have shown that increased thalamic neuronal loss in chronically stressed mice was associated with dampening of microglia activation (272), suggesting a complicated

`

relationship between the SND and microglia activity. The second aim of this study was to investigate closely this relationship by using LOPC as intervention. In particular, by evaluating neuronal loss and inflammation at two different time points, I could observe their interconnection from a unique perspective.

`

Contributions

As co-authors of the paper: **Pietrogrande G**, Zalewska K, Zhao Z, Johnson SJ, Nilsson M, Walker FR *(2018).*

Low Oxygen Post Conditioning prevents thalamic secondary neuronal loss caused by excitotoxicity in a murine model of cortical stroke.

T be submitted Scientific reports, we confirm that **Giovanni Pietrogrande** has made the following contribution;

75% conception and design of research;

75% experimental procedures;

75% analysis and interpretation of the findings;

80% writing of the paper and critical appraisal of content

Katarzyna Zalewska		*27.03.2018*
Name of Co-author	*Signature*	*Date*
Zhao Zidan		*27.03.2018*
Name of Co-author	*Signature*	*Date*
Sarah J. Johnson		*27/03/2018*
Name of Co-author	*Signature*	*Date*
Michael Nilsson		*27/03/2018*
Name of Co-author	*Signature*	*Date*
Frederick Rohan Walker		*27/03/2018*
Name of Co-author	*Signature*	*Date*

`

PAPER 3

Title page

Low oxygen post conditioning prevents thalamic secondary neuronal loss caused by excitotoxicity after cortical stroke

Giovanni Pietrogrande [1, 2], Katarzyna Zalewska [1, 2], Zidan Zhao [1, 2], Mahmoud Abdolhoseini [3], Wei Zhen Chow [1, 2], Sonia Sanchez-Bezanilla [1, 2], Lin Kooi Ong [1, 2, 4], Sarah J Johnson [3], Michael Nilsson [2, 4, 5], Frederick R Walker [1, 2 ,4]

1 - School of Biomedical Sciences and Pharmacy and Priority Research Centre for Stroke and Brain Injury, University of Newcastle, Australia.

2 - Hunter Medical Research Institute, Australia.

3- School of Electrical Engineering and Computing, University of Newcastle, Australia.

4 - NHMRC Centre of Research Excellence Stroke Rehabilitation and Brain Recovery, Australia.

5 - Priority Research Centre for Stroke and Brain Injury, University of Newcastle, Australia.

Hunter Medical Research Institute, Australia.

Address correspondence: Frederick Rohan Walker, Hunter Medical Research Institute, Level 3 East Kookaburra Circuit, New Lambton Heights NSW 2305, Australia.

Email: rohan.walker@newcastle.edu.au

Abstract

In the current study, we were interested in investigating whether Low oxygen post-conditioning (LOPC) was capable of limiting the severity of stroke-induced secondary neurodegeneration (SND). To investigate the effect of LOPC we exposed adult male C57/BL6 mice to photothrombotic occlusion (PTO) of the motor and somatosensory cortex. This is known to induce progressive neurodegeneration in the thalamus within two weeks of infarction. Two days after PTO induction mice were randomly assigned to one of four groups: (i) LOPC-15 day exposure group; (ii) a LOPC 15 day exposure followed by a 15 day exposure to normal atmosphere; (iii) normal atmosphere for 15 days and (iv) normal atmosphere for 30 days (n = 20/group). We observed that LOPC reduced the extent of neuronal loss, as indicated by assessment of both area of loss and $NeuN^+$ cell counts, within the thalamus. Additionally, we identified that LOPC reduced microglial activity and decreased activity within the excitotoxic signalling pathway of the NMDAR axis. Together, these findings suggest that LOPC limits neuronal death caused by excitotoxicity in sites of secondary damage and promotes neuronal survival. In conclusion, this work supports the potential of utilising LOPC to intervene in the sub-acute phase post-stroke to restrict the severity of SND.

Introduction

Ischemic stroke is caused by the sudden interruption of the blood supply to the CNS. In most instances this interruption leads to neuronal loss and impaired brain function [1]. While the severity of the damage induced by stroke can be greatly reduced through hyper-acute interventions such as thrombolysis and thrombectomy, it is nearly always the case that patients are left with some degree of functional impairment. Currently, there are very few effective treatments available that are capable of reversing these persistent deficits. Adding to this challenge, research has identified secondary neurodegeneration (SND) as a related and significant problem with high clinical relevance [2]. SND is described as the progressive loss of neurons at sites that were connected to the infarct site but not directly impacted at the time of infarction.

While the processes driving SND are not yet well understood, it is clear that one of the mechanisms involves the spread of death through white matter tracts [3]. Currently, several experimental studies have demonstrated that a likely contributor to the spread of damage is glutamate mediated excitotoxicity [4,5]. While the process is relatively complex, its core is identified by the presence of excess glutamate that cannot be efficiently processed. The consequence of improper glutamate clearance can lead to the excessive stimulation of the ionotropic N-methyl-D-aspartate (NMDARs) receptors, massive influx of Ca^{2+} and unregulated intracellular signalling, which is known to ultimately cause cell death. One specific pathway of note in glutamate mediated excitotoxcity is the interaction of NMDARs with the scaffold postsynaptic density protein 95 (PSD-95). PSD-95 facilitates the coupling of NMDAR's with neuronal nitric oxide synthetise (nNOS), which in turn can result in the production of nitric oxide (NO), which contributes to the formation of peroxynitrite, a compound that can drive cell death by apoptosis or necrosis [6-8].

While inhibiting NMDAR activity has been of interest because of its potential to limit excitotoxicity, modulation has been difficult because of the central role that this receptor plays in normal CNS function [9]. To overcome this challenge, it has been demonstrated that suppressing PSD-95 binding to NMDAR acutely post-stroke can restrict excitotoxicity without markedly influencing NMDA activity [10], such effects, however have not been demonstrated over longer time frames.

Recently, our team has been exploring the therapeutic potential of low oxygen post conditioning (LOPC). As a therapy LOPC has several advantages including that it has a well-characterised and acceptable safety profile [11]. Moreover, LOPC has already been shown in experimental stroke models to reduce infarct size [12], promote neurogenesis and limit stroke induced deficits in motor [13,14] and memory impairment [15,16]. More pertinent to the context of SND, a recent study showed that exposure to 8% oxygen for 5 days post-stroke reduces thalamic atrophy in a model of MCAO [17].

In the current study, we aimed to examine if the neuroprotective actions LOPC could be underpinned by the interventions ability to modulate NMDA-PSD-95-nNOS signalling. To consider if LOPC modulated NMDAR mediated excitotoxicity we chose an experimental model of photothrombotic (PT) ischemia targeting the motor-cortex. We considered this model the most suitable as it induces a highly focal infarct region and as such degenerative effects occurring at distance are only driven by SND related processes [18]. 48h after stroke we began the LOPC protocol, which involved exposing male mice to normobaric 11% oxygen for 8 hours/day for 14 days (Fig.1). Our previous studies have

shown that SND become apparent in the thalamus after 14 days from stroke, specifically in the thalamic regions posterior complex (PO) and ventral posterolateral nucleus (VPL) which are connected to the motor-sensory cortical area. Therefore we focused our intervention within this time window and we investigated whether LOPC treatment disturbed NMDAR mediated excitotoxicity. As SND is a dynamic process, we also extended our observations to include an additional time point at 30 days post stroke. The aim of including this latter time point was to verify how SND and associated microgliosis evolved over time and if LOPC effects were maintained.

Results

LOPC prevents thalamic neuronal death

In order to investigate the neuroprotective activity of LOPC, we estimated the number of neurons by counting NeuN+ cells in thalamic posterior (PO) and ventral posterolateral nuclei (VPL) (Fig 2a). We also evaluated neuronal loss in the PO also by measuring the area of NeuN+ cell loss (Fig 2b). The area of SND in VPL could not be evaluated since the neuronal loss wasn't as evident as in the PO. Data show that LOPC group at 30 days have significantly more $NeuN^+$ cells in thalamus ($p<0.01$) and inside the regions VPL ($p<0.01$) and PO ($p<0.05$), and that the area of PO affected by SND was smaller after LOPC both at 15 and 30 days ($p<0.05$ and $p<0.01$ respectively).

Thalamic inflammation is resolved at 1 month after LOPC

Regions of secondary damage are associated with extensive microgliosis. Therefore we evaluated microglia activation in the thalamus by investigating changes in the immunohistochemical expression of Iba1 (Fig 3a) as well as CD68 (Fig 3b). We further cross-validated these findings using western blot quantification of another marker of microglial 'activation', CD11b (Fig 4). Analysing the thalamic area we observed extensive microgliosis at 15 days post stroke in both stroke and LOPC groups, while at 30 days microglia activation was significantly decreased in LOPC treated (Iba1 $p<0.01$, CD68 $p<0.01$, CD11b $p<0.05$). 2-way ANOVA analysis of the % of thresholded material showed that Iba1 (at pixel intensity 50) and CD68 (pixel intensity 100) decrease in the VPL area, with significant contribution from both time (Iba1 $p<0.0001$, CD68 $p<0.001$) and LOPC ($p<0.05$ both Iba1 and CD68) (Supp Fig 1 and 2). Instead in the PO area, only LOPC treatment was found giving a significant contribution ($p<0.05$), with a significant difference between stroke and LOPC at 30 days for both Iba1 and CD68 ($p<0.05$) as assessed by post-hoc analysis.

Thalamic calcium accumulation is not affected by LOPC

Calcium induced excitotoxicity has been proposed as potential cause of thalamic SND, therefore we evaluated by Alizarin red S staining the accumulation of calcium in the thalamus after 15 days post stroke [19]. We could not find any difference in the calcium accumulation between stroke and LOPC at 15 days (see, Fig 5a).

Decreased NMDAR/PSD-95 interaction after LOPC treatment

We analysed in the thalamus the expression levels of the components of the complex NMDAR/PSD-95/nNOS that can mediate calcium excitotoxicity. In particular NMDAR is composed by one NR1 and 2 NR2 (N2A and/or N2B) subunits, being N2B the subunit interacting with PSD-95. We could not find any statistical evidence to support the notion that LOPC altered the expression of NR1, N2B or nNOS (Fig 5a). We did, however, identify that LOPC induced a significant decrease in PSD-95 expression ($p<0.01$) (Fig 5b). To verify if there was a disturbance in synapse formation we also quantified the expression of Synapsin1 but we couldn't find any statistical evidence to support a LOPC mediated change, suggesting that the decrease in PSD-95 was specific. Next we determined whether decreased PSD-95 expression involved decreased PSD-95/NMDAR interaction as determined via co-immunoprecipitation of PSD-95 with N2B subunit. PSD-95 was successfully pulled down, as we verified by using a different PSD-95 antibody to probe the membrane, and co-immunoprecipitated specifically with N2B (Fig 4c, left panel). We ruled out that the signal could be

due to non specific binding to the beads since β-actin was neither detectable in CO-IP samples nor in samples of beads not antibody-coated incubated with same amount of lysates (-Ab lane, Fig 5c right panel). As further control antibody-coated beads not incubated with lysates did not give any PSD-95, N2B or β-actin signal (-Lysate, Fig 4c). The results showed a decreased co-immunoprecipitation of PSD-95 with N2B in LOPC samples ($p<0.05$). This experiment was replicated with similar results.

LOPC ameliorates white matter disturbances

Since SND is a disconnection injury we evaluated white matter tract alterations using Sudan Black staining of myelin. We found a significant decrease in white matter structural loss in corpus callosum at Bregma -1.5, as a difference between the contralateral (CL) and ipsilateral (IL) hemispheric area (mm^2), at 15 days post stroke in LOPC mice ($p<0.05$). The LOPC protective effects of white matter disturbances were sustained at 30 days post-stroke ($p<0.05$) (Supp Fig 4).

Discussion

The specificity and precision of occlusion that can be induced via use of photothrombosis, makes it an ideal model to study secondary neurodegeneration. Our group and others have used this model extensively to study the progression of secondary neurodegeneration in the thalamus. The thalamus is recognised to be mono-synaptically connected to the motor and somatosensory corticies but is not directly affected by the primary occlusion [20-22]. In the current study we were interested in exploring a specific question, to what extent could low oxygen post-conditioning (LOPC) influence the severity of thalamic degeneration, and in particular whether it could modulate the excitotoxic processes within the degenerating thalamus. In short, we observed a striking ability of LOPC to induce robust neuroprotection within the thalamus in terms of mature neurons cell count. Importantly, we also have observed, for the first time, that LOPC reduced the interaction of PSD-95 with the N2B subunit of NMDAR, a key interaction in eleciting excitotoxic cell death. These results provide novel evidence that one of the potential mechanisms underlying LOPC neuroprotection may be reduction in exitotoxicity mediated by the NMDAR-PSD-95-nNOS pathway.

To quantify the extent of neuroprotection offered by LOPC we used two different but complementary measurements to estimate the extent of secondary thalamic tissue loss: the area of thalamic injury that is affected by SND and the degree of neuronal loss in that area. Both these methods have previously been used to identify thalamic neuronal death [20,23-25]. When considering the area of loss we observed that the SND area in the thalamus did not significantly change over time between 15 and 30 days. This suggests that in our model the event defining the perimeter of SND has largely developed within 15 days after stroke, an observation that was mirrored in the LOPC group. Our $NeuN^+$ cell count results, however, suggested that loss of cells within this perimeter continued to increasing over time between 15 and 30 days ($NeuN^+$ cell count, PO 183.5 vs 69.5, VPN 136.6 vs 95.5), an observation that also aligns with [26]. Based on these results and other studies [27], we conclude that $NeuN^+$ cell counts represent a more sensitive indicator of SND than area measurement, and deduce that the SND takes some time to fully manifest in the model of ischemic injury. The progressive nature of the cell death could be driven by a number of mechanisms but is most likely caused by the spreading of death by apoptosis over time [28] which is consistent with an excitotoxic mechanism [29,30]. Of note, in the LOPC group we did not observe further neuronal death after 15 days. This result suggests that 2 weeks of LOPC was sufficient to constrain those processes that contribute to neuronal loss and appear to significantly slow its progression. Further, the results from Sudan Black staining suggest that LOPC provides protective effects on white matter structural loss.

Microgliosis, in conjunction with selective neuronal loss, is recognised to be another characteristic feature of SND [31]. Our results show that SND was associated with a considerable change in microglial morphology (Fig 3a) as well as enhanced expression of CD68, a putative marker of phagocytosis (Fig 3b) and CD11b a putative marker of complement recognition (Fig 4) at day 15 post stroke. These changes are highly consistent with a phenotype observed in microglia that are responding to injury and damage within the CNS [32] and were confirmed by analysis of the immunolabelling intensity (Supp Fig 1 and 2). LOPC was observed to significantly reduce microglial 'activation' on day 30 (15 days after the end of LOPC treatment) but not earlier. We find this observation particularly interesting when taken in conjunction with our neuronal loss findings. As the benefit of LOPC on neuronal loss was already evident by day 15 and as there was no measurable

LOPC effect on microglia until 30 days, it would suggest that the benefits of LOPC are not primarily attributable to modulation of microglial activity.

Since we observed a direct effect on LOPC at 15 days on thalamic cell loss we next evaluated the involvement of LOPC on excitotoxicity at this time point. We first confirmed an accumulation of calcium within the ipsilateral thalamus (Fig 5a), effectively establishing the possibility that calcium-dependent excitotoxicity was occurring within this region. We could not identify any differences between stroke alone and LOPC treated animals in calcium build up. We next considered the expression levels within the thalamus of the main elements involved in the excitotoxic axis: NMDAR, PSD-95 and nNOS. Here we identified a significant and specific decrease of 30% in PSD-95 expression after LOPC compared to stroke alone at 15 days (Fig 5b). We considered the reduction in PSD-95 to be specific and not likely due to altered plasticity, since the level of Synapsin-1 was not altered. This decrease suggested a potential alteration of the excitotoxic signalling initiated by NMDAR, as the crucial event for this signalling cascade is the binding of PSD-95 to NMDAR. Therefore, we next investigated by co-immunoprecipitation (CO-IP) the levels of interaction between the PSD-95 and the NMDAR subunit N2B [33]. The results showed that in tissue obtained from the ipsilateral thalamus of mice exposed to LOPC there was a lower level N2B being pulled down with PSD-95 (50% decrease, Fig 5c). As we could find no evidence of non-specific proteins such as β-actin on the pull down, we are inclined to conclude that LOPC reduces also NMDAR and PSD-95 interaction, a finding that is consistent with the ability of LOPC to dampen the severity of excitotoxicity.

While we have found that the neuroprotective effect of LOPC may be mediated via an effect of excitotoxicity it is important to recognise that the LOPC may effect neuroprotection via numerous mechanisms. For instance it has been shown that LOPC promotes post-translational modification of neuroprotective heat shock protein [34], inactivation of the ERK pathway [35] and promotion of VEGF signalling [36]. Although previous work has already suggested that exposure to low oxygen environments may dampen NMDAR mediated activation of nNOS [37], to our knowledge this is the first report proposing to exploit LOPC to interfere with the excitotoxic signalling leading to SND, by decreasing PSD-95 expression [10] and the interaction between NMDAR and PSD-95. While LOPC has been shown to be safe in humans [11], more studies are needed to identify potential unwanted effects of this treatment after stroke.

In conclusion we have shown that LOPC can prevent stroke-associated secondary neuronal loss within the thalamus by interfering with the excitotoxic process mediated by the NMDAR/PSD-95 interaction. However, further studies are required to dissect the mechanism by which the excitotoxic signal originating from the primary injury can induce SND and define its contribution to distal neuronal death. In this study, we focused on the sub-acute phase, commencing low oxygen exposure 48 hours after stroke, when the primary damage is mostly developed. Considering that in the mouse the peak of SND occurs at one month after ischemia, it was vital to begin the treatment within this time window. The time scale for humans is quite different, since distal neuronal death and microglia activation lasts for months after stroke [38,39]. In a translational perspective, the efficacy of LOPC at later time still needs to be validated. In addition to duration of effect further consideration needs to be given to issues including the optimal oxygen concentration [40], atmospheric pressure [41], dosage [42] as well as consider the interaction of the treatment with common comorbidities [43,44]. At this stage,

however, LOPC is a promising treatment with theoretically few side effects and an excellent candidate for translational approaches.

Materials and Methods

Procedures: Animals were obtained from the Animal Services Unit at the University of Newcastle. Experiments were approved by the University of Newcastle Animal Care and Ethics Committee and conducted in accordance with the New South Wales Animals Research Act and the Australian Code of Practice for the use of animals for scientific purposes.

Stroke: On day 0 mice were anesthetised by using 2% of isoflurane followed by intraperitoneal injection of 0.2 ml rose Bengal at10 mg/ml concentration. After eight minutes a cold light source with a fibre optic end of 4.5 mm diameter was placed at 2.2 mm left lateral to Bregma onto the exposed skull for 15 minutes (Fig 1) [20]. Mice were excluded if negative for stroke by histological evaluation at the relative endpoint. The sample size was estimated based on previous experiments (data not shown).

LOPC: 48 hours after stroke induction (day 0), a total of 80 mice were randomly allocated to control (atmospheric oxygen) or LOPC group. LOPC was delivered using a customized hypoxic environment IVC rack provided 11% oxygen for 8 h/day, at atmospheric CO_2 concentration (300 ±50 ppm) and atmospheric pressure (100kPa).Following 14 days half of each group was euthanized for tissue collection (n. 6-10 depending on experiment). The remaining half of both groups was continuously exposed to atmospheric air for further 14 days before the endpoint (day 30).

Tissue processing: At the scheduled endpoint (day 15 or 30) mice were deeply anaesthetised with sodium pentabarbitol and perfused via the ascending aorta with ice cold PBS followed by ice cold 4% paraformaldehyde (pH 7.4) for immunohistochemical analysis or with cold PBS only for western blotting. For immune-histochemical analysis, brains were dissected, post-fixed in 4% paraformaldehyde for 4 h and transferred to 12.5% sucrose in PBS for storage for a maximum of 1 month. Coronal sections of the brains were sectioned with a freezing microtome (Leica) at a thickness of 30 µm. For cohorts dedicated to western blot analysis, brains were dissected and flash-frozen in -80°C isopentane. Frozen brains were sliced using the cryostat at a thickness of 200 µm. Tissue was then punched using 2mm tissue punch in the thalamus region (Bregma -1.2 to -2.2). Samples were stored frozen in -80 °C until further analysis.

Western blot: Thalamic samples were sonicated in 150 µl lysis buffer (50 mM TRIS buffer pH 7.4, 1 mM EDTA, 1 mM DTT, 80 µM ammonium molybdate, 1 mM sodium pyrophosphate, 1 mM sodium vanadate, 5 mM b-glycerolphosphate, 1 protease inhibitor cocktail tablet, 1 phosphatase inhibitor cocktail tablet, final concentration) and centrifuged for 20 min at 4°C. Next, supernatants were collected and protein levels were estimated by Pierce BCA protein assay kit according to the manufacturer's instructions. 15µg of lysate were loaded per lane. After transfer and blocking, the membranes were probed with the appropriate antibody: CD11b (Cat#ab75476, Abcam), N2B (Cat#14544, Cell Signalling), NeuN (Cat#MAB377, Millipore), nNOS (Cat#4236, Cell Signalling), NR1(Cat#5704, Cell Signalling), PSD-95 (Cat#3409, Cell Signalling), Synapsin 1 (Cat#5297, Cell Signalling), β-actin (Cat#A3854, Sigma-Aldrich). Analysis was performed with the Amersham Imager 600 Analysis Software.

Immunohistochemistry: Free-floating sections were immunostained as described with minor modification. All reactions for labels marker were run at the same time, with same reagents, at the

same concentrations. Briefly, brain sections were incubated with 1% hydrogen peroxidase for 30 min at 25°C and followed by 3% horse serum for 30 min at 25°C. Incubation with primary antibodies was performed for 72 h at 4°C followed by incubation with the proper secondary antibody for 1 h at 25°C. Next, brain sections were incubated for 2 h at 25°C with avidin–biotin-peroxidase complex and finally developed using DAB peroxidase substrate. Brain sections were washed with PBS in between each incubation step. After processing was complete, sections were mounted onto polylysine coated slides and cover slipped. For calcium staining, brain sections were mounted on polylysine coated slides and incubated in 2% Azalin Red S (Sigma) in distilled water (pH 4.1) for 30 seconds [19], dehydrated and cover slipped. Sudan Black B (Sigma-Aldrich, USA) protocol was performed as previously described [45]. Briefly, sections were mounted and rinsed with 70% ethanol followed by 15 min incubation with Sudan Black B solution. After staining sections were rinsed with 70% ethanol and water and 5 min counterstained with nuclear fast red solution (Sigma-Aldrich, USA). Images were taken at 20X with an Aperio AT2 (Leica). ImageJ software (1.50, NIH) or Matlab custom script (R2015a, MathWorks) were used to measure $NeuN^+$ cell number and area coverage of immunolabelling by cumulative tresholding [46].The estimated corpus callosum loss area was determined using ImageJ software [area of contralateral hemisphere - area of ipsilateral hemisphere].

Co-IP: n=16 mice underwent stroke procedure and after 48 hours were randomly allocated to atmospheric oxygen or LOPC for 14 days. One mouse was excluded since negative for stroke by histological evaluation. The tissue was collected as for the western blot procedure. The thalamic area was punched and tissue was gently homogenised with a pestle in 50 mM tris, 150 mM NaCl and 1% Triton-X 100 with protease inhibitor cocktail (Roche). Protein concentration was quantified by Pierce BSA assay. Beads from Dynabeads™ Protein A Immunoprecipitation Kit (Invitrogen) were washed 3x in PBS-T 0.05% and incubated with PSD-95 antibody (Cat#2507, Cell Signalling) at 1:50 concentration in a volume of 800ul for 3 hours in rotation at RT. After 2 washes in PBS-T, beads were resuspended in Lysis buffer and an equivalent amount of 50ul of starting beads was added to 75 ug of proteins in a final volume of 400ul and incubated by rotation O.N. at 4°C. The following day beads were washed 2 times in Lysis buffer changing the tube, spinned down, resuspended in 15 ul of Laemmli buffer and boiled for 10 minutes. Finally the samples were centrifuged 4000g for 3 minutes to pellet the beads and loaded. Blot was hybridised with antibodies for PSD-95 (Cat#3409, Cell Signalling), N2B (Cat #14544 Cell Signalling) and β-Actin. Beads coated with the N2B antibody successfully pulled down the target protein but failed to coimmunoprecipitate PSD-95 (not shown).

Statistics: Data were analysed with either Mann-Whitney U test or 2-way ANOVA followed by Tukey's multiple comparison post-test using Prism 7 (GraphPad). $P<0.05$ was considered significant.

`

References

1 Howard, G. & Goff, D. C. Population shifts and the future of stroke: forecasts of the future burden of stroke. *Ann N Y Acad Sci* **1268**, 14-20, doi:10.1111/j.1749-6632.2012.06665.x (2012).

2 Zhang, J., Zhang, Y., Xing, S., Liang, Z. & Zeng, J. Secondary neurodegeneration in remote regions after focal cerebral infarction: a new target for stroke management? *Stroke* **43**, 1700-1705, doi:10.1161/strokeaha.111.632448 (2012).

3 Weishaupt, N., Zhang, A., Deziel, R. A., Tasker, R. A. & Whitehead, S. N. Prefrontal Ischemia in the Rat Leads to Secondary Damage and Inflammation in Remote Gray and White Matter Regions. *Frontiers in neuroscience* **10**, 81, doi:10.3389/fnins.2016.00081 (2016).

4 Ross, D. T. & Ebner, F. F. Thalamic retrograde degeneration following cortical injury: an excitotoxic process? *Neuroscience* **35**, 525-550 (1990).

5 Lai, T. W., Zhang, S. & Wang, Y. T. Excitotoxicity and stroke: identifying novel targets for neuroprotection. *Prog Neurobiol* **115**, 157-188, doi:10.1016/j.pneurobio.2013.11.006 (2014).

6 Liu, P. K., Robertson, C. S. & Valadka, A. The association between neuronal nitric oxide synthase and neuronal sensitivity in the brain after brain injury. *Ann N Y Acad Sci* **962**, 226-241 (2002).

7 Eliasson, M. J. *et al.* Neuronal nitric oxide synthase activation and peroxynitrite formation in ischemic stroke linked to neural damage. *J Neurosci* **19**, 5910-5918 (1999).

8 Bonfoco, E., Krainc, D., Ankarcrona, M., Nicotera, P. & Lipton, S. A. Apoptosis and necrosis: two distinct events induced, respectively, by mild and intense insults with N-methyl-D-aspartate or nitric oxide/superoxide in cortical cell cultures. *Proc Natl Acad Sci U S A* **92**, 7162-7166 (1995).

9 Ikonomidou, C. & Turski, L. Why did NMDA receptor antagonists fail clinical trials for stroke and traumatic brain injury? *Lancet Neurol* **1**, 383-386 (2002).

10 Sattler, R. *et al.* Specific coupling of NMDA receptor activation to nitric oxide neurotoxicity by PSD-95 protein. *Science* **284**, 1845-1848 (1999).

11 Baillieul, S. *et al.* Hypoxic conditioning and the central nervous system: A new therapeutic opportunity for brain and spinal cord injuries? *Exp Biol Med (Maywood)* **242**, 1198-1206, doi:10.1177/1535370217712691 (2017).

12 Joo, S. P., Xie, W., Xiong, X., Xu, B. & Zhao, H. Ischemic postconditioning protects against focal cerebral ischemia by inhibiting brain inflammation while attenuating peripheral lymphopenia in mice. *Neuroscience* **243**, 149-157, doi:10.1016/j.neuroscience.2013.03.062 (2013).

13 Nguyen, H. L., Ruhoff, A. M., Fath, T. & Jones, N. M. Hypoxic postconditioning enhances functional recovery following endothelin-1 induced middle cerebral artery occlusion in conscious rats. *Exp Neurol* **306**, 177-189, doi:10.1016/j.expneurol.2018.05.018 (2018).

14 Pietrogrande, G. *et al.* Low Oxygen Post Conditioning as an Efficient Non-pharmacological Strategy to Promote Motor Function After Stroke. *Translational stroke research*, doi:10.1007/s12975-018-0656-5 (2018).

15 Tsai, Y. W., Yang, Y. R., Sun, S. H., Liang, K. C. & Wang, R. Y. Post ischemia intermittent hypoxia induces hippocampal neurogenesis and synaptic alterations and alleviates long-term memory impairment. *J Cereb Blood Flow Metab* **33**, 764-773, doi:10.1038/jcbfm.2013.15 (2013).

16 Tsai, Y. W., Yang, Y. R., Wang, P. S. & Wang, R. Y. Intermittent hypoxia after transient focal ischemia induces hippocampal neurogenesis and c-Fos expression and reverses spatial memory deficits in rats. *PLoS One* **6**, e24001, doi:10.1371/journal.pone.0024001 (2011).

17 Leconte, C. *et al.* Delayed hypoxic postconditioning protects against cerebral ischemia in the mouse. *Stroke* **40**, 3349-3355, doi:10.1161/STROKEAHA.109.557314 (2009).

18 Dihne, M., Grommes, C., Lutzenburg, M., Witte, O. W. & Block, F. Different mechanisms of secondary neuronal damage in thalamic nuclei after focal cerebral ischemia in rats. *Stroke* **33**, 3006-3011 (2002).

19 Makinen, S. *et al.* Coaccumulation of calcium and beta-amyloid in the thalamus after transient middle cerebral artery occlusion in rats. *J Cereb Blood Flow Metab* **28**, 263-268, doi:10.1038/sj.jcbfm.9600529 (2008).

20 Zalewska, K. *et al.* Sustained administration of corticosterone at stress-like levels after stroke suppressed glial reactivity at sites of thalamic secondary neurodegeneration. *Brain, behavior, and immunity* **69**, 210-222, doi:10.1016/j.bbi.2017.11.014 (2018).

21 Kluge, M. G. *et al.* Impaired microglia process dynamics post-stroke are specific to sites of secondary neurodegeneration. *Glia* **65**, 1885-1899, doi:10.1002/glia.23201 (2017).

22 Ong, L. K., Zhao, Z., Kluge, M., Walker, F. R. & Nilsson, M. Chronic stress exposure following photothrombotic stroke is associated with increased levels of Amyloid beta accumulation and altered oligomerisation at sites of thalamic secondary neurodegeneration in mice. *J Cereb Blood Flow Metab*, doi:10.1177/0271678X16654920 (2016).

23 Weishaupt, N., Riccio, P., Dobbs, T., Hachinski, V. C. & Whitehead, S. N. Characterization of Behaviour and Remote Degeneration Following Thalamic Stroke in the Rat. *Int J Mol Sci* **16**, 13921-13936, doi:10.3390/ijms160613921 (2015).

24 Jones, K. A. *et al.* Chronic stress exacerbates neuronal loss associated with secondary neurodegeneration and suppresses microglial-like cells following focal motor cortex ischemia in the mouse. *Brain Behav Immun* **48**, 57-67, doi:10.1016/j.bbi.2015.02.014 (2015).

25 Cao, Z. *et al.* TRPV1-mediated Pharmacological Hypothermia Promotes Improved Functional Recovery Following Ischemic Stroke. *Sci Rep* **7**, 17685, doi:10.1038/s41598-017-17548-y (2017).

26 Kluge, M. G. *et al.* Spatiotemporal analysis of impaired microglia process movement at sites of secondary neurodegeneration post-stroke. *Journal of cerebral blood flow and metabolism : official journal of the International Society of Cerebral Blood Flow and Metabolism*, 271678x18797346, doi:10.1177/0271678x18797346 (2018).

27 Zuo, X. *et al.* Inhibition of Cathepsin B Alleviates Secondary Degeneration in Ipsilateral Thalamus After Focal Cerebral Infarction in Adult Rats. *J Neuropathol Exp Neurol* **75**, 816-826, doi:10.1093/jnen/nlw054 (2016).

28 Chen, Y. *et al.* 2-Cl-MGV-1 Ameliorates Apoptosis in the Thalamus and Hippocampus and Cognitive Deficits After Cortical Infarct in Rats. *Stroke* **48**, 3366-3374, doi:10.1161/strokeaha.117.019439 (2017).

29 Dong, X. X., Wang, Y. & Qin, Z. H. Molecular mechanisms of excitotoxicity and their relevance to pathogenesis of neurodegenerative diseases. *Acta pharmacologica Sinica* **30**, 379-387, doi:10.1038/aps.2009.24 (2009).

30 Paz, J. T., Christian, C. A., Parada, I., Prince, D. A. & Huguenard, J. R. Focal cortical infarcts alter intrinsic excitability and synaptic excitation in the reticular thalamic nucleus. *The Journal of neuroscience : the official journal of the Society for Neuroscience* **30**, 5465-5479, doi:10.1523/jneurosci.5083-09.2010 (2010).

31 Block, F., Dihne, M. & Loos, M. Inflammation in areas of remote changes following focal brain lesion. *Prog Neurobiol* **75**, 342-365, doi:10.1016/j.pneurobio.2005.03.004 (2005).

32 Kawabori, M. & Yenari, M. A. The role of the microglia in acute CNS injury. *Metab Brain Dis* **30**, 381-392, doi:10.1007/s11011-014-9531-6 (2015).

33 Kornau, H. C., Schenker, L. T., Kennedy, M. B. & Seeburg, P. H. Domain interaction between NMDA receptor subunits and the postsynaptic density protein PSD-95. *Science* **269**, 1737-1740 (1995).

34 Zhan, L. *et al.* Neuroprotection of hypoxic postconditioning against global cerebral ischemia through influencing posttranslational regulations of heat shock protein 27 in adult rats. *Brain pathology (Zurich, Switzerland)* **27**, 822-838, doi:10.1111/bpa.12472 (2017).

35 Zhan, L. *et al.* Activation of Akt/FoxO and inactivation of MEK/ERK pathways contribute to induction of neuroprotection against transient global cerebral ischemia by delayed hypoxic postconditioning in adult rats. *Neuropharmacology* **63**, 873-882, doi:10.1016/j.neuropharm.2012.06.035 (2012).

36 Zhu, T. *et al.* Hypoxia-inducible factor 1alpha mediates neuroprotection of hypoxic postconditioning against global cerebral ischemia. *J Neuropathol Exp Neurol* **73**, 975-986, doi:10.1097/NEN.0000000000000118 (2014).
37 Coleman, C. G. *et al.* Chronic intermittent hypoxia induces NMDA receptor-dependent plasticity and suppresses nitric oxide signaling in the mouse hypothalamic paraventricular nucleus. *J Neurosci* **30**, 12103-12112, doi:10.1523/jneurosci.3367-10.2010 (2010).
38 Pappata, S. *et al.* Thalamic microglial activation in ischemic stroke detected in vivo by PET and [11C]PK1195. *Neurology* **55**, 1052-1054 (2000).
39 Gerhard, A., Schwarz, J., Myers, R., Wise, R. & Banati, R. B. Evolution of microglial activation in patients after ischemic stroke: a [11C](R)-PK11195 PET study. *NeuroImage* **24**, 591-595, doi:10.1016/j.neuroimage.2004.09.034 (2005).
40 Jackman, K. A. *et al.* Dichotomous effects of chronic intermittent hypoxia on focal cerebral ischemic injury. *Stroke* **45**, 1460-1467, doi:10.1161/STROKEAHA.114.004816 (2014).
41 Coppel, J., Hennis, P., Gilbert-Kawai, E. & Grocott, M. P. The physiological effects of hypobaric hypoxia versus normobaric hypoxia: a systematic review of crossover trials. *Extreme physiology & medicine* **4**, 2, doi:10.1186/s13728-014-0021-6 (2015).
42 Navarrete-Opazo, A. & Mitchell, G. S. Therapeutic potential of intermittent hypoxia: a matter of dose. *Am J Physiol Regul Integr Comp Physiol* **307**, R1181-1197, doi:10.1152/ajpregu.00208.2014 (2014).
43 Karatepe, A. G., Gunaydin, R., Kaya, T. & Turkmen, G. Comorbidity in patients after stroke: impact on functional outcome. *J Rehabil Med* **40**, 831-835, doi:10.2340/16501977-0269 (2008).
44 Fischer, U. *et al.* Impact of comorbidity on ischemic stroke outcome. *Acta Neurol Scand* **113**, 108-113, doi:10.1111/j.1600-0404.2005.00551.x (2006).
45 Carriel, V., Campos, A., Alaminos, M., Raimondo, S. & Geuna, S. Staining Methods for Normal and Regenerative Myelin in the Nervous System. *Methods in molecular biology (Clifton, N.J.)* **1560**, 207-218, doi:10.1007/978-1-4939-6788-9_15 (2017).
46 Pietrogrande, G. *et al.* Chronic stress induced disturbances in Laminin: A significant contributor to modulating microglial pro-inflammatory tone? *Brain Behav Immun*, doi:10.1016/j.bbi.2017.09.012 (2017).
47 This article was published in The mouse brain in stereotaxic coordinates. Compact 2nd edn, Paxinos, G. & Franklin, K. B. J., Page 145-212, Copyright Elsevier (2004).

Additional information

Author Contribution

GP, KZ, ZZ, CWZ, SSB and LKO performed experiments and analysed the results; GP and FRW designed the experiments and interpreted the data; MA and SJJ developed the software for analysis; GP, FRW, SJJ and MN wrote and reviewed the manuscript.

Additional Information

The authors declare no competing interests.

Figure legends

Fig 1. Experimental plan. Layout of the experimental design of LOPC and follow up protocol. Diagram illustrating the site of phototrombotic stroke induction (red arrow) at bregma 0 mm adapted from [47] and representative cresyl violet stained coronal sections of a PTO stroke-affected hemisphere showing somatosensory cortex ablation (Bregma -0.6 to +1.5).

Fig 2. Secondary neuronal death is prevented by LOPC at 30 days. (**A**) Brain map adapted from [47] and exemplificative NeuN staining showing the infarct region (*) and the thalamic regions VPL and PO. (**B**) Identified area of PO SND (dash line, scalebar=400 μm) and representative images of the PO (scalebar=70 μm) and VPL (scalebar=40 μm) areas used for $NeuN^+$ cells count. On the right, quantification shows that LOPC decreases the area of SND in PO and prevents $NeuN^+$ cells decrease in the VPL and PO. Results are shown as the mean ± SD. * $p<0.05$, ** $p<0.01$, 2-way ANOVA with Tukey's multiple comparison test.

Fig 3. Thalamic microglia activation is resolved at 30 days after LOPC. (**A**) Decreased microglia activation area in thalamus of LOPC mice at 30 days, as estimated by Iba1 and CD68 (**B**) staining (scalebar=300 μm). ** $p<0.01$, 2-way ANOVA with Tukey's multiple comparison test.

Fig 4. Thalamic microglia expression of inflammatory marker CD11b. Representative western blot showing changes in CD11b expression (n=8-10). Quantification revealed decreased expression of CD11b in LOPC mice at 30 days. Results are shown as the mean ± SD. * $p<0.05$, 2-way ANOVA with Tukey's multiple comparison test.

Fig 5. NMDAR mediated nNOS activation is prevented by LOPC at 15 days. (A) Calcium accumulation in the thalamus is not affected by LOPC at all pixel intensities as shown by cumulative tresholding analysis (scalebar=400 μm). (**B**) The thalamic expression NR1, N2B and nNOS do not change in time or with treatment as assessed by WB. At 15 days, WB analysis show that the expression of synaptic marker PSD-95 is decreased by 50% in LOPC while Synapsin 1 expression is unchanged. (**C**) Co-immunoprecipitation of N2B and PSD-95 shows decreased interaction in LOPC samples between NMDAR and PSD-95 at 15 days (-Ab: beads not coated incubated in lysate; -Lysate: beads coated incubated in PBS). Images cropped from Supp Fig 3. Results are shown as the mean ± SD. * $p<0.05$, Mann Whitney U test.

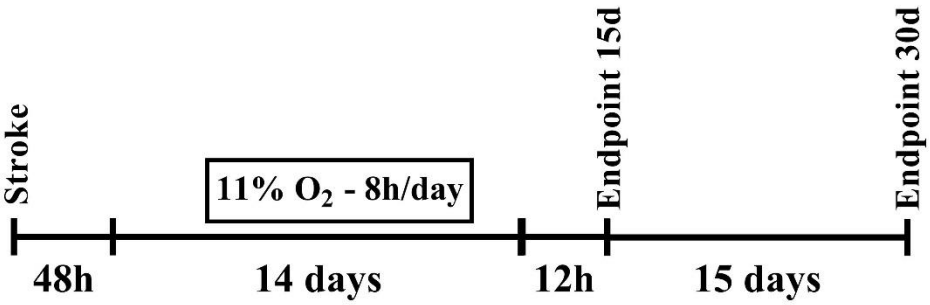
Stroke
11% O_2 - 8h/day
Endpoint 15d
Endpoint 30d
48h
14 days
12h
15 days

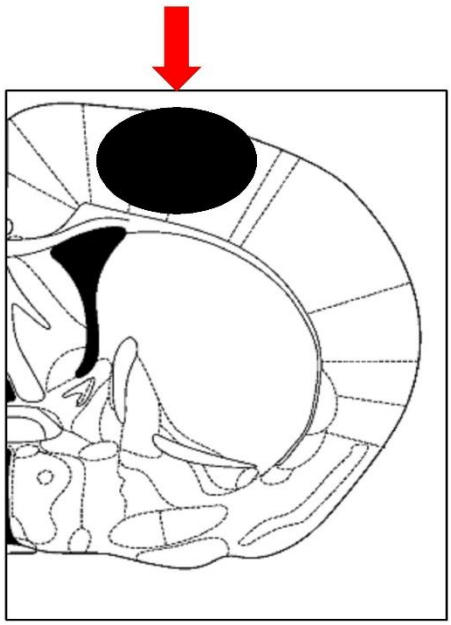

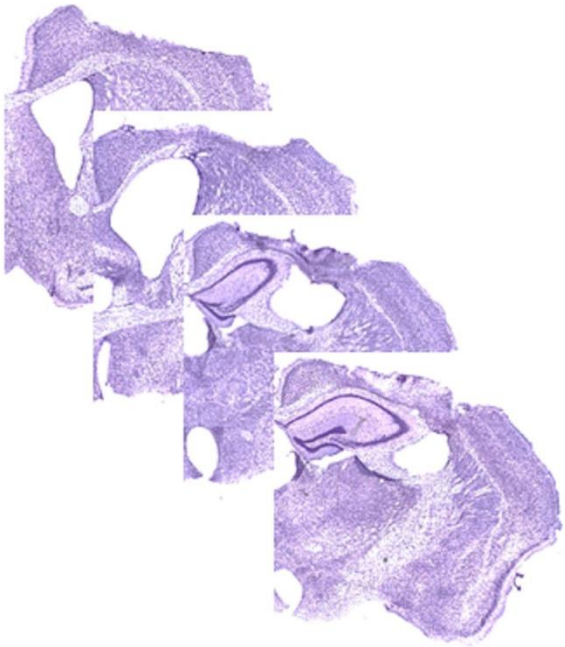

`

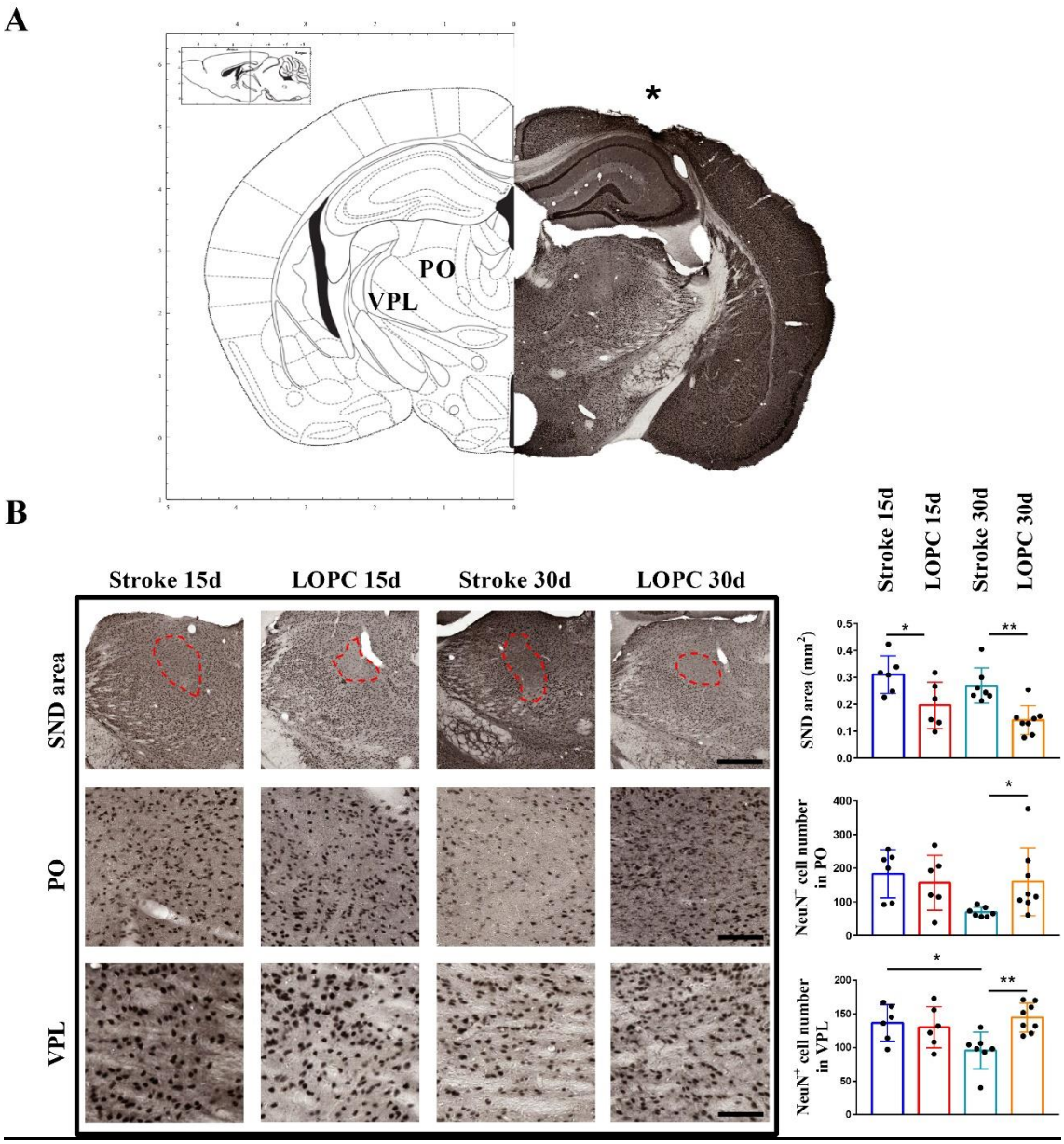
A
*
PO
VPL
B
Stroke 15d
LOPC 15d
Stroke 30d
LOPC 30d
SND area
PO
VPL
Stroke 15d
LOPC 15d
Stroke 30d
LOPC 30d
SND area (mm²)
NeuN⁺ cell number in PO
NeuN⁺ cell number in VPL
*
**
*
*
**

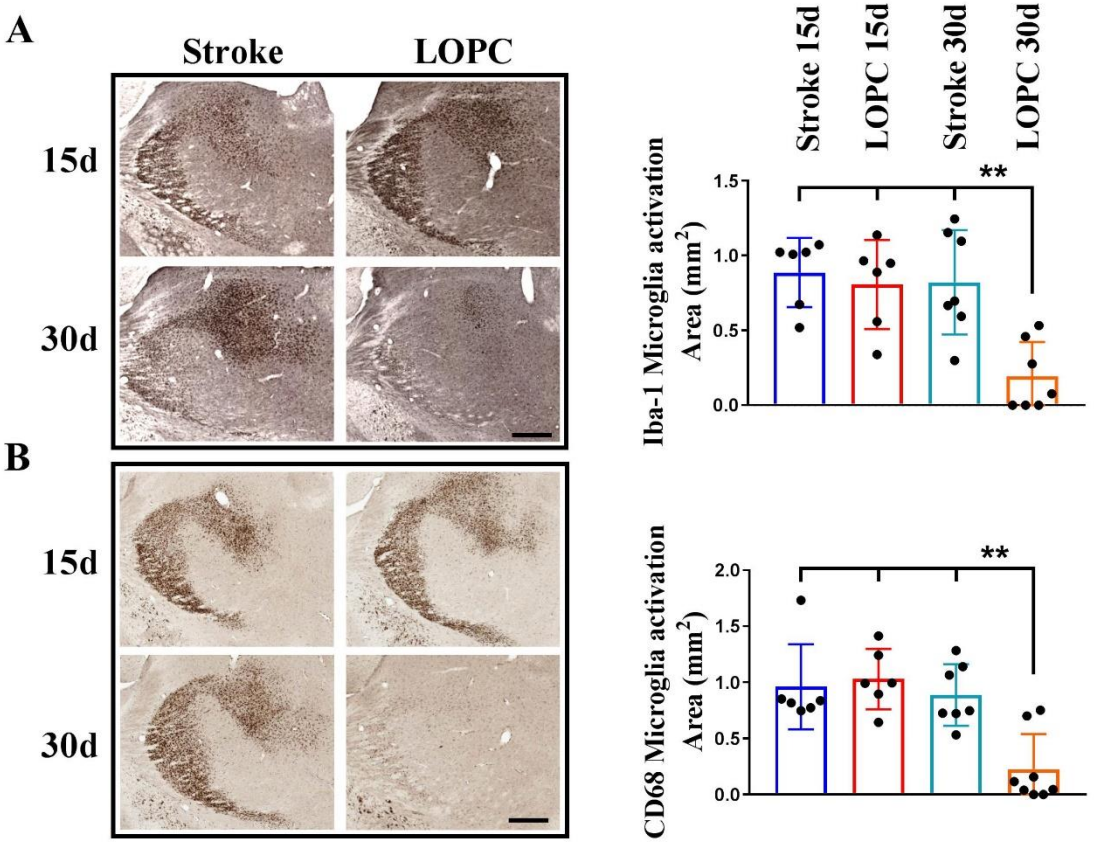
A
Stroke
LOPC
15d
30d
B
15d
30d
Stroke 15d
LOPC 15d
Stroke 30d
LOPC 30d
Iba-1 Microglia activation
Area (mm2)
**
CD68 Microglia activation
Area (mm2)
**

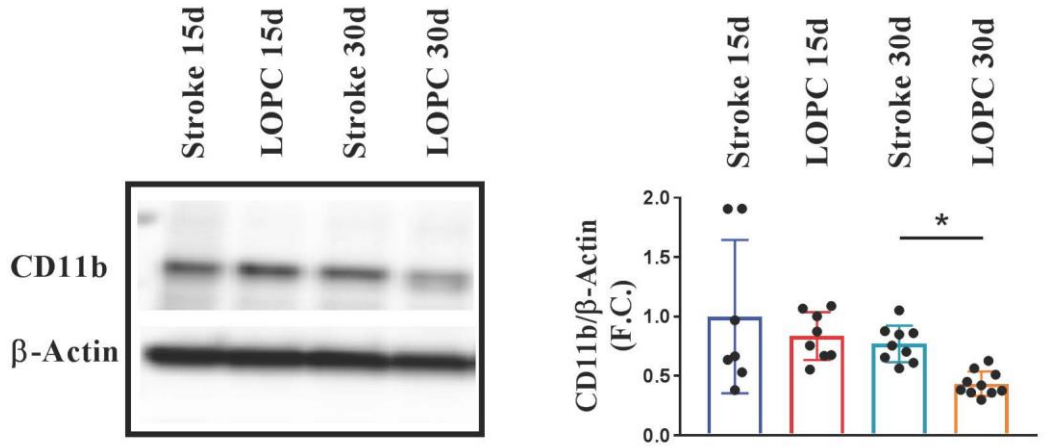
Stroke 15d
LOPC 15d
Stroke 30d
LOPC 30d
CD11b
β-Actin
CD11b/β-Actin
(F.C.)
*

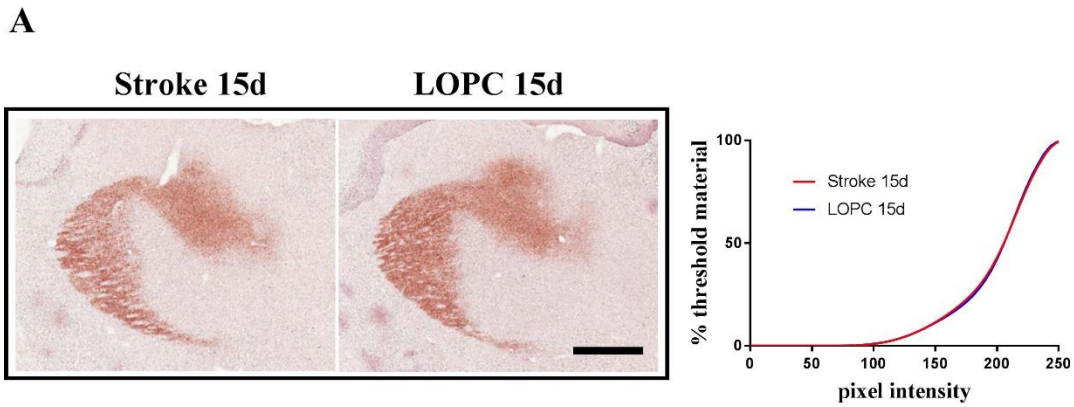
A
Stroke 15d
LOPC 15d
% threshold material
pixel intensity
Stroke 15d
LOPC 15d
B
Stroke 15d
LOPC 15d
NR1
nNOS
β-Act
N2B
β-Act
PSD-95
β-Act
Syn 1
β-Act
Fold change
NR1
N2B
nNOS
Syn 1
PSD-95
**
C
Stroke 15d
LOPC 15d
-Ab
-Lysate
1 µg Lysate
N2B
PSD-95
β-Act
N2B/PSD-95 ratio
Stroke 15d
LOPC 15d
*

`

Low Oxygen Post Conditioning prevents thalamic secondary neuronal loss caused by excitotoxicity after cortical stroke

Authors:

Giovanni Pietrogrande, Katarzyna Zalewska, Zidan Zhao, Mahmoud Abdolhoseini, Wei Zhen Chow, Sonia Sanchez-Bezanilla , Lin Kooi Ong, Sarah J Johnson, Michael Nilsson, Frederick R Walker

Supplementary Information

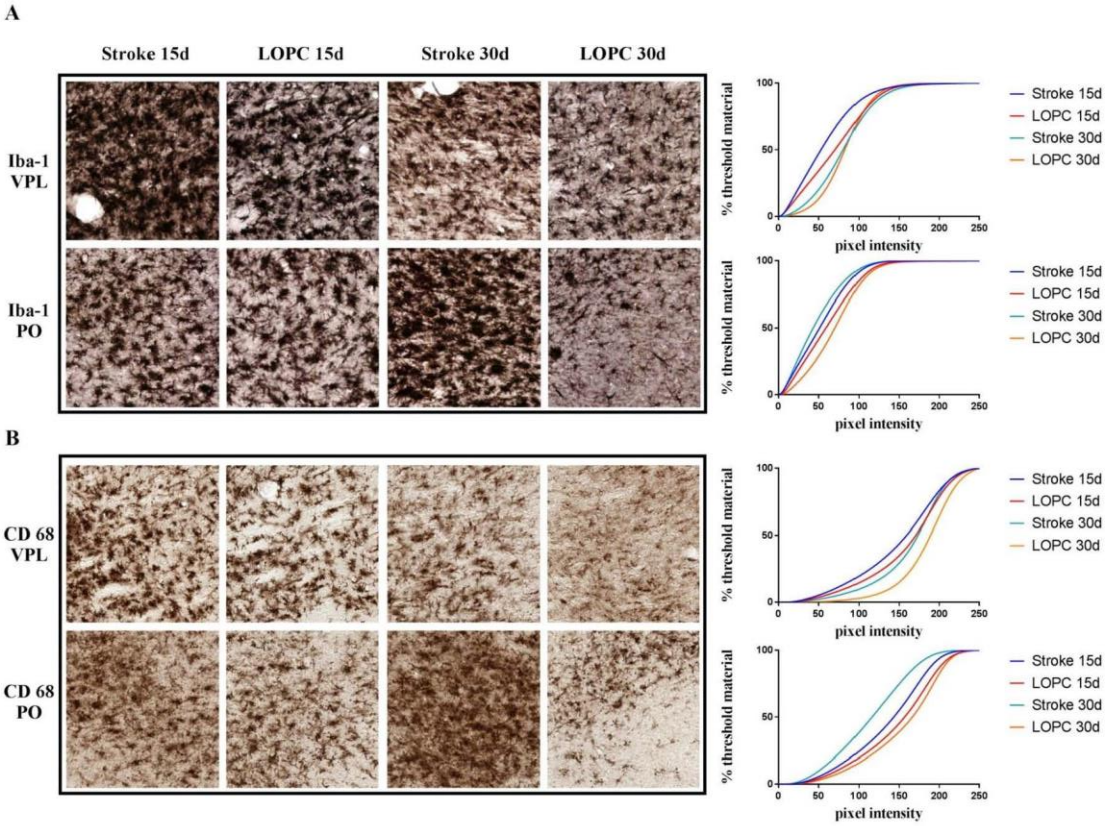
A
Stroke 15d
LOPC 15d
Stroke 30d
LOPC 30d
Iba-1 VPL
Iba-1 PO
% threshold material
pixel intensity
Stroke 15d
LOPC 15d
Stroke 30d
LOPC 30d
B
CD 68 VPL
CD 68 PO

`

Supp Fig 1. Quantification of immunolabelling for Iba1 and CD68 in the PO and VPL. Cumulative thresholding analysis of the intensity of immunolabelling confirms general decrease in the levels of microglia activation at 30 days after LOPC compared to stroke alone.

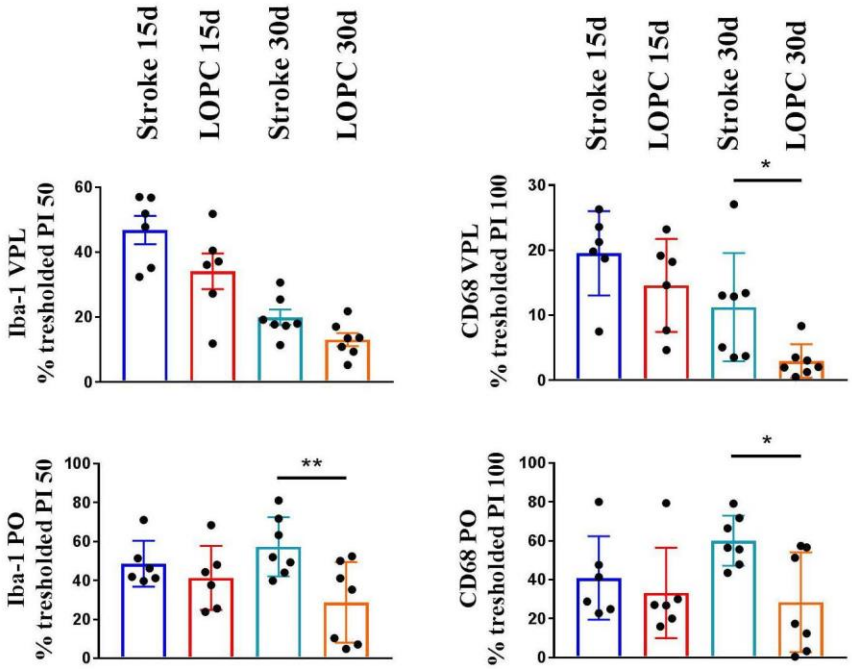

Supp Fig 2. Specific quantification of cumulative thresholding. Analysis of the thresholded material of Iba-1 and CD68 staining in the VPL and PO. The optimal pixel intensity (PI) was assessed manually.

`

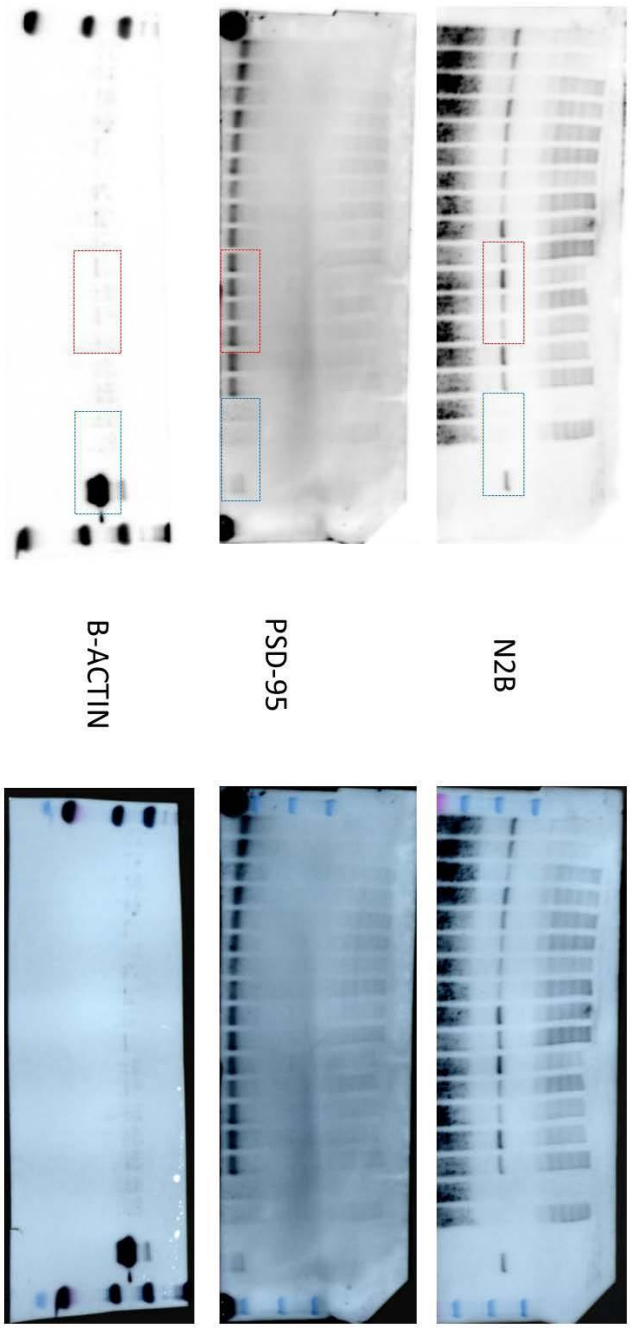
B-ACTIN
PSD-95
N2B

`

Supp Fig 3. CO-IP original western blot. Picture of the original western blot cropped for Fig. 5c and overlay with white light for molecular weight marker (Bio Rad, Cat# 161-0374) visualization. Loading order: Stroke1, Stroke2, LOPC1, LOPC2, Stroke3, Stroke4, LOPC 3, LOPC4, Stroke5, Stroke6, Stroke7, LOPC5, LOPC6, LOPC7, LOPC8, -Ab, -Lys, empty lane, 1µg Stroke thalamus lysate. Red box highlights the left part of panel Fig 5c, blue box the right panel of Fig 5c.

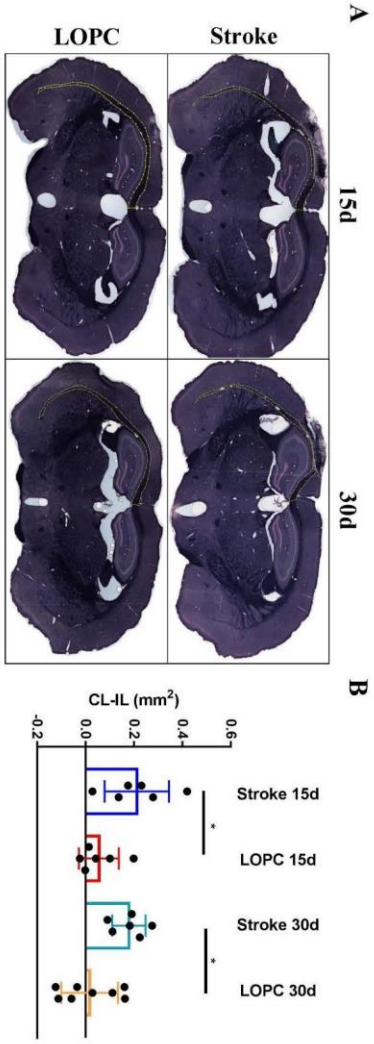

Supp Fig.4 LOPC ameliorates white matter loss. (A) Sudan Black B staining at Bregma levels -1.5. Yellow line represents the corpus callosum traced using ImageJ. **(B)** Quantification of corpus callosum area measured as a difference between the contralateral (CL) and ipisilateral (IL) hemisphere revealed a significant decrease in white matter structural loss at both 15 and 30 days post-stroke. Results are shown as the mean ± SD. * $p<0.05$, Mann Whitney U test.

`

Discussion

In the previous study I have identified that vascular regeneration, BDNF expression and decreased inflammation after exposure to LOPC protocol were associated with a considerable reduction in neuronal loss within peri-infarct regions, concomitant with a promising improvement in motor function. In this study, I extended my findings by giving specific consideration to the effects of LOPC within the ipsilateral thalamus and the neuronal loss that affects this area after cortical stroke, in a process called secondary neurodegeneration (SND). Previous data generated in the lab have shown that the protocol of LOPC adopted can ameliorate SND at some extent (Appendix 1). However, after this study, it was still unknown whether this effect was temporary and if the damage in the area would deteriorated after the end of the treatment. Furthermore, the involvement of microglia activation was only marginally elaborated, and the excitotoxic process not considered.

The thalamus has the key function to relay peripheral sensory information to the cortex. Previously, our and other groups have reported that stroke in the sensory motor cortex area induces SND specifically in two thalamic area: the ventral posterior nucleus (VPN) and the posterior nucleus (PO). These nuclei are involved in the relay of somatosensory and motor information and are connected, via corticothalamic and thalamocortical projections, to the area targeted by phototrombotic stroke. (325, 326). Using immunohistochemistry I was able to estimate the neuronal loss specifically in these areas. To identify neurons I used NeuN, a very specific marker of mature neurons, and as primary analysis I quantified SND as estimated area affected by evident low density presence of $NeuN^+$ cells. Then, by neuronal count, I accurately evaluated SND within the dorsal thalamus and specifically inside the areas affected by SND. This analysis allowed

`

me to evaluate SND on different levels and revealed that SND worsen with time and LOPC can prevent this degeneration. Specifically, analysis showed a wider area affected by SND in stroke alone samples compared to LOPC, significantly different at both time points. On the other hand, cell count analysis within the dorsal thalamus area, PO and VPN all showed significantly less NeuN+ cells in stroke alone mice at 30 days compared to 15 days, while in LOPC samples neurons number was constant over time and similar to stroke alone at 15 days. These results show that LOPC decreased the extent of SND area at 15 days and, even more importantly, it strongly prevented further neurodegeneration, that instead occurred in the subsequent weeks in stroke alone mice. SND leads to progressive neuronal loss and clinical studies in humans showed that SND develops in the months following ischemic injury. This temporal analysis suggests that even a relatively small neuroprotective effect in the first phase of SND development, like the one observed, can have an important impact on the degree of neuronal loss at latter stages. However, an explanation can be also found in the results of Chapter 4, since the infarct size could correlate with the extent of SND and LOPC decreases neuronal loss in the peri-infarct area. A potential approach to elucidate this point would be to further delay the beginning of LOPC treatment, when neuronal death in the peri-infarct is unlikely to be prevented anymore.

After confirming the neuroprotective activity of LOPC, I proceeded to investigate the potential underlying mechanism. As extensively highlighted across this thesis, microglia activation can promote neuronal death by inducing release of neurotoxic factors or by stimulating phagocytosis of injured neurons. I identified the areas of microgliosis by immunostaining for two markers of microglia activation: Iba-1 and CD68. As previously

`

described also by others, at 15 days the microglia activation was restricted to PO and VPN, the same areas affected by neuronal loss. Intriguingly, while the global area of activation was similar in stroke alone animals between 15 and 30 days, LOPC samples showed very little to none microglia activation at 30 days. These results were consistent with western blot analysis of CD11b, another marker overexpressed in microglia after activation. As in other reports, also in this study I could see that decreased SND is accompanied by less microgliosis; however, using the data produced in this longitudinal study, I can bring my considerations a bit further. At 15 days data showed that SND is ameliorated by LOPC, while microglia activity is not. If inflammation was the only driver of SND, I would have expected the same level of thalamic neuronal death. Instead at 30 days, after LOPC I found constant SND and marked decrease of microglia activation, while with time SND is strongly exacerbated in stroke alone. Altogether these data suggest that inflammation is more a consequence than a cause for SND, and stopping the progression of SND promoted the natural resolution of inflammation. This model does not preclude a contribution of microgliosis to SND, but points out that LOPC is interfering on an alternative mechanism that lead to SND in first place. Thus, as potential primary cause of SND I investigated excitotoxicity and the involvement of LOPC in disrupting this mechanism at 15 days, right after the end of the treatment. It is important to underline that both neuronal death and microglia activation are only attenuated by our LOPC intervention, and their presence is clearly detected at 15 days.

As extensively detailed in the introduction and in the paper itself, neuronal death by excitotoxicity is caused by abnormal Ca^{2+} influx and consequent over-activation of signalling cascades leading to cell death. Of particular interest is the activation of nNOS caused by activation of NMDAR and Ca^{2+} influx, that induces the production of highly cytotoxic elements. In order for Ca^{2+} influx to induce nNOS activation, nNOS needs to

`

be localised in a complex together with NMDAR. However this interaction is not direct, and needs the mediation of a specific scaffold protein, the post synaptic density protein PSD95. The formation of this complex formed by NMDAR/PSD95/nNOS ultimately allows the activation of nNOS following CA^{2+} influx, and excessive influx translates in excessive nNOS activation and excessive production of free radicals (327). Intriguingly, overexpression of nNOS does not automatically translates in cytotoxicity, but at the same time silencing of nNOS or PSD95 protects from excitotoxicity (328, 329). To investigate this signalling cascade, at first I verified calcium accumulation specifically in the SND areas, which was not influenced by LOPC. Then I quantified by western blot the expression of all the elements involved in this pathway, specifically: the NMDAR subunits NR1 and N2B, PSD95 and nNOS. The data showed that LOPC thalamic samples presented a small (35%) but significant decrease in PSD95 expression, while the other components of this pathway were unchanged. Since the expression of another synaptic protein, Synapsin-1, was unaffected, it seemed unlikely that the decrease in PSD95 was due to a general synaptic deregulation. However, it must be also considered that Synapsin-1 is an ubiquitous pre-synaptic marker and it is plausible that other mechanisms could be compensating for the decreased levels of PSD95 that I observed. To corroborate the evidence of LOPC disrupting the NMDAR/PSD95/nNOS signalling, I generated another cohort of mice to specifically investigate the levels of interaction between NMDAR and PSD95 by co-immunoprecipitation (CO-IP). Unfortunately, I could not find commercially available polyclonal antibodies targeting NR1 or N2B capable of pulling down PSD95. However, in preliminary experiments I successfully optimised the protocol and found a PSD95 antibody capable of co-immunoprecipitate PSD95 with N2B, the NMDAR subunit interacting with the PSD95. The results showed that thalamic LOPC samples have decreased levels of N2B pulled down with PSD-95 by

`

a polyclonal PSD-95 antibody. Since a protein unrelated to the complex like β-actin was undetectable in the PSD-95 pull down samples, this indicated a *bone fide* decreased interaction between NMDAR and PSD-95 in ipsilateral thalamic neurons after 2 weeks LOPC. These results strongly suggest that LOPC have the potential to decrease SND by interfering in the excitotoxic mechanism, but further studies are need to validate this finding and elucidate the exact mechanism leading to the disruption of the NMDAR/PSD95/nNOS complex.

In conclusion, this study showed that LOPC treatment strongly prevents the development of SND, also suggesting that longer expositions to LOPC is unlikely to induce further benefits since deterioration of SND was already stopped by 2 weeks of treatment. LOPC blocking SND development also induced a faster resolution of inflammation, providing a new, important clue about the causal dichotomy between secondary neuronal death and microgliosis. Further, I identified a new mechanism that can mediate the neuroprotective activity of LOPC. Altogether, the data from the studies in chapters 4 and 5 prove the potential of LOPC as a non-pharmacological treatment to induce neuroprotection after ischemia.

`

`

CHAPTER 6

Conclusion

In conclusion, this thesis has demonstrated several new findings. I identified a new mechanism that can lead to microglia disturbances linked to pathologies and described a new therapeutic approach that can induce neuroprotection after stroke, while analysing the role of microglia activation in stroke peri-infarct and SND areas.

There are several models of experimental stroke that can be used by researchers. The most common models of ischemic stroke in rodents include mechanical MCAO, thrombotic occlusion by injection of preformed clots or micro-emboli, injection of the vasoconstrictor endothelin-1 and the photo-thrombosis (reviewed in (330)).Each of these models has a set of well described advantages and disadvantages, and I will now discuss some of these limitations.

The model of MCAO in rats was first described in the 1986 by Koizumi et al. (331) and then modified to reduce complications and adapted to mice (332). Briefly, an occluding suture or injection of clots is applied via the common carotid artery towards the junction of the anterior and middle cerebral arteries, resulting in ischemia of MAC vascular territory. The main advantages of this technique are that it closely mimics the stroke event in human, it does not require cranial surgery and models focal infarction in a large vascular territory. However MCAO induces a very variable level of damage that affects thalamus and substantia nigra at variable degrees (333). Therefore the MCAO model does not readily lend itself to tightly controlled studies considering interventions with moderate effect sizes. Further, exactly because MCAO damages multiple areas of the brain, it is not optimal to investigate thalamic damage and SND as consequences of the circuit interruptions between cortex and thalamus. MACO

`

can also causes serious complications as subarachnoid haemorrhage (334), visual dysfunction (335) and the muscles mastication and swallow ischemia, resulting in eating difficulty and weight loss (336). Such complications can influence post-stroke measurement of motor function, which is one of the primary aims of my studies. Furthermore, it has been reported that the infarct size caused by MACO is highly variable (337). A second widely used model of stroke consists in the application of the vasoconstrictor endothelin-1 that acts on endothelial cells (338). The advantages of endothelin-1 model are that it can be intracerebrally injected in specific regions to produce cortical ischemic lesion aiming the brain circuits of interest with minimal tissue edema (339, 340). However, endothelin-1 receptor are also expressed in astrocytes and neurons (341, 342) and promotes astrocytosis and facilitates axonal sprouting in spinal cord injury (343), a potential bias when investigating a neuroprotective treatment as LOPC.

The last model I will now discuss is the PT model of focal cerebral ischemia (344). The PT model induces ischemic damage within a limited and highly controllable cortical area by photo-activation of Rose Bengal, a light-sensitive dye that is delivered by intraperitoneal injection. The stimulation with light is applied on the intact skull with minimal surgery and target the cortical area of interest with precision within a tenth of a millimetre and small variability (345). The photo-activated Rose Bengal produces singlet oxygen that damages endothelia cell membranes leading to platelet aggregation and an occlusion that results in local blood interruption (346, 347). One clear limitation of PT stroke is that it can only induce the obstruction of superficial vessels, while the vast majority of human stroke are caused by the occlusion or rupture of one artery. Another limitation is that PT stroke is not able to produce ischemic penumbral zone like MCAO. I chose this model for my studies because it provides a clear and highly reproducible output and it is suitable for studying cellular and molecular mechanisms of cortical

`

remodelling (348). Furthermore my research goal had a focus on the effect of interventions in a relatively long term, up to 4 weeks. Therefore I did not consider the absence of penumbra within the tissue during the acute (few days) phase post stroke as a dramatic limitation. On the contrary, as described in chapter 5 the absence of penumbra makes PT stroke an optimal model to investigate SND.

The key findings of this thesis can be summarised in the following points:

- I validated the development of higher basal inflammatory status in a model of murine chronic stress. Concomitantly, I proved with different techniques that the expression of ECM components, in particular Laminin, is deregulated in this model. To investigate whether ECM disturbances can potentially modulate microglial level of activation, I used a wide array of *in vitro* approaches using both cell lines and primary microglia. Altogether, the data suggested that Laminin can induce a higher microglia inflammatory status, assessed as expression of pro-inflammatory cytokines and phagocytosis, enhanced response to pro-inflammatory stimuli and delayed resolution of inflammation. This study provides strong proof of concept implying the involvement of ECM alterations in the context of psychopathologies.

- I evaluated a new therapeutic intervention after cortical stroke, LOPC, and showed that it can be highly beneficial for motor function. These benefits correlated with a neuroprotective phenotype, increased neovascularization, production of neurotrophic factors and a marked decrease of microglia activation markers. Moreover, the positive effects of LOPC were maintained after treatment, highlighting the clinical potential of LOPC.

`

- SND is a pathology closely related to stroke that leads to neuronal death over time in regions distant from the infarct core. I evaluated the potential of LOPC to ameliorate this neuronal loss and found that LOPC can interfere with the excitotoxic signalling that leads to neuronal death. Moreover, I used this model to study the involvement of microglia activation in the development of SND, and the data suggests that preventing SND also accelerates the resolution of inflammation at later times. This report adds a piece of very important information in understanding the involvement of microglia activation in SND.

Inflammation in the CNS is believed to play a pivotal role in many neurodegenerative diseases and microglia activation is a hallmark of an existing pathological state within the brain (349). Studying microglial behaviour in different pathologies provided us with a unique perspective on microglia disturbances. In these studies I dissected microglia and microglia activation role in very different CNS pathologies. While at first glance stroke interventions and chronic stress might not seem connected, they are linked at different levels. For example, I contributed to studies from our lab showing that chronic stress after stroke exacerbates brain damage, while perceived psychological stress is associated with an increased risk of stroke (350).

10 to 30% of patient with major depression disorder do not respond to pharmaceutical treatment (351, 352), and in stroke none of the neuroprotective compounds screened up to date in preclinical studies showed efficacy in clinical trials (157). These reports highlight the urgent need of changing our approach while studying CNS pathologies. This thesis provides new insights about microglia activation and its involvement in the

`

development of CNS pathologies, proposing new mechanisms of microglia activation after chronic stress and new potential treatments to improve motor functional outcome after stroke, with important implications for future directions.

CHAPTER 7

References

`

1. Katan M, and Luft A. Global Burden of Stroke. *Seminars in neurology.* 2018;38(2):208-11.
2. Xavier AL, Menezes JR, Goldman SA, and Nedergaard M. Fine-tuning the central nervous system: microglial modelling of cells and synapses. *Philosophical transactions of the Royal Society of London Series B, Biological sciences.* 2014;369(1654):20130593.
3. Tremblay ME, Lecours C, Samson L, Sanchez-Zafra V, and Sierra A. From the Cajal alumni Achucarro and Rio-Hortega to the rediscovery of never-resting microglia. *Front Neuroanat.* 2015;9:45.
4. Solito E, and Sastre M. Microglia function in Alzheimer's disease. *Frontiers in pharmacology.* 2012;3:14.
5. Subramaniam SR, and Federoff HJ. Targeting Microglial Activation States as a Therapeutic Avenue in Parkinson's Disease. *Front Aging Neurosci.* 2017;9:176.
6. Jack C, Ruffini F, Bar-Or A, and Antel JP. Microglia and multiple sclerosis. *J Neurosci Res.* 2005;81(3):363-73.
7. Crotti A, and Glass CK. The choreography of neuroinflammation in Huntington's disease. *Trends Immunol.* 2015;36(6):364-73.
8. Mondelli V, Vernon AC, Turkheimer F, Dazzan P, and Pariante CM. Brain microglia in psychiatric disorders. *Lancet Psychiatry.* 2017;4(7):563-72.
9. Ginhoux F, Greter M, Leboeuf M, Nandi S, See P, Gokhan S, et al. Fate mapping analysis reveals that adult microglia derive from primitive macrophages. *Science.* 2010;330(6005):841-5.
10. Chang PK, Khatchadourian A, McKinney RA, and Maysinger D. Docosahexaenoic acid (DHA): a modulator of microglia activity and dendritic spine morphology. *J Neuroinflammation.* 2015;12:34.
11. Antony JM, Paquin A, Nutt SL, Kaplan DR, and Miller FD. Endogenous microglia regulate development of embryonic cortical precursor cells. *J Neurosci Res.* 2011;89(3):286-98.
12. Marin-Teva JL, Dusart I, Colin C, Gervais A, van Rooijen N, and Mallat M. Microglia promote the death of developing Purkinje cells. *Neuron.* 2004;41(4):535-47.
13. Schafer DP, Lehrman EK, Kautzman AG, Koyama R, Mardinly AR, Yamasaki R, et al. Microglia sculpt postnatal neural circuits in an activity and complement-dependent manner. *Neuron.* 2012;74(4):691-705.
14. Paolicelli RC, Bolasco G, Pagani F, Maggi L, Scianni M, Panzanelli P, et al. Synaptic pruning by microglia is necessary for normal brain development. *Science.* 2011;333(6048):1456-8.
15. Davalos D, Grutzendler J, Yang G, Kim JV, Zuo Y, Jung S, et al. ATP mediates rapid microglial response to local brain injury in vivo. *Nat Neurosci.* 2005;8(6):752-8.
16. Tremblay ME, Lowery RL, and Majewska AK. Microglial interactions with synapses are modulated by visual experience. *PLoS biology.* 2010;8(11):e1000527.
17. Wu Y, Dissing-Olesen L, MacVicar BA, and Stevens B. Microglia: Dynamic Mediators of Synapse Development and Plasticity. *Trends Immunol.* 2015;36(10):605-13.
18. Grabert K, Michoel T, Karavolos MH, Clohisey S, Baillie JK, Stevens MP, et al. Microglial brain region-dependent diversity and selective regional sensitivities to aging. *Nat Neurosci.* 2016;19(3):504-16.
19. Wohleb ES. Neuron-Microglia Interactions in Mental Health Disorders: "For Better, and For Worse". *Frontiers in immunology.* 2016;7:544.
20. Zusso M, Methot L, Lo R, Greenhalgh AD, David S, and Stifani S. Regulation of postnatal forebrain amoeboid microglial cell proliferation and development by the transcription factor Runx1. *J Neurosci.* 2012;32(33):11285-98.
21. Schlegelmilch T, Henke K, and Peri F. Microglia in the developing brain: from immunity to behaviour. *Curr Opin Neurobiol.* 2011;21(1):5-10.

`

22. Ueno M, and Yamashita T. Bidirectional tuning of microglia in the developing brain: from neurogenesis to neural circuit formation. *Curr Opin Neurobiol.* 2014;27:8-15.
23. Nimmerjahn A, Kirchhoff F, and Helmchen F. Resting microglial cells are highly dynamic surveillants of brain parenchyma in vivo. *Science.* 2005;308(5726):1314-8.
24. Karperien A, Jelinek H, and Buchan A. *Box-Counting Analysis of Microglia Form in Schizophrenia, Alzheimer's Disease and Affective Disorder.* 2008.
25. Lehnardt S. Innate immunity and neuroinflammation in the CNS: the role of microglia in Toll-like receptor-mediated neuronal injury. *Glia.* 2010;58(3):253-63.
26. Sadasivan S, Zanin M, O'Brien K, Schultz-Cherry S, and Smeyne RJ. Induction of microglia activation after infection with the non-neurotropic A/CA/04/2009 H1N1 influenza virus. *PLoS One.* 2015;10(4):e0124047.
27. Wake H, Moorhouse AJ, Jinno S, Kohsaka S, and Nabekura J. Resting microglia directly monitor the functional state of synapses in vivo and determine the fate of ischemic terminals. *J Neurosci.* 2009;29(13):3974-80.
28. Dissing-Olesen L, LeDue JM, Rungta RL, Hefendehl JK, Choi HB, and MacVicar BA. Activation of neuronal NMDA receptors triggers transient ATP-mediated microglial process outgrowth. *J Neurosci.* 2014;34(32):10511-27.
29. Eyo UB, Peng J, Swiatkowski P, Mukherjee A, Bispo A, and Wu LJ. Neuronal hyperactivity recruits microglial processes via neuronal NMDA receptors and microglial P2Y12 receptors after status epilepticus. *J Neurosci.* 2014;34(32):10528-40.
30. Weinhard L, di Bartolomei G, Bolasco G, Machado P, Schieber NL, Neniskyte U, et al. Microglia remodel synapses by presynaptic trogocytosis and spine head filopodia induction. *Nat Commun.* 2018;9(1):1228.
31. Salter MW, and Beggs S. Sublime microglia: expanding roles for the guardians of the CNS. *Cell.* 2014;158(1):15-24.
32. Vinet J, Weering HR, Heinrich A, Kalin RE, Wegner A, Brouwer N, et al. Neuroprotective function for ramified microglia in hippocampal excitotoxicity. *J Neuroinflammation.* 2012;9:27.
33. Shinozaki Y, Nomura M, Iwatsuki K, Moriyama Y, Gachet C, and Koizumi S. Microglia trigger astrocyte-mediated neuroprotection via purinergic gliotransmission. *Sci Rep.* 2014;4:4329.
34. Kettenmann H, Hanisch UK, Noda M, and Verkhratsky A. Physiology of microglia. *Physiol Rev.* 2011;91(2):461-553.
35. Chen Z, and Trapp BD. Microglia and neuroprotection. *J Neurochem.* 2016;136 Suppl 1:10-7.
36. Block ML, Zecca L, and Hong JS. Microglia-mediated neurotoxicity: uncovering the molecular mechanisms. *Nat Rev Neurosci.* 2007;8(1):57-69.
37. Cardona AE, Pioro EP, Sasse ME, Kostenko V, Cardona SM, Dijkstra IM, et al. Control of microglial neurotoxicity by the fractalkine receptor. *Nat Neurosci.* 2006;9(7):917-24.
38. Lull ME, and Block ML. Microglial activation and chronic neurodegeneration. *Neurotherapeutics : the journal of the American Society for Experimental NeuroTherapeutics.* 2010;7(4):354-65.
39. Qin L, Wu X, Block ML, Liu Y, Breese GR, Hong JS, et al. Systemic LPS causes chronic neuroinflammation and progressive neurodegeneration. *Glia.* 2007;55(5):453-62.
40. Giulian D, and Baker TJ. Characterization of ameboid microglia isolated from developing mammalian brain. *J Neurosci.* 1986;6(8):2163-78.
41. Walker FR, Beynon SB, Jones KA, Zhao Z, Kongsui R, Cairns M, et al. Dynamic structural remodelling of microglia in health and disease: a review of the models, the signals and the mechanisms. *Brain Behav Immun.* 2014;37:1-14.

`

42. Thored P, Heldmann U, Gomes-Leal W, Gisler R, Darsalia V, Taneera J, et al. Long-term accumulation of microglia with proneurogenic phenotype concomitant with persistent neurogenesis in adult subventricular zone after stroke. *Glia.* 2009;57(8):835-49.
43. Imai Y, Ibata I, Ito D, Ohsawa K, and Kohsaka S. A novel gene iba1 in the major histocompatibility complex class III region encoding an EF hand protein expressed in a monocytic lineage. *Biochem Biophys Res Commun.* 1996;224(3):855-62.
44. Cao T, Thomas TC, Ziebell JM, Pauly JR, and Lifshitz J. Morphological and genetic activation of microglia after diffuse traumatic brain injury in the rat. *Neuroscience.* 2012;225:65-75.
45. Morrison HW, and Filosa JA. A quantitative spatiotemporal analysis of microglia morphology during ischemic stroke and reperfusion. *J Neuroinflammation.* 2013;10:4.
46. Buttini M, Limonta S, and Boddeke HW. Peripheral administration of lipopolysaccharide induces activation of microglial cells in rat brain. *Neurochem Int.* 1996;29(1):25-35.
47. Hoek RM, Ruuls SR, Murphy CA, Wright GJ, Goddard R, Zurawski SM, et al. Down-regulation of the macrophage lineage through interaction with OX2 (CD200). *Science.* 2000;290(5497):1768-71.
48. Fontainhas AM, Wang M, Liang KJ, Chen S, Mettu P, Damani M, et al. Microglial morphology and dynamic behavior is regulated by ionotropic glutamatergic and GABAergic neurotransmission. *PLoS One.* 2011;6(1):e15973.
49. Chang RC, Chen W, Hudson P, Wilson B, Han DS, and Hong JS. Neurons reduce glial responses to lipopolysaccharide (LPS) and prevent injury of microglial cells from over-activation by LPS. *J Neurochem.* 2001;76(4):1042-9.
50. Stansley B, Post J, and Hensley K. A comparative review of cell culture systems for the study of microglial biology in Alzheimer's disease. *J Neuroinflammation.* 2012;9:115.
51. Henn A, Lund S, Hedtjarn M, Schrattenholz A, Porzgen P, and Leist M. The suitability of BV2 cells as alternative model system for primary microglia cultures or for animal experiments examining brain inflammation. *ALTEX.* 2009;26(2):83-94.
52. Gosselin D, Skola D, Coufal NG, Holtman IR, Schlachetzki JCM, Sajti E, et al. An environment-dependent transcriptional network specifies human microglia identity. *Science.* 2017;356(6344).
53. Lund S, Christensen KV, Hedtjarn M, Mortensen AL, Hagberg H, Falsig J, et al. The dynamics of the LPS triggered inflammatory response of murine microglia under different culture and in vivo conditions. *J Neuroimmunol.* 2006;180(1-2):71-87.
54. Laurenzi MA, Arcuri C, Rossi R, Marconi P, and Bocchini V. Effects of microenvironment on morphology and function of the microglial cell line BV-2. *Neurochem Res.* 2001;26(11):1209-16.
55. Tanaka J, Toku K, Matsuda S, Sudo S, Fujita H, Sakanaka M, et al. Induction of resting microglia in culture medium devoid of glycine and serine. *Glia.* 1998;24(2):198-215.
56. Schilling T, Nitsch R, Heinemann U, Haas D, and Eder C. Astrocyte-released cytokines induce ramification and outward K+ channel expression in microglia via distinct signalling pathways. *Eur J Neurosci.* 2001;14(3):463-73.
57. Sola C, Casal C, Tusell JM, and Serratosa J. Astrocytes enhance lipopolysaccharide-induced nitric oxide production by microglial cells. *Eur J Neurosci.* 2002;16(7):1275-83.
58. Butovsky O, Jedrychowski MP, Moore CS, Cialic R, Lanser AJ, Gabriely G, et al. Identification of a unique TGF-beta-dependent molecular and functional signature in microglia. *Nat Neurosci.* 2014;17(1):131-43.
59. Tanaka J, and Maeda N. Microglial ramification requires nondiffusible factors derived from astrocytes. *Exp Neurol.* 1996;137(2):367-75.

`

60. Tanaka J, Toku K, Sakanaka M, and Maeda N. Morphological differentiation of microglial cells in culture: involvement of insoluble factors derived from astrocytes. *Neurosci Res.* 1999;34(4):207-15.
61. Yeh WL, Lu DY, Liou HC, and Fu WM. A forward loop between glioma and microglia: glioma-derived extracellular matrix-activated microglia secrete IL-18 to enhance the migration of glioma cells. *J Cell Physiol.* 2012;227(2):558-68.
62. Lu YC, Yeh WC, and Ohashi PS. LPS/TLR4 signal transduction pathway. *Cytokine.* 2008;42(2):145-51.
63. Hines DJ, Choi HB, Hines RM, Phillips AG, and MacVicar BA. Prevention of LPS-induced microglia activation, cytokine production and sickness behavior with TLR4 receptor interfering peptides. *PLoS One.* 2013;8(3):e60388.
64. Persson M, Brantefjord M, Hansson E, and Ronnback L. Lipopolysaccharide increases microglial GLT-1 expression and glutamate uptake capacity in vitro by a mechanism dependent on TNF-alpha. *Glia.* 2005;51(2):111-20.
65. Sheng W, Zong Y, Mohammad A, Ajit D, Cui J, Han D, et al. Pro-inflammatory cytokines and lipopolysaccharide induce changes in cell morphology, and upregulation of ERK1/2, iNOS and sPLA(2)-IIA expression in astrocytes and microglia. *J Neuroinflammation.* 2011;8:121.
66. Levi BZ, Hashmueli S, Gleit-Kielmanowicz M, Azriel A, and Meraro D. ICSBP/IRF-8 transactivation: a tale of protein-protein interaction. *J Interferon Cytokine Res.* 2002;22(1):153-60.
67. Minten C, Terry R, Deffrasnes C, King NJ, and Campbell IL. IFN regulatory factor 8 is a key constitutive determinant of the morphological and molecular properties of microglia in the CNS. *PLoS One.* 2012;7(11):e49851.
68. Ilschner S, and Brandt R. The transition of microglia to a ramified phenotype is associated with the formation of stable acetylated and detyrosinated microtubules. *Glia.* 1996;18(2):129-40.
69. abd-el-Basset E, and Fedoroff S. Effect of bacterial wall lipopolysaccharide (LPS) on morphology, motility, and cytoskeletal organization of microglia in cultures. *J Neurosci Res.* 1995;41(2):222-37.
70. Stossel TP. On the crawling of animal cells. *Science.* 1993;260(5111):1086-94.
71. Hoffmann A, Hofmann F, Just I, Lehnardt S, Hanisch UK, Bruck W, et al. Inhibition of Rho-dependent pathways by Clostridium botulinum C3 protein induces a proinflammatory profile in microglia. *Glia.* 2008;56(11):1162-75.
72. Park JY, Kim HY, Jou I, and Park SM. GM1 induces p38 and microtubule dependent ramification of rat primary microglia in vitro. *Brain Res.* 2008;1244:13-23.
73. Lively S, and Schlichter LC. The microglial activation state regulates migration and roles of matrix-dissolving enzymes for invasion. *J Neuroinflammation.* 2013;10:75.
74. Imai Y, and Kohsaka S. Intracellular signaling in M-CSF-induced microglia activation: role of Iba1. *Glia.* 2002;40(2):164-74.
75. Martin KH, Slack JK, Boerner SA, Martin CC, and Parsons JT. Integrin connections map: to infinity and beyond. *Science.* 2002;296(5573):1652-3.
76. Hynes RO. Integrins: versatility, modulation, and signaling in cell adhesion. *Cell.* 1992;69(1):11-25.
77. Campbell ID, and Humphries MJ. Integrin structure, activation, and interactions. *Cold Spring Harbor perspectives in biology.* 2011;3(3).
78. Lock JG, Wehrle-Haller B, and Stromblad S. Cell-matrix adhesion complexes: master control machinery of cell migration. *Seminars in cancer biology.* 2008;18(1):65-76.
79. Guan JL. Role of focal adhesion kinase in integrin signaling. *The international journal of biochemistry & cell biology.* 1997;29(8-9):1085-96.

`

80. Schaller MD. Cellular functions of FAK kinases: insight into molecular mechanisms and novel functions. *Journal of cell science.* 2010;123(Pt 7):1007-13.
81. Golubovskaya VM, Finch R, and Cance WG. Direct interaction of the N-terminal domain of focal adhesion kinase with the N-terminal transactivation domain of p53. *The Journal of biological chemistry.* 2005;280(26):25008-21.
82. Lim ST, Chen XL, Lim Y, Hanson DA, Vo TT, Howerton K, et al. Nuclear FAK promotes cell proliferation and survival through FERM-enhanced p53 degradation. *Molecular cell.* 2008;29(1):9-22.
83. Kloss CU, Bohatschek M, Kreutzberg GW, and Raivich G. Effect of lipopolysaccharide on the morphology and integrin immunoreactivity of ramified microglia in the mouse brain and in cell culture. *Exp Neurol.* 2001;168(1):32-46.
84. Ohsawa K, Irino Y, Sanagi T, Nakamura Y, Suzuki E, Inoue K, et al. P2Y12 receptor-mediated integrin-beta1 activation regulates microglial process extension induced by ATP. *Glia.* 2010;58(7):790-801.
85. Milner R, and Campbell IL. Cytokines regulate microglial adhesion to laminin and astrocyte extracellular matrix via protein kinase C-dependent activation of the alpha6beta1 integrin. *J Neurosci.* 2002;22(5):1562-72.
86. Milner R, Crocker SJ, Hung S, Wang X, Frausto RF, and del Zoppo GJ. Fibronectin- and vitronectin-induced microglial activation and matrix metalloproteinase-9 expression is mediated by integrins alpha5beta1 and alphavbeta5. *Journal of immunology (Baltimore, Md : 1950).* 2007;178(12):8158-67.
87. Kim C, Cho ED, Kim HK, You S, Lee HJ, Hwang D, et al. beta1-integrin-dependent migration of microglia in response to neuron-released alpha-synuclein. *Exp Mol Med.* 2014;46:e91.
88. Burnside ER, and Bradbury EJ. Manipulating the extracellular matrix and its role in brain and spinal cord plasticity and repair. *Neuropathol Appl Neurobiol.* 2014;40(1):26-59.
89. Cragg B. Brain extracellular space fixed for electron microscopy. *Neurosci Lett.* 1979;15(2-3):301-6.
90. Nicholson C, and Sykova E. Extracellular space structure revealed by diffusion analysis. *Trends Neurosci.* 1998;21(5):207-15.
91. Mi H, Haeberle H, and Barres BA. Induction of astrocyte differentiation by endothelial cells. *J Neurosci.* 2001;21(5):1538-47.
92. Keely PJ. Mechanisms by which the extracellular matrix and integrin signaling act to regulate the switch between tumor suppression and tumor promotion. *Journal of mammary gland biology and neoplasia.* 2011;16(3):205-19.
93. Lau LW, Cua R, Keough MB, Haylock-Jacobs S, and Yong VW. Pathophysiology of the brain extracellular matrix: a new target for remyelination. *Nat Rev Neurosci.* 2013;14(10):722-9.
94. de Vivo L, Landi S, Panniello M, Baroncelli L, Chierzi S, Mariotti L, et al. Extracellular matrix inhibits structural and functional plasticity of dendritic spines in the adult visual cortex. *Nat Commun.* 2013;4:1484.
95. Deepa SS, Carulli D, Galtrey C, Rhodes K, Fukuda J, Mikami T, et al. Composition of perineuronal net extracellular matrix in rat brain: a different disaccharide composition for the net-associated proteoglycans. *The Journal of biological chemistry.* 2006;281(26):17789-800.
96. Gaudet AD, and Popovich PG. Extracellular matrix regulation of inflammation in the healthy and injured spinal cord. *Exp Neurol.* 2014;258:24-34.
97. Fitch MT, and Silver J. CNS injury, glial scars, and inflammation: Inhibitory extracellular matrices and regeneration failure. *Exp Neurol.* 2008;209(2):294-301.

`

98. Moeendarbary E, Weber IP, Sheridan GK, Koser DE, Soleman S, Haenzi B, et al. The soft mechanical signature of glial scars in the central nervous system. *Nat Commun.* 2017;8:14787.
99. Rolls A, Shechter R, and Schwartz M. The bright side of the glial scar in CNS repair. *Nat Rev Neurosci.* 2009;10(3):235-41.
100. Myer DJ, Gurkoff GG, Lee SM, Hovda DA, and Sofroniew MV. Essential protective roles of reactive astrocytes in traumatic brain injury. *Brain.* 2006;129(Pt 10):2761-72.
101. Huang L, Wu ZB, Zhuge Q, Zheng W, Shao B, Wang B, et al. Glial scar formation occurs in the human brain after ischemic stroke. *International journal of medical sciences.* 2014;11(4):344-8.
102. Shibuya S, Yamamoto T, and Itano T. Glial and axonal regeneration following spinal cord injury. *Cell Adh Migr.* 2009;3(1):99-106.
103. Liddelow SA, and Barres BA. Regeneration: Not everything is scary about a glial scar. *Nature.* 2016;532(7598):182-3.
104. Ricard-Blum S. The collagen family. *Cold Spring Harbor perspectives in biology.* 2011;3(1):a004978.
105. Cheng JS, Dubal DB, Kim DH, Legleiter J, Cheng IH, Yu GQ, et al. Collagen VI protects neurons against Abeta toxicity. *Nat Neurosci.* 2009;12(2):119-21.
106. Kosmehl H, Berndt A, and Katenkamp D. Molecular variants of fibronectin and laminin: structure, physiological occurrence and histopathological aspects. *Virchows Arch.* 1996;429(6):311-22.
107. Pankov R, and Yamada KM. Fibronectin at a glance. *Journal of cell science.* 2002;115(Pt 20):3861-3.
108. Mohri H. Fibronectin and integrins interactions. *Journal of investigative medicine : the official publication of the American Federation for Clinical Research.* 1996;44(8):429-41.
109. Sakai T, Johnson KJ, Murozono M, Sakai K, Magnuson MA, Wieloch T, et al. Plasma fibronectin supports neuronal survival and reduces brain injury following transient focal cerebral ischemia but is not essential for skin-wound healing and hemostasis. *Nat Med.* 2001;7(3):324-30.
110. Khan MM, Gandhi C, Chauhan N, Stevens JW, Motto DG, Lentz SR, et al. Alternatively-spliced extra domain A of fibronectin promotes acute inflammation and brain injury after cerebral ischemia in mice. *Stroke.* 2012;43(5):1376-82.
111. Stoffels JM, de Jonge JC, Stancic M, Nomden A, van Strien ME, Ma D, et al. Fibronectin aggregation in multiple sclerosis lesions impairs remyelination. *Brain.* 2013;136(Pt 1):116-31.
112. Scheele S, Nystrom A, Durbeej M, Talts JF, Ekblom M, and Ekblom P. Laminin isoforms in development and disease. *J Mol Med (Berl).* 2007;85(8):825-36.
113. Omar MH, Campbell MK, Xiao X, Zhong Q, Brunken WJ, Miner JH, et al. CNS Neurons Deposit Laminin alpha5 to Stabilize Synapses. *Cell reports.* 2017;21(5):1281-92.
114. Lei WL, Xing SG, Deng CY, Ju XC, Jiang XY, and Luo ZG. Laminin/beta1 integrin signal triggers axon formation by promoting microtubule assembly and stabilization. *Cell research.* 2012;22(6):954-72.
115. Chen Z-L, Indyk JA, and Strickland S. The Hippocampal Laminin Matrix Is Dynamic and Critical for Neuronal Survival. *Molecular Biology of the Cell.* 2003;14(7):2665-76.
116. Milner R, and Campbell IL. The extracellular matrix and cytokines regulate microglial integrin expression and activation. *Journal of immunology (Baltimore, Md : 1950).* 2003;170(7):3850-8.
117. Tam WY, Au NP, and Ma CH. The association between laminin and microglial morphology in vitro. *Sci Rep.* 2016;6:28580.

118. Tynan RJ, Naicker S, Hinwood M, Nalivaiko E, Buller KM, Pow DV, et al. Chronic stress alters the density and morphology of microglia in a subset of stress-responsive brain regions. *Brain Behav Immun.* 2010;24(7):1058-68.
119. Szabo S. Hans Selye and the development of the stress concept. Special reference to gastroduodenal ulcerogenesis. *Ann N Y Acad Sci.* 1998;851:19-27.
120. McEwen BS, and Wingfield JC. What is in a name? Integrating homeostasis, allostasis and stress. *Horm Behav.* 2010;57(2):105-11.
121. de Kloet ER, Joels M, and Holsboer F. Stress and the brain: from adaptation to disease. *Nat Rev Neurosci.* 2005;6(6):463-75.
122. Cohen S, Janicki-Deverts D, Doyle WJ, Miller GE, Frank E, Rabin BS, et al. Chronic stress, glucocorticoid receptor resistance, inflammation, and disease risk. *Proc Natl Acad Sci U S A.* 2012;109(16):5995-9.
123. Caspi A, Sugden K, Moffitt TE, Taylor A, Craig IW, Harrington H, et al. Influence of life stress on depression: moderation by a polymorphism in the 5-HTT gene. *Science.* 2003;301(5631):386-9.
124. Fried EI, Nesse RM, Guille C, and Sen S. The differential influence of life stress on individual symptoms of depression. *Acta Psychiatr Scand.* 2015;131(6):465-71.
125. Lagraauw HM, Kuiper J, and Bot I. Acute and chronic psychological stress as risk factors for cardiovascular disease: Insights gained from epidemiological, clinical and experimental studies. *Brain Behav Immun.* 2015;50:18-30.
126. Sapolsky RM, Romero LM, and Munck AU. How do glucocorticoids influence stress responses? Integrating permissive, suppressive, stimulatory, and preparative actions. *Endocr Rev.* 2000;21(1):55-89.
127. Edeleva EV, and Shcherbata HR. Stress-induced ECM alteration modulates cellular microRNAs that feedback to readjust the extracellular environment and cell behavior. *Front Genet.* 2013;4:305.
128. Sorrells SF, Caso JR, Munhoz CD, and Sapolsky RM. The stressed CNS: when glucocorticoids aggravate inflammation. *Neuron.* 2009;64(1):33-9.
129. Hinwood M, Morandini J, Day TA, and Walker FR. Evidence that microglia mediate the neurobiological effects of chronic psychological stress on the medial prefrontal cortex. *Cereb Cortex.* 2012;22(6):1442-54.
130. Yirmiya R. Endotoxin produces a depressive-like episode in rats. *Brain Res.* 1996;711(1-2):163-74.
131. O'Reilly B, Vander AJ, and Kluger MJ. Effects of chronic infusion of lipopolysaccharide on food intake and body temperature of the rat. *Physiol Behav.* 1988;42(3):287-91.
132. Crestani F, Seguy F, and Dantzer R. Behavioural effects of peripherally injected interleukin-1: role of prostaglandins. *Brain Res.* 1991;542(2):330-5.
133. Vollmer-Conna U, Fazou C, Cameron B, Li H, Brennan C, Luck L, et al. Production of pro-inflammatory cytokines correlates with the symptoms of acute sickness behaviour in humans. *Psychological medicine.* 2004;34(7):1289-97.
134. Bennett BK, Hickie IB, Vollmer-Conna US, Quigley B, Brennan CM, Wakefield D, et al. The relationship between fatigue, psychological and immunological variables in acute infectious illness. *The Australian and New Zealand journal of psychiatry.* 1998;32(2):180-6.
135. Capuron L, and Miller AH. Immune system to brain signaling: neuropsychopharmacological implications. *Pharmacology & therapeutics.* 2011;130(2):226-38.
136. Raison CL, Borisov AS, Broadwell SD, Capuron L, Woolwine BJ, Jacobson IM, et al. Depression during pegylated interferon-alpha plus ribavirin therapy: prevalence and prediction. *The Journal of clinical psychiatry.* 2005;66(1):41-8.

`

137. Musselman DL, Lawson DH, Gumnick JF, Manatunga AK, Penna S, Goodkin RS, et al. Paroxetine for the prevention of depression induced by high-dose interferon alfa. *N Engl J Med.* 2001;344(13):961-6.
138. Sluzewska A, Rybakowski JK, Laciak M, Mackiewicz A, Sobieska M, and Wiktorowicz K. Interleukin-6 serum levels in depressed patients before and after treatment with fluoxetine. *Ann N Y Acad Sci.* 1995;762:474-6.
139. Alesci S, Martinez PE, Kelkar S, Ilias I, Ronsaville DS, Listwak SJ, et al. Major depression is associated with significant diurnal elevations in plasma interleukin-6 levels, a shift of its circadian rhythm, and loss of physiological complexity in its secretion: clinical implications. *The Journal of clinical endocrinology and metabolism.* 2005;90(5):2522-30.
140. Mikova O, Yakimova R, Bosmans E, Kenis G, and Maes M. Increased serum tumor necrosis factor alpha concentrations in major depression and multiple sclerosis. *European neuropsychopharmacology : the journal of the European College of Neuropsychopharmacology.* 2001;11(3):203-8.
141. Owen BM, Eccleston D, Ferrier IN, and Young AH. Raised levels of plasma interleukin-1beta in major and postviral depression. *Acta Psychiatr Scand.* 2001;103(3):226-8.
142. Thomas AJ, Davis S, Morris C, Jackson E, Harrison R, and O'Brien JT. Increase in interleukin-1beta in late-life depression. *Am J Psychiatry.* 2005;162(1):175-7.
143. Varnum MM, and Ikezu T. The classification of microglial activation phenotypes on neurodegeneration and regeneration in Alzheimer's disease brain. *Arch Immunol Ther Exp (Warsz).* 2012;60(4):251-66.
144. Hestad KA, Tonseth S, Stoen CD, Ueland T, and Aukrust P. Raised plasma levels of tumor necrosis factor alpha in patients with depression: normalization during electroconvulsive therapy. *The journal of ECT.* 2003;19(4):183-8.
145. Chen E, and Miller GE. Stress and inflammation in exacerbations of asthma. *Brain Behav Immun.* 2007;21(8):993-9.
146. Black PH, and Garbutt LD. Stress, inflammation and cardiovascular disease. *J Psychosom Res.* 2002;52(1):1-23.
147. Collins SM. Stress and the Gastrointestinal Tract IV. Modulation of intestinal inflammation by stress: basic mechanisms and clinical relevance. *Am J Physiol Gastrointest Liver Physiol.* 2001;280(3):G315-8.
148. Silverman MN, and Sternberg EM. Neuroendocrine-immune interactions in rheumatoid arthritis: mechanisms of glucocorticoid resistance. *Neuroimmunomodulation.* 2008;15(1):19-28.
149. Silverman MN, and Sternberg EM. Glucocorticoid regulation of inflammation and its functional correlates: from HPA axis to glucocorticoid receptor dysfunction. *Ann N Y Acad Sci.* 2012;1261:55-63.
150. Kumar R, and Thompson EB. Gene regulation by the glucocorticoid receptor: structure:function relationship. *The Journal of steroid biochemistry and molecular biology.* 2005;94(5):383-94.
151. Nelson G, Wilde GJ, Spiller DG, Kennedy SM, Ray DW, Sullivan E, et al. NF-kappaB signalling is inhibited by glucocorticoid receptor and STAT6 via distinct mechanisms. *Journal of cell science.* 2003;116(Pt 12):2495-503.
152. De Bosscher K, Vanden Berghe W, and Haegeman G. Cross-talk between nuclear receptors and nuclear factor kappaB. *Oncogene.* 2006;25(51):6868-86.
153. Barnes PJ. Corticosteroid effects on cell signalling. *The European respiratory journal.* 2006;27(2):413-26.
154. Heiss WD. The ischemic penumbra: correlates in imaging and implications for treatment of ischemic stroke. The Johann Jacob Wepfer award 2011. *Cerebrovasc Dis.* 2011;32(4):307-20.

155. Liang W, Ou Z, and Luo R. Solitaire Stent in the Treatment of Acute Ischemic Stroke with Large Cerebral Artery Occlusion. *Translational neuroscience.* 2017;8:97-101.
156. Pena ID, Borlongan C, Shen G, and Davis W. Strategies to Extend Thrombolytic Time Window for Ischemic Stroke Treatment: An Unmet Clinical Need. *J Stroke.* 2017;19(1):50-60.
157. O'Collins VE, Macleod MR, Donnan GA, Horky LL, van der Worp BH, and Howells DW. 1,026 experimental treatments in acute stroke. *Annals of neurology.* 2006;59(3):467-77.
158. Turner RC, Dodson SC, Rosen CL, and Huber JD. The science of cerebral ischemia and the quest for neuroprotection: navigating past failure to future success. *J Neurosurg.* 2013;118(5):1072-85.
159. Patel AR, Ritzel R, McCullough LD, and Liu F. Microglia and ischemic stroke: a double-edged sword. *Int J Physiol Pathophysiol Pharmacol.* 2013;5(2):73-90.
160. Szalay G, Martinecz B, Lenart N, Kornyei Z, Orsolits B, Judak L, et al. Microglia protect against brain injury and their selective elimination dysregulates neuronal network activity after stroke. *Nat Commun.* 2016;7:11499.
161. Erblich B, Zhu L, Etgen AM, Dobrenis K, and Pollard JW. Absence of colony stimulation factor-1 receptor results in loss of microglia, disrupted brain development and olfactory deficits. *PLoS One.* 2011;6(10):e26317.
162. Elmore MR, Najafi AR, Koike MA, Dagher NN, Spangenberg EE, Rice RA, et al. Colony-stimulating factor 1 receptor signaling is necessary for microglia viability, unmasking a microglia progenitor cell in the adult brain. *Neuron.* 2014;82(2):380-97.
163. Lalancette-Hébert M, Swarup V, Beaulieu JM, Bohacek I, Abdelhamid E, Weng YC, et al. Galectin-3 is required for resident microglia activation and proliferation in response to ischemic injury. *The Journal of Neuroscience.* 2012;32(30):10383-95.
164. Gowing G, Vallieres L, and Julien JP. Mouse model for ablation of proliferating microglia in acute CNS injuries. *Glia.* 2006;53(3):331-7.
165. Neumann H, Kotter MR, and Franklin RJ. Debris clearance by microglia: an essential link between degeneration and regeneration. *Brain.* 2009;132(Pt 2):288-95.
166. Neher JJ, Emmrich JV, Fricker M, Mander PK, Théry C, and Brown GC. Phagocytosis executes delayed neuronal death after focal brain ischemia. *Proceedings of the National Academy of Sciences.* 2013;110(43):E4098-E107.
167. Liu Z, Fan Y, Won SJ, Neumann M, Hu D, Zhou L, et al. Chronic treatment with minocycline preserves adult new neurons and reduces functional impairment after focal cerebral ischemia. *Stroke.* 2007;38(1):146-52.
168. Fan R, Xu F, Previti ML, Davis J, Grande AM, Robinson JK, et al. Minocycline reduces microglial activation and improves behavioral deficits in a transgenic model of cerebral microvascular amyloid. *J Neurosci.* 2007;27(12):3057-63.
169. Kobayashi K, Imagama S, Ohgomori T, Hirano K, Uchimura K, Sakamoto K, et al. Minocycline selectively inhibits M1 polarization of microglia. *Cell death & disease.* 2013;4:e525.
170. Scholz R, Sobotka M, Caramoy A, Stempfl T, Moehle C, and Langmann T. Minocycline counter-regulates pro-inflammatory microglia responses in the retina and protects from degeneration. *J Neuroinflammation.* 2015;12:209.
171. Tikka TM, and Koistinaho JE. Minocycline provides neuroprotection against N-methyl-D-aspartate neurotoxicity by inhibiting microglia. *Journal of immunology (Baltimore, Md : 1950).* 2001;166(12):7527-33.
172. Brugniaux JV, Schmitt L, Robach P, Nicolet G, Fouillot JP, Moutereau S, et al. Eighteen days of "living high, training low" stimulate erythropoiesis and enhance aerobic performance in elite middle-distance runners. *J Appl Physiol (1985).* 2006;100(1):203-11.

`

173. Wehrlin JP, Zuest P, Hallen J, and Marti B. Live high-train low for 24 days increases hemoglobin mass and red cell volume in elite endurance athletes. *J Appl Physiol (1985).* 2006;100(6):1938-45.
174. Rodriguez FA, Truijens MJ, Townsend NE, Stray-Gundersen J, Gore CJ, and Levine BD. Performance of runners and swimmers after four weeks of intermittent hypobaric hypoxic exposure plus sea level training. *J Appl Physiol (1985).* 2007;103(5):1523-35.
175. Faiss R, Girard O, and Millet GP. Advancing hypoxic training in team sports: from intermittent hypoxic training to repeated sprint training in hypoxia. *Br J Sports Med.* 2013;47 Suppl 1:i45-50.
176. Dempsey JA, and Morgan BJ. Humans In Hypoxia: A Conspiracy Of Maladaptation?! *Physiology (Bethesda).* 2015;30(4):304-16.
177. Serebrovskaya TV, and Xi L. Intermittent hypoxia training as non-pharmacologic therapy for cardiovascular diseases: Practical analysis on methods and equipment. *Exp Biol Med (Maywood).* 2016;241(15):1708-23.
178. Vinit S, Lovett-Barr MR, and Mitchell GS. Intermittent hypoxia induces functional recovery following cervical spinal injury. *Respir Physiol Neurobiol.* 2009;169(2):210-7.
179. Fuller DD, Johnson SM, Olson EB, Jr., and Mitchell GS. Synaptic pathways to phrenic motoneurons are enhanced by chronic intermittent hypoxia after cervical spinal cord injury. *J Neurosci.* 2003;23(7):2993-3000.
180. Astorino TA, Harness ET, and White AC. Efficacy of Acute Intermittent Hypoxia on Physical Function and Health Status in Humans with Spinal Cord Injury: A Brief Review. *Neural Plast.* 2015;2015:409625.
181. Dale EA, Ben Mabrouk F, and Mitchell GS. Unexpected benefits of intermittent hypoxia: enhanced respiratory and nonrespiratory motor function. *Physiology (Bethesda).* 2014;29(1):39-48.
182. Baillieul S, Chacaroun S, Doutreleau S, Detante O, Pepin JL, and Verges S. Hypoxic conditioning and the central nervous system: A new therapeutic opportunity for brain and spinal cord injuries? *Exp Biol Med (Maywood).* 2017;242(11):1198-206.
183. Trumbower RD, Jayaraman A, Mitchell GS, and Rymer WZ. Exposure to acute intermittent hypoxia augments somatic motor function in humans with incomplete spinal cord injury. *Neurorehabil Neural Repair.* 2012;26(2):163-72.
184. Hayes HB, Jayaraman A, Herrmann M, Mitchell GS, Rymer WZ, and Trumbower RD. Daily intermittent hypoxia enhances walking after chronic spinal cord injury: a randomized trial. *Neurology.* 2014;82(2):104-13.
185. Navarrete-Opazo A, Alcayaga J, Sepulveda O, Rojas E, and Astudillo C. Repetitive Intermittent Hypoxia and Locomotor Training Enhances Walking Function in Incomplete Spinal Cord Injury Subjects: A Randomized, Triple-Blind, Placebo-Controlled Clinical Trial. *Journal of neurotrauma.* 2017;34(9):1803-12.
186. Trumbower RD, Hayes HB, Mitchell GS, Wolf SL, and Stahl VA. Effects of acute intermittent hypoxia on hand use after spinal cord trauma: A preliminary study. *Neurology.* 2017;89(18):1904-7.
187. Mateika JH, El-Chami M, Shaheen D, and Ivers B. Intermittent hypoxia: a low-risk research tool with therapeutic value in humans. *J Appl Physiol (1985).* 2015;118(5):520-32.
188. Fu Y, Sun JL, Ma JF, Geng X, Sun J, Liu JR, et al. The neuroprotection of prodromal transient ischaemic attack on cerebral infarction. *Eur J Neurol.* 2008;15(8):797-801.
189. Wegener S, Gottschalk B, Jovanovic V, Knab R, Fiebach JB, Schellinger PD, et al. Transient ischemic attacks before ischemic stroke: preconditioning the human brain? A multicenter magnetic resonance imaging study. *Stroke.* 2004;35(3):616-21.
190. Moncayo J, de Freitas GR, Bogousslavsky J, Altieri M, and van Melle G. Do transient ischemic attacks have a neuroprotective effect? *Neurology.* 2000;54(11):2089-94.

`

191. Weih M, Kallenberg K, Bergk A, Dirnagl U, Harms L, Wernecke KD, et al. Attenuated stroke severity after prodromal TIA: a role for ischemic tolerance in the brain? *Stroke.* 1999;30(9):1851-4.
192. Schaller B, and Graf R. Cerebral ischemic preconditioning. An experimental phenomenon or a clinical important entity of stroke prevention? *J Neurol.* 2002;249(11):1503-11.
193. Schaller B, Graf R, and Jacobs AH. Ischaemic tolerance: a window to endogenous neuroprotection? *Lancet.* 2003;362(9389):1007-8.
194. Hadjikhani N, Sanchez Del Rio M, Wu O, Schwartz D, Bakker D, Fischl B, et al. Mechanisms of migraine aura revealed by functional MRI in human visual cortex. *Proc Natl Acad Sci U S A.* 2001;98(8):4687-92.
195. Schaller B. Ischemic preconditioning as induction of ischemic tolerance after transient ischemic attacks in human brain: its clinical relevance. *Neurosci Lett.* 2005;377(3):206-11.
196. Sandu N, Cornelius J, Filis A, Arasho B, Perez-Pinzon M, and Schaller B. Ischemic tolerance in stroke treatment. *Expert review of cardiovascular therapy.* 2009;7(10):1255-61.
197. Sharp FR, Ran R, Lu A, Tang Y, Strauss KI, Glass T, et al. Hypoxic preconditioning protects against ischemic brain injury. *NeuroRx.* 2004;1(1):26-35.
198. Leconte C, Tixier E, Freret T, Toutain J, Saulnier R, Boulouard M, et al. Delayed hypoxic postconditioning protects against cerebral ischemia in the mouse. *Stroke.* 2009;40(10):3349-55.
199. Zhu LL, Zhao T, Li HS, Zhao H, Wu LY, Ding AS, et al. Neurogenesis in the adult rat brain after intermittent hypoxia. *Brain Res.* 2005;1055(1-2):1-6.
200. Tsai YW, Yang YR, Sun SH, Liang KC, and Wang RY. Post ischemia intermittent hypoxia induces hippocampal neurogenesis and synaptic alterations and alleviates long-term memory impairment. *J Cereb Blood Flow Metab.* 2013;33(5):764-73.
201. Tsai YW, Yang YR, Wang PS, and Wang RY. Intermittent hypoxia after transient focal ischemia induces hippocampal neurogenesis and c-Fos expression and reverses spatial memory deficits in rats. *PLoS One.* 2011;6(8):e24001.
202. Zhan L, Liu L, Li K, Wu B, Liu D, Liang D, et al. Neuroprotection of hypoxic postconditioning against global cerebral ischemia through influencing posttranslational regulations of heat shock protein 27 in adult rats. *Brain pathology (Zurich, Switzerland).* 2017;27(6):822-38.
203. Zhan L, Li D, Liang D, Wu B, Zhu P, Wang Y, et al. Activation of Akt/FoxO and inactivation of MEK/ERK pathways contribute to induction of neuroprotection against transient global cerebral ischemia by delayed hypoxic postconditioning in adult rats. *Neuropharmacology.* 2012;63(5):873-82.
204. Zhu T, Zhan L, Liang D, Hu J, Lu Z, Zhu X, et al. Hypoxia-inducible factor 1alpha mediates neuroprotection of hypoxic postconditioning against global cerebral ischemia. *J Neuropathol Exp Neurol.* 2014;73(10):975-86.
205. Huang T, Huang W, Zhang Z, Yu L, Xie C, Zhu D, et al. Hypoxia-inducible factor-1alpha upregulation in microglia following hypoxia protects against ischemia-induced cerebral infarction. *Neuroreport.* 2014;25(14):1122-8.
206. Qiao Y, Liu Z, Yan X, and Luo C. Effect of intermittent hypoxia on neuro-functional recovery post brain ischemia in mice. *J Mol Neurosci.* 2015;55(4):923-30.
207. Teo JD, Morris MJ, and Jones NM. Hypoxic postconditioning reduces microglial activation, astrocyte and caspase activity, and inflammatory markers after hypoxia-ischemia in the neonatal rat brain. *Pediatr Res.* 2015;77(6):757-64.

`

208. Wise R, Gibbs J, Frackowiak R, Marshall J, and Jones T. No evidence for transhemispheric diaschisis after human cerebral infarction. *Stroke.* 1986;17(5):853-61.
209. Feeney DM, and Baron JC. Diaschisis. *Stroke.* 1986;17(5):817-30.
210. Carrera E, and Tononi G. Diaschisis: past, present, future. *Brain.* 2014;137(Pt 9):2408-22.
211. Gupta RK, Saksena S, Hasan KM, Agarwal A, Haris M, Pandey CM, et al. Focal Wallerian degeneration of the corpus callosum in large middle cerebral artery stroke: serial diffusion tensor imaging. *Journal of magnetic resonance imaging : JMRI.* 2006;24(3):549-55.
212. Thomalla G, Glauche V, Koch MA, Beaulieu C, Weiller C, and Rother J. Diffusion tensor imaging detects early Wallerian degeneration of the pyramidal tract after ischemic stroke. *NeuroImage.* 2004;22(4):1767-74.
213. Buss A, Brook GA, Kakulas B, Martin D, Franzen R, Schoenen J, et al. Gradual loss of myelin and formation of an astrocytic scar during Wallerian degeneration in the human spinal cord. *Brain.* 2004;127(Pt 1):34-44.
214. Buss A, Pech K, Merkler D, Kakulas BA, Martin D, Schoenen J, et al. Sequential loss of myelin proteins during Wallerian degeneration in the human spinal cord. *Brain.* 2005;128(Pt 2):356-64.
215. Johnson AC, Mc NA, and Rossiter RJ. Chemistry of wallerian degeneration; a review of recent studies. *Arch Neurol Psychiatry.* 1950;64(1):105-21.
216. Lampert PW, and Cressman MR. Fine-structural changes of myelin sheaths after axonal degeneration in the spinal cord of rats. *Am J Pathol.* 1966;49(6):1139-55.
217. Pierpaoli C, Barnett A, Pajevic S, Chen R, Penix LR, Virta A, et al. Water diffusion changes in Wallerian degeneration and their dependence on white matter architecture. *NeuroImage.* 2001;13(6 Pt 1):1174-85.
218. Thomalla G, Glauche V, Weiller C, and Rother J. Time course of wallerian degeneration after ischaemic stroke revealed by diffusion tensor imaging. *J Neurol Neurosurg Psychiatry.* 2005;76(2):266-8.
219. DeVetten G, Coutts SB, Hill MD, Goyal M, Eesa M, O'Brien B, et al. Acute corticospinal tract Wallerian degeneration is associated with stroke outcome. *Stroke.* 2010;41(4):751-6.
220. Radlinska B, Ghinani S, Leppert IR, Minuk J, Pike GB, and Thiel A. Diffusion tensor imaging, permanent pyramidal tract damage, and outcome in subcortical stroke. *Neurology.* 2010;75(12):1048-54.
221. Liang Z, Zeng J, Liu S, Ling X, Xu A, Yu J, et al. A prospective study of secondary degeneration following subcortical infarction using diffusion tensor imaging. *J Neurol Neurosurg Psychiatry.* 2007;78(6):581-6.
222. Hinman JD. The back and forth of axonal injury and repair after stroke. *Curr Opin Neurol.* 2014;27(6):615-23.
223. Tamura A, Tahira Y, Nagashima H, Kirino T, Gotoh O, Hojo S, et al. Thalamic atrophy following cerebral infarction in the territory of the middle cerebral artery. *Stroke.* 1991;22(5):615-8.
224. Ogawa T, Yoshida Y, Okudera T, Noguchi K, Kado H, and Uemura K. Secondary thalamic degeneration after cerebral infarction in the middle cerebral artery distribution: evaluation with MR imaging. *Radiology.* 1997;204(1):255-62.
225. Nakane M, Tamura A, Sasaki Y, and Teraoka A. MRI of secondary changes in the thalamus following a cerebral infarct. *Neuroradiology.* 2002;44(11):915-20.
226. Li C, Ling X, Liu S, Xu A, Zhang Y, Xing S, et al. Early detection of secondary damage in ipsilateral thalamus after acute infarction at unilateral corona radiata by diffusion tensor imaging and magnetic resonance spectroscopy. *BMC Neurology.* 2011;11(1):49.

`

227. Herve D, Molko N, Pappata S, Buffon F, LeBihan D, Bousser MG, et al. Longitudinal thalamic diffusion changes after middle cerebral artery infarcts. *J Neurol Neurosurg Psychiatry.* 2005;76(2):200-5.
228. De Bilbao F, Guarin E, Nef P, Vallet P, Giannakopoulos P, and Dubois-Dauphin M. Cell death is prevented in thalamic fields but not in injured neocortical areas after permanent focal ischaemia in mice overexpressing the anti-apoptotic protein Bcl-2. *The European journal of neuroscience.* 2000;12(3):921-34.
229. Schroeter M, Zickler P, Denhardt DT, Hartung HP, and Jander S. Increased thalamic neurodegeneration following ischaemic cortical stroke in osteopontin-deficient mice. *Brain.* 2006;129(Pt 6):1426-37.
230. Zhang J, Zhang Y, Xing S, Liang Z, and Zeng J. Secondary neurodegeneration in remote regions after focal cerebral infarction: a new target for stroke management? *Stroke.* 2012;43(6):1700-5.
231. Binkofski F, Seitz RJ, Arnold S, Classen J, Benecke R, and Freund HJ. Thalamic metbolism and corticospinal tract integrity determine motor recovery in stroke. *Annals of neurology.* 1996;39(4):460-70.
232. Fernandez-Andujar M, Doornink F, Dacosta-Aguayo R, Soriano-Raya JJ, Miralbell J, Bargallo N, et al. Remote thalamic microstructural abnormalities related to cognitive function in ischemic stroke patients. *Neuropsychology.* 2014;28(6):984-96.
233. Seitz RJ, Azari NP, Knorr U, Binkofski F, Herzog H, and Freund HJ. The role of diaschisis in stroke recovery. *Stroke.* 1999;30(9):1844-50.
234. Hunnicutt BJ, Long BR, Kusefoglu D, Gertz KJ, Zhong H, and Mao T. A comprehensive thalamocortical projection map at the mesoscopic level. *Nat Neurosci.* 2014;17(9):1276-85.
235. Baron JC, Yamauchi H, Fujioka M, and Endres M. Selective neuronal loss in ischemic stroke and cerebrovascular disease. *J Cereb Blood Flow Metab.* 2014;34(1):2-18.
236. Loos M, Dihne M, and Block F. Tumor necrosis factor-alpha expression in areas of remote degeneration following middle cerebral artery occlusion of the rat. *Neuroscience.* 2003;122(2):373-80.
237. Ashkar S, Weber GF, Panoutsakopoulou V, Sanchirico ME, Jansson M, Zawaideh S, et al. Eta-1 (osteopontin): an early component of type-1 (cell-mediated) immunity. *Science.* 2000;287(5454):860-4.
238. Guo H, Cai CQ, Schroeder RA, and Kuo PC. Osteopontin is a negative feedback regulator of nitric oxide synthesis in murine macrophages. *Journal of immunology (Baltimore, Md : 1950).* 2001;166(2):1079-86.
239. Chabas D, Baranzini SE, Mitchell D, Bernard CC, Rittling SR, Denhardt DT, et al. The influence of the proinflammatory cytokine, osteopontin, on autoimmune demyelinating disease. *Science.* 2001;294(5547):1731-5.
240. Xing S, Zhang Y, Li J, Zhang J, Li Y, Dang C, et al. Beclin 1 knockdown inhibits autophagic activation and prevents the secondary neurodegenerative damage in the ipsilateral thalamus following focal cerebral infarction. *Autophagy.* 2012;8(1):63-76.
241. Ross DT, and Ebner FF. Thalamic retrograde degeneration following cortical injury: an excitotoxic process? *Neuroscience.* 1990;35(3):525-50.
242. Christopherson KS, Hillier BJ, Lim WA, and Bredt DS. PSD-95 assembles a ternary complex with the N-methyl-D-aspartic acid receptor and a bivalent neuronal NO synthase PDZ domain. *The Journal of biological chemistry.* 1999;274(39):27467-73.
243. Liu PK, Robertson CS, and Valadka A. The association between neuronal nitric oxide synthase and neuronal sensitivity in the brain after brain injury. *Ann N Y Acad Sci.* 2002;962:226-41.

244. Davis SM, Lees KR, Albers GW, Diener HC, Markabi S, Karlsson G, et al. Selfotel in acute ischemic stroke : possible neurotoxic effects of an NMDA antagonist. *Stroke.* 2000;31(2):347-54.
245. Ikonomidou C, and Turski L. Why did NMDA receptor antagonists fail clinical trials for stroke and traumatic brain injury? *Lancet Neurol.* 2002;1(6):383-6.
246. Cook DJ, Teves L, and Tymianski M. Treatment of stroke with a PSD-95 inhibitor in the gyrencephalic primate brain. *Nature.* 2012;483(7388):213-7.
247. Tymianski M. Emerging mechanisms of disrupted cellular signaling in brain ischemia. *Nat Neurosci.* 2011;14(11):1369-73.
248. Dietrich WD, Busto R, Watson BD, Scheinberg P, and Ginsberg MD. Photochemically induced cerebral infarction. II. Edema and blood-brain barrier disruption. *Acta Neuropathol.* 1987;72(4):326-34.
249. Sommer CJ. Ischemic stroke: experimental models and reality. *Acta Neuropathol.* 2017;133(2):245-61.
250. Bidmon HJ, Jancsik V, Schleicher A, Hagemann G, Witte OW, Woodhams P, et al. Structural alterations and changes in cytoskeletal proteins and proteoglycans after focal cortical ischemia. *Neuroscience.* 1998;82(2):397-420.
251. Dihne M, Grommes C, Lutzenburg M, Witte OW, and Block F. Different mechanisms of secondary neuronal damage in thalamic nuclei after focal cerebral ischemia in rats. *Stroke.* 2002;33(12):3006-11.
252. Calcia MA, Bonsall DR, Bloomfield PS, Selvaraj S, Barichello T, and Howes OD. Stress and neuroinflammation: a systematic review of the effects of stress on microglia and the implications for mental illness. *Psychopharmacology (Berl).* 2016;233(9):1637-50.
253. Zhang L, Zhang ZG, Zhang RL, Lu M, Krams M, and Chopp M. Effects of a selective CD11b/CD18 antagonist and recombinant human tissue plasminogen activator treatment alone and in combination in a rat embolic model of stroke. *Stroke.* 2003;34(7):1790-5.
254. Prestigiacomo CJ, Kim SC, Connolly ES, Jr., Liao H, Yan SF, and Pinsky DJ. CD18-mediated neutrophil recruitment contributes to the pathogenesis of reperfused but not nonreperfused stroke. *Stroke.* 1999;30(5):1110-7.
255. Kohler E, Prentice DA, Bates TR, Hankey GJ, Claxton A, van Heerden J, et al. Intravenous minocycline in acute stroke: a randomized, controlled pilot study and meta-analysis. *Stroke.* 2013;44(9):2493-9.
256. Medzhitov R. Recognition of microorganisms and activation of the immune response. *Nature.* 2007;449(7164):819-26.
257. Dantzer R, O'Connor JC, Freund GG, Johnson RW, and Kelley KW. From inflammation to sickness and depression: when the immune system subjugates the brain. *Nat Rev Neurosci.* 2008;9(1):46-56.
258. Benton T, Staab J, and Evans DL. Medical co-morbidity in depressive disorders. *Annals of clinical psychiatry : official journal of the American Academy of Clinical Psychiatrists.* 2007;19(4):289-303.
259. Brites D, and Fernandes A. Neuroinflammation and Depression: Microglia Activation, Extracellular Microvesicles and microRNA Dysregulation. *Front Cell Neurosci.* 2015;9:476.
260. Saha RN, and Pahan K. Regulation of inducible nitric oxide synthase gene in glial cells. *Antioxidants & redox signaling.* 2006;8(5-6):929-47.
261. Kreisel T, Frank MG, Licht T, Reshef R, Ben-Menachem-Zidon O, Baratta MV, et al. Dynamic microglial alterations underlie stress-induced depressive-like behavior and suppressed neurogenesis. *Mol Psychiatry.* 2014;19(6):699-709.

`

262. Hinwood M, Tynan RJ, Charnley JL, Beynon SB, Day TA, and Walker FR. Chronic stress induced remodeling of the prefrontal cortex: structural re-organization of microglia and the inhibitory effect of minocycline. *Cereb Cortex.* 2013;23(8):1784-97.
263. Westhoff MA, Zhou S, Bachem MG, Debatin KM, and Fulda S. Identification of a novel switch in the dominant forms of cell adhesion-mediated drug resistance in glioblastoma cells. *Oncogene.* 2008;27(39):5169-81.
264. Adamson IY, King GM, and Young L. Influence of extracellular matrix and collagen components on alveolar type 2 cell morphology and function. *In vitro cellular & developmental biology : journal of the Tissue Culture Association.* 1989;25(6):494-502.
265. Lu P, Takai K, Weaver VM, and Werb Z. Extracellular matrix degradation and remodeling in development and disease. *Cold Spring Harbor perspectives in biology.* 2011;3(12).
266. Frantz C, Stewart KM, and Weaver VM. The extracellular matrix at a glance. *Journal of cell science.* 2010;123(Pt 24):4195-200.
267. Thivolet CH, Chatelain P, Nicoloso H, Durand A, and Bertrand J. Morphological and functional effects of extracellular matrix on pancreatic islet cell cultures. *Experimental cell research.* 1985;159(2):313-22.
268. Hansen NU, Genovese F, Leeming DJ, and Karsdal MA. The importance of extracellular matrix for cell function and in vivo likeness. *Experimental and molecular pathology.* 2015;98(2):286-94.
269. Krishnan V, and Nestler EJ. Animal models of depression: molecular perspectives. *Curr Top Behav Neurosci.* 2011;7:121-47.
270. Campos AC, Fogaca MV, Aguiar DC, and Guimaraes FS. Animal models of anxiety disorders and stress. *Rev Bras Psiquiatr.* 2013;35 Suppl 2:S101-11.
271. Zhao Z, Ong LK, Johnson S, Nilsson M, and Walker FR. Chronic stress induced disruption of the peri-infarct neurovascular unit following experimentally induced photothrombotic stroke. *J Cereb Blood Flow Metab.* 2017;37(12):3709-24.
272. Jones KA, Zouikr I, Patience M, Clarkson AN, Isgaard J, Johnson SJ, et al. Chronic stress exacerbates neuronal loss associated with secondary neurodegeneration and suppresses microglial-like cells following focal motor cortex ischemia in the mouse. *Brain Behav Immun.* 2015;48:57-67.
273. Ong LK, Zhao Z, Kluge M, Walker FR, and Nilsson M. Chronic stress exposure following photothrombotic stroke is associated with increased levels of Amyloid beta accumulation and altered oligomerisation at sites of thalamic secondary neurodegeneration in mice. *J Cereb Blood Flow Metab.* 2016.
274. Glavin GB, Pare WP, Sandbak T, Bakke HK, and Murison R. Restraint stress in biomedical research: an update. *Neurosci Biobehav Rev.* 1994;18(2):223-49.
275. Buynitsky T, and Mostofsky DI. Restraint stress in biobehavioral research: Recent developments. *Neurosci Biobehav Rev.* 2009;33(7):1089-98.
276. Toth I, and Neumann ID. Animal models of social avoidance and social fear. *Cell Tissue Res.* 2013;354(1):107-18.
277. Rybkin, II, Zhou Y, Volaufova J, Smagin GN, Ryan DH, and Harris RB. Effect of restraint stress on food intake and body weight is determined by time of day. *Am J Physiol.* 1997;273(5 Pt 2):R1612-22.
278. Chotiwat C, Kelso EW, and Harris RB. The effects of repeated restraint stress on energy balance and behavior of mice with selective deletion of CRF receptors. *Stress.* 2010;13(3):203-13.
279. Jeong JY, Lee DH, and Kang SS. Effects of chronic restraint stress on body weight, food intake, and hypothalamic gene expressions in mice. *Endocrinol Metab (Seoul).* 2013;28(4):288-96.

280. Pare WP, and Glavin GB. Restraint stress in biomedical research: a review. *Neurosci Biobehav Rev.* 1986;10(3):339-70.
281. Krugers HJ, Lucassen PJ, Karst H, and Joels M. Chronic stress effects on hippocampal structure and synaptic function: relevance for depression and normalization by anti-glucocorticoid treatment. *Front Synaptic Neurosci.* 2010;2:24.
282. Narayanan R, and Chattarji S. Computational analysis of the impact of chronic stress on intrinsic and synaptic excitability in the hippocampus. *J Neurophysiol.* 2010;103(6):3070-83.
283. Stewart MG, Davies HA, Sandi C, Kraev IV, Rogachevsky VV, Peddie CJ, et al. Stress suppresses and learning induces plasticity in CA3 of rat hippocampus: a three-dimensional ultrastructural study of thorny excrescences and their postsynaptic densities. *Neuroscience.* 2005;131(1):43-54.
284. Joels M, Karst H, Alfarez D, Heine VM, Qin Y, van Riel E, et al. Effects of chronic stress on structure and cell function in rat hippocampus and hypothalamus. *Stress.* 2004;7(4):221-31.
285. Dong H, Goico B, Martin M, Csernansky CA, Bertchume A, and Csernansky JG. Modulation of hippocampal cell proliferation, memory, and amyloid plaque deposition in APPsw (Tg2576) mutant mice by isolation stress. *Neuroscience.* 2004;127(3):601-9.
286. Gould E, and Tanapat P. Stress and hippocampal neurogenesis. *Biol Psychiatry.* 1999;46(11):1472-9.
287. Moser E, Moser MB, and Andersen P. Spatial learning impairment parallels the magnitude of dorsal hippocampal lesions, but is hardly present following ventral lesions. *J Neurosci.* 1993;13(9):3916-25.
288. Bellani R, Luecken LJ, and Conrad CD. Peripubertal anxiety profile can predict predisposition to spatial memory impairments following chronic stress. *Behav Brain Res.* 2006;166(2):263-70.
289. Sousa N, Lukoyanov NV, Madeira MD, Almeida OF, and Paula-Barbosa MM. Reorganization of the morphology of hippocampal neurites and synapses after stress-induced damage correlates with behavioral improvement. *Neuroscience.* 2000;97(2):253-66.
290. Conrad CD, Galea LA, Kuroda Y, and McEwen BS. Chronic stress impairs rat spatial memory on the Y maze, and this effect is blocked by tianeptine pretreatment. *Behav Neurosci.* 1996;110(6):1321-34.
291. Kim DM, and Leem YH. Chronic stress-induced memory deficits are reversed by regular exercise via AMPK-mediated BDNF induction. *Neuroscience.* 2016;324:271-85.
292. Mehta V, Parashar A, and Udayabanu M. Quercetin prevents chronic unpredictable stress induced behavioral dysfunction in mice by alleviating hippocampal oxidative and inflammatory stress. *Physiol Behav.* 2017;171:69-78.
293. Pearson-Leary J, Eacret D, Chen R, Takano H, Nicholas B, and Bhatnagar S. Inflammation and vascular remodeling in the ventral hippocampus contributes to vulnerability to stress. *Transl Psychiatry.* 2017;7(6):e1160.
294. Wang YL, Han QQ, Gong WQ, Pan DH, Wang LZ, Hu W, et al. Microglial activation mediates chronic mild stress-induced depressive- and anxiety-like behavior in adult rats. *J Neuroinflammation.* 2018;15(1):21.
295. Seil FJ. The extracellular matrix molecule, laminin, induces purkinje cell dendritic spine proliferation in granule cell depleted cerebellar cultures. *Brain Res.* 1998;795(1-2):112-20.
296. Plantman S, Patarroyo M, Fried K, Domogatskaya A, Tryggvason K, Hammarberg H, et al. Integrin-laminin interactions controlling neurite outgrowth from adult DRG neurons in vitro. *Mol Cell Neurosci.* 2008;39(1):50-62.

`

297. Flanagan LA, Rebaza LM, Derzic S, Schwartz PH, and Monuki ES. Regulation of human neural precursor cells by laminin and integrins. *J Neurosci Res.* 2006;83(5):845-56.
298. Levy AD, Omar MH, and Koleske AJ. Extracellular matrix control of dendritic spine and synapse structure and plasticity in adulthood. *Front Neuroanat.* 2014;8:116.
299. Dansie LE, and Ethell IM. Casting a net on dendritic spines: the extracellular matrix and its receptors. *Dev Neurobiol.* 2011;71(11):956-81.
300. Thyboll J, Kortesmaa J, Cao R, Soininen R, Wang L, Iivanainen A, et al. Deletion of the laminin alpha4 chain leads to impaired microvessel maturation. *Mol Cell Biol.* 2002;22(4):1194-202.
301. Chen ZL, Yao Y, Norris EH, Kruyer A, Jno-Charles O, Akhmerov A, et al. Ablation of astrocytic laminin impairs vascular smooth muscle cell function and leads to hemorrhagic stroke. *J Cell Biol.* 2013;202(2):381-95.
302. Yurchenco PD, Quan Y, Colognato H, Mathus T, Harrison D, Yamada Y, et al. The alpha chain of laminin-1 is independently secreted and drives secretion of its beta- and gamma-chain partners. *Proc Natl Acad Sci U S A.* 1997;94(19):10189-94.
303. Lai AY, and Todd KG. Microglia in cerebral ischemia: molecular actions and interactions. *Can J Physiol Pharmacol.* 2006;84(1):49-59.
304. Wood PL. Microglia as a unique cellular target in the treatment of stroke: potential neurotoxic mediators produced by activated microglia. *Neurol Res.* 1995;17(4):242-8.
305. Yang GY, Gong C, Qin Z, Ye W, Mao Y, and Bertz AL. Inhibition of TNFalpha attenuates infarct volume and ICAM-1 expression in ischemic mouse brain. *Neuroreport.* 1998;9(9):2131-4.
306. Yamasaki Y, Matsuura N, Shozuhara H, Onodera H, Itoyama Y, and Kogure K. Interleukin-1 as a pathogenetic mediator of ischemic brain damage in rats. *Stroke.* 1995;26(4):676-80; discussion 81.
307. Boutin H, LeFeuvre RA, Horai R, Asano M, Iwakura Y, and Rothwell NJ. Role of IL-1alpha and IL-1beta in ischemic brain damage. *J Neurosci.* 2001;21(15):5528-34.
308. Zhang N, Komine-Kobayashi M, Tanaka R, Liu M, Mizuno Y, and Urabe T. Edaravone reduces early accumulation of oxidative products and sequential inflammatory responses after transient focal ischemia in mice brain. *Stroke.* 2005;36(10):2220-5.
309. Yrjanheikki J, Tikka T, Keinanen R, Goldsteins G, Chan PH, and Koistinaho J. A tetracycline derivative, minocycline, reduces inflammation and protects against focal cerebral ischemia with a wide therapeutic window. *Proc Natl Acad Sci U S A.* 1999;96(23):13496-500.
310. Schilling M, Besselmann M, Muller M, Strecker JK, Ringelstein EB, and Kiefer R. Predominant phagocytic activity of resident microglia over hematogenous macrophages following transient focal cerebral ischemia: an investigation using green fluorescent protein transgenic bone marrow chimeric mice. *Exp Neurol.* 2005;196(2):290-7.
311. Ramprasad MP, Terpstra V, Kondratenko N, Quehenberger O, and Steinberg D. Cell surface expression of mouse macrosialin and human CD68 and their role as macrophage receptors for oxidized low density lipoprotein. *Proc Natl Acad Sci U S A.* 1996;93(25):14833-8.
312. Neher JJ, Neniskyte U, Zhao JW, Bal-Price A, Tolkovsky AM, and Brown GC. Inhibition of microglial phagocytosis is sufficient to prevent inflammatory neuronal death. *Journal of immunology (Baltimore, Md : 1950).* 2011;186(8):4973-83.
313. Nakada Y, Canseco DC, Thet S, Abdisalaam S, Asaithamby A, Santos CX, et al. Hypoxia induces heart regeneration in adult mice. *Nature.* 2017;541(7636):222-7.
314. Galle AA, and Jones NM. The neuroprotective actions of hypoxic preconditioning and postconditioning in a neonatal rat model of hypoxic-ischemic brain injury. *Brain Res.* 2013;1498:1-8.

315. Rybnikova E, Vorobyev M, Pivina S, and Samoilov M. Postconditioning by mild hypoxic exposures reduces rat brain injury caused by severe hypoxia. *Neurosci Lett.* 2012;513(1):100-5.
316. Miller FD, and Kaplan DR. Neurotrophin signalling pathways regulating neuronal apoptosis. *Cellular and molecular life sciences : CMLS.* 2001;58(8):1045-53.
317. Zhang Y, and Pardridge WM. Blood-brain barrier targeting of BDNF improves motor function in rats with middle cerebral artery occlusion. *Brain Res.* 2006;1111(1):227-9.
318. Schabitz WR, Steigleder T, Cooper-Kuhn CM, Schwab S, Sommer C, Schneider A, et al. Intravenous brain-derived neurotrophic factor enhances poststroke sensorimotor recovery and stimulates neurogenesis. *Stroke.* 2007;38(7):2165-72.
319. Schabitz WR, Berger C, Kollmar R, Seitz M, Tanay E, Kiessling M, et al. Effect of brain-derived neurotrophic factor treatment and forced arm use on functional motor recovery after small cortical ischemia. *Stroke.* 2004;35(4):992-7.
320. Chen A, Xiong LJ, Tong Y, and Mao M. The neuroprotective roles of BDNF in hypoxic ischemic brain injury. *Biomedical reports.* 2013;1(2):167-76.
321. Weber JT. Altered calcium signaling following traumatic brain injury. *Frontiers in pharmacology.* 2012;3:60.
322. Kluge MG, Kracht L, Abdolhoseini M, Ong LK, Johnson SJ, Nilsson M, et al. Impaired microglia process dynamics post-stroke are specific to sites of secondary neurodegeneration. *Glia.* 2017;65(12):1885-99.
323. Rupalla K, Allegrini PR, Sauer D, and Wiessner C. Time course of microglia activation and apoptosis in various brain regions after permanent focal cerebral ischemia in mice. *Acta Neuropathol.* 1998;96(2):172-8.
324. Zuo X, Hou Q, Jin J, Zhan L, Li X, Sun W, et al. Inhibition of Cathepsin B Alleviates Secondary Degeneration in Ipsilateral Thalamus After Focal Cerebral Infarction in Adult Rats. *J Neuropathol Exp Neurol.* 2016;75(9):816-26.
325. Viaene AN, Petrof I, and Sherman SM. Properties of the thalamic projection from the posterior medial nucleus to primary and secondary somatosensory cortices in the mouse. *Proc Natl Acad Sci U S A.* 2011;108(44):18156-61.
326. Diamond ME. In: Jones EG, and Diamond IT eds. *The Barrel Cortex of Rodents*. Boston, MA: Springer US; 1995:189-219.
327. Piserchio A, Salinas GD, Li T, Marshall J, Spaller MR, and Mierke DF. Targeting specific PDZ domains of PSD-95; structural basis for enhanced affinity and enzymatic stability of a cyclic peptide. *Chem Biol.* 2004;11(4):469-73.
328. Ayata C, Ayata G, Hara H, Matthews RT, Beal MF, Ferrante RJ, et al. Mechanisms of reduced striatal NMDA excitotoxicity in type I nitric oxide synthase knock-out mice. *J Neurosci.* 1997;17(18):6908-17.
329. Cui H, Hayashi A, Sun HS, Belmares MP, Cobey C, Phan T, et al. PDZ protein interactions underlying NMDA receptor-mediated excitotoxicity and neuroprotection by PSD-95 inhibitors. *J Neurosci.* 2007;27(37):9901-15.
330. Braeuninger S, and Kleinschnitz C. Rodent models of focal cerebral ischemia: procedural pitfalls and translational problems. *Exp Transl Stroke Med.* 2009;1:8.
331. Koizumi J YY, Nakazawa T, Ooneda G. Experimental studies of ischemic brain edema, I: a new experimental model of cerebral embolism in rats in which recirculation can be introduced in the ischemic area. *Jpn J Stroke.* 1986;8:1-8.
332. Clark WM, Lessov NS, Dixon MP, and Eckenstein F. Monofilament intraluminal middle cerebral artery occlusion in the mouse. *Neurol Res.* 1997;19(6):641-8.
333. Kanemitsu H, Nakagomi T, Tamura A, Tsuchiya T, Kono G, and Sano K. Differences in the extent of primary ischemic damage between middle cerebral artery coagulation and intraluminal occlusion models. *Journal of cerebral blood flow and metabolism :*

`

official journal of the International Society of Cerebral Blood Flow and Metabolism. 2002;22(10):1196-204.

334. Schmid-Elsaesser R, Zausinger S, Hungerhuber E, Baethmann A, and Reulen HJ. A critical reevaluation of the intraluminal thread model of focal cerebral ischemia: evidence of inadvertent premature reperfusion and subarachnoid hemorrhage in rats by laser-Doppler flowmetry. *Stroke; a journal of cerebral circulation.* 1998;29(10):2162-70.
335. Steele EC, Jr., Guo Q, and Namura S. Filamentous middle cerebral artery occlusion causes ischemic damage to the retina in mice. *Stroke; a journal of cerebral circulation.* 2008;39(7):2099-104.
336. Dittmar M, Spruss T, Schuierer G, and Horn M. External carotid artery territory ischemia impairs outcome in the endovascular filament model of middle cerebral artery occlusion in rats. *Stroke; a journal of cerebral circulation.* 2003;34(9):2252-7.
337. McColl BW, Carswell HV, McCulloch J, and Horsburgh K. Extension of cerebral hypoperfusion and ischaemic pathology beyond MCA territory after intraluminal filament occlusion in C57Bl/6J mice. *Brain Res.* 2004;997(1):15-23.
338. Masaki T, and Yanagisawa M. Endothelins. *Essays Biochem.* 1992;27:79-89.
339. Adkins-Muir DL, and Jones TA. Cortical electrical stimulation combined with rehabilitative training: enhanced functional recovery and dendritic plasticity following focal cortical ischemia in rats. *Neurol Res.* 2003;25(8):780-8.
340. Hughes PM, Anthony DC, Ruddin M, Botham MS, Rankine EL, Sablone M, et al. Focal lesions in the rat central nervous system induced by endothelin-1. *J Neuropathol Exp Neurol.* 2003;62(12):1276-86.
341. Nakagomi S, Kiryu-Seo S, and Kiyama H. Endothelin-converting enzymes and endothelin receptor B messenger RNAs are expressed in different neural cell species and these messenger RNAs are coordinately induced in neurons and astrocytes respectively following nerve injury. *Neuroscience.* 2000;101(2):441-9.
342. Naidoo V, Naidoo S, Mahabeer R, and Raidoo DM. Cellular distribution of the endothelin system in the human brain. *J Chem Neuroanat.* 2004;27(2):87-98.
343. Carmichael ST. Rodent models of focal stroke: size, mechanism, and purpose. *NeuroRx : the journal of the American Society for Experimental NeuroTherapeutics.* 2005;2(3):396-409.
344. Wood NI, Sopesen BV, Roberts JC, Pambakian P, Rothaul AL, Hunter AJ, et al. Motor dysfunction in a photothrombotic focal ischaemia model. *Behav Brain Res.* 1996;78(2):113-20.
345. Li H, Zhang N, Lin HY, Yu Y, Cai QY, Ma L, et al. Histological, cellular and behavioral assessments of stroke outcomes after photothrombosis-induced ischemia in adult mice. *BMC Neurosci.* 2014;15:58.
346. Watson BD, Dietrich WD, Busto R, Wachtel MS, and Ginsberg MD. Induction of reproducible brain infarction by photochemically initiated thrombosis. *Ann Neurol.* 1985;17(5):497-504.
347. Lee JK, Park MS, Kim YS, Moon KS, Joo SP, Kim TS, et al. Photochemically induced cerebral ischemia in a mouse model. *Surg Neurol.* 2007;67(6):620-5; discussion 5.
348. Labat-gest V, and Tomasi S. Photothrombotic ischemia: a minimally invasive and reproducible photochemical cortical lesion model for mouse stroke studies. *J Vis Exp.* 2013(76).
349. Dheen ST, Kaur C, and Ling EA. Microglial activation and its implications in the brain diseases. *Curr Med Chem.* 2007;14(11):1189-97.
350. Booth J, Connelly L, Lawrence M, Chalmers C, Joice S, Becker C, et al. Evidence of perceived psychosocial stress as a risk factor for stroke in adults: a meta-analysis. *BMC Neurol.* 2015;15:233.

`

351. Al-Harbi KS. Treatment-resistant depression: therapeutic trends, challenges, and future directions. *Patient preference and adherence.* 2012;6:369-88.
352. Penn E, and Tracy DK. The drugs don't work? antidepressants and the current and future pharmacological management of depression. *Therapeutic advances in psychopharmacology.* 2012;2(5):179-88.

`

Appendix 1 additional publications

Publication 4

Title: Normobaric post-conditioning hypoxia improves stroke-induced cognitive impairment through improved glymphatic flow

Manuscript number: STROKE/2018/021491

Author(s): Zidan Zhao
Lin Kooi Ong
Giovanni Pietrogrande
Ole Ottersen
Sarah Johnson
Michael Nilsson
Frederick Walker

Normobaric post-conditioning hypoxia improves stroke-induced cognitive impairment through improved glymphatic flow.

Zidan Zhao, PhD

School of Biomedical Sciences and Pharmacy and Priority Research Centre for Stroke and Brain Injury, University of Newcastle, NSW, Australia. Hunter Medical Research Institute, NSW, Australia.

Lin Kooi Ong, PhD

School of Biomedical Sciences and Pharmacy and Priority Research Centre for Stroke and Brain Injury, University of Newcastle, NSW, Australia. Hunter Medical Research Institute, NSW, Australia. NHMRC Centre of Research Excellence Stroke Rehabilitation and Brain Recovery, Australia.

Giovanni Pietrogrande, MSc

School of Biomedical Sciences and Pharmacy and Priority Research Centre for Stroke and Brain Injury, University of Newcastle, NSW, Australia. Hunter Medical Research Institute, NSW, Australia.

Ole P. Ottersen, PhD

Division of Anatomy, Department of Molecular Medicine, Institute of Basic Medical Sciences, University of Oslo, Norway.

Sarah J Johnson, PhD

School of Electrical Engineering and Computing, University of Newcastle, NSW, Australia.

Michael Nilsson, MD, PhD†

Priority Research Centre for Stroke and Brain Injury, University of Newcastle, NSW, Australia. Hunter Medical Research Institute, NSW, Australia. NHMRC Centre of Research Excellence Stroke Rehabilitation and Brain Recovery, Australia.

Frederick R Walker, PhD†

School of Biomedical Sciences and Pharmacy and Priority Research Centre for Stroke and Brain Injury, University of Newcastle, NSW, Australia. Hunter Medical Research Institute, NSW, Australia. NHMRC Centre of Research Excellence Stroke Rehabilitation and Brain Recovery, Australia.

Address for correspondence: University of Newcastle, Callaghan, NSW, Australia. Phone: +612 4921 5012; Email: rohan.walker@newcastle.edu.au

† Contributed equally to senior authorship.

Cover title: Normobaric hypoxia promotes post-stroke cognition

Figures = 6

Keywords: Stroke recovery, glymphatic system, neurovascular unit, amyloid-beta, cognitive function

Word Count = 6536

Abstract

Background and Purpose – Cognitive impairment is a common and disruptive outcome for stroke survivors. Deterioration in cognitive function post-stroke has proven to be notoriously difficult to treat. Although little is understood about the potential mechanisms involved, recent studies on traumatic brain injury have suggested that changes in glymphatic clearance may be involved.

Methods – Experimental stroke was induced by photothrombotic occlusion in adult mice. Firstly, we assessed the effects of stroke on glymphatic flow and the cellular structures that support normal glymphatic flow. Secondly, we considered whether exposure to delayed normobaric post-conditioning mild hypoxia could improve these deficits, as it is one the few experimental interventions previously shown to improve cognitive function post-stroke. We additionally assessed cognitive performance using a rodent touchscreen platform.

Results – Utilising real time in vivo imaging we established for the first time that experimental stroke reduced glymphatic flow at 17 days post-stroke, an effect that was underpinned by reduced Aquaporin-4 (AQP4) polarisation, marked accumulation of soluble amyloid-beta oligomers, and significant learning and memory impairment. Exposure to mild hypoxia post-stroke (for either 8h or 24h/day for 14 days) improved nearly all deficits induced by stroke including the reduction in glymphatic flow. Most importantly, stroked animals exposed to hypoxia exhibited robust improvements in cognitive function post-stroke, assessed using a touchscreen based paired-associate learning task.

Conclusions – These findings provide compelling pre-clinical evidence of the potential clinical utility of normobaric mild hypoxic exposure for enhancing recovery post-stroke.

Introduction

Stroke is the leading cause of long-term disability in the world.[1] While the nature of disability load post-stroke is heterogeneous and complex, a major common problem is cognitive impairment.[2] However, there are currently no generally accepted interventions for improving cognition post-stroke.[3, 4] Notwithstanding the paucity of demonstrated clinical interventions, there has been substantive and on-going efforts to develop approaches that could safely promote improved cognitive performance post-stroke.[5, 6]

A promising approach identified so far as a potential pro-cognitive stimulus is intermittent exposure to a reduced oxygen environment. A compelling body of literature has clearly described the neuroprotective actions of transient exposure to hypoxia when delivered prior to ischemic injury (an intervention often referred to as pre-conditioning hypoxia).[7] The effectiveness of the procedure in contexts where ischemic events are predictable has in turn led several research teams to consider whether the same neuroprotective benefits could be obtained in the hypoxia procedure was deployed post-ischemic injury (i.e. post-conditioning).[7] It has been shown that the transient reduction of inspired oxygen can enhance levels of neurogenesis and long term memory function.[8-12] Tsai et al. has demonstrated that delayed intermittent hypoxia appears to have utility in the context of stroke, with mice exposed to hypoxia post-stroke exhibiting significant improvements in learning and memory as well as in neurogenesis and synaptogenesis.[10] Different hypoxia exposure protocols are already widely used to enhance athletic physical performance. For example, athletes from various sporting codes have identified that living at high altitude, usually for between 2 to 6 weeks, can translate into significantly enhanced athletic performance at sea level.[13] While several physiological adaptions are triggered by exposure to hypoxia, it is considered that the main drivers of improved performance are the enhancements that occur in erythropoiesis and

angiogenesis,[14, 15] systems that have been consistently targeted in the context of promoting recovery from brain injury.[16-19]

One of the major question relating to reduced oxygen environments following stroke is how the therapeutic benefits are mediated. An interesting possibility is that the intervention enhances glymphatic mediated interstitial bulk flow processes (otherwise referred to as glymphatic flow). Glymphatic flow refers to the recently described trafficking of cerebrospinal fluid through the peri-arterial space and subsequent transit via astrocytic Aquaporin-4 (AQP4) into and out of the parenchyma.[20, 21] A known benefit of glymphatic flow is the removal of soluble amyloid-β (Aβ), a protein known for its significant neurotoxic potential.[20] Of relevance, disturbances in glymphatic flow have been observed in experimental models of traumatic brain injury[22] and micro-emboli[23] but have not yet been reported in the context of experimental stroke. Impairment of glymphatic flow, however, could explain the significant levels of soluble Aβ accumulation that we and others have observed after stroke.[24-28] Further, increased levels of soluble Aβ accumulation, and in particular high molecular weight oligomers have been linked to cognitive decline.[29, 30]

In the current study we had two major objectives. The first was to examine how stroke influenced glymphatic flow and the cellular structures that support normal glymphatic flow. Specifically, we examined changes in vascular density, AQP4 polarization, and glymphatic flow, as well as the levels of soluble Aβ. Secondly, we examined whether exposure to delayed normobaric mild hypoxia (dHPX) (11% oxygen, either 8h or 24h/day for 14 days) could modulate glymphatic flow dynamics post-stroke. We also assessed cognitive performance using a rodent touchscreen platform for paired-associate learning (PAL) task.

Materials and Methods

The data that support the findings of this study are available from the corresponding author(s) upon reasonable request. A detailed materials and methods section is available in the online-only Data Supplement.

Ethical statements

Animal research was undertaken in accordance to the ARRIVE guidelines. Experiments were approved by the University of Newcastle Animal Care and Ethics Committee (A-2013-338), and conducted in accordance with the New South Wales Animals Research Act and the Australian Code of Practice for the use of animals for scientific purposes.

Experimental design

A total of 144 C57BL/6 adult male mice were each randomly allocated to one of the following four groups: sham, stroke, stroke with exposure to 8h/daily of hypoxia (dHPX 8h), and stroke with 24h/daily of hypoxia (dHPX 24h). The first cohort of 32 mice (8 per group) were used for behavioural testing, the second cohort of 32 mice (8 per group) were used for fixed tissue analysis (immunohistochemistry), the third cohort of 32 mice (8 per group) was used for western blotting analysis, the fourth cohort of 32 mice (8 per group) was used for PCR analysis, and the last cohort of 16 mice (4 per group) were used for real time in vivo imaging. Brains and blood samples were collected at day 17 post-stroke. All outcome analyses were performed by independent study team members blinded to the treatment condition.

Animal surgery and delayed normobaric post-conditioning mild hypoxia

Photothrombotic vascular occlusion was performed as described.[25, 31] Mice were subjected to the hypoxic environment starting at 3 days post-stroke. Hypoxic exposure was achieved using a customized ventilated cage racking system that was retrofitted to accept 11% oxygen, provided by a pressure swing adaptor based hypoxic generator. The levels for CO_2 were monitored and remained at atmospheric levels with a concentration of (~350ppm) and normal sea level atmospheric pressure (101kPa) within the conditioned chambers. Mice from the two hypoxic exposure conditions, dHPX 8h and dHPX 24h groups were maintained in hypoxic environment for either 8h (10am to 6pm) or 24h daily for two weeks, respectively.

Assessment of cognitive deficits

Mice were subjected to the mouse touchscreen platform for paired-associate learning (PAL) task to assess the associative memory cognitive domain.[32, 33]

Haematocrit assessment

Blood haematocrit levels were measured using the i-STAT system and CG8 cartridges (Abbott Point of Care).

Histology and immunohistochemistry analysis

For immunoperoxidase labelling, free floating sections were immunostained as described.[31, 34] Images were acquired at 20 X using Aperio AT2 (Leica, Germany). ImageJ (1.50, NIH) and Matlab (R2015a, MathWorks) were used to estimate tissue loss, cell count, APQ4 vessel/parenchymal ratio, and to analyse intensity of immunolabelling.[25, 31, 35-37]

Biochemical analysis

Protein homogenates from the peri-infarct samples were obtained and Western blotting was performed as described.[25, 31] RNA was isolated from the peri-infarct samples using the Illustra RNAspin Kit (GE Healthcare, Cat# 25-0500-70) according to manufacturer's specifications. Quantitative RT-PCR was performed as described.[38]

In vivo confocal scanning microscopy

Intracisternal tracer injection and in vivo confocal laser scanning microscopy were performed as previously described with minor modification.[20]

Statistical analysis

All data for sham, stroke, dHPX 8h, and dHPX 24h groups were expressed as mean±SEM and were analysed using Prism 6 for Windows Version 6.01, GraphPad Software. Two-way ANOVA was used to determine whether there were time and treatment effects across groups in the PAL touchscreen task and in vivo imaging experiments. All other experiments used a One-Way ANOVA to determine whether there were any significant treatment effects across the groups. Additional Tukey multiple comparisons, which controls family wise error, were used to analyse differences between the mean of each group with the mean of every other group. The significant differences shown on the graphs with asterisks (*) refer to the post hoc tests. All differences were considered to be significant at $p<0.05$.

Results

dHPX increases haematocrit in mice

To confirm the effect of our normobaric hypoxic exposure protocol, the haematocrit in mice was measured. We identified that there was no significant difference between sham and stroke mice (0.38±0.006 vs. 0.38±0.005, $p=0.97$). The stroked dHPX 8h (0.48±0.005) and dHPX 24h (0.49±0.008) animals had a significantly higher haematocrit than stroke only animals ($p<0.001$ and $p<0.001$, respectively).

dHPX ameliorates the cognitive function deficit after stroke

Three days after stroke, animals started dHPX 8h or 24h daily respectively. At the same time, they performed PAL touch screen task daily.

Repeat trials per task: Analysis of the number of repeated trials per task revealed a significant main effect for group ($F=77.90$, $p<0.001$) and time ($F=6.36$, $p<0.01$) but no significant interaction. In Week 1, stroked animals performed significantly more repeated trials when compared to the sham ($p<0.01$), dHPX 8h ($p<0.05$) and dHPX 24h ($p<0.05$) groups. In the second week of training stroked animals still performed a greater number of repeated trials when compared to sham ($p<0.05$), however there was no significant difference between stroke and dHPX 8h animals ($p=0.08$) or dHPX 24h animals ($p=0.07$) (Figure. 1C).

% of correct responses: Analysis of the % of correct responses indicated that there was a main effect for each of treatment group ($F=118.3$, $p<0.001$) and time ($F=4.16$, $p<0.05$). The interaction term between the factors did not achieve significance ($F=1.17$, $p=0.3$). In the second week of testing we identified that the animals exposed to stroke performed significantly lower than both the sham and dHPX groups ($p<0.05$) (Figure. 1D). There were no differences between the two dHPX conditions.

dHPX reduces tissue loss and neuron loss after stroke

The average volume of tissue loss in the dHPX 8h and dHPX 24h animals was significantly smaller than observed in stroke only animals ($F=25.35$, $p<0.001$ and $p<0.001$, respectively, Figure 2C). Mature neuron marker NeuN labelling was also used to assess the neuron loss in the peri-infarct region after stroke. ANOVA indicated that photothrombotic stroke significantly reduced the number of NeuN positive cells in the peri-infarct territory, compared to sham animals ($F=21.30$, $p<0.001$), while both dHPX 8h and dHPX 24h limited the reduction of NeuN positive cells compared to the stroke only animals ($p<0.05$ and $p<0.05$, respectively. Figure 2D).

dHPX promotes NVU remodelling and reduces IgG leakage after stroke

To investigate how dHPX influenced the NVU remodelling in the peri-infarct territory following stroke, the blood vessel marker Collagen IV, astrocyte marker GFAP and microglia marker Iba-1 were used. For the thresholding analysis, the data for each group was expressed as a fold increase of the mean±SEM for each group relative to the mean of the sham group (for cumulative threshold analysis see Figure II in the online-only Data Supplement). The thresholding analysis indicated that stroke resulted in a significant decrease in the formation of vessels labelled by Collagen IV ($F=28.47$, $p<0.05$, Figure 3A), but this response was substantially improved by exposure to dHPX 8h and 24h ($p<0.001$ and $p<0.001$, Figure 3B). The thresholding analysis of glial markers, GFAP and Iba-1, demonstrated a similar pattern. Stroke alone induced a significant increase in both GFAP and Iba-1 relative to sham animals ($F=84.95$, $p<0.001$ and $F=31.72$, $p<0.01$, respectively), and dHPX 8h and dHPX 24h exhibited modestly elevated levels of both GFAP and Iba-1 relative to stroked animals ($p<0.01$ and $p<0.01$, respectively. Figure 3C and D).

Blood vessel leakage was assessed by IgG staining in the peri-infarct regions. For the thresholding analysis, ANOVA indicated that photothrombosis drove a significant increase in IgG ($F=13.87$, $p<0.001$) compared to sham animals. This increase was improved significantly by exposure to dHPX 24h ($p<0.001$), but there was no significant difference between dHPX 8h and stroke only animals ($p=0.45$, Figure 3B).

dHPX reduces Aβ oligomer accumulation after stroke

The tissue samples from the peri-infarct territory were analysed by western blot using anti-Aβ for soluble Aβ oligomers. The results for Aβ oligomers at 56kDa (dodecamer), 50kDa (decamer), 25kDa (pentamer), 5kDa (monomer) and total Aβ (5-200kDa) levels were normalized to β-actin as loading control (Figure 4A). The data for all groups were expressed as a fold increase of the mean±SEM for each group relative to the mean of the sham group. All Aβ oligomers showed similar patterns. Specifically, at 56kDa, 50kDa, 25kDa, and total Aβ levels, were elevated in the stroke group relative to sham animals ($F=10.44$, $p<0.001$; $F=28.60$, $p<0.001$; $F=12.10$, $p<0.001$ and $F=12.14$, $p<0.001$, respectively). Both the dHPX 8h and dHPX 24h displayed lower levels of oligomerization relative to the stroke alone condition (dHPX 8h; $p<0.05$, $p<0.001$, $p<0.05$, $p<0.05$ and dHPX 24h; $p<0.01$, $p<0.001$, $p<0.05$, $p<0.001$, respectively). At 5kDa level, stroke induced a significant increase relative to sham animals ($F=3.01$, $p<0.05$) but there was no significant difference compared to dHPX 8h and dHPX 24h ($p=0.23$ and $p=0.15$, respectively).

dHPX facilitates CSF Flow through the brain parenchyma and the clearance of small molecule.

The fluorescent intensity of the CSF tracer (AF 594, red) along the paravascular space was assessed over time. The first image taken was used as the baseline, and the following images

at 30-min intervals were analysed to calculate the relative fluorescence change from baseline for 2 hours. Two-way ANOVA noted significant differences for group x time interaction ($F=11.11$, $p<0.001$), groups ($F=13.18$, $p<0.001$), and time ($F=11.59$, $p<0.001$). Over 2h, sham, dHPX 8h and dHPX 24h animals all showed significantly reduced florescence compared to their baseline level ($p<0.001$, $p<0.001$ and $p<0.001$ respectively, Figure 5D), while stroke only animals demonstrated a significant increase in fluorescence compared to its baseline ($p<0.001$). Specifically at 135min, the relative florescence change of stroke alone animals was significantly higher than sham, dHPX 8h and dHPX 24h animals ($p<0.001$, $p<0.001$ and $p<0.001$ respectively, Figure 5D).

dHPX improves AQP4 polarization after stroke

The AQP4 polarization was calculated as the ratio of AQP4 labelling on the vessel wall to that in the parenchymal tissue directly adjacent to the vessel. One-way ANOVA indicated that compared to sham animals, the AQP4 polarization in peri-infarct regions of stroke was reduced significantly ($F=29.46$, $p<0.001$), but this reduction was improved by both dHPX 8h and dHPX 24h ($p<0.05$ and $p<0.05$ respectively, Figure 6).

Discussion

In the current study we have shown, for the first time that a focal cortical photothrombotic stroke is associated with significant impairment of glymphatic flow, in addition to producing marked disturbances in the key cellular components responsible for supporting glymphatic flow. We have further determined that transient exposure to normobaric hypoxia substantially ameliorates stroke-induced deficits in glymphatic flow. Co-incident with these improvements we have also further determined that normobaric hypoxic exposure lowers the burden of soluble Aβ and improves cognitive function as assessed through the touchscreen delivered paired-associate learning (PAL) task.

We were motivated to consider glymphatic flow in the context of stroke for a number of reasons. Firstly, glymphatic flow has been demonstrated to play an important role in the removal of waste products from the brain, including the removal of the highly neurotoxic protein Aβ. Specifically, it has been demonstrated that glymphatic mediated waste clearance [20, 39] involves the movement of the water component of CSF from the paravascular space into the parenchyma through AQP4 water channels, potentially creating a convective and/or solute gradient that flushes metabolic waste, including proteins such as Aβ, towards the venous surfaces whereby it is removed from the brain by active or passive transport processes.[20, 21] Illif et al. have documented that experimentally induced traumatic brain injury (TBI) disrupts glymphatic flow.[22] Specifically, the authors identified using real time in vivo imaging that TBI reduces glymphatic flow, and further determined that this impairment was partly dependent upon the disruption of regular polarisation of AQP4 to the vascular surface. A similar observation has recently also been reported in an experimental model of cholesterol-induced micro-emboli.[23]

Given the apparent consistency with which quite distinct models of brain injury-induced glymphatic disturbances we considered it worthwhile to investigate whether stroke

would do the same. We examined glymphatic flow using real time in vivo imaging.[20] This procedure involves introducing a small molecular weight dye (Alexa Fluor 594, 758.79 Da) into the cisterna magna, which is known to supply CSF into the paravascular space, and imaging the dye efflux into the parenchyma via a thin skull window (see Figure 5 and V in the online-only Data Supplement). We imaged dye efflux every 30 min over the course of 2 h. The analysis of changes in flow indicated that sham animals cleared the dye steadily exhibiting a reduction of nearly 70% by the final observation point. In contrast, parenchymal fluorescence was observed to increase in animals exposed to stroke and unlike the sham condition did not substantially dissipate, indicating impaired glymphatic flow in these animals. We further identified that stroked animals exposed to dHPX exhibited a robust improvement in glymphatic clearance relative to the stroke alone group, and were found to have similar rates of clearance at 2 h compared to sham non-stroked animals. Together, these results indicate that stroke induces a deficit in glymphatic flow and that dHPX effectively corrects this deficit.

Amongst the most likely mechanisms involved in mediating the changes in glymphatic flow observed with stroke and normobaric hypoxia were changes in AQP4 polarization.[21] Significant disturbances in AQP4, have been identified previously, occurring across the first 72 h post-stroke.[40] In the context of TBI, changes in AQP4 polarisation have been linked to reductions in glymphatic flow.[22] Interestingly, the disturbances in AQP4 polarisation in the tg-ArcSwe mouse model of Alzheimer's disease have been linked to the accumulation of Aβ.[41] Of particular relevance, we observed that exposure to hypoxia resulted in a substantial improvement in AQP4 polarisation in stroke animals. The changes in AQP4 polarisation associated with hypoxia led us to consider the vasculature, as arterioles and venules effectively act as the scaffold upon which the perivascular space is structured. Here we identified that those animals exposed to hypoxia after stroke exhibited a robust increase in

capillary density relative to the stroke alone group. Furthermore, we identified that in addition to increasing vascular density hypoxia appeared to limit stroke induced blood barrier leakage, as indicated by reduced IgG leakage into the parenchyma. We also identified that hypoxic exposure elicited a mild stimulatory effect on microglia and astrocytes, which is of note given these cells described roles in repair.[42, 43] The generation of a neurotrophic environment is also supported by the fact that hypoxic exposure was associated with less tissue loss and greater neuronal density in the damaged hemisphere. We would propose that these results suggest that hypoxia acts as a neurotrophic and pro-angiogenic stimulus. Together, this encourages the development of new vessels and in doing so, facilitates restoration of AQP4 polarisation and improved glymphatic flow.

Stroke-induced dysfunction of glymphatic flow and AQP4 polarisation provides a robust explanation for the accumulation of Aβ after stroke.[22, 41] Considering the ability of hypoxic exposure to improve glymphatic flow, and AQP4 polarisation we reasoned that it may also be able to reduce the Aβ burden. As expected we identified that stroked animals exhibit greater levels of the soluble oligomers of Aβ. In comparison, stroked animals exposed to hypoxia exhibited significant reductions in total levels of Aβ, as well as exhibiting specific reductions in 25, 50 and 56 kDa oligomers relative to the stroke alone condition. To our knowledge, this is the first report to demonstrate that exposure to normobaric hypoxia is capable of inducing robust decreases in total levels of amyloid and reducing aggregation of soluble Aβ oligomers post-stroke.

While improved glymphatic clearance represents a pathway through which hypoxia may trigger Aβ removal, it is also possible that the intervention altered other clearance pathways. Accordingly, we investigated changes in the expression levels of several key genes involved in the generation, degradation and export of Aβ (Figure IV in the online-only Data Supplement). Here we identified that hypoxic exposure normalized stroke induced

disturbances in amyloid precursor protein and beta-secretase mRNA expression but did not influence the expression of TNFα converting enzyme, neprilysin, or insulin-degrading enzyme. Modest elevations were observed in dHPX 8 h exposed animals over stroke alone in mRNA expression of the transport protein low density lipoprotein receptor-related protein-1 and the receptor for advanced glycation end products. Together these results suggest dHPX does not reduce Aβ through reducing rates of production or degradation but rather indicates that it occurs through enhanced transportation.[44]

Finally, we considered changes in cognitive function post-stroke using the paired-associate learning (PAL) task. The PAL test is a well described cognitive assessment task and was chosen as PAL deficits have been identified in patients post-stroke and in the earliest stages of Alzheimer's disease.[45-47] The rodent version of the PAL task used in the current study has been validated as a sensitive tool for identifying complex cognitive deficits in rodents.[32] We identified that mice exposed to stroke exhibited robust deficits in two key metrics, namely the % of correct trials performed, which is considered to reference both learning and memory[32], and the number of repeated trials, which is considered to index perseveration.[48, 49] Both the hypoxic exposure paradigms limited these deficits to a level that was not different from that observed in sham animals. These findings align well with previous data illustrating the effectiveness of hypoxic exposure to enhance long term memory performance in rats/mice following stroke.[9, 10]

The findings from the current study provide several critical advances upon existing knowledge. Firstly, we have identified that stroke is associated with persistent disturbances in critical components that support glymphatic flow, including blood vessels and AQP4 polarisation. Extending from this we have directly identified that stroke is associated with a significant reduction in glymphatic flow. To our knowledge, this is the first time that these impairments have been reported. Our findings also align particularly well with prior work

examining glymphatic disturbances following other forms of brain injury.[22, 23] Secondly, we have demonstrated that exposure to normobaric hypoxia beginning 72 h after stroke improves the glymphatic apparatus as well as glymphatic flow. Perhaps most significantly, this improvement is coupled with a significant decrease in the accumulation of Aβ oligomers. Functionally, these improvements in glymphatic flow and Aβ reduction are significant, as we have identified that animals exposed to hypoxia post-stroke also exhibit substantial improvements in cognitive function, as assessed through the PAL task.

Conclusions

The ability of hypoxia exposure (pre-conditioning and post-conditioning) has long been recognised to be potently neuroprotective.[7, 50] Indeed, the therapeutic effects do not appear to be confined to the CNS, with Nakada et al., recently demonstrating the effectiveness of hypoxic exposure to improve heart regeneration following cardio myocyte loss.[51] One of the principle advantages associated with reduced oxygen exposure interventions is that the approach triggers system-wide compensatory adaptions. In addition to stimulating significant vascular growth, hypoxia was identified to improve glymphatic flow, reduce Aβ loading and enhance cognitive performance. Given, that stroke is known to trigger cognitive impairment and under certain circumstance trigger the emergence of dementia-like symptoms[26], a therapeutic strategy to reduce Aβ and improve cognitive performance is highly desirable. As several human specific technologies already exist for controlled hypoxic exposure, it is not inconceivable that future safety trials for this promising pro-cognitive intervention could be undertaken rapidly.

Acknowledgments

We express our gratitude to HMRI Core Histology Facility for assistance with the immunohistochemistry images. We also would like to acknowledge the insights and comments provided by Prof Jorgen Isgaard and Prof Neil Spratt on early versions of the manuscript.

Sources of Funding

This study was supported by the NHMRC project grant (APP1142862), Hunter Medical Research Institute, The Brawn Bequest, Priority Research Centre for Stroke and Brain Injury Research Support Grant, Faculty of Health and Medicine Pilot Grant and University of Newcastle, Australia.

Disclosures

None.

References

1. Thrift AG, Cadilhac DA, Thayabaranathan T, Howard G, Howard VJ, Rothwell PM, et al. Global stroke statistics. *Int J Stroke*. 2014;9:6-18
2. Levine DA, Galecki AT, Langa KM, Unverzagt FW, Kabeto MU, Giordani B, et al. Trajectory of cognitive decline after incident stroke. *JAMA*. 2015;314:41-51
3. Chung CS, Pollock A, Campbell T, Durward BR, Hagen S. Cognitive rehabilitation for executive dysfunction in adults with stroke or other adult non-progressive acquired brain damage. *Cochrane Database Syst Rev*. 2013:CD008391
4. Loetscher T, Lincoln NB. Cognitive rehabilitation for attention deficits following stroke. *Cochrane Database Syst Rev*. 2013:CD002842
5. Shigaki CL, Frey SH, Barrett AM. Rehabilitation of poststroke cognition. *Semin Neurol*. 2014;34:496-503
6. Sun JH, Tan L, Yu JT. Post-stroke cognitive impairment: Epidemiology, mechanisms and management. *Ann Transl Med*. 2014;2:80
7. Baillieul S, Chacaroun S, Doutreleau S, Detante O, Pepin JL, Verges S. Hypoxic conditioning and the central nervous system: A new therapeutic opportunity for brain and spinal cord injuries? *Exp Biol Med (Maywood)*. 2017;242:1198-1206
8. Leconte C, Tixier E, Freret T, Toutain J, Saulnier R, Boulouard M, et al. Delayed hypoxic postconditioning protects against cerebral ischemia in the mouse. *Stroke*. 2009;40:3349-3355
9. Tsai YW, Yang YR, Wang PS, Wang RY. Intermittent hypoxia after transient focal ischemia induces hippocampal neurogenesis and c-fos expression and reverses spatial memory deficits in rats. *PLoS One*. 2011;6:e24001
10. Tsai YW, Yang YR, Sun SH, Liang KC, Wang RY. Post ischemia intermittent hypoxia induces hippocampal neurogenesis and synaptic alterations and alleviates long-term memory impairment. *J Cereb Blood Flow Metab*. 2013;33:764-773
11. Galle AA, Jones NM. The neuroprotective actions of hypoxic preconditioning and postconditioning in a neonatal rat model of hypoxic-ischemic brain injury. *Brain Res*. 2013;1498:1-8
12. Rybnikova E, Vorobyev M, Pivina S, Samoilov M. Postconditioning by mild hypoxic exposures reduces rat brain injury caused by severe hypoxia. *Neurosci Lett*. 2012;513:100-105
13. Faiss R, Girard O, Millet GP. Advancing hypoxic training in team sports: From intermittent hypoxic training to repeated sprint training in hypoxia. *Br J Sports Med*. 2013;47 Suppl 1:i45-50
14. Brugniaux JV, Schmitt L, Robach P, Nicolet G, Fouillot JP, Moutereau S, et al. Eighteen days of "living high, training low" stimulate erythropoiesis and enhance aerobic performance in elite middle-distance runners. *J Appl Physiol (1985)*. 2006;100:203-211
15. Wehrlin JP, Zuest P, Hallen J, Marti B. Live high-train low for 24 days increases hemoglobin mass and red cell volume in elite endurance athletes. *J Appl Physiol (1985)*. 2006;100:1938-1945
16. LaManna JC, Vendel LM, Farrell RM. Brain adaptation to chronic hypobaric hypoxia in rats. *J Appl Physiol (1985)*. 1992;72:2238-2243
17. Shweiki D, Itin A, Soffer D, Keshet E. Vascular endothelial growth factor induced by hypoxia may mediate hypoxia-initiated angiogenesis. *Nature*. 1992;359:843-845
18. Boroujerdi A, Milner R. Defining the critical hypoxic threshold that promotes vascular remodeling in the brain. *Exp Neurol*. 2015;263:132-140

19. Howell K, Preston RJ, McLoughlin P. Chronic hypoxia causes angiogenesis in addition to remodelling in the adult rat pulmonary circulation. *J Physiol*. 2003;547:133-145
20. Iliff JJ, Wang M, Liao Y, Plogg BA, Peng W, Gundersen GA, et al. A paravascular pathway facilitates csf flow through the brain parenchyma and the clearance of interstitial solutes, including amyloid beta. *Sci Transl Med*. 2012;4:147ra111
21. Nagelhus EA, Ottersen OP. Physiological roles of aquaporin-4 in brain. *Physiol Rev*. 2013;93:1543-1562
22. Iliff JJ, Chen MJ, Plog BA, Zeppenfeld DM, Soltero M, Yang L, et al. Impairment of glymphatic pathway function promotes tau pathology after traumatic brain injury. *J Neurosci*. 2014;34:16180-16193
23. Wang M, Ding F, Deng S, Guo X, Wang W, Iliff JJ, et al. Focal solute trapping and global glymphatic pathway impairment in a murine model of multiple microinfarcts. *J Neurosci*. 2017;37:2870-2877
24. Liu W, Wong A, Au L, Yang J, Wang Z, Leung EY, et al. Influence of amyloid-beta on cognitive decline after stroke/transient ischemic attack: Three-year longitudinal study. *Stroke*. 2015;46:3074-3080
25. Ong LK, Zhao Z, Kluge M, Walker FR, Nilsson M. Chronic stress exposure following photothrombotic stroke is associated with increased levels of amyloid beta accumulation and altered oligomerisation at sites of thalamic secondary neurodegeneration in mice. *J Cereb Blood Flow Metab*. 2017;37:1338-1348
26. Ong LK, Walker FR, Nilsson M. Is stroke a neurodegenerative condition? A critical review of secondary neurodegeneration and amyloid-beta accumulation after stroke. *AIMS Medical Science*. 2017;4:1-16
27. Aho L, Jolkkonen J, Alafuzoff I. Beta-amyloid aggregation in human brains with cerebrovascular lesions. *Stroke*. 2006;37:2940-2945
28. van Groen T, Puurunen K, Maki HM, Sivenius J, Jolkkonen J. Transformation of diffuse beta-amyloid precursor protein and beta-amyloid deposits to plaques in the thalamus after transient occlusion of the middle cerebral artery in rats. *Stroke*. 2005;36:1551-1556
29. Lesne S, Koh MT, Kotilinek L, Kayed R, Glabe CG, Yang A, et al. A specific amyloid-beta protein assembly in the brain impairs memory. *Nature*. 2006;440:352-357
30. Lesne SE, Sherman MA, Grant M, Kuskowski M, Schneider JA, Bennett DA, et al. Brain amyloid-beta oligomers in ageing and alzheimer's disease. *Brain*. 2013;136:1383-1398
31. Zhao Z, Ong LK, Johnson S, Nilsson M, Walker FR. Chronic stress induced disruption of the peri-infarct neurovascular unit following experimentally induced photothrombotic stroke. *J Cereb Blood Flow Metab*. 2017:271678X17696100
32. Horner AE, Heath CJ, Hvoslef-Eide M, Kent BA, Kim CH, Nilsson SR, et al. The touchscreen operant platform for testing learning and memory in rats and mice. *Nat Protoc*. 2013;8:1961-1984
33. Oomen CA, Hvoslef-Eide M, Heath CJ, Mar AC, Horner AE, Bussey TJ, et al. The touchscreen operant platform for testing working memory and pattern separation in rats and mice. *Nat Protoc*. 2013;8:2006-2021
34. Tynan RJ, Naicker S, Hinwood M, Nalivaiko E, Buller KM, Pow DV, et al. Chronic stress alters the density and morphology of microglia in a subset of stress-responsive brain regions. *Brain, behavior, and immunity*. 2010;24:1058-1068
35. Johnson SJ, Walker FR. Strategies to improve quantitative assessment of immunohistochemical and immunofluorescent labelling. *Sci Rep*. 2015;5:10607

36. Kongsui R, Johnson SJ, Graham BA, Nilsson M, Walker FR. A combined cumulative threshold spectra and digital reconstruction analysis reveal structural alterations of microglia within the prefrontal cortex following low-dose lps administration. *Neuroscience*. 2015;310:629-640
37. Ong LK, Zhao Z, Kluge M, TeBay C, Zalewska K, Dickson PW, et al. Reconsidering the role of glial cells in chronic stress-induced dopaminergic neurons loss within the substantia nigra? Friend or foe? *Brain, behavior, and immunity*. 2017;60:117-125
38. Pietrogrande G, Mabotuwana N, Zhao Z, Abdolhoseini M, Johnson SJ, Nilsson M, et al. Chronic stress induced disturbances in laminin: A significant contributor to modulating microglial pro-inflammatory tone? *Brain, behavior, and immunity*. 2018;68:23-33
39. Xie L, Kang H, Xu Q, Chen MJ, Liao Y, Thiyagarajan M, et al. Sleep drives metabolite clearance from the adult brain. *Science*. 2013;342:373-377
40. Frydenlund DS, Bhardwaj A, Otsuka T, Mylonakou MN, Yasumura T, Davidson KG, et al. Temporary loss of perivascular aquaporin-4 in neocortex after transient middle cerebral artery occlusion in mice. *Proc Natl Acad Sci U S A*. 2006;103:13532-13536
41. Yang J, Lunde LK, Nuntagij P, Oguchi T, Camassa LM, Nilsson LN, et al. Loss of astrocyte polarization in the tg-arcswe mouse model of alzheimer's disease. *J Alzheimers Dis*. 2011;27:711-722
42. Szalay G, Martinecz B, Lenart N, Kornyei Z, Orsolits B, Judak L, et al. Microglia protect against brain injury and their selective elimination dysregulates neuronal network activity after stroke. *Nat Commun*. 2016;7:11499
43. Li L, Lundkvist A, Andersson D, Wilhelmsson U, Nagai N, Pardo AC, et al. Protective role of reactive astrocytes in brain ischemia. *J Cereb Blood Flow Metab*. 2008;28:468-481
44. Storck SE, Meister S, Nahrath J, Meissner JN, Schubert N, Di Spiezio A, et al. Endothelial lrp1 transports amyloid-beta(1-42) across the blood-brain barrier. *J Clin Invest*. 2016;126:123-136
45. Pergola G, Gunturkun O, Koch B, Schwarz M, Daum I, Suchan B. Recall deficits in stroke patients with thalamic lesions covary with damage to the parvocellular mediodorsal nucleus of the thalamus. *Neuropsychologia*. 2012;50:2477-2491
46. Weinstein G, Preis SR, Beiser AS, Au R, Kelly-Hayes M, Kase CS, et al. Cognitive performance after stroke--the framingham heart study. *Int J Stroke*. 2014;9 Suppl A100:48-54
47. Barnett JH, Lewis L, Blackwell AD, Taylor M. Early intervention in alzheimer's disease: A health economic study of the effects of diagnostic timing. *BMC Neurol*. 2014;14:101
48. Montgomery C, Fisk JE, Newcombe R. The nature of ecstasy-group related deficits in associative learning. *Psychopharmacology (Berl)*. 2005;180:141-149
49. Rich JB, Campodonico JR, Rothlind J, Bylsma FW, Brandt J. Perseverations during paired-associate learning in huntington's disease. *J Clin Exp Neuropsychol*. 1997;19:191-203
50. Ergul A, Alhusban A, Fagan SC. Angiogenesis: A harmonized target for recovery after stroke. *Stroke*. 2012;43:2270-2274
51. Nakada Y, Canseco DC, Thet S, Abdisalaam S, Asaithamby A, Santos CX, et al. Hypoxia induces heart regeneration in adult mice. *Nature*. 2017;541:222-227

Figure Legends.

Figure 1. Illustration of the paired-associate learning (PAL) task. (A) The Campden Instruments touchscreen chamber apparatus. To obtain the strawberry milkshake reward, the animal needs to choose the correct stimulus on the touchscreen. **(B)** An illustration of the two different trial types and the correct location object pairing (red crosses) in PAL. Bar graphs show the animals' performance of the four groups, sham, stroke, dHPX 8h and dHPX 24h in **(C)** the number of repeated trials per PAL task and **(D)** the correct rate. Data expressed as mean±SEM for n=8 per group. ns: not significant, *p<0.05, **p<0.01 (one-way ANOVA followed by Tukey's multiple comparisons).

Figure 2. Illustration of the neural tissue loss. (A) The location of the infarct (red circle) and the four different levels (dash lines) chosen for tissue loss analysis. **(B)** The stroke sections from Bregma +1.0mm to Bregma -2.0mm. **(C)** The bar graph shows that dHPX 8h and dHPX 24h animals had smaller % tissue loss, compared to the stroke only animals. % Tissue loss was calculated as (Contralateral hemisphere size – ipsilateral hemisphere size) / contralateral hemisphere size x 100%. **(D)** Four left images illustrate representative labelling for NeuN for the four groups, sham, stroke, dHPX 8h and dHPX 24h. The right bar graph illustrates the number of NeuN positive cells for four groups. Data expressed as mean±SEM for n=8 per group. ***p<0.001 (one-way ANOVA followed by Tukey's multiple comparisons). White scale bar represents 3mm and black scale bar represents 1mm.

Figure 3. dHPX promotes NVU remodelling within the peri-infarct region (Bregma 0.0mm) following stroke. Four left most panels in each row illustrate representative labelling for each protein investigated for the four groups, sham, stroke, dHPX 8h and dHPX 24h. The

right most panel illustrates quantification of the fold change of thresholded material for each of the proteins, **(A)** Collagen IV, **(B)** IgG, **(C)** GFAP and **(D)** Iba-1. Data expressed as a fold change of mean ± SEM for each group relative to the mean of the sham group (n = 8 per group). For cumulative threshold analysis refer to Figure II in the online-only Data Supplement. *p< 0.05, ***p<0.001 (ANOVA followed by Tukey's multiple comparisons). All scale bars represent 100μm.

Figure 4. dHPX reduces Aβ in the peri-infarct territory after stroke. (A) The left panel is the representative western blot of protein samples in peri-infarct territory from sham, stroke, dHPX 8h and dHPX 24h animals. Bands were detected using D3D2N anti-Aβ antibody. Loading controls were performed by analysis of β-actin. **(B)** The bar graphs at the right are quantification of Aβ oligomers at 56kDa (dodecamer), 50kDa (decamer), 25kDa (pentamer), 5kDa (monomer) and total Aβ (5-200kDa) deposition. Data expressed as a fold change of mean±SEM for each group relative to the mean of the sham group (n=8 per group). ns: not significant, *p<0.05, **p<0.01 ***p<0.001 (one-way ANOVA followed by Tukey's multiple comparisons).

Figure 5. Glymphatic in vivo imaging experiment. (A) An anaesthetized mouse fixed in a stereotaxic frame for thinned skull window preparation. Schematic diagram on the right depicts a thinned skull window was made over the cortex proximal to the infarct site. **(B)** The setting for in vivo imaging. The influx into the cerebral cortex of fluorescent tracer injected intracisternally into the subarachnoid CSF was assessed in vivo by confocal imaging through a closed cranial window. Schematic diagram on the right shows the imaging conducted between 0 and 100 μm below the cortical surface at 5-min intervals for 2 hours. **(C)** The cerebral vasculature was visualized with tail vein injected FITC-d2000 (green) and CSF

tracer AF 594 (red) moved along the outside of cerebral arteries. After 5 min intracisternal injection of the AF 594 and 15 min of image setup preparation, images were taken every 30 min for 2 hours. Veins were identified morphologically and the fluorescent intensity of CSF tracer (AF 594, red) along the vein (the white circle) was assessed over time. **(D)** The line graph demonstrates the relative fluorescence change of CSF tracer along the outside of cerebral surface arteries at 30-min intervals for 2 hours for all groups. Data expressed as relative change of mean±SEM for each group over time (n=4 per group). Sham vs. stroke ***p<0.001, stroke vs. dHPX 8h ###p<0.001, stroke vs. dHPX 24h +++ p<0.001 at 135 min. Two-way ANOVA was used to determine whether there were time and treatment effects across groups. White scale bar represents 100μm.

Figure 6. dHPX improves AQP4 polarity within peri-infarct region (Bregma 0.0mm) following stroke. Four left most images illustrate representative labelling of AQP4 for the four groups, sham, stroke, dHPX 8h and dHPX 24h. Insets show APQ4 polarity on vessels at high magnification. The right bar graph illustrates the AQP4 polarization. Data expressed as a fold change of mean±SEM for each group relative to the mean of the sham group (n=8 per group). ns: not significant, *p<0.05, **p<0.01 ***p<0.001 (one-way ANOVA followed by Tukey's multiple comparisons). Black scale bar represents100μm and white scale bar represents of inset represents 10μm.

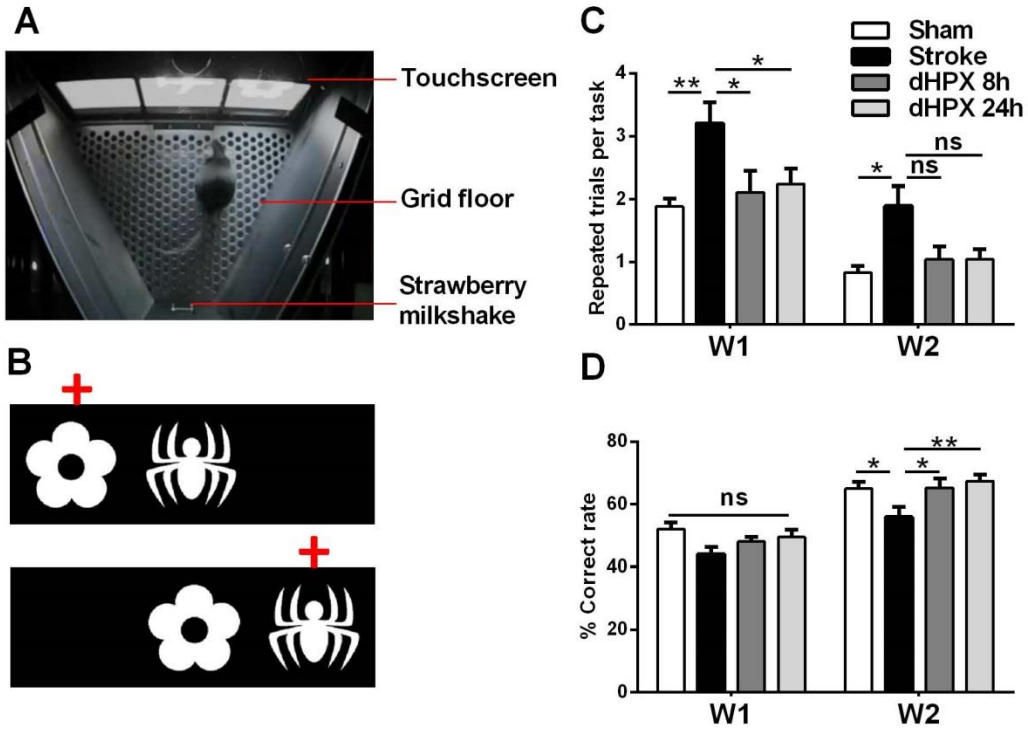
A
Touchscreen
Grid floor
Strawberry milkshake
B
C
Sham
Stroke
dHPX 8h
dHPX 24h
Repeated trials per task
0
1
2
3
4
**
*
*
*
ns
ns
W1
W2
D
% Correct rate
0
20
40
60
80
ns
*
*
**
W1
W2

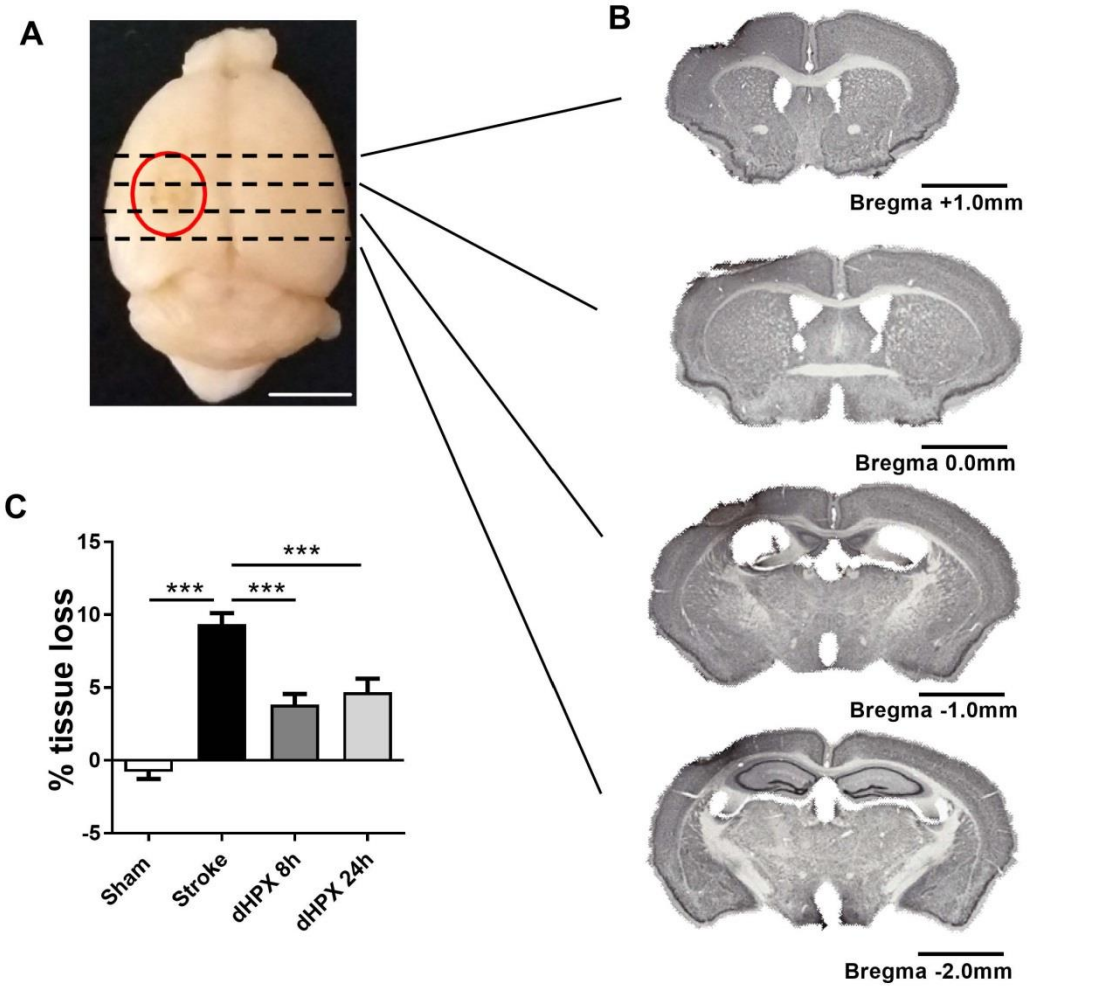
A
B
Bregma +1.0mm
Bregma 0.0mm
Bregma -1.0mm
Bregma -2.0mm
C
% tissue loss
15
10
5
0
-5
***
***
***
Sham
Stroke
dHPX 8h
dHPX 24h

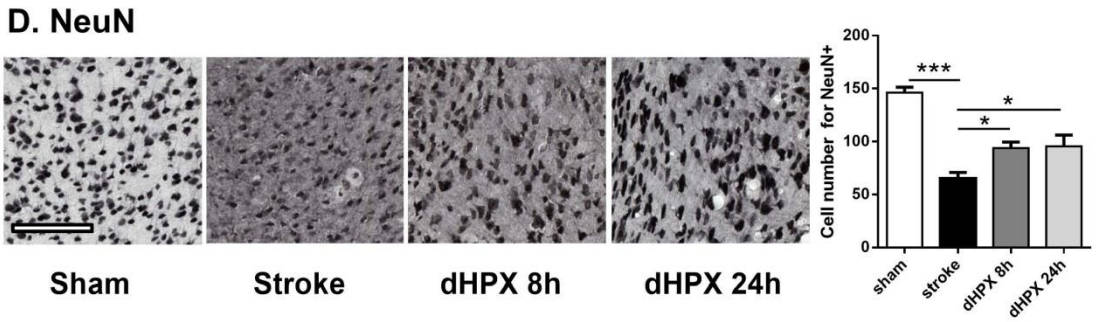
D. NeuN
Sham
Stroke
dHPX 8h
dHPX 24h
Cell number for NeuN+
200
150
100
50
0
***
*
*
sham
stroke
dHPX 8h
dHPX 24h

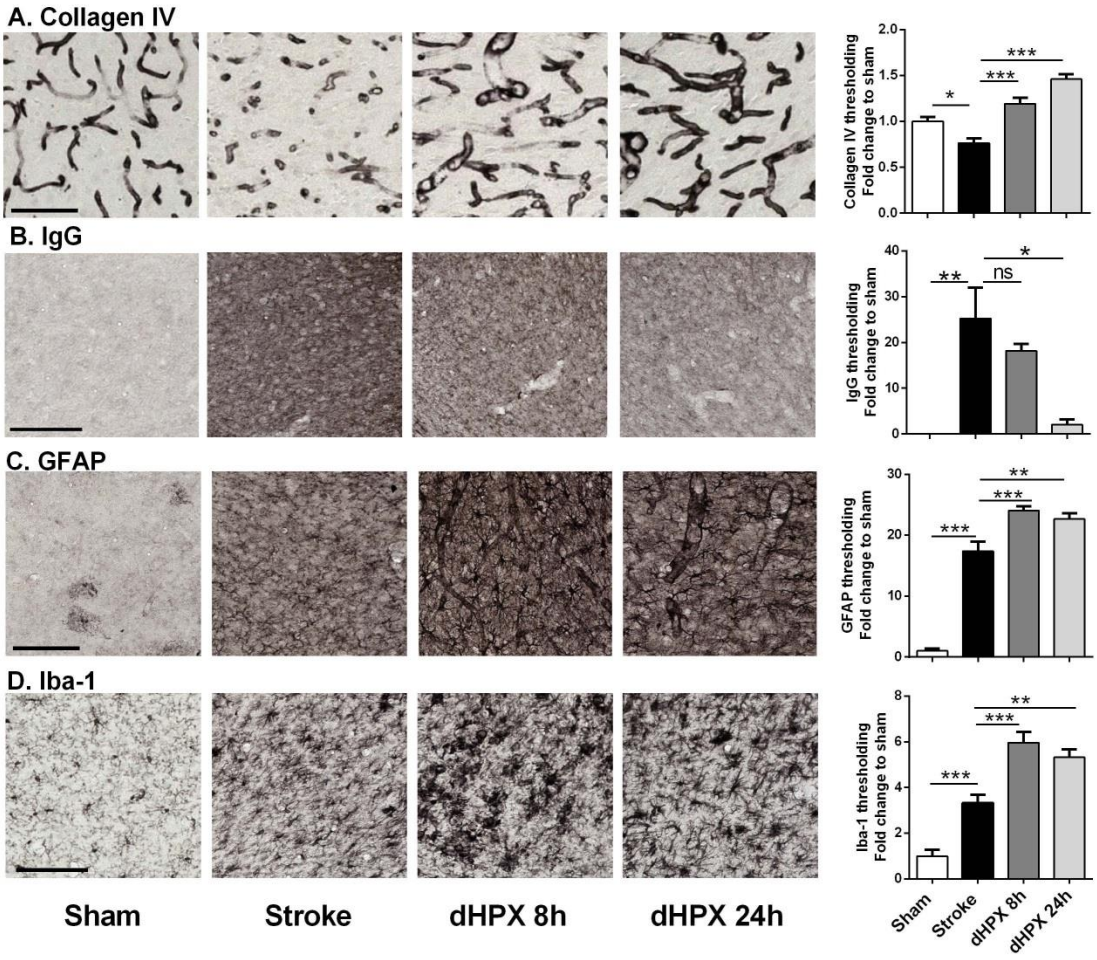
A. Collagen IV
B. IgG
C. GFAP
D. Iba-1
Collagen IV thresholding Fold change to sham
IgG thresholding Fold change to sham
GFAP thresholding Fold change to sham
Iba-1 thresholding Fold change to sham
Sham
Stroke
dHPX 8h
dHPX 24h
ns

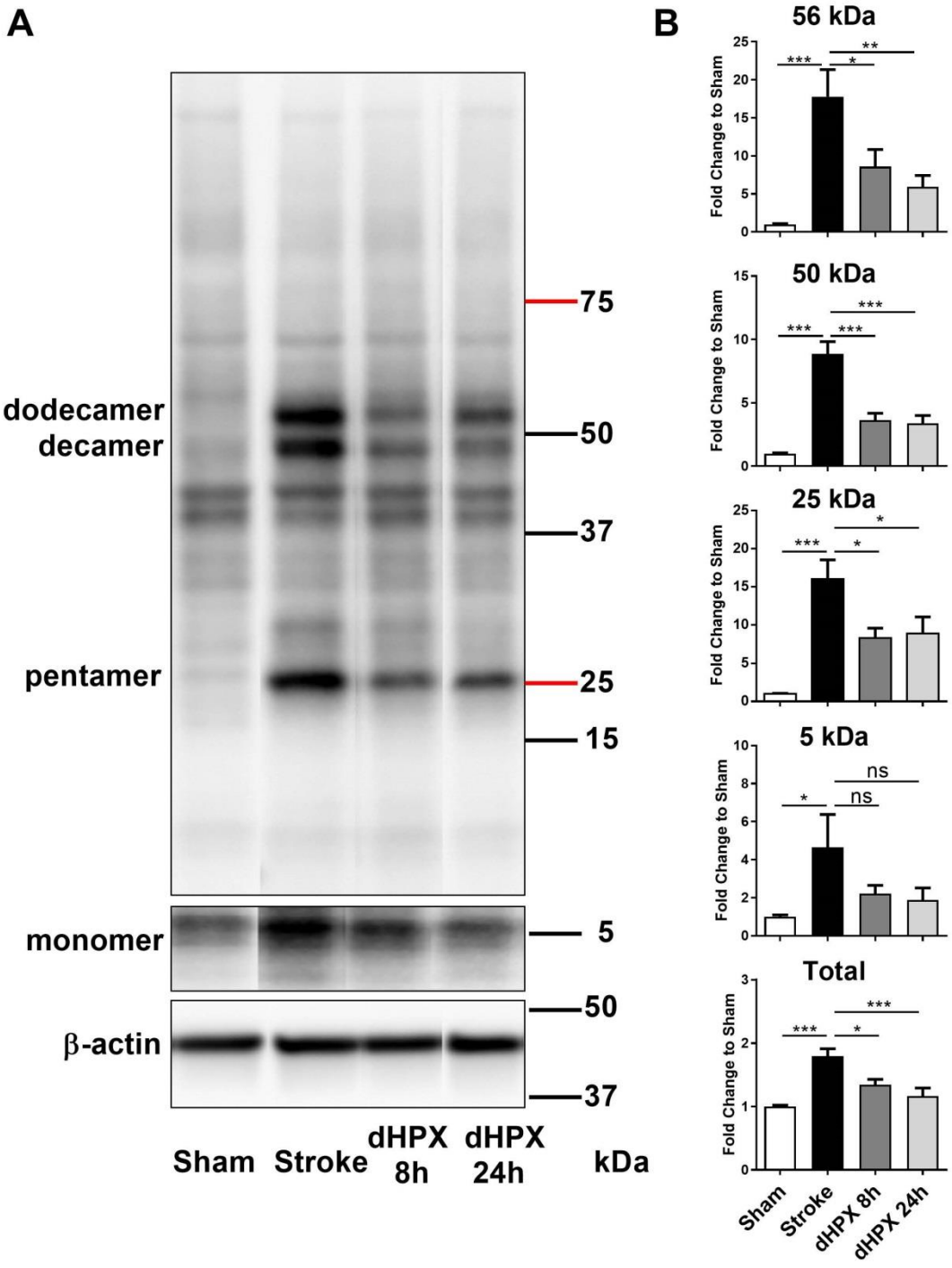
A
dodecamer
decamer
pentamer
monomer
β-actin
75
50
37
25
15
5
50
37
Sham
Stroke
dHPX 8h
dHPX 24h
kDa
B
56 kDa
50 kDa
25 kDa
5 kDa
Total
Fold Change to Sham
***
**
*
ns
Sham
Stroke
dHPX 8h
dHPX 24h

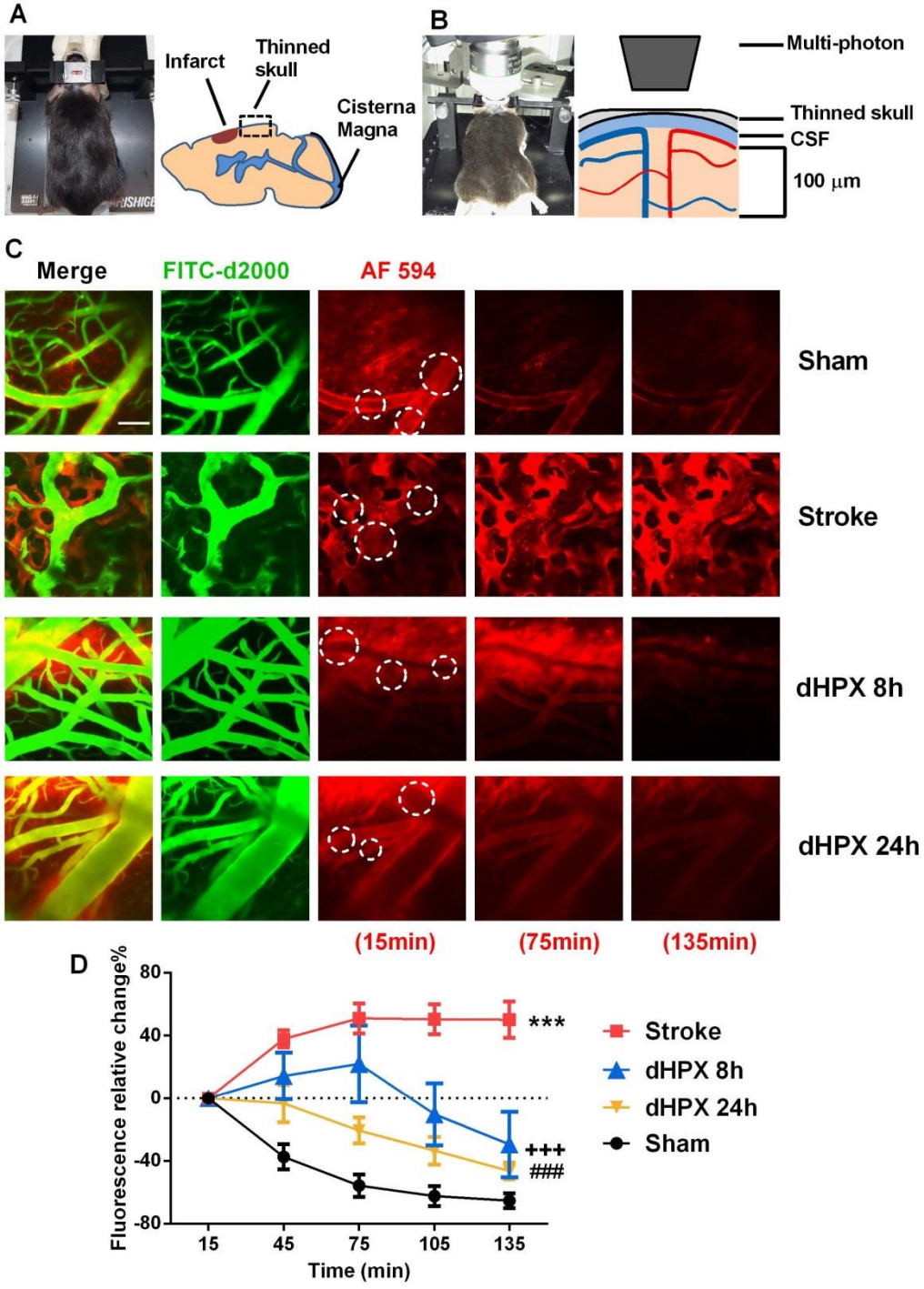
A
Infarct
Thinned skull
Cisterna Magna
B
Multi-photon
Thinned skull
CSF
100 μm
C
Merge
FITC-d2000
AF 594
Sham
Stroke
dHPX 8h
dHPX 24h
(15min)
(75min)
(135min)
D
Fluorescence relative change%
80
40
0
-40
-80
15
45
75
105
135
Time (min)
***
+++
###
Stroke
dHPX 8h
dHPX 24h
Sham

`

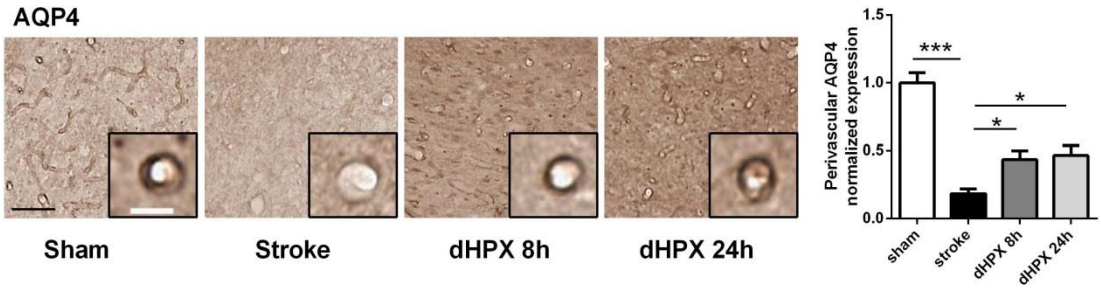
AQP4
Sham
Stroke
dHPX 8h
dHPX 24h
Perivascular AQP4 normalized expression
1.5
1.0
0.5
0.0
***
*
*
sham
stroke
dHPX 8h
dHPX 24h

`

Publication 5

Delayed normobaric hypoxic exposure rescued neuron loss and reduced Amyloid beta accumulation at thalamic secondary neurodegeneration post-stroke.

Zidan Zhao, Lin Kooi Ong, **Giovanni Pietrogrande**, Sarah J Johnson, Michael Nilsson, Frederick R Walker

Abstract

Despite the fact that quite a lot is known about the cellular events involved in brain repair, the number of options that are therapeutically available remains small. Motivated by the significant gains demonstrated by elite athletes, the current study has investigated the potential therapeutic benefits of high altitude training. One of the primary mechanisms considered to underpin the benefits of high altitude training in athletes is the ability of the intervention to potently stimulate new vessel growth. Of interest, this has also been a major objective of research in the field of brain repair. In the current study, we investigated whether high altitude training following stroke could improve secondary neurodegeneration. Undertaken in male C57B6 mice, we examined how exposure to consistent (24h/day) hypoxic environment (11% oxygen) for two weeks following photothrombotic stroke, altered neuron loss, amyloid beta (Aβ) accumulation and vascular remodelling within the thalamus, a major site of secondary neurodegeneration. The results from this study indicate that exposure to hypoxia limited neuronal loss, reduced Aβ deposition and promoted vessels. We further noted the ability of hypoxic exposure to partially restore Aquaporin-4 polarization. Collectively, these results highlight that high altitude training following photothrombotic stroke can limit the severity of secondary neurodegeneration. Preliminary, these suggest some consideration be given to evaluating the potential of high altitude training in those recovering from stroke.

5.1 Introduction

Focal cortical infarction, induced by photothrombosis, has been extensively used a controllable model of stroke. This model has been shown to not only induce cellular damage at the site of infarction but also induce neuronal death, axonal degeneration and gliosis in remote brain regions (1). The ability of focal infarction to induce secondary neurodegeneration (SND) is of considerable interest, as a highly analogous phenomenon is observed in humans following stroke. SND has been consistently observed in humans using MRI (2-5), CT (6-9) and PET (10-12) imaging from one week, up to at least two years.

While the relevance of SND in the human context is yet to be definitively established, a number of studies have indicated that SND is associated significantly with impaired functional recovery in clinical (13-15) and experimental (1, 16-20) studies.

From a histological perspective, the most characteristic aspect of SND is neuronal loss. It is not completely understood why neuronal loss occurs. However, it has been hypothesised that the Wallerian degeneration initiated by the severing of axons at the infarct site, significant neuronal inflammation in secondary regions. This neuro inflammatory response, involving often extreme microgliosis, is considered to produce an environment that is unfavourable for neuronal survival. Typically, sites of SND contain high levels of pro-inflammatory cytokines, reactive oxygen species, highly phagocytic cells, including cells from the peripheral immune system. Also common at sites of SND are high levels of neurotoxic proteins, most notably Amyloid-beta (Aβ) (20).

The appearance of significant amounts of amyloid has attracted considerable interest because of the role that amyloid issues in a number of neurodegenerative diseases. Most notably, Aβ has consistently been identified to be neurotoxic and linked to cognitive decline in Alzheimer's disease (21, 22).

The Aβ is a peptide of 36 to 43 amino acids and can self-assemble into different forms. Small Aβ intermediates, soluble oligomers, can disrupt synaptic structure and plasticity in the aggregation process, while large insoluble deposits may function as reservoirs of the bioactive oligomers (23).

The clearance of soluble Aβ out of the brain depends on the glymphatic system, a paravascular pathway formed by the end-feet of astrocytes that carries out the functions of conventional lymphatic vasculature to clean soluble proteins and metabolites from the central nervous system (24). In our previous study, we identified vasculogenesis driven by delayed normobaric hypoxic exposure (dHPX) was associated with considerable reduction in Aβ loading in peri-infarct region, concomitant with an enhancement in cognitive performance. Additionally, we observed that paravascular cerebrospinal fluid (CSF) mediated clearance was enhanced in animals undergoing dHPX. Such reduction in Aβ within peri-infarct region may be due to the enhanced paravascular CSF efflux, via Aquaporin-4 (AQP4) water channels which has been reported to contribute to the clearance of Aβ (24).

Given the ability of ischemic injury to robustly increase Aβ loads and oligomerization at sites of SND, increased cerebral capillary density may potentially reduce Aβ accumulation by improved interstitial bulk flow (ISBF) and thereby rescue the neuronal loss occurring in the thalamic SND site. Problematically, however, it is not easy to directly image deeper sub cortical structures. Accordingly, we can at the present time only obtain information on the effects of hypoxia rather than directly imaging its ability to improve glymphatic flow.

To our knowledge, no studies have examined whether dHPX is able to reduce neuron loss and Aβ accumulation in ipsilateral thalamus after focal cerebral infarction. In the current study, we employed a mouse model of the photothrombotic vascular occlusion and have chosen to run three experimental groups: shams, stroke alone, and stroke with dHPX. Neuron loss in the ipsilateral thalamus was examined by immunohistochemistry. Soluble Aβ oligomerization within thalamus was measured by western blotting and immunohistochemistry. The expression levels of Aβ deposition related genes were examined by PCR. Vessel formation and the polarization of AQP4 on peri-vasculature were also measured by immunohistochemistry. Briefly, these investigations have provided evidence suggesting that dHPX treatment rescues the neuron loss and Aβ accumulation with the thalamic SND site after photothrombotic vascular occlusion.

5.2 Materials and Methods

Animals

72 C57BL/6 adult male mice, each randomly allocated to one of the following groups: sham, stroke, and stroke dHPX, 24 animals per group. Animals were obtained from the Animal Services Unit at the University of Newcastle. This study also complies with the ARRIVE guidelines. Animals were maintained in a temperature (21 °C ± 1) and humidity controlled environment with food and water available *ad libitum*. Lighting was on a 12:12h reverse light–dark cycle (lights on 19:00 h) with all procedures conducted in the dark phase under low-level red lighting (40 Lux). All animals were allowed to acclimate for a minimum of seven days prior to the start of the experiment. All experiments were approved by the University of Newcastle Animal Care and Ethics Committee, and conducted in accordance with the New South Wales Animals Research Act and the Australian Code of Practice for the use of animals for scientific purposes.

Photothrombotic occlusion

On Day 0 (D0), mice were anaesthetized by isoflurane in a transparent induction chamber (4% for induction, 2% for maintaining) in 100% oxygen. The skin along the midline of the scalp, from the eye level down to the neck, was incised and the skull was exposed. Photothrombotic vascular occlusion was achieved by intraperitoneal injection of mice with 0.2mL of 10mg/mL of Rose Bengal 8 minutes prior to 15 min of illumination, using a cold light source with a fibre optic end of 4.5mm diameter placed 2.2mm left lateral of Bregma onto the exposed skull. The interaction of light with the dye initiates the generation of free radicals that damage the endothelial membranes, and subsequently trigger a thrombotic reaction resulting in microvessel occlusion. After 15 min of illumination, the skin of the scalp was closed using surgical cyanoacrylate glue. Surgeries for stroke animals were operated in a blind manner. For the sham group, similar procedure was applied except Rose Bengal was replaced with 0.2mL of 0.9% saline.

Delay hypoxia (dHPX) protocol

Post-stroke animals were allowed to recover for 3 days before receiving the dHPX training. A custom-made hypoxic environment rack which can hold 14 animal cages were built to provide 11% oxygen, normal CO_2 concentration (250-350ppm), and normal atmospheric pressure (101kPa) environment. Animals from stroke dHPX group were maintained in hypoxic environment for 24h daily for two weeks. Sham and stroke only animals were handled for 2 min twice daily throughout the duration of experiment. All animals were weighed on D0 before stroke and D17 post-stroke.

Tissue processing

At day 17 post-stroke animals were euthanized. For immunohistochemistry analysis, animals (n=8 per group) were deeply anesthetized via intraperitoneal injection of sodium pentobarbital and transcardially perfused with ice cold 0.9% saline for 2 mins followed by ice cold 4% paraformaldehyde (pH 7.4) for 13 mins. Brains were removed and post-fixed for 4 hours in the same fixative then transferred to a 12.5% sucrose solution in 0.1M PBS for storage and cyroprotection. Serial coronal sections were sliced on a freezing microtome (-25°C) at a thickness of 30µm. For western blot and PCR analysis, animals (n=8 per group for western blot and PCR analysis, respectively) were deeply anesthetized via intraperitoneal injection of sodium pentobarbital and transcardially perfused with ice cold 0.1 % diethylpyrocarbonate in 0.9 % saline for 2 mins. Brains were dissected and rapidly frozen in -80°C isopentane. Section were sliced in a cryostat (-20°C) at a thickness of 200µm and the ipsilateral thalamus (Bregma -1.0 to -2.2 mm) were punched using a 2mm tissue punch. Samples were kept frozen at all times until protein and mRNA extraction.

Immunohistochemistry

For immunoperoxidase labelling, free-floating sections (Bregma -2.0 mm) were immunostained as previously described (25) with one of the following primary antibodies: (mouse anti-amyloid β (D3D2N), 1:1000Cell Signaling Technology; mouse anti-NeuN, 1:500, Millipore; rabbit anti-Aquaporin 4 (AQP4, 1:500). Sections immunostained by rabbit anti-collagen IV (1:1000, Abcam) were carried out pepsin antigen retrieval as described by S. Franciosi et al. (26) before immunohistochemistry. Sections were rinsed with 0.1 M PB and then endogenous peroxidases were

destroyed in 0.1 M PB containing 3% hydrogen peroxide. Non-specific binding was blocked with 3% normal horse serum. Sections were incubated in primary antibody with 2% normal horse serum for 48 hours at 4 C° and then were washed by 0.1 M PBS for 30 min and incubated with biotinylated goat a secondary antibody (1:500; Jackson ImmunoResearch) of corresponding species for 2h at room temperature, rinsed, incubated in 0.1% extravadin peroxidase for 1 h, and then rinsed again. Immunolabelling was developed using a nickel-enhanced 3, 3'-diaminobenzidine (DAB) reaction. Tissues of three groups were performed simultaneously and the DAB reactions were developed for exactly the same length of time following the addition of glucose oxidase (1:1000). Negative control sections, in which no primary antibodies were added at a time, were developed at the same time. After processing was complete, sections were washed, mounted onto chrome alum-coated slides, and coverslipped.

Image acquisition, thresholding and AQP4 polarization analysis

Images were acquired at 20 X using Aperio AT2 (Leica, Germany). The quantitative analysis was undertaken specifically in the ipsilateral thalamus (Bregma -2.0 mm). The cumulative threshold spectra analysis was evaluated for Aβ and Collagen IV as previously described (1, 27, 28). Briefly, Matlab software R2015a was used to crop regions of interest, these cropped regions were thresholded and the data exported. Pixel intensity level considered to be optimal for detecting genuine differences in immunoreactive signal was determined using ImageJ software. The term 'Thresholded area %' refers to the percentage of pixels that were captured at and below the optimal pixel intensity to the total number of pixels in each image. For NeuN labelling, the area of NeuN^{+} labelling regions in thalamus was traced by using ImageJ. To analyse the AQP4 polarity on vessels, the thresholding of AQP4 labelling on vessels and background were measured. The AQP4 polarization was calculated as the ratio of thresholding of AQP4 labelling on vessels to that on background. All images were analysed in a blinded manner.

Protein extraction and Western blot

Protein extraction and western blot were performed as previously described with minor modification (29). Samples were sonicated in 300 µL of lysis buffer (50 mM TRIS buffer pH 7.4, 1 mM EDTA, 1 mM DTT, 80 µM ammonium molybdate, 1 mM sodium pyrophosphate, 1 mM sodium vanadate, 5 mM b-glycerolphosphate, 1 protease inhibitor cocktail tablet, 1 phosphatase inhibitor cocktail tablet, final concentration) with a UP50H microsonicator (Hielscher Ultrasonics GmbH, Germany) for 3 x 30 s pulses at 4°C. Samples were centrifuged at 14 000 g for 20 min at 4°C. The clear supernatants were collected and protein concentrations were determined by Pierce BCA protein assay kit according to the manufacturer's instructions. Samples were diluted with lysis buffer to equalize protein concentrations (1.5 mg/mL) and stored at -80°C until further analysis. Samples were mixed with sample buffer (2 % sodium dodecyl sulfate, 50 mM Tris, 10 % glycerol, 1 % DTT, 0.1 % bromophenol blue, pH 6.8) and 15 µg of total tissue protein samples were electrophoresed to Biorad Criterion TGC Stain-Free 4-20 % gels. Gels were transferred to PVDF membranes by in transfer buffer (25 mM Tris, 200 mM glycine, and 20 % methanol pH 8.3). PVDF membranes were washed in Tris-buffered saline with tween (TBST) (150 mM NaCl, 10 mM Tris, 0.075% Tween-20, pH 7.5) and blocked in 5% skim milk powder (SMP) in TBST for 1 h at 25°C. Membranes were incubated with primary antibodies (anti-amyloid β (D3D2N), Cell Signaling Technology, 1:1000) and secondary antibody (horseradish peroxidase conjugated goat anti-mouse, Biorad, 1:10,000). In between each incubation step, membranes were washed in TBST. Membranes were visualized on Amersham Imager 600 using Luminata Forte Western blotting detection reagents. The density of the bands was measured using Amersham Imager 600 Analysis Software.

mRNA extraction and PCR

RNA was isolated using the Illustra RNAspin Kit (GE Healthcare, Cat# 25-0500-70) according to manufacturer's specifications from tissue punched from thalamus areas of frozen brain slices. cDNA was generated using SuperScript™ III First Strand Synthesis System for RT-PCR (Invitrogen, Cat# 18080-044) according to manufacturer's instructions on a GeneAmp PCR System 9700 instrument (Applied Biosystems). Quantitative RT-PCR was performed on an Applied Biosystems® 7500 (Applied Biosystems) or ViiA7 (Thermofisher) instruments using SensiFAST SYBR® Lo-ROX

Master Mix (Bioline, Cat# BIO-94020). Genes of interest (Table 5-1) were normalized on the housekeeping gene GAPDH and data are expressed as $2^{-\Delta\Delta Ct}$ as fold change relative to sham.

Table 5-1. PCR primer sequences

Genes	Forward	Reverse
APP	CCCACGACAGCAGCCAG	GCTCTGCCTCTTCCCATTC
BACE1	GCTTTGTGGAGATGGTGGAC	AGGATGTTGAGCGTCTGTGG
TACE	CATCGTTGGGTCTGTTCTGG	AGGGATTCATACTGCTTGTC
NEP	CTGGAGGTCAATGGGAAGTC	TCGGCTGAGGCTGCTTAC
ECE	TCCTTCGCTGCCCTCCT	GGACAACATCAAAAGACCCAC
IDE	AGTTCCCTGAGCACCCTTTC	ACCCAGCCCTTTGATTTGAG
LRP1	AGACTATCAGGGCGGCAAG	CAAACACGGACACGGAGAAC
RAGE	CCGATGGCAAAGAAACACTC	GCAGGAGAAGGTAGGATGGG
GAPDH	TCGGTGTGAACGGATTTGGC	TGTTAGTGGGGTCTCGCTCC

APP, amyloid precursor protein; BACE1, Beta-secretase 1; TACE, TNFα converting enzyme; NEP, neprilysin; ECE, endothelin-converting enzymes; IDE, insulin-degrading enzyme; LRP1, low-density lipoprotein receptor-related protein; RAGE, receptor for advanced glycation end products; GAPDH, glycolytic glyceraldehyde-3-phosphate dehydrogenase.

Data analysis

All data for sham, stroke, and stroke dHPX groups was expressed as mean ± SEM and was analysed using Prism 6 for Windows Version 6.01, GraphPad Software. One-Way ANOVA was used to determine whether there were any significant treatment effects across the groups. Additional Tukey multiple comparisons were used to analyse differences between the mean of each group with the mean

of every other group. The significant differences shown on the graphs with asterisks (*) refer to the post hoc tests. All differences were considered to be significant at $p < 0.05$.

5.3 Results

dHPX reduces neuron loss in the thalamic secondary neurodegeneration site

Mature neuron marker NeuN labelling was used to assess the neuronal loss in the ipsilateral thalamus region after stroke. Photothrombotic occlusion significantly induced neuronal loss in the thalamic secondary neurodegeneration site. To analyse the extent of neuronal loss, the area of NeuN$^-$ region was traced in both stroke groups. dHPX reduced the area of neuronal loss significantly compared to the stroke only group ($p < 0.05$, Fig. 5-1).

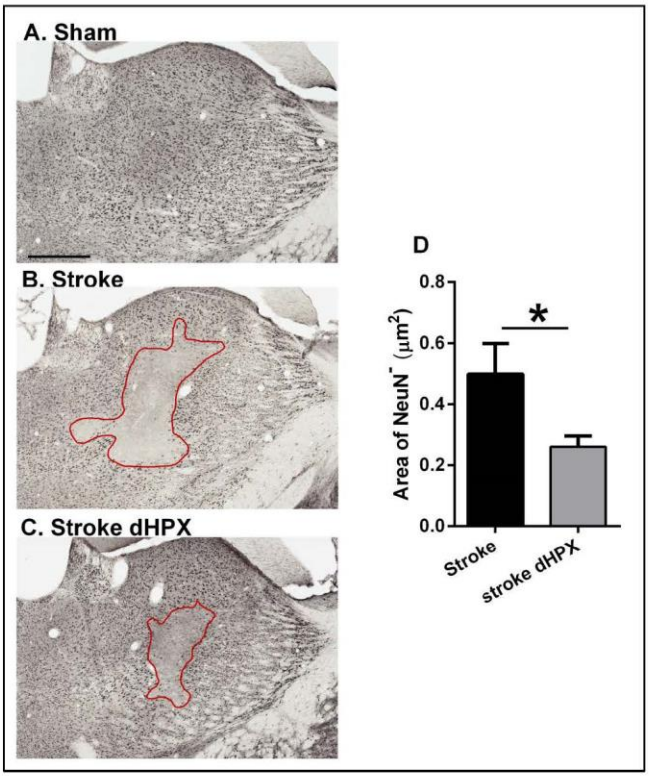

Figure 5-1. Three left images illustrate representative labelling for NeuN in thalamus region (Bregma -2.0 mm) for the three groups, sham (A), stroke (B), and stroke dHPX (C). Within the red line areas are the NeuN negative regions which were traced in ImageJ. (D) The bar graph shows the area of

NeuN negative regions in the thalamus for stroke alone and stroke dHPX animals. Data expressed as mean ± SEM for each group relative (n = 8 per group). * $p < 0.05$ (two tail t-test). Scale bar represents 500μm.

dHPX reduces Aβ oligomer accumulation in thalamus after stroke

The tissue from the thalamus territory of all groups was analysed by western blot using anti-amyloid β for soluble Aβ oligomers. The results for Aβ oligomers at 70kDa (high molecular weight species, HMW), 50kDa (decamer), and 25kDa (pentamer) levels were normalized to β-actin as loading control (Fig.5-2). The data for all groups were expressed as a fold increase of the mean ± SEM for each group relative to the mean of the sham group. All Aβ oligomers showed similar patterns. Specifically, at HMW, decamer and pentamer levels, stroke increased Aβ oligomerization significantly compared to sham animals ($p < 0.05$, $p < 0.05$, and $p < 0.01$, respectively), and dHPX reversed this response significantly at HMW and pentamer levels ($p < 0.05$ and $p < 0.001$), but not at decamer level.

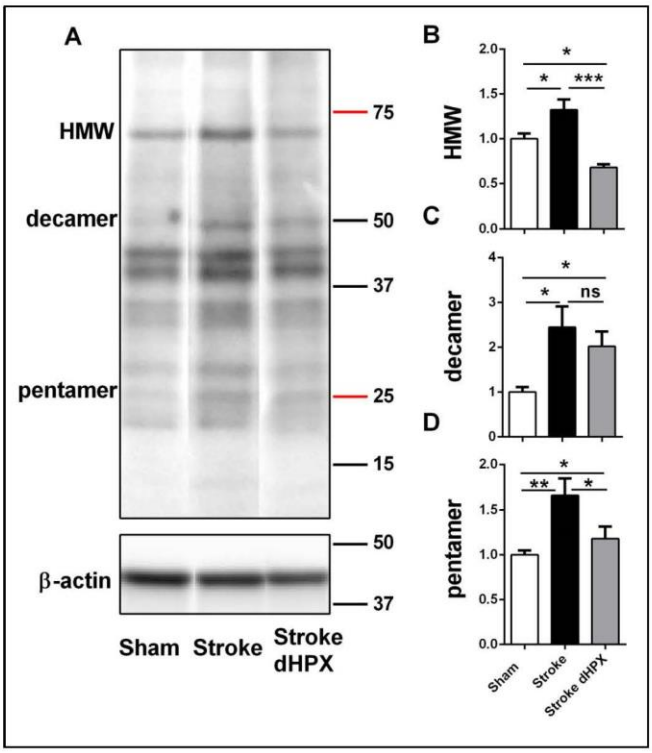

Figure 5-2. dHPX reduces Aβ deposits in the thalamus after stroke. A. The left panel is the representative western blot of protein samples within the thalamus region (Bregma -1.0 to -2.2 mm) for the three groups, sham, stroke and stroke dHPX from sham, stroke, and stroke dHPX animals. Bands were detected using D3D2N anti-Aβ antibody. Loading controls were performed by analysis of β-actin. The bar graphs (B-D) at the right are quantification of Aβ oligomers at 70kDa (high molecular weight species, HMW), 50kDa (decamer), and 25kDa (pentamer) deposition. Data expressed as a fold change of mean ± SEM for each group relative to the mean of the sham group (n = 8 per group). ns: not significant, * $p < 0.05$, ** $p < 0.01$ *** $p < 0.001$ (one-way ANOVA followed by Tukey's multiple comparisons).

Semi-quantitative immunohistochemistry of Aβ accumulation in thalamus

Immunohistochemistry staining of anti- Aβ (D3D2N) antibody was used at a single level (Bregma -2.0 mm) to validate western blot results and to better understand the spatial distribution of Aβ accumulation following stroke (Fig. 5-3). Optical density of anti Aβ staining within thalamus was then semi-quantitatively assessed using the threshold analysis.

There is a significant increase in Aβ accumulation in the thalamus of stroke animals ($p < 0.001$) compared to sham animals and dHPX rescued such increase in stroke animals ($p < 0.001$).

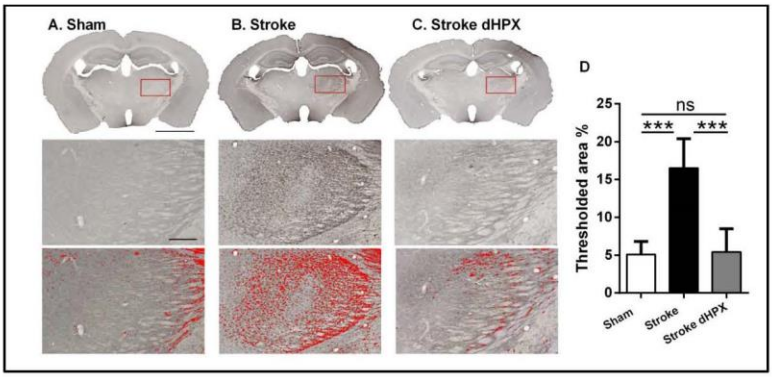

Figure 5-3. The top three images illustrate representative labelling for Amyloid β (Aβ) on the whole sections (Bregma -2.0 mm) for the three groups, sham (A), stroke (B), and stroke dHPX (C). Scale bar represents 2 mm. Red rectangles indicates the thalamus regions analysed by thresholding. The middle three images are the red rectangle regions at high magnification. Scale bar represents 300μm. The bottom three images are the representative images of thresholding analysis. Pixel intensity level considered to be optimal for detecting genuine differences in immunoreactive signal (in red) was determined using ImageJ software. The term 'Thresholded area %' refers to the percentage of pixels that were captured at and below the optimal pixel intensity to the total number of pixels in each image. (D) The bar graph illustrates quantification of the change % of thresholded material for

Amyloid β. Data expressed as mean ± SEM for each group relative (n = 8 per group). *** $p < 0.001$; ns, not significant (one-way ANOVA followed by Tukey's multiple comparisons).

dHPX modifies the Aβ production, degradation and transportation related genes expression

mRNA was extracted from tissue punched in the thalamus area, retrotranscribed and analysed for the expression of elements involved in the production, degradation and transport of Aβ (Fig. 5-4). Aβ is a peptide derived from the cleavage of β-amyloid precursor protein (APP) (30, 31). Although stroke did not increase the APP mRNA expression level, there was a significant reduction by dHPX treatment, compared to sham and stroke only animals ($p < 0.001$).

Proteolytic enzymes cleave the extracellular domain of APP (32). The cleavage of APP by the beta secretase-1 (BACE) is essential for Aβ generation (33). However, the cleavage of APP by alpha secretase TNF-α converting enzyme (TACE) can preclude Aβ generation (34). Although there was no difference across three groups in TACE mRNA expression level, but a significant reduction of BACE mRNA expression level induced by dHPX in stroke animals, compared to stroke only animals, was observed ($p < 0.01$).

Neprilysin (NEP) (35), insulin degrading enzyme (IDE) (36) and endothelin converting enzyme (ECE2) (37) are involved in extracellular or intracellular degradation of Aβ. Our transcriptional expression analysis revealed that stroke increased ECE mRNA expression level ($p < 0.01$) and decreased IDE mRNA expression level significantly ($p < 0.01$) compared to sham animals, but there was no dHPX effect in stroke animals. There was no difference across three groups for NEP mRNA expression level.

Finally, we analysed the mRNA expression of factors involved in the export and uptake of Aβ, specifically low-density lipoprotein receptor related protein-1 (LRP1) (38) and receptor for advanced glycation end products (RAGE) (39). There was no difference across three groups for LRP1 mRNA

expression level, while stroke induced a significant increase in RAGE mRNA expression level compared to sham animals ($p < 0.01$) and dHPX treatment reversed such response ($p < 0.05$).

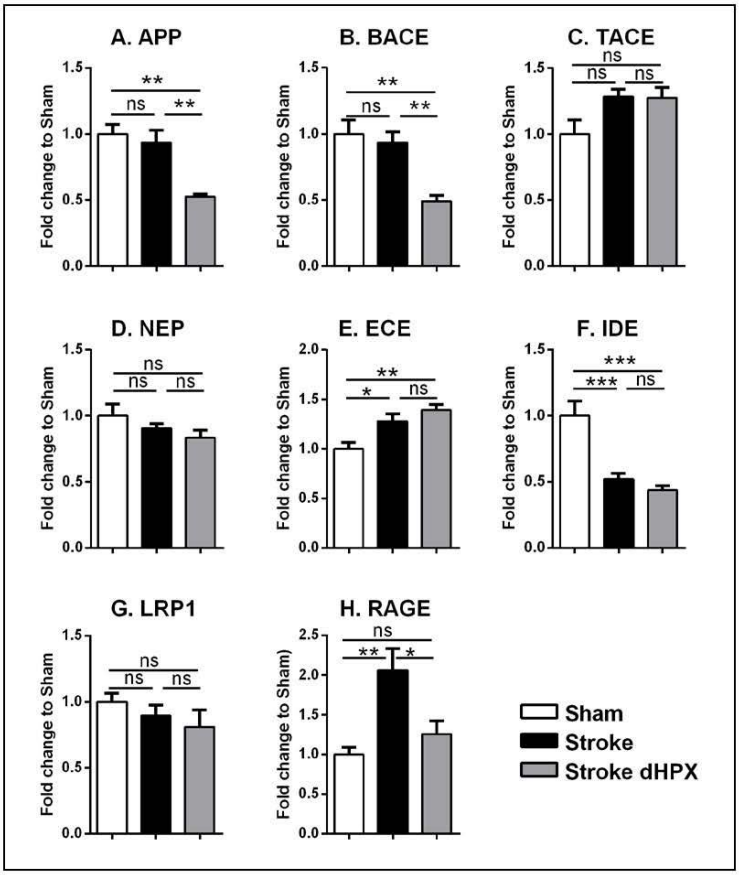

Figure 5-4. The expression of the Aβ accumulation relevant genes, APP (A), BACE (B) TACE (C), NEP (D), ECE (E), IDE (F), LRP1 (G) and RAGE (H) within the thalamus region (Bregma -1.0 to -2.2 mm) for the three groups, sham, stroke and stroke dHPX.. Data expressed as a fold change of mean ± SEM for each group relative to the mean of the sham group (n = 8 per group). ns: not significant, * $p < 0.05$, **** $p < 0.001$ (one-way ANOVA followed by Tukey's multiple comparisons).

dHPX promotes Collagen labelling in the thalamus post stroke

The thresholding analysis indicated that there was no difference between sham and stroke alone groups, but dHPX induced a significant increase in the formation of vessels labelled by Collagen IV in ipsilateral thalamus ($p < 0.05$, Fig. 5-5).

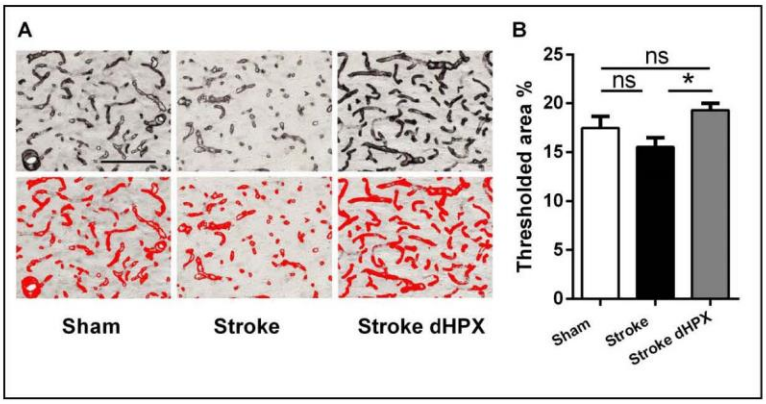

Figure 5-5. (A) The top three images are Collagen-IV labelling within the ipsilateral thalamus region (Bregma -2.0 mm) for the three groups, sham, stroke and stroke dHPX. The bottom three images are the representative images of threshold analysis. Pixel intensity level considered to be optimal for detecting genuine differences in immunoreactive signal (in red) was determined using ImageJ software. The term 'Thresholded area %' refers to the percentage of pixels that were captured at and below the optimal pixel intensity to the total number of pixels in each image. (B) illustrates quantification of the change % of thresholded material for Collagen IV. Data expressed as mean ± SEM for each group relative (n = 8 per group). * $p < 0.05$; ns, not significant (one-way ANOVA followed by Tukey's multiple comparisons). Scale bar represents 100µm.

dHPX improves AQP4 polarity after stroke

The AQP4 polarization was calculated as the ratio of AQP4 labelling on the vessel wall to that in the parenchymal tissue directly adjacent to the vessel.

A one-way ANOVA indicated that compared to sham animals the AQP4 polarization in peri-infarct regions of stroke was reduced significantly ($p < 0.05$), but dHPX treatment rescued such reduction ($p < 0.05$, Fig. 5-6).

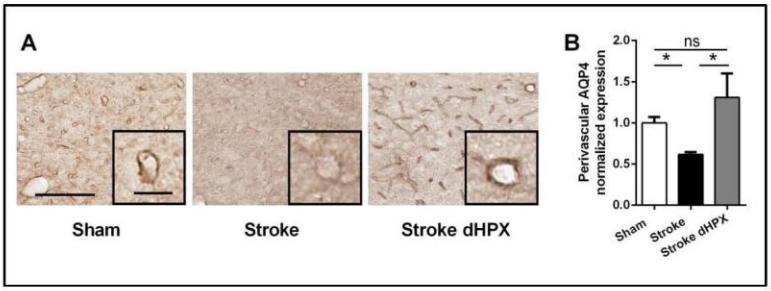

Figure 5-6. dHPX improves AQP4 polarity within the thalamus region (Bregma -2.0 mm) following stroke. (A) Three left most images illustrate representative labelling of AQP4 for the three groups, sham, stroke, and stroke dHPX. Scale bar represents 100μm. Insets show APQ4 polarity on vessels at high magnification. Scale bar represents 20μm. (B)The right bar graph illustrates the AQP4 polarization. Data expressed as a fold change of mean ± SEM for each group relative to the mean of the sham group (n = 8 per group). ns: not significant, * $p < 0.05$; ns, not significant (one-way ANOVA followed by Tukey's multiple comparisons).

5.4 Discussion

Normobaric high-altitude training regimens are well recognised to be capable of enhancing athletic performance at sea (40-42). It has been widely suggested that these beneficial effects are largely driven by the ability of the intervention to promote vasculogenesis and erythropoiesis and in doing so increasing the oxygen delivering capacity of the body (41, 43, 44). Interestingly, the promotion of cortical vasculature and erythropoiesis has been amongst the most investigated strategies in the field of brain repair post-stroke (45, 46).

In the context of stroke recovery research, the enhancement of vasculature and erythropoiesis has been attempted through the delivery of specific growth factors. One of the most intensively studied growth factors in stroke is vascular endothelial growth factor (VEGF). Numerous experimental studies have indicated that VEGF induces neuroprotection, neurogenesis and angiogenesis after stroke (47). The clinical trials of VEGF treatment in stroke patients, however, have failed, due to the fact that VEGF is also associated with significant problems including BBB leakage, brain oedema and haemorrhage during stroke recovery (47, 48).

We are certainly not the first group to consider the potential therapeutic utility of high altitude training. Indeed several other groups have already described the ability of the hypoxia intervention to significantly improve cognitive function post stroke (49-53). For example, Tsai et al. has demonstrated that delayed intermittent hypoxia post-stroke rescued spatial learning and memory impairment by inducing hippocampal neurogenesis and functional synaptogenesis in the rat model of occlusion of the middle cerebral artery (51).

In the current study, we adopted a pre-clinical experimental model of stroke (photothrombotic occlusion). Beginning 72 h after the stroke event animals were exposed to normal atmospheric conditions for 24 h of hypoxia (~11% 0_2) using a customized normobaric living environment, an approach that we refer to as delayed hypoxia (dHPX). The key findings of the study were that animals exposed to dHPX exhibited significantly reduced neuronal loss, reduced Aβ levels and aggregation and enhanced vasculogenesis in the thalamic SND site. Additionally, we observed that the disrupted

AQP4 polarization within the thalamus was improved by dHPX. Together, these results indicate that dHPX could represent a potentially useful therapeutic modality to Aβ loads and SND post-stroke.

We first evaluated the ability of dHPX to reduce SND damage in thalamus by using NeuN labelling. Photothrombotic occlusion robustly induced neuronal loss in the ipsilateral thalamus. By tracing the area of NeuN negative labelling, we identified that mice exposed to stroke and dHPX exhibited significantly less neuronal loss in the ipsilateral thalamus than that measured in the stroke alone condition. This finding aligns well with previous data illustrating the effectiveness of hypoxic exposure to reduce thalamic atrophy after cerebral focal ischemia in mouse (49) and suggests that dHPX can limit secondary thalamic degeneration or limit delayed apoptotic neuronal death in the thalamus.

To examine changes in Aβ, we have again primarily utilised western blotting. Specifically we identified that stroked animals exhibited higher levels of the 25, 50 and 75 kDa Aβ oligomers and sham animals. In contrast animals exposed to stroke and dHPX exhibited significant reductions in the 25 and 75 kDa Aβ oligomers relative to the stroke alone condition. To our knowledge, this is the first report to demonstrate that exposure to normobaric hypoxic is capable of decreaseing aggregation of soluble Aβ oligomers in the thalamic SND site after stroke. We also examined the total Aβ by using immunohistochemistry labelling within ipsilateral thalamus. We found that the Aβ labelling was significantly increased in stroke alone animals but such response was suppressed in stroke dHPX animals.

The ability of dHPX to reduce total Aβ and limit the shift towards higher molecular weight Aβ soluble oligomers may be associated with numerous changes in the underlying apparatus responsible for the generation of Aβ. Accordingly, we screened, using real-time PCR, changes in the transcription of genes known to be involved in the production, degradation and transportation of Aβ. Here we identified that dHPX normalized stroke induced significant decrease in APP and BACE, which are both essential for Aβ production (30-32), but did not influence the expression of TACE, the enzyme that can preclude Aβ production (34). For the degradation pathway, data shows that dHPX exposure

had no effect on the transcription levels of NEP, ECE and IDE. In terms of the transportation, the transcription level of LRP, the receptor contributing to Aβ efflux from brain to blood via BBB (38), was no difference across three experimental groups. However, the increased level of RAGE transcription, the receptor responsible for the Aβ influx from blood into brain across BBB (39), induced by stroke was significantly suppressed by exposure to dHPX. Taken together, the real-time PCR results suggest that the dHPX induced Aβ reduction in stroke animals may involve in limiting not only the production of Aβ but also the influx of Aβ.

While we could not directly assess CSF flow in the thalamus, we could examine changes in the vasculature and in AQP4 polarization, both essential in glymphatic clearance. Here we identified that dHPX induced a considerable enhancement in the density of ipsilateral thalamic vasculature in stroke animals. This finding aligns well with previous studies showing that hypoxia can robustly increase cerebral vessel density (54, 55). We next considered AQP4 polarization. Here it is worthwhile to recall that AQP4 is normally located in the vascular facing end-feet of astrocytes. Previous studies have quantified changes in the extent to which AQP4 ears or localised to the luminal surface. Accordingly in the current study, as we did in Chapter 4, changes in the distribution of AQP4 by determining the ratio of luminal to parenchymal labelling were assessed. This analysis indicated that stroke was associated with a significant reduction in AQP4 polarization, a finding remarkably consistent with that observed after the Hit & Run model of moderate TBI (56). We further identified that dHPX was associated with a significant restoration of AQP4 polarization. These results suggest that the reduced Aβ aggregation and accumulation in the thalamic SND site by dHPX might be due to the rescued AQP4 polarization on vessels and increased vasculogenesis, which could possibly drive the soluble Aβ in ISBF into paravascular pathway through AQP4 channels, and eventually clear out of the brain.

Taken together, in terms of accounting for lower levels of Aβ oligomerisation and accumulation, there are at least three possible explanations. First, dHPX has direct effects on the thalamus, rather instead in reducing the extent of neuronal loss in the peri-infarct region, which in turns limits the secondary neurodegenerative changes in the thalamus. Second, dHPX directly lowers levels of Aβ generation.

This explanation is supported by the finding in current study that the genes expression levels of APP, BACE, and RAGE were observed to significantly reduce by exposure to dHPX. These three factors are well recognised as contributors to Aβ generation. Third, the Aβ clearance pathway, glymphatic system, might be promoted by dHPX. In Chapter 4, by assessing ISBF using real time confocal imaging through the cortex, the approach first reported by Illif et al (24), we found that stroked animals exhibit a deficit in ISBF and that dHPX effectively corrects this deficit. However, due to the practical limitation that confocal in vivo imaging can only be applied on the surface of cerebral cortex, no deeper than 200 μm, the in vivo status of glymphatic system within thalamus thereby cannot be detected as Chapter 4 described. The findings in current study, indicate that the vasculature and AQP4 polarization which are both essential for Aβ clearance were considerably improved by dHPX in stroke animals, still supporting the possibility of the third explanation.

To conclude, the findings from the current study provide several knowledge advances. Firstly, the study has demonstrated that 24h dHPX, beginning three days post stroke and continuing for two weeks thereafter, induces a neuroprotective effect by significantly reducing the neuronal loss in the ipsilateral thalamic SND site. Secondly and most importantly, we have identified that for the first time, that dHPX is capable of significantly reducing the aggregation of soluble oligomers within the ipsilateral thalamus territory. Thirdly, to examine the possible mechanisms, we have provided evidence that the reduced levels of Aβ production and import receptor related gene expression might be the contributors to the dHPX induced Aβ reduction, and the clearance of Aβ could be possibly facilitated by improved AQP4 polarization and significantly promoted vasculogenesis within ipsilateral thalamus regions.

In our previous study, we have identified that the vascular regeneration induced by dHPX after stroke is associated with considerable reduction in Aβ loading within peri-infarct regions concomitant with an enhancement in cognitive performance. In the current study, we further confirmed that dHPX can also induce similar effect in the thalamic SND site. Given, that the extent of SND is associated with impaired functional recovery (13-15) and stroke is known to trigger accelerated cognitive decline and

result in rapid emergence of dementia like symptoms, a therapeutic strategy that can induce reduction of neurodegeneration at multiple sites would be highly desirable.

Funding acknowledgements

This study was supported by the Hunter Medical Research Institute, Faculty of Health and Medicine Pilot Grant and The University of Newcastle, Australia.

Declaration of conflicting interests

The authors declared no potential conflicts of interest with respect to the research, authorship, and/or publication of this article.

References

1. Jones KA, Zouikr I, Patience M, Clarkson AN, Isgaard J, Johnson SJ, et al. Chronic stress exacerbates neuronal loss associated with secondary neurodegeneration and suppresses microglial-like cells following focal motor cortex ischemia in the mouse. *Brain Behav Immun.* 2015;48:57-67.
2. Duering M, Righart R, Wollenweber FA, Zietemann V, Gesierich B, and Dichgans M. Acute infarcts cause focal thinning in remote cortex via degeneration of connecting fiber tracts. *Neurology.* 2015;84(16):1685-92.
3. Duering M, Righart R, Csanadi E, Jouvent E, Herve D, Chabriat H, et al. Incident subcortical infarcts induce focal thinning in connected cortical regions. *Neurology.* 2012;79(20):2025-8.
4. Liang Z, Zeng J, Zhang C, Liu S, Ling X, Xu A, et al. Longitudinal investigations on the anterograde and retrograde degeneration in the pyramidal tract following pontine infarction with diffusion tensor imaging. *Cerebrovasc Dis.* 2008;25(3):209-16.
5. Nakane M, Tamura A, Sasaki Y, and Teraoka A. MRI of secondary changes in the thalamus following a cerebral infarct. *Neuroradiology.* 2002;44(11):915-20.
6. Shan DE. An explanation for putaminal CT, MR, and diffusion abnormalities secondary to nonketotic hyperglycemia. *AJNR Am J Neuroradiol.* 2005;26(1):194; author reply -5.
7. Ohara S, Kondo K, Kagoshima M, and Yanagisawa N. [Secondary degeneration of substantia nigra following massive basal ganglia infarction]. *Rinsho Shinkeigaku.* 1989;29(11):1352-6.
8. Kazui S, Kuriyama Y, Sawada T, and Imakita S. Very early demonstration of secondary pyramidal tract degeneration by computed tomography. *Stroke.* 1994;25(11):2287-9.
9. Tamura A, Tahira Y, Nagashima H, Kirino T, Gotoh O, Hojo S, et al. Thalamic atrophy following cerebral infarction in the territory of the middle cerebral artery. *Stroke.* 1991;22(5):615-8.
10. Nagasawa H, Kogure K, Fujiwara T, Itoh M, and Ido T. Metabolic disturbances in exo-focal brain areas after cortical stroke studied by positron emission tomography. *J Neurol Sci.* 1994;123(1-2):147-53.
11. Gerhard A, Schwarz J, Myers R, Wise R, and Banati RB. Evolution of microglial activation in patients after ischemic stroke: a [11C](R)-PK11195 PET study. *Neuroimage.* 2005;24(2):591-5.
12. Pappata S, Levasseur M, Gunn RN, Myers R, Crouzel C, Syrota A, et al. Thalamic microglial activation in ischemic stroke detected in vivo by PET and [11C]PK1195. *Neurology.* 2000;55(7):1052-4.
13. Binkofski F, Seitz R, Arnold S, Classen J, Benecke R, and Freund HJ. Thalamic metabolism and corticospinal tract integrity determine motor recovery in stroke. *Annals of neurology.* 1996;39(4):460-70.
14. Fernández-Andújar M, Doornink F, Dacosta-Aguayo R, Soriano-Raya JJ, Miralbell J, Bargalló N, et al. Remote Thalamic Microstructural Abnormalities Related to Cognitive Function in Ischemic Stroke Patients. 2014.
15. Seitz RJ, Azari NP, Knorr U, Binkofski F, Herzog H, and Freund H-J. The role of diaschisis in stroke recovery. *Stroke.* 1999;30(9):1844-50.
16. Winter B, Brunecker P, Fiebach JB, Jungehulsing GJ, Kronenberg G, and Endres M. Striatal Infarction Elicits Secondary Extrafocal MRI Changes in Ipsilateral Substantia Nigra. *PLoS One.* 2015;10(9):e0136483.
17. Prinz V, Hetzer AM, Muller S, Balkaya M, Leithner C, Kronenberg G, et al. MRI heralds secondary nigral lesion after brain ischemia in mice: a secondary time window for neuroprotection. *J Cereb Blood Flow Metab.* 2015;35(12):1903-9.
18. Baron JC, Yamauchi H, Fujioka M, and Endres M. Selective neuronal loss in ischemic stroke and cerebrovascular disease. *J Cereb Blood Flow Metab.* 2014;34(1):2-18.

19. Kronenberg G, Balkaya M, Prinz V, Gertz K, Ji S, Kirste I, et al. Exofocal dopaminergic degeneration as antidepressant target in mouse model of poststroke depression. *Biol Psychiatry.* 2012;72(4):273-81.
20. Zhang J, Zhang Y, Xing S, Liang Z, and Zeng J. Secondary neurodegeneration in remote regions after focal cerebral infarction: a new target for stroke management? *Stroke; a journal of cerebral circulation.* 2012;43(6):1700-5.
21. Lesne SE, Sherman MA, Grant M, Kuskowski M, Schneider JA, Bennett DA, et al. Brain amyloid-beta oligomers in ageing and Alzheimer's disease. *Brain.* 2013;136(Pt 5):1383-98.
22. Lesne S, Koh MT, Kotilinek L, Kayed R, Glabe CG, Yang A, et al. A specific amyloid-beta protein assembly in the brain impairs memory. *Nature.* 2006;440(7082):352-7.
23. Haass C, and Selkoe DJ. Soluble protein oligomers in neurodegeneration: lessons from the Alzheimer's amyloid beta-peptide. *Nat Rev Mol Cell Biol.* 2007;8(2):101-12.
24. Iliff JJ, Wang M, Liao Y, Plogg BA, Peng W, Gundersen GA, et al. A paravascular pathway facilitates CSF flow through the brain parenchyma and the clearance of interstitial solutes, including amyloid beta. *Sci Transl Med.* 2012;4(147):147ra11.
25. Tynan RJ, Naicker S, Hinwood M, Nalivaiko E, Buller KM, Pow DV, et al. Chronic stress alters the density and morphology of microglia in a subset of stress-responsive brain regions. *Brain Behav Immun.* 2010;24(7):1058-68.
26. Franciosi S, De Gasperi R, Dickstein DL, English DF, Rocher AB, Janssen WG, et al. Pepsin pretreatment allows collagen IV immunostaining of blood vessels in adult mouse brain. *J Neurosci Methods.* 2007;163(1):76-82.
27. Johnson SJ, and Walker FR. Strategies to improve quantitative assessment of immunohistochemical and immunofluorescent labelling. *Sci Rep.* 2015;5:10607.
28. Patience MJ, Zouikr I, Jones K, Clarkson AN, Isgaard J, Johnson SJ, et al. Photothrombotic stroke induces persistent ipsilateral and contralateral astrogliosis in key cognitive control nuclei. *Neurochem Res.* 2015;40(2):362-71.
29. Ong LK, Guan L, Damanhuri H, Goodchild AK, Bobrovskaya L, Dickson PW, et al. Neurobiological consequences of acute footshock stress: effects on tyrosine hydroxylase phosphorylation and activation in the rat brain and adrenal medulla. *J Neurochem.* 2014;128(4):547-60.
30. Glenner GG, and Wong CW. Alzheimer's disease: initial report of the purification and characterization of a novel cerebrovascular amyloid protein. *Biochem Biophys Res Commun.* 1984;120(3):885-90.
31. Kang J, Lemaire HG, Unterbeck A, Salbaum JM, Masters CL, Grzeschik KH, et al. The precursor of Alzheimer's disease amyloid A4 protein resembles a cell-surface receptor. *Nature.* 1987;325(6106):733-6.
32. Sisodia SS. Beta-amyloid precursor protein cleavage by a membrane-bound protease. *Proc Natl Acad Sci U S A.* 1992;89(13):6075-9.
33. Cai H, Wang Y, McCarthy D, Wen H, Borchelt DR, Price DL, et al. BACE1 is the major beta-secretase for generation of Abeta peptides by neurons. *Nat Neurosci.* 2001;4(3):233-4.
34. Black RA, Rauch CT, Kozlosky CJ, Peschon JJ, Slack JL, Wolfson MF, et al. A metalloproteinase disintegrin that releases tumour-necrosis factor-alpha from cells. *Nature.* 1997;385(6618):729-33.
35. Iwata N, Tsubuki S, Takaki Y, Shirotani K, Lu B, Gerard NP, et al. Metabolic regulation of brain Abeta by neprilysin. *Science.* 2001;292(5521):1550-2.
36. Kurochkin IV, and Goto S. Alzheimer's beta-amyloid peptide specifically interacts with and is degraded by insulin degrading enzyme. *FEBS Lett.* 1994;345(1):33-7.
37. Eckman EA, Reed DK, and Eckman CB. Degradation of the Alzheimer's amyloid beta peptide by endothelin-converting enzyme. *The Journal of biological chemistry.* 2001;276(27):24540-8.

38. Deane R, Wu Z, Sagare A, Davis J, Du Yan S, Hamm K, et al. LRP/amyloid beta-peptide interaction mediates differential brain efflux of Abeta isoforms. *Neuron.* 2004;43(3):333-44.
39. Deane R, Du Yan S, Submamaryan RK, LaRue B, Jovanovic S, Hogg E, et al. RAGE mediates amyloid-beta peptide transport across the blood-brain barrier and accumulation in brain. *Nat Med.* 2003;9(7):907-13.
40. Rodriguez FA, Truijens MJ, Townsend NE, Stray-Gundersen J, Gore CJ, and Levine BD. Performance of runners and swimmers after four weeks of intermittent hypobaric hypoxic exposure plus sea level training. *J Appl Physiol (1985).* 2007;103(5):1523-35.
41. Wehrlin JP, Zuest P, Hallen J, and Marti B. Live high-train low for 24 days increases hemoglobin mass and red cell volume in elite endurance athletes. *J Appl Physiol (1985).* 2006;100(6):1938-45.
42. Brugniaux JV, Schmitt L, Robach P, Nicolet G, Fouillot JP, Moutereau S, et al. Eighteen days of "living high, training low" stimulate erythropoiesis and enhance aerobic performance in elite middle-distance runners. *J Appl Physiol (1985).* 2006;100(1):203-11.
43. Meeuwsen T, Hendriksen IJ, and Holewijn M. Training-induced increases in sea-level performance are enhanced by acute intermittent hypobaric hypoxia. *Eur J Appl Physiol.* 2001;84(4):283-90.
44. Dufour SP, Ponsot E, Zoll J, Doutreleau S, Lonsdorfer-Wolf E, Geny B, et al. Exercise training in normobaric hypoxia in endurance runners. I. Improvement in aerobic performance capacity. *J Appl Physiol (1985).* 2006;100(4):1238-48.
45. Wang L, Zhang Z, Wang Y, Zhang R, and Chopp M. Treatment of stroke with erythropoietin enhances neurogenesis and angiogenesis and improves neurological function in rats. *Stroke.* 2004;35(7):1732-7.
46. Sun Y, Jin K, Xie L, Childs J, Mao XO, Logvinova A, et al. VEGF-induced neuroprotection, neurogenesis, and angiogenesis after focal cerebral ischemia. *J Clin Invest.* 2003;111(12):1843-51.
47. Greenberg DA, and Jin K. Vascular endothelial growth factors (VEGFs) and stroke. *Cellular and molecular life sciences : CMLS.* 2013;70(10):1753-61.
48. Lapchak PA. Erythropoietin molecules to treat acute ischemic stroke: a translational dilemma! *Expert Opin Investig Drugs.* 2010;19(10):1179-86.
49. Leconte C, Tixier E, Freret T, Toutain J, Saulnier R, Boulouard M, et al. Delayed hypoxic postconditioning protects against cerebral ischemia in the mouse. *Stroke; a journal of cerebral circulation.* 2009;40(10):3349-55.
50. Tsai YW, Yang YR, Wang PS, and Wang RY. Intermittent hypoxia after transient focal ischemia induces hippocampal neurogenesis and c-Fos expression and reverses spatial memory deficits in rats. *PLoS One.* 2011;6(8):e24001.
51. Tsai YW, Yang YR, Sun SH, Liang KC, and Wang RY. Post ischemia intermittent hypoxia induces hippocampal neurogenesis and synaptic alterations and alleviates long-term memory impairment. *J Cereb Blood Flow Metab.* 2013;33(5):764-73.
52. Galle AA, and Jones NM. The neuroprotective actions of hypoxic preconditioning and postconditioning in a neonatal rat model of hypoxic-ischemic brain injury. *Brain Res.* 2013;1498:1-8.
53. Rybnikova E, Vorobyev M, Pivina S, and Samoilov M. Postconditioning by mild hypoxic exposures reduces rat brain injury caused by severe hypoxia. *Neurosci Lett.* 2012;513(1):100-5.
54. LaManna JC, Vendel LM, and Farrell RM. Brain adaptation to chronic hypobaric hypoxia in rats. *J Appl Physiol (1985).* 1992;72(6):2238-43.
55. LaManna JC, Chavez JC, and Pichiule P. Structural and functional adaptation to hypoxia in the rat brain. *J Exp Biol.* 2004;207(Pt 18):3163-9.

56. Iliff JJ, Chen MJ, Plog BA, Zeppenfeld DM, Soltero M, Yang L, et al. Impairment of glymphatic pathway function promotes tau pathology after traumatic brain injury. *J Neurosci.* 2014;34(49):16180-93.

`

Publication 6

Brain, Behavior, and Immunity 69 (2018) 210–222

Contents lists available at ScienceDirect

Brain, Behavior, and Immunity

journal homepage: www.elsevier.com/locate/ybrbi

Sustained administration of corticosterone at stress-like levels after stroke suppressed glial reactivity at sites of thalamic secondary neurodegeneration

Katarzyna Zalewska [a,b], Giovanni Pietrogrande [a,b], Lin Kooi Ong [a,b,c], Mahmoud Abdolhoseini [d], Murielle Kluge [a,b], Sarah J. Johnson [d], Frederick R. Walker [a,b,c,*], Michael Nilsson [a,b,c]

[a] School of Biomedical Sciences and Pharmacy and the Priority Research Centre for Stroke and Brain Injury, University of Newcastle, Callaghan, NSW, Australia
[b] Hunter Medical Research Institute, Newcastle, NSW, Australia
[c] NHMRC Centre of Research Excellence Stroke Rehabilitation and Brain Recovery, Australia
[d] School of Electrical Engineering and Computer Science, University of Newcastle, Callaghan, NSW, Australia

ARTICLE INFO

Article history:
Received 5 July 2017
Received in revised form 7 November 2017
Accepted 17 November 2017
Available online 21 November 2017

Keywords:
Neurovascular unit
Corticosterone
Microglia
Astrocytes
Neurons
Stroke
Vessels

ABSTRACT

Secondary neurodegeneration (SND) is an insidious and progressive condition involving the death of neurons in regions of the brain that were connected to but undamaged by the initial stroke. Our group have published compelling evidence that exposure to psychological stress can significantly exacerbate the severity SND, a finding that has considerable clinical implications given that stroke-survivors often report experiencing high and unremitting levels of psychological stress. It may be possible to use one or more targeted pharmacological approaches to limit the negative effects of stress on the recovery process but in order to move forward with this approach the most critical stress signals have to be identified. Accordingly, in the current study we have directed our attention to examining the potential effects of corticosterone, delivered orally at stress-like levels. Our interest is to determine how similar the effects of corticosterone are to stress on repair and remodelling that is known to occur after stroke. The study involved 4 groups, sham and stroke, either administered corticosterone or normal drinking water. The functional impact was assessed using the cylinder task for paw asymmetry, grid walk for sensorimotor function, inverted grid for muscle strength and coordination and open field for anxiety-like behaviour. Biochemically and histologically, we considered disturbances in main cellular elements of the neurovascular unit, including microglia, astrocytes, neurons and blood vessels using both immunohistochemistry and western blotting. In short, we identified that corticosterone delivery after stroke results in significant suppression of key microglial and astroglial markers. No changes were observed on the vasculature and in neuronal specific markers. No changes were identified for sensorimotor function or anxiety-like behaviour. We did, however, observe a significant change in motor function as assessed using the inverted grid walk test. Collectively, these results suggest that pharmacologically targeting corticosterone levels in the future may be warranted but that such an approach is unlikely to limit all the negative effects associated with exposure to chronic stress.

1. Introduction

Stroke survivors often experience high levels of psychological stress (Hilari et al., 2010; Lyon, 2002). Although few clinical studies, have systematically dissected out the specific causes of the stress burden, even the slightest consideration of the changes in personal circumstances reveal a multitude of probable factors. Amongst the most compelling, is the fact that stroke survivors frequently report significant levels of motor and cognitive impairment, outcomes which can also directly impact on the survivor's quality of social interactions. A further dimension to the stress experienced by stroke survivors is persistence, with several studies reporting that the level of stress for stroke survivors is unremitting and has detrimental effect on the recovery in both clinical and preclinical research (Angeleri et al., 1993; Elmstahl et al., 1996; Espinosa-Garcia et al., 2017; Feibel et al., 1977; Hilari et al.,

* Corresponding author at: School of Biomedical Sciences and Pharmacy and the Priority Research Centre for Stroke and Brain Injury, University of Newcastle, Callaghan, NSW, Australia. Hunter Medical Research Institute, Newcastle, NSW, Australia.
E-mail address: rohan.walker@newcastle.edu.au (F.R. Walker).

https://doi.org/10.1016/j.bbi.2017.11.014
0889-1591/

2010; Jones et al., 2015; Kirkland et al., 2008; Lyon, 2002; Ong et al., 2016; Tyson, 1995; Walker et al., 2014; Zhao et al., 2017).

Recently, our research team has directed it's focus towards exploring the potential implications of chronic stress exposure during the recovery process on the severity of secondary neurodegeneration (SND) post-stroke. SND involves the progressive death of neurons in regions that are connected to but not originally damaged by the infarction. In our initial study into this phenomenon we identified that exposure to chronic stress was associated with a significant exacerbation of the neuronal loss within the thalamus after induction of a somatosensory cortex stroke (Jones et al., 2015; Ong et al., 2016). Interestingly, our team also observed that the increased loss of neurons in the thalamus co-occurred with a suppression of makers indicative of microglial activity (Jones et al., 2015). This observation, aligned well with a number of results that have suggested that microglia play a central role in brain repair following CNS trauma (Myers et al., 1991; Pappata et al., 2000; Sugama et al., 2009). We have also identified that chronic stress markedly alters the accumulation of neurotoxic proteins within the thalamus while concomitantly reducing synaptic density (Alfarez et al., 2009; Karten et al., 1999; Ong et al., 2016). Collectively, these findings suggest that chronic stress exerts a broadly negative influence over repair processes at sites of SND.

Limiting the negative effects of stress from a biomedical standpoint poses a number of significant challenges, foremost amongst which is the fact that the 'stress response' evokes changes in the activity of multiple subsystems. This creates a significant challenge for the development of targeted strategies that restrict the negative effects of stress. One potential solution to this challenge is to target which stress signals are the most biologically active and have the strongest evidence implicating their role in immunomodulation and immunosuppression. To this end, there is one compelling candidate; corticosterone. Corticosterone is one of the major immunomodulatory hormones released during the stress response. It's release from the adrenal cortex is initiated by the coordinated actions of the hypothalamic–pituitary–adrenal axis (De Kloet, 2004).

In the current study, we aimed to investigate the effect of corticosterone administration on the severity of SND post-stroke within the thalamus. This study is a continuation of previously reported corticosterone impact in peri-infarct regions (Zalewska et al., 2017). In terms of the design of the current study we chose to use a photothrombotic (PT) model to induce a focal cortically directed stroke. This model has a number of advantages, including that it is highly steerable and repeatable, has low experiment to experiment variance, and is widely used and extensively validated (Labat-gest and Tomasi, 2013). Importantly, it is also recognised to possess a number of limitations, including the fact that it produces only a relatively small penumbral area (at risk tissue around the primary infarct) and by its nature does not permit the study of cortical reperfusion, as the occlusion induced is permanent in nature (Labat-gest and Tomasi, 2013). We have previously used the PT model across a large number of studies and have consistently identified the ability of PT stroke directed towards the somatosensory cortex to robustly induced thalamic SND (Jones et al., 2015; Ong et al., 2016; Patience et al., 2015). To consider the influence of corticosterone, we used the same administration paradigm as previously reported by Zalewska et al., to simulate stress-like levels of corticosterone (Zalewska et al., 2017). Specifically, we delivered 100 μg/ml of corticosterone in the drinking water to mice following stroke. This concentration has been shown to increase level of corticosterone in blood to around 5 times that seen in sham animals (Zalewska et al., 2017). A similar level of increase has been shown after exposure of mice to a 30 min swim stress (Barriga et al., 2001) a 6 h session of restraint stress, or after 23 days of mild unpredictable stress (Gong et al., 2015) Corticosterone administration began 72 h after the induction of stroke. Three days of recovery reduced chances of surgery related infections and allows wound healing which could be delayed due to corticosterone administration (Padgett et al., 1998).

Corticosterone was administered via drinking water for 14 days. We assessed motor function using the cylinder task, grid walk and inverted grid test to determine functional recovery. Anxiety-like behaviour and locomotor activity was assessed by open field test. We examined changes of a variety of markers; neuronal (NeuN, PSD-95), astroglial (GFAP, S100β), microglial (CD68, CD11b) and vascular proteins (Collagen-IV, CD31) within the thalamus. Additionally, we also examined changes in microglial morphology. We hypothesised that exposure to corticosterone at stress-like levels would result in greater neuronal loss. Moreover, we expected that corticosterone would result in significant suppression of glial activation and that this will be linked to suppression of vascular growth.

2. Materials and methods

2.1. Materials

A full list of antibodies used during this experiment is listed in Table 1. Corticosterone hemisuccinate (4-PREGNEN-11β, 21-DIOL-3, 20-DIONE 21-HEMISUCCINATE) was obtained from Steraloids

Table 1
List of antibodies used for western blot and immunohistochemistry.

	Sources of antibodies	Application	Dilution
Collagen IV	Abcam, rabbit anti-collagen IV, ab6586	IHC	1:1000
	Abcam, rabbit anti-collagen IV, ab6586	WB	1:1000
GFAP	Sigma, mouse anti-GFAP, G3893	IHC	1:1000
	Cell Signalling, mouse anti-GFAP, #3670	WB	1:5000
Iba-1	WAKO, rabbit anti-Iba-1, 019-19741	IHC	1:1000
NeuN	Millipore, mouse anti-NeuN, MAB377	IHC	1:500
	Cell signalling, monoclonal rabbit anti-NeuN, #12943	WB	1:2000
CD11b	Abcam, rabbit anti- CD11b, #ab75476	WB	1:2000
CD31	Cell signalling, monoclonal rabbit- anti CD31, #77699	WB	1:1000
CD68	Abcam, monoclonal rabbit anti-CD68, #76308	IHC	1:500
	Abcam, monoclonal rabbit anti-CD68, #76308	WB	1:2000
PSD95	Cell signalling, rabbit anti-PSD95, #3409	WB	1:1000
S100B	Cell signalling, monoclonal rabbit- anti S100B, #9550	WB	1:1000
β-actin	Sigma-Aldrich, Monoclonal anti-β-actin-HRP, A3854	WB	1:50000
Rabbit IgG	Biorad, anti-Rabbit-HRP antibody, #170-6515	WB	1:5000
	Jackson ImmunoResearch, goat anti-rabbit-biotin, #111-065-003	IHC	1:500
Mouse IgG	Biorad, anti-Mouse-HRP antibody, #170-6516	WB	1:10000
	Jackson ImmunoResearch, goat anti-mouse-biotin, #115-065-003	IHC	1:500

Inc. (Newport, RI, USA). Paraformaldehyde, rose bengal and other reagents were purchased from Sigma-Aldrich (St. Louis, MO, USA).

2.2. Animals

All experiments were approved by the University of Newcastle Animal Care and Ethics Committee and conducted in accordance with the New South Wales Animals Research Act (1985) and the Australian Code of Practice for the use of animals for scientific purposes. This study was planned and conducted according to ARRIVE guidelines. See Fig. 1A for experimental design. Mice were maintained at 21 °C ± 1 in a humidity controlled environment with water and food available *ad libitum*. Lighting was on 12:12 h reverse light–dark cycle (light on at 7 pm). All procedures were conducted in the dark phase under low-level red light. Mice were grouped-housed with 2–4 animals per cage and acclimatised for 7 days before commencing the procedures. Animals were weighed throughout the procedures.

2.2.1. Sample size calculations

Sample sizes were estimated using the formula to compare between groups with quantitate endpoints.

$$SS = \frac{2SD^2(z_1 - \alpha/2 + z_{1-\beta})^2}{d^2}$$

Using preliminary data on corticosterone treatment of sham animals, we obtained standard deviation SD = 11 and an effect size of d = 20. Allowing a type 1 error of 5%, $\alpha = 0.05$ with the power of 90%, $\beta = 0.1$ we calculated a sample size of 7 animals per group. More than 7 animals per group would ensure that a treatment effect will be detected, if present, with a greater than 90% chance.

C57BL/6 male mice (7 weeks old) were obtained from the Animal Services Unit at the University of Newcastle, each randomly allocated to one of the following groups before any of procedures started: sham ($n_{fixed} = 7$, $n_{fresh} = 9$), sham + CORT ($n_{fixed} = 7$, $n_{fresh} = 10$), stroke ($n_{fixed} = 7$, $n_{fresh} = 11$) and stroke + CORT ($n_{fixed} = 5$, $n_{fresh} = 8$). At time of death if we histologically identified that the stroke had not occurred, or was placed clearly beyond the somatosensory territory that animal was removed from the study.

2.3. Behavioural tasks

2.3.1. Open field test

In order to assess changes in locomotor activity and exploration level all mice were tested in an open field environment on D0, prior to sham or stroke surgery, and again on D16. As described previously (Zhao et al., 2017) mice were placed in the centre of open field arena (40 cm × 40 cm × 40 cm). Locomotor activity was recorded for 5 min, light in the testing room was kept below 50Lux. Assessment of locomotor parameters was performed using EthoVision XT system (Noldus, Wageningen, The Netherlands). The software detected and tracked the mouse and reported total distance travelled, the time spent in the center (12 cm × 12 cm, the center of the arena) and four corners (14 cm × 14 cm) (see Fig. 2D and Appendix 1). Total of 30 mice was used for this test.

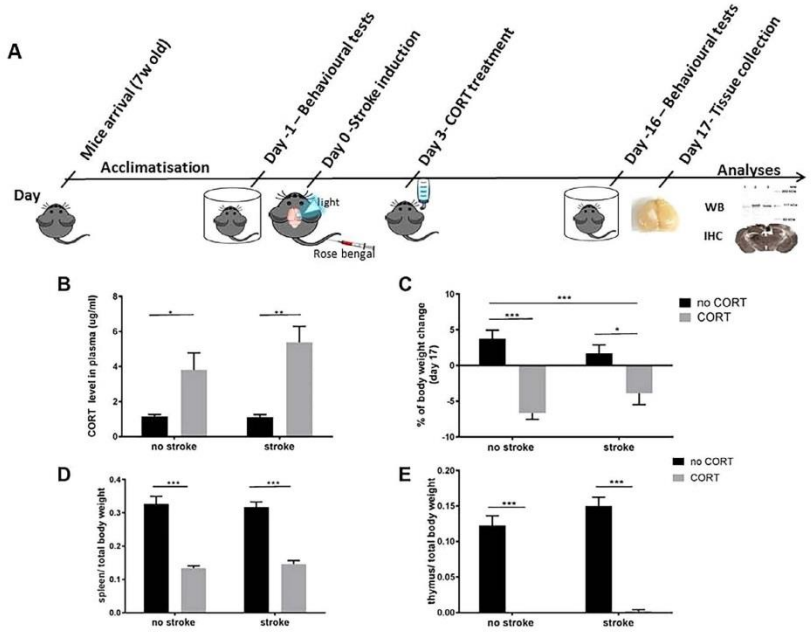

Fig. 1. The effect of stroke and CORT treatment on physiological parameters A. experimental design timeline B. CORT administration significantly increased level of CORT in blood serum compared to non- CORT treated groups C. CORT administration significantly decreased the body weight. Animals were weighed on Day 0 before the photothrombotic occlusion and then again on the day 17 th. D. CORT treatment significantly decreased the spleen weight. E. CORT treatment irrespective of stroke reduces weight of the thymus. Changes in spleen and thymus size were normalised to the body weight. Graphs report the mean ± SEM $^{***}p < .001$, $^{**}p < .01$, $^{*}p < .05$.

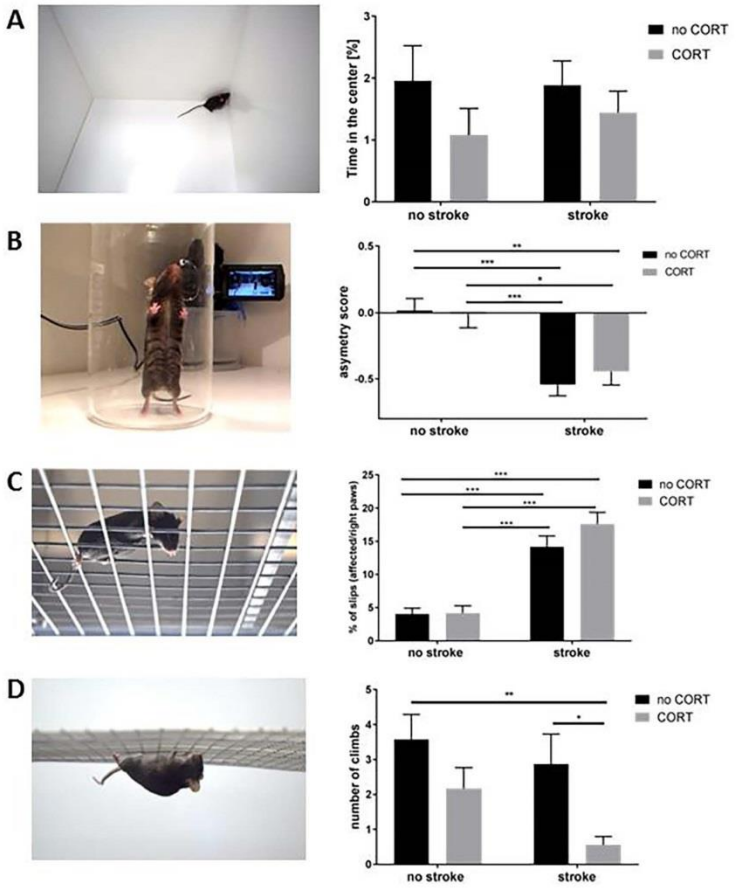

Fig. 2. Assessments of behavioural parameters. A. Mouse placed in open field box (left). Time spent in the centre of the box suggest level of anxiety (right) B. Mouse placement during cylinder test adapted from (Zhao et al., 2017) (left). Cylinder task asymmetry score (right panel) B. Left panel shows mouse placement on the grid walk, right panel shows increased right paws "foot fault". C. Mouse placement during inverted grid test (left). Number of climbs on top of the screen within 4 min of test (right). $^{*}P < .05$, $^{**}P < .01$ $^{***}P < .001$ (two-way ANOVA followed by Tukey's multiple comparisons).

2.3.2. Paw asymmetry assessment using the cylinder task

In the study we used the cylinder task, consistent with how we have used the test previously; (Schaar et al., 2010). Briefly described, the day before the stroke (day -1) and day before sacrifice (day 16 – see Fig. 1A) the mouse was placed in a glass cylinder 9 cm diameter and 15 cm in height and videotaped from both sides during the test. Afterward paw placed was determined by researcher blinded to the experimental condition. The scoring matrix was as follows: (1) the first forelimb to contact the wall during a full rear was recorded as an independent wall placement for that limb. (2) Simultaneous use of both the left and right forelimb by contacting the wall of the cylinder during a full rear and for lateral movements along the wall was recorded as "both" movement. A total of 20 movements were recorded during the 4 min test. A final asymmetry score was calculated as the ratio of non-impaired forelimb movement minus impaired forelimb movement to total forelimb movement (see Fig. 2A). The final score was calculated as a difference scores between the asymmetry score before and after.

2.3.3. Sensorimotor function assessment using grid walk

This test determines sensorimotor function, motor coordination and placing deficits during locomotion (Schaar et al., 2010). Mouse was placed on elevated grid with openings. Healthy mouse during walk on the grid place paws precisely on the bars. After the stroke this coordination is disturbed. Each mouse was recorded and number of "foot faults" on each side was calculated of total of 60 steps (see Fig. 2B and Appendix 1).

2.3.4. Inverted grid walk to determine changes in muscle strength

We used modified version of inverted grid test to measure motor impairment and coordination (Coughenour et al., 1977).

Each animal was placed in the middle of the wire screen and then inverted to 180°. Mice were allowed to climb on the top of the screen and after were inverted back until the end of the test. A maximum time of 4 min was given if an animal did not fall. The time at which hind paws and fore paws were no longer in contact with the screen, number and time of climbing on the top of the screen was recorded (see Fig. 2C and Appendix 1).

2.4. Photothrombotic occlusion

Photothrombotic occlusion was performed as described previously by (Ong et al., 2016; Zalewska et al., 2017). Briefly, on day 0 mice were anesthetised by using 2% of isoflurane and injected intraperitoneally with 0.2 mL of 10 mg/mL of rose bengal eight minutes prior to 15 min of illumination, using a cold light source with a fibre optic end of 4.5 mm diameter placed 2.2 mm left lateral of Bregma onto the exposed skull. Occlusion was directed into somatosensory and motor cortices (based on Mouse Brain Atlas (Paxinos and Franklin, 2004). For the sham group, a similar procedure was applied except Rose Bengal was replaced with 0.2 mL of 0.9% saline.

2.5. Oral delivery of corticosterone (CORT)

CORT administration began 72 h after the stroke. The drinking water solution was prepared so that the final concentration was 100 μg/ml as described previously (Gourley et al., 2006; Gourley and Taylor, 2009; Zalewska et al., 2017). Briefly, the protocol for achieving the desired amount of CORT involved the solution being stirred in pH 11–12 water solution (using NaOH) until completely dissolved and then pH adjusted to pH 7–7.5 (using HCl). The CORT – water solution, henceforth referred to as CORT, was given to animals instead of drinking water. The solution was refreshed every 72 h over the 14 days of protocol. For the half of animals in non CORT treated groups drinking water was prepared by increasing and reduction of pH without CORT addition.

2.6. Tissue collection

Tissue and blood samples were collected for all of groups at the same time of the day between 10 am and 2 pm to avoid changes in CORT level caused by circadian rhythm. Mice were deeply anaesthetised with sodium pentabarbitol. Blood samples were collected transcardially. Following removal of 0.3 mL of blood, mice were perfused via the ascending aorta with ice cold 0.9% saline followed by ice cold 4% paraformaldehyde (pH 7.4) for immunohistochemical analysis or with cold 0.9% saline only for western blotting. Spleen and thymus were dissected and weighed.

2.6.1. Tissue collection for immunohistochemical analysis

Brains were dissected, post-fixed in 4% paraformaldehyde for 4 h and transferred to 12.5% sucrose in PBS for storage and cryoprotection. Coronal sections of the brains were sectioned with a freezing microtome (Leica, North Ryde, NSW, Australia) at 30 μm.

2.6.2. Tissue collection for western blotting

Brains were dissected and rapidly frozen in -80 °C isopentane. Frozen brains were sliced using the cryostat at the thickness of 200 μm. Tissue was punched using 2 mm tissue punch in the thalamus region (Bregma −1.0 to −2.2). Samples were stored frozen in −80 °C until further analysis.

2.7. Analysis of serum corticosterone

Blood samples were incubated for 20 min at RT and then centrifuged 5000*g* for 5 min at 4 °C, serum was collected and frozen in −80 °C for future analyses. The levels of CORT were determined using a commercially available Corticosterone Enzyme Immunoassay kit (Arbor Assays, Ann Arbor, MI, USA) according to the manufacturer's instruction. All samples were run in duplicate. The final concentration is presented in μg/ml of serum. 1 value from sham + CORT group which exceeded maximum sensitivity of immunoassay was excluded from analyses.

2.8. Immunohistochemistry procedure

For immunoperoxidase labelling, free-floating sections were immunostained as described with minor modification (Tynan et al., 2010). All reactions for labels marker were run at the same time, with same reagents, at the same concentrations. Briefly, brain sections were incubated with 1 μg/ml pepsin in 0.01 M HCl for 2 min at 37 °C to retrieve antigen. Brain sections were then incubated with 1% hydrogen peroxidase for 30 min at 25 °C and followed by 3% horse serum for 30 min at 25 °C. Brain sections were incubated with primary antibodies (see Table 1) for 72 h at 4 °C and followed by secondary antibodies (see Table 1) for 1 h at 25 °C. Next, brain sections were incubated for 2 h at 25 °C with avidin–biotin-peroxidase complex and finally developed using DAB peroxidase substrate. Brain sections were washed with PBS in between each incubation step. After processing was complete, brain sections were mounted onto chrome alum-coated slides and cover slipped.

2.9. Protein extraction

Protein extraction protocol was described before (Ong et al., 2016). Briefly, thalamic samples were sonicated in 300 μl lysis buffer (50 mM TRIS buffer pH 7.4, 1 mM EDTA, 1 mM DTT, 80 μM ammonium molybdate, 1 mM sodium pyrophosphate, 1 mM sodium vanadate, 5 mM b-glycerolphosphate, 1 protease inhibitor cocktail tablet, 1 phosphatase inhibitor cocktail tablet, final concentration) and centrifuged for 20 min at 4 °C. Next, supernatants were collected and protein levels were estimated by using commercially available Pierce BCA protein assay kit according to the manufacturer's instructions.

2.10. Western blotting

Western blotting was conducted as described previously at (Ong et al., 2017; Ong et al., 2016). Supernatants were added with sample buffer (2% sodium dodecyl sulfate, 50 mM Tris, 10% glycerol, 1% DTT, 0.1% bromophenol blue, pH 6.8), followed by electrophoresis of 15 μg of total tissue protein in to Biorad Criterion TGC Stain-Free 4–20% gels. Proteins were transferred onto PVDF membranes in transfer buffer (25 mM Tris, 200 mM glycine, and 20% methanol pH 8.3).

2.11. Image acquisition and analysis

The following analyses were performed by a researcher blinded to the experimental conditions during the experiment.

2.11.1. Fixed tissue

Images of immunolabelling were obtained and analysed as described previously at (Ong et al., 2017; Zalewska et al., 2017). Briefly images were taken in the magnification 20 X by using an Aperio AT2 (Leica). Whole mosaic SVS images were converted into TIFF images in Matlab v2015b followed by conversion into uncompressed JPEG images using Irfanview v4.37 before finally being passed into Matlab v2015b for further analysis. Brain regions were identified by reference to the Mouse Brain in Stereotaxic Coordinate (Paxinos and Franklin, 2004). The mosaic images were cropped in thalamic territories (Bregma −1.34 to 2.06 mm).

For analysis of the acquired cropped images, we determined the pixel intensity that clearly reflected full inclusion of the immunolabelled signal. The individual pixel intensities, at which this occurred were then determined and passed through to quantitative analysis.

Secondary neurodegeneration area was determined manually as territories with an approximate loss of 50% of neurons using imageJ 1.48v.

2.11.2. Fresh tissue

Membranes obtained during western blotting procedures were visualized using Amersham Imager 600 with Luminata Classico Western blotting detection reagents. The density of the bands was measured using Amersham Imager 600 Analysis Software.

2.12. Digital reconstruction of Collagen IV and Iba1 immunostaining

2.12.1. Collagen IV

The morphological digital reconstruction of collagen IV was performed as described at (Kongsui et al., 2015; Zalewska et al., 2017). Collagen IV positive cells were isolated from the background using multi-level Otsu's thresholding method which calculates the threshold that minimizes the interclass pixel intensity variance between groups. Using Matlab we examined number of the cells and area covered by the labelling (the total amount of pixels in the region).

2.12.2. Iba1

3 regions of interest (posterior thalamic nuclear group (Po), ventralposterior thalamic nucleus (vpl) and ventral postmedial thalamic nucleus (vpm) were cropped within thalamus. Automatic reconstructions and quantifications was performed using GliaTrace script (Abdolhoseini, 2016; Pietrogrande et al., 2017). It received 2D/3D microscopy images of microglia as inputs, and after processing the data, it output all results in spreadsheets. The program also stores cellular reconstructions in standard SWC file format. The method implemented in GliaTrace includes soma segmentation, tracing of the cell processes, and quantification of the cell features. Soma segmentation and background removal are performed using multilevel thresholding as the first step. Different intensity levels output by the first step are sampled to create seed points. Connecting seed points is started from the soma centroid, then proceeded through the centreline of the processes and ended with the last significant intensity level. The process is designed to output a tree-like structure for each cell which fulfils the topology of the microglial cell. Finally the reconstructed images are visualized and the features of the cells are automatically quantified.

2.13. Statistical analyses

All of the statistical analyses were performed as a difference between 4 groups: sham, sham + CORT, stroke and stroke + CORT. Those differences were determined by using two-way ANOVA followed by Tukey's multiple comparisons test using GraphPad Prism v.7.02. All data sets are presented as mean ± SEM and statistical significance accepted at $p < .05$. For analyses of secondary neurodegeneration area (see Fig. 2B) unpaired *t*-test was used.

3. Results

3.1. Oral administration of CORT reduced body, spleen and thymus weight and increased circulating CORT levels

To asses efficiency of CORT administration we measured changes in body weight, blood circulating CORT level and weight of spleen and thymus. Groups for fixed and fresh tissue were calculated together.

We found that the circulating levels of CORT were significantly different across groups ($F_{CORT(1,62)} = 27.16$; $p < .001$) with increased levels in sham + CORT (sham, 1.143 μg/ml vs sham + CORT, 3.8 μg/ml; $p < .05$) and stroke + CORT groups (sham, 1.143 μg/ml vs stroke + CORT, 5.379 μg/ml; $p < .001$) without significant differences between sham and stroke groups (see Fig. 1B).

Body weight change was calculated as percentage (%) change from baseline (day 0) to the last day of CORT treatment (day 17). CORT significantly impact on body weight ($F_{CORT(1,65)} = 42.15$; $p < .001$) while there was no effect of stroke ($F_{Stroke(1,65)} = 0.08633$) (see Fig. 1C).

The whole body to spleen ($F_{CORT(1,65)} = 141.5$; $p < .001$) and thymus weights ($F_{CORT(1,65)} = 185.6$; $p < .001$) ratios were found significantly reduced in CORT treated groups (see Fig. 1D and E).

3.2. CORT administration does not impact on paw recovery and anxiety level but impairs muscle strength and endurance

Analyses of open field data did not reveal an effect for stroke or CORT on locomotor activity ($F_{Stroke(1,26)} = 2.55$, $p = .1224$, $F_{CORT(1,26)} = 0.7597$, $p = .3914$). There was also no significant effect on time spent in the centre of the box ($F_{Stroke(1,26)} = 0.111$, $p = .7417$, $F_{CORT(1,26)} = 2.281$, $p = .1430$, see Fig. 2A).

To measure changes in paw preference for mice we used the cylinder task. The effect of stroke was highly significant, while CORT treatment didn't exert a significant effect ($F_{Stroke(1,64)} = 26.88$, $p < .001$, $F_{CORT(1,64)} = 0.1356$, see Fig. 2B).

Sensorimotor function was assessed by the grid walk test. Number of "foot faults" on the right/affected side was significantly higher in stroke groups compare to sham ("foot faults" for sham = 4%, for stroke = 14% $p < .001$, for stroke CORT = 18% $p < .001$). There was no significant effect of CORT ($F_{CORT(1,26)} = 1.352$, $p = .25$). Left/not affected paw "foot faults" was consistent to all 4 groups at the level of ~5%. Assessment of grid walk before the stroke did not show any differences between the groups (see Fig. 2C).

The inverted grid walk test was used to measure deficits in muscle strength and coordination. While there was no difference between stroke and stroke CORT in number of complete releases from the grid ($p = .9$), stroke CORT group had significantly lower number of climbs compared to sham and stroke alone (sham = 3.57 climbs vs. stroke CORT = 0.56 climbs $p < .01$, stroke = 2.87 climbs, $p < .05$). There was no statistical difference between sham, sham CORT and stroke group (see Fig. 2D).

3.3. Stroke but not CORT induced changes in neuronal specific markers NeuN and PSD95

Analyses of the thalamic secondary neurodegeneration area using manual calculation in ImageJ did not show changes between stroke and stroke CORT groups (mean ± SEM of stroke 0.2928 ± 0.04462 px, vs. mean ± SEM of stroke CORT, 0.3172 ± 0.03494 px). NeuN positive cell counting was conducted using a code in MatLab and revealed a significant decrease of neurons in the area of SND caused by stroke ($F_{stroke(1,22)} = 17.3$, $p < .001$) but not by CORT exposure after stroke ($F_{CORT(1,22)} = 1.111$) (See Fig. 3B and D).

Western blot analysis of protein level identified a decrease in NeuN (mean protein fold change in stroke = 0.6953, mean fold change in stroke CORT = 0.6553, $F_{Stroke(1,34)} = 52.92$, $p < .001$, $F_{CORT(1,34)} = 0.04943$) and PSD95 (mean protein fold change in stroke = 0.7658 and for stroke CORT = 0.8066, $F_{Stroke(1,34)} = 10.06$, $p < .01$ and $F_{CORT(1,34)} = 0.006052$) after stroke. Statistical analyses did not identify changes between sham and sham + CORT groups (see Fig. 3E and F).

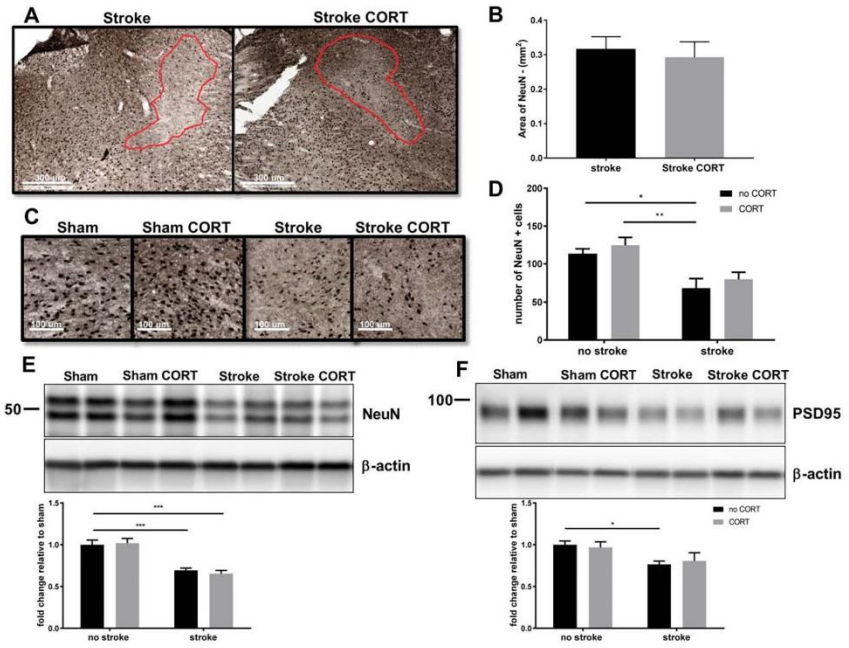

Fig. 3. Stroke induced changes in neuronal markers NeuN and PSD95. A. Two images represent NeuN immunolabelling in thalamus. Within red circle are areas of secondary neurodegeneration. Area was estimated using ImageJ. Scale bar 300 μm. B. The bar graph shows the area (mm^2) of NeuN loss in the thalamus for stroke alone and stroke + CORT animals. Data expressed as mean ± SEM for each group $^{*}p < .05$ (two tail *t*-test) C. Panel of representative images representing NeuN positive immunolabelling in thalamus. Scale bar 100 μm. D. NeuN cell counting in the regions of secondary neurodegeneration. E - F. Representative WB of NeuN and PSD for each of experimental groups. Below the bar graphs showed protein fold change relative to sham group. Data expressed as mean ± SEM for each group relative to the mean of the sham group $^{*}P < .05$, $^{**}P < .01$ $^{***}P < .001$ (two-way ANOVA followed by Tukey's multiple comparisons).

3.4. CORT administration decreased the level of the astrocytic specific markers GFAP and S100B

Pixel intensity level have been chosen at the level of 110 based on cumulative threshold spectra analyses (see Fig. 4D) Analysis of GFAP immunolabelling showed that stroke results in a significant increase in relation to the control group. This effect was suppressed by additional treatment with CORT ($F_{Stroke(1,21)} = 95.13$, $p < .001$, sham 2.278% of thresholding vs. 34.32% of thresholding for stroke group, $F_{CORT(1,21)} = 5.934$, $p < .05$, 22.07% of thresholding for stroke CORT group) (see Fig. 4E). Measurement of GFAP protein levels in the thalamus showed a significant increase in animals exposed to stroke ($F_{Stroke(1,34)} = 14.13$, $p < .001$, mean fold change in stroke = 2.402) and a decrease in protein levels in stroked animals additionally exposed to CORT ($F_{CORT(1,34)} = 11.62$, $p < .01$, mean fold change in stroke CORT = 1.08, $p < .01$). There was no significant change between sham and sham + CORT group.

Measurement of S100β protein levels showed a significant decrease between stroke and stroke CORT (mean fold change for stroke = 1.312 to mean fold change for stroke CORT = 0.479, $p < .001$), (see Fig. 4F and G).

3.5. Orally delivered CORT decreased level of microglial markers of immunoreactivity CD68 and CD11b

The pixel intensity used for the thresholding analysis was set a 100, based on the cumulative threshold spectra analyses (see Fig. 4D). Analysis of CD68 immunolabelling indicated that stroke induction resulted in enhanced expression (from 2.52% of thresholded material in sham group to 32.22% of thresholded material in stroke, $p < .00{,}1$ $F_{Stroke(1,19)} = 569$, $p < .001$) and that additional CORT administration resulted in decreased expression (7.982% of thresholded material, $p < .001$, $F_{CORT(1,19)} = 277.7$, $p < .001$) (see Fig. 5E).

Data obtained from protein analyses showed that the level of CD11b was increased after the stroke and decreased after CORT administration (from mean protein fold change in stroke = 2.151 to mean protein fold change in stroke CORT = 0.982, $p < .001$, $F_{Stroke(1,34)} = 22.25$, $p < .001$, $F_{CORT(1,34)} = 23.5$, $p < .001$). The level of CD68 also increased after the stroke and decreased after CORT but without reaching significance (mean fold change in stroke = 4.331 to mean fold change in stroke CORT = 2.521, $p < .0587$, $F_{Stroke(1,34)} = 24.54$, $p < .001$, $F_{CORT(1,34)} = 3.276$, $p < .0792$) (see Fig. 5F and G).

3.6. CORT administration reduced the number of Iba1 positive cells but did not change their morphology

Morphological analyses showed that the number of Iba1 positive cells increased after stroke and decreased after CORT treatment and they were both greater relative to control (from 17.43 cells found in sham group to 168 in stroke, $p < .001$, $F_{Stroke(1,20)} = 208.8$, $p < .001$, from 168 to 120 cells, $p < .01$, $F_{CORT(1,20)} = 8.355$, $p < .01$). Total branch length was significantly smaller in both

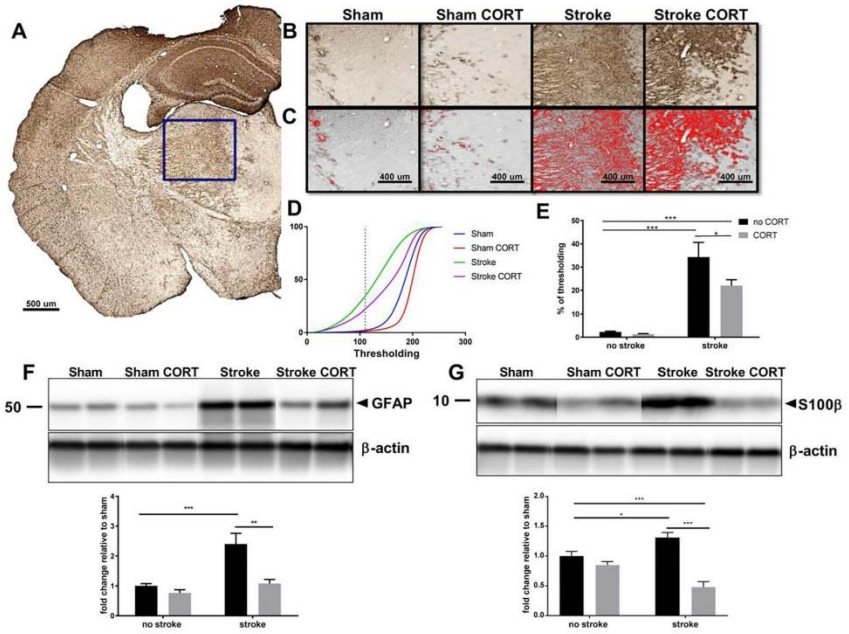

Fig. 4. The effect of stroke and CORT administration on astrocytic specific markers: GFAP and S100b A. Representative brain section from a single animal 17 days post stroke exhibiting increased activity of GFAP (blue rectangle). Scale bar = 500 μm. B. Panel of representative GFAP immunolabelling across all of the groups. Scale bar = 400 μm. C. The lower panels show material thresholded at the pixel intensity (PI) 110 in thalamus. The number of pixels that were captured at and below PI 110 was then expressed as a percentage of the total number of pixels in each image and this data were used to investigate between-group differences D. Graph represents cumulative threshold, represent each of possible pixel intensity (0–255). Cropped line indicate pixel intensity where analyses were performed E. The bar graph represents changes in GFAP thresholded material at PI = 110. F–G. Representative WB for GFAP and S100b markers across all of the groups. Data expressed as a fold change of mean ± SEM for each group relative to the mean of the sham group $^{*}P < .05$, $^{**}P < .01$ $^{***}P < .001$ (two-way ANOVA followed by Tukey's multiple comparisons).

stroke and stroke + CORT groups relative to sham (from 141.7 pixels in sham to 35.82 pixels in stroke, $p < .001$ and 67.97 pixels in stroke + CORT, $p < .001$) but there were no statistically significant differences between stroke and stroke + CORT total branch length, however two way ANOVA analyses revealed CORT influenced this variable ($F_{Stroke(1,20)} = 69.74$, $p < .001$, $F_{CORT(1,20)} = 6.297$, $p < .05$, see Fig. 6C and D).

Evaluation of cell area showed that stroke significantly reduced cell area compared to sham animals ($F_{Stroke(1,20)} = 40.36$, $p < .001$, from 418.5 pixels in sham to 233.2 pixels in stroke, $p < .001$). No differences were found between stroke and stroke + CORT (233.2 pixels in stroke to 305.5 pixels in stroke CORT, $F_{CORT(1,20)} = 5.997$, $p < .05$, see Fig. 6E).

3.7. The number and area of blood vessels and endothelial cell markers CD31 and Collagen IV were not altered by stroke or by CORT

Digital reconstruction of Collagen IV and assessment of protein levels using WB indicated that there were no identifiable differences in the vessel numbers or the total vessel area between groups that received stroke or CORT (see Fig. 7C, D and F).

Our WB analysis of CD31 indicated that there was no difference between stroke and stroke and CORT treated animals ($F_{Stroke(1,34)} = 3.286$, $p = .0787$, $F_{CORT(1,34)} = 0.007502$, $p = .9315$) (see Fig. 7E).

4. Discussion

The main objective of the current study was to examine the degree to which exposure to corticosterone at stress-like levels may influence the severity of secondary neurodegeneration. Our motivation to undertake this work based on the fact, that patients recovering from stroke often reported high and unremitting levels of psychological stress. We and others have consistently documented that exposure to chronic stress during the recovery period can negatively impact on the cellular recovery, exacerbating both functional deficits and the extent of neuronal loss (Balkaya et al., 2011; Jin et al., 2010; Jones et al., 2015; Kirkland et al., 2008; Ong et al., 2016; Zhao et al., 2017). While this information is important for confirming that exposure to stress is negative, delivering solutions to ameliorate stress linked disturbances is certainly less straightforward. The complexity here is driven by the fact that the stress response is multifactorial, involving numerous signalling systems (De Kloet, 2004). If we can identify that one of the signals generated during the stress response was accounting for a significant number of the stress-induced disturbances we would overall be in a better position to move ahead with future intervention strategies, such as using specific antagonists of the glucocorticoid receptor block the negative effects of stress hormones on brain repair.

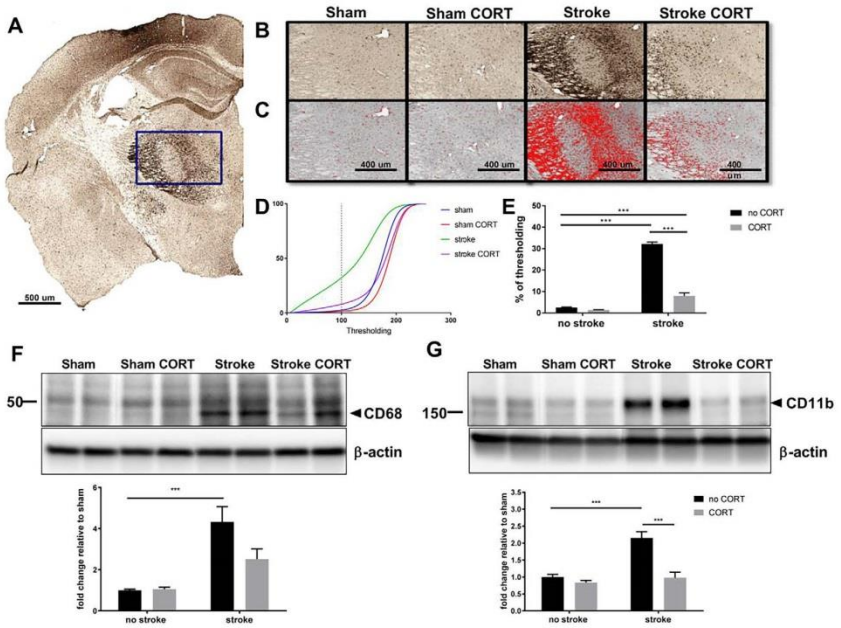

Fig. 5. The effect of stroke and CORT administration on microglial specific markers CD68 and CD11b A. Representative brain section from a single animal 17 days post stroke exhibiting enhancing expression of CD68 (blue rectangle). Scale bar = 500 μm. B. Panel of representative CD68 immunolabelling across all of the groups in the thalamic territories. Scale bar = 400 μm. C. The lower panels show material thresholded at the pixel intensity (PI) 100 in thalamus. The number of pixels that were captured at and below PI 100 was then expressed as a percentage of the total number of pixels in each image and this data was used to investigate between-group differences D. The graph represents the cumulative threshold, which illustrates the amount of material included in the threshold analysis at each of the 256 possible threshold levels. Cropped line indicates pixel intensity where analyses were performed D. The bar graph represents changes in CD68 thresholded material at PI = 100. E–F. Representative WB for CD68 and CD11b markers across all of the groups. Data expressed as a fold change of mean ± SEM for each group relative to the mean of the sham group $^{*}P < .05$, $^{**}P < .01$ $^{***}P < .001$ (two-way ANOVA followed by Tukey's multiple comparisons).

The results from the current study have identified that exposure to corticosterone at stress-like levels, while exerting clear biological effects like including reduced mass of glucocorticoid-sensitive organs and suppression of glial cell markers of 'activity' did not significantly exacerbate neuronal or vascular loss in thalamic territories or impact sensorimotor function. We did find, however, identify that corticosterone exposure post-stroke did impair motor function, as assessed using the inverted grid walk tests, as well as suppress markers typically linked with astro- and microglial activity. In short, these findings together suggest that pharmacological strategies only directed at limiting corticosterone release are unlikely to limit all of the effects of stress on neurovascular unit. This is a significant conclusion in the context of our current understanding of how environmental events influence the progression of secondary neurodegeneration. Corticosterone, is one of the most extensively studied signalling molecules release during the stress response (Carter et al., 2013; Cooper and Stewart, 2009; Faraji et al., 2011; Gourley et al., 2008a; Gourley et al., 2006; Gourley et al., 2008b; Joels and de Kloet, 1992; Nacher et al., 2004; Olausson et al., 2013; Zalewska et al., 2017; Zhang et al., 2015a; Zhang et al., 2015b). The molecule itself is a steroid hormone, released from the adrenal cortex in response to the activity of adrenocorticotrophic release hormone (ACTH). Corticosterone, which can freely enter the brain via the circulation, exerts the majority of its effects (in the context of stress) through the glucocorticoid receptor (GCR) (Ramamoorthy and Cidlowski, 2016). In the current study we chose to orally deliver a dose 100 μg/ml of drinking water. We have previously established that delivery at this concentration elevates levels within the blood around 5 times above baseline level which is typically observed after both chronic and acute stress exposition (Barriga et al., 2001; Gong et al., 2015; Malisch et al., 2007; Zalewska et al., 2017; Zhao et al., 2017).

Although corticosterone administration clearly impacted a number of systems, we did not find evidence indicate that it could influence the extent of SND post-stroke, as measured through the loss of neuronal or synaptic markers or the area of tissue loss within the thalamus. The finding that exposure to corticosterone did not significantly alter the severity of SND was, to some extent, was an unanticipated finding. We consider it important to emphasize that the absence of an effect was confirmed using several complimentary techniques. Specifically we assessed neuronal disruption by manually tracing the area of loss, by counting cells within the affected territories, as well as by assessing protein expression of the key neuronal markers NeuN and PSD-95 obtained from the site of SND. This result indicated that corticosterone delivery did not produce the same impact that can be observed after exposure to chronic stress post-stroke (Jones et al., 2015; Ong et al., 2016).

One explanation for the absence of corticosterone mediated effects on neuronal loss is that the corticosterone administration

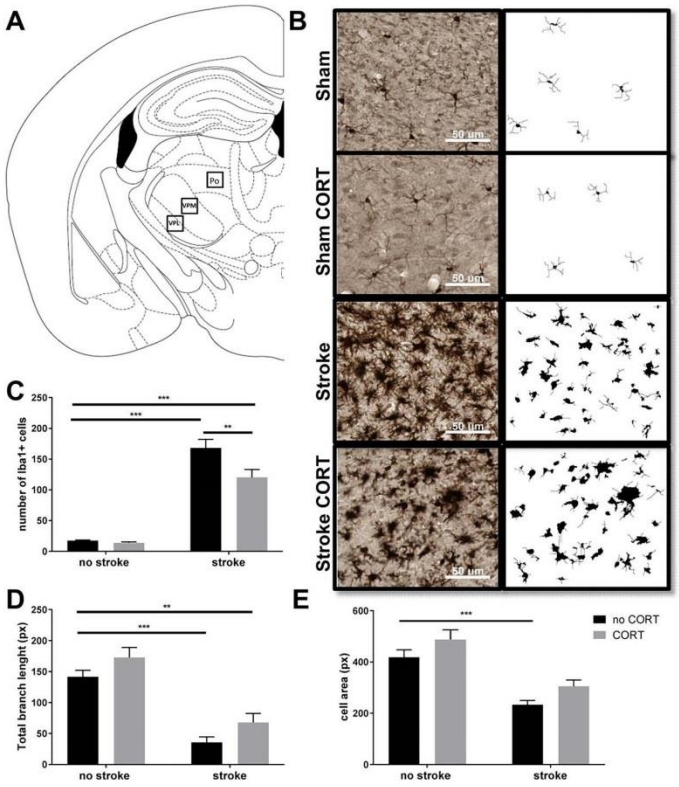

Fig. 6. Microglia morphology digital reconstruction conducted for 3 regions of the thalamus: posterior thalamic nuclear group (Po), ventral posterior thalamic nucleus (vpl) and ventral postmedial thalamic nucleus (vpm) A. Schematic illustration of the thalamus with selected regions of interest. B. Left panel shows representative Iba1 immunolabelling across all of the groups. Right panel shows digital reconstruction of left panel. Cells on the border were removed. Scale bar = 50 μm. C–E. Bar graphs display changes in number of Iba1 positive cells – sum of 3 regions (C), total branch length (D) and cell area (E) – average from 3 regions. Data expressed as a mean ± SEM for each group, $^{*}P < .05$, $^{**}P < .01$ $^{***}P < .001$ (two-way ANOVA followed by Tukey's multiple comparisons).

paradigm used in the current study was insufficient to elicit differences. All the available evidence that we have gathered, however, does not support this possibility. For instance, in an earlier study using an identical administration paradigm we directly established the ability of orally delivered corticosterone to increased tissue loss within the peri-infarct regions after stroke (Zalewska et al., 2017). We have also identified in the current study that corticosterone administration exerted a marked suppressive effect on body, thymus and spleen weight and increased circulating corticosterone levels to a level equivalent to that seen after exposure to chronic stress, all of which are observations that mirror our earlier work (Zalewska et al., 2017) (see Fig. 1). Taken together, these results suggest that the corticosterone administration procedure was effective in altering various biological functions but simply did not meaningfully impact on neuronal loss in areas of SND.

Interestingly, we did observe a clear impact of corticosterone administration on both markers of astro- and microglial activity. Specifically, we observed corticosterone mediated reductions in the expression of the astrocyte markers S100β and GFAP and the microglial markers CD11b and CD68. This finding is totally consistent with what we have observed within the thalamus after chronic stress exposure and in the peri-infarct after chronic corticosterone administration (Jones et al., 2015; Zalewska et al., 2017; Zhao et al., 2017). As such, we would conclude that glial activity, measured by classical markers of the activity used in the current study, is sensitive to the effects of corticosterone. Given the neuroprotective actions of both astrocytes and microglia, we expected to see increased severity of SND (Becerra-Calixto and Cardona-Gomez, 2017; Patel et al., 2013). As no obvious impacts were noted, however, we would surmise that glia either (i) do not exert neuroprotective actions at sites of SND, (ii) that the timing of assessment was out of phase with the peak periods of neuronal loss or (iii) the stroke produced a floor effect, whereby cell loss within the thalamus was so complete that modulatory effects of corticosterone could not be identified. Given these alterative outcomes, we suggest that it would be of benefit to consider undertaking systematic time-line evaluation of how corticosterone influences on SND. These experiments together will significantly increase the ability to make an unequivocal determination of the neuroprotective role of glia in mediating SND.

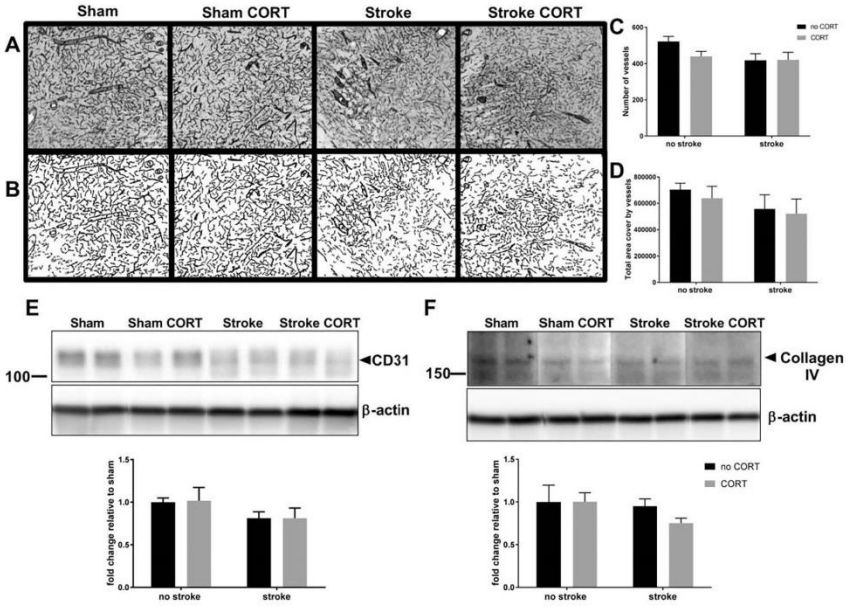

Fig. 7. Effects of CORT administration on vascular specific markers Collagen IV and CD31. A. Panel of representative Collagen IV staining across the groups B. Digital reconstruction of Collagen IV staining C. Number of vessels in the cropped area found by digital reconstruction D. Total area covered by vessels in the cropped area shown in pixels F- G. Representative WB of CD31 across the groups. There were no significant changes between the groups in CD31 and Collagen IV expression.

We also undertook a detailed examination of the extent to which corticosterone administration influenced behaviour. We have previously noted in our study on the peri-infarct that corticosterone administration, using the same paradigm used in the current study, did not elicit any noticeable changes in the cylinder task, as general assessment of functional deficit. Similarly, we confirmed this finding in the current study. However, unlike our previous investigation of the influence of corticosterone administration of the peri-infarct we also examined sensorimotor and motor function as well as anxiety-like behaviour in the current study. Here we identified that corticosterone resulted in clear impairments of motor function using the inverted grid walk but did not noticeably alter behaviour in either the open field or grid walk task. We believe this represents an interesting advancement of knowledge and taken with previous work suggests that the corticosterone administration may preferentially influence motor over sensorimotor pathways. A finding we will explore across future studies. Specifically, we wish to introduce specific tracers in motor and sensorimotor pathways to examine whether the pathways are equally influenced by stroke. Moreover, these tracing studies will also allow us to examine whether myelination may act as a modulator of these findings. The absence of anxiety-like behaviour was also noteworthy. However, it was very much consistent with the idea that corticosterone administration alone is not 'stressful' and therefore does not elicit stress like effects on behaviour (Walker et al., 2014).

Stroke both for the individual and for their family is a detrimental experience. The outcomes of stroke, while sometimes mild are more often than not quite severe, eliciting a sudden and often dramatic decrease in quality life. This transition, unsurprisingly, is routinely reported as being an incredibly stressful period for most stroke survivors. Unfortunately, several decades of research into the impacts of chronic stress have made an absolutely unequivocal case for uniformly negative effect of chronic stress of CNS function. We and several other labs have demonstrated this consistently at the pre-clinical level (Espinosa-Garcia et al., 2017; Faraji et al., 2011; Jin et al., 2010; Jones et al., 2015; Kirkland et al., 2008; Ong et al., 2016; Walker et al., 2014; Zhao et al., 2017) an effect that is increasingly been supported to translate clinically (Ben Assayag et al., 2012; Ben Assayag et al., 2017). The question is what could be done to mitigate the inevitable presence of chronic stress during the recovery period. There are very few established strategies, and none that are proven to work in the context of chronic stress. One option is the ability to attenuate stress effects through pharmacological treatment. Highly specific glucocorticoid antagonists like mifepristone, have been developed for clinical use and therefore could be considered in the context of stroke. Prior to moving to this pathway, however, we should closely examine how corticosterone simulated the effects of chronic stress. To this end, in our previous studies we evaluated the effects of corticosterone administration on the peri-infarct territories and in the current one within the thalamus, a major site of SND. Here across both investigations we have identified that corticosterone administration produces some but not all the same effects of chronic stress. Accordingly, we believe that the case for supporting clinical evaluation of glucocorticoid agonists is relatively weak and potentially other options should be considered first before these agents are utilised. Although this conclusion is somewhat downcast, it is nevertheless important as it provides a signal that modulation of HPA signalling is unlikely to be a productive course to pursue improvements in patient quality of life.

Acknowledgments

This work was supported by the National Health & Medical Research Council, Hunter Medical Research Institute Research Grant, Faculty of Health and Medicine Pilot Grant and the University of Newcastle, Australia. We also express our gratitude to Dr Rick Thorne and HMRI CORE Histology Facility for assistance with the immunohistochemistry images.

Authors' contributions

KZ and FRW designed the experiment. KZ performed the majority of the experiments with assistance of GP. SJJ and MA designed and prepared the Matlab program for the image analysis. KZ, LKO, GP, MK and FRW analysed the data and interpreted the results. KZ, LKO and FRW wrote the manuscript. KZ, FRW, SJJ, GP, MK, MA and MN helped revise the manuscript.

Appendix A. Supplementary data

Supplementary data associated with this article can be found, in the online version, at https://doi.org/10.1016/j.bbi.2017.11.014.

References

Abdolhoseini M., W.F., and Johnson S., 2016. Automated tracing of microglia using multilevel thresholding and minimum spanning trees. In: 38th Annual International Conference of the IEEE Engineering in Medicine and Biology Society (EMBC). EMBC, pp. 1208–1211.

Alfarez, D.N., De Simoni, A., Velzing, E.H., Bracey, E., Joels, M., Edwards, F.A., Krugers, H.J., 2009. Corticosterone reduces dendritic complexity in developing hippocampal CA1 neurons. Hippocampus 19, 828–836.

Angeleri, F., Angeleri, V.A., Foschi, N., Giaquinto, S., Nolfe, G., 1993. The influence of depression, social activity, and family stress on functional outcome after stroke. Stroke 24, 1478–1483.

Balkaya, M., Prinz, V., Custodis, F., Gertz, K., Kronenberg, G., Kroeber, J., Fink, K., Plehm, R., Gass, P., Laufs, U., Endres, M., 2011. Stress worsens endothelial function and ischemic stroke via glucocorticoids. Stroke 42, 3258–3264.

Barriga, C., Martin, M.I., Tabla, R., Ortega, E., Rodriguez, A.B., 2001. Circadian rhythm of melatonin, corticosterone and phagocytosis: effect of stress. J. Pineal. Res. 30, 180–187.

Becerra-Calixto, A., Cardona-Gomez, G.P., 2017. The role of astrocytes in neuroprotection after brain stroke: potential in cell therapy. Front. Mol. Neurosci. 10, 88.

Ben Assayag, E., Korczyn, A.D., Giladi, N., Goldbourt, U., Berliner, A.S., Shenhar-Tsarfaty, S., Kliper, E., Hallevi, H., Shopin, L., Hendler, T., Baashat, D.B., Aizenstein, O., Soreq, H., Katz, N., Solomon, Z., Mike, A., Usher, S., Hausdorff, J. M., Auriel, E., Shapira, I., Bornstein, N.M., 2012. Predictors for poststroke outcomes: the Tel Aviv Brain Acute Stroke Cohort (TABASCO) study protocol. Int. J. Stroke 7, 341–347.

Ben Assayag, E., Tene, O., Korczyn, A.D., Shopin, L., Auriel, E., Molad, J., Hallevi, H., Kirschbaum, C., Bornstein, N.M., Shenhar-Tsarfaty, S., Kliper, E., Stalder, T., 2017. High hair cortisol concentrations predict worse cognitive outcome after stroke: Results from the TABASCO prospective cohort study. Psychoneuroendocrinology 82, 133–139.

Carter, B.S., Hamilton, D.E., Thompson, R.C., 2013. Acute and chronic glucocorticoid treatments regulate astrocyte-enriched mRNAs in multiple brain regions in vivo. Front. Neurosci. 7, 139.

Cooper, M.S., Stewart, P.M., 2009. 11Beta-hydroxysteroid dehydrogenase type 1 and its role in the hypothalamus-pituitary-adrenal axis, metabolic syndrome, and inflammation. J. Clin. Endocrinol. Metab. 94, 4645–4654.

Coughenour, L.L., McLean, J.R., Parker, R.B., 1977. A new device for the rapid measurement of impaired motor function in mice. Pharmacol. Biochem. Behav. 6, 351–353.

De Kloet, E.R., 2004. Hormones and the stressed brain. Ann. N. Y. Acad. Sci. 1018, 1–15.

Elmstahl, S., Malmberg, B., Annerstedt, L., 1996. Caregiver's burden of patients 3 years after stroke assessed by a novel caregiver burden scale. Arch. Phys. Med. Rehabil. 77, 177–182.

Espinosa-Garcia, C., Sayeed, I., Yousuf, S., Atif, F., Sergeeva, E.G., Neigh, G.N., Stein, D. G., 2017. Stress primes microglial polarization after global ischemia: Therapeutic potential of progesterone. Brain Behav. Immun.

Faraji, J., Ejaredar, M., Metz, G.A., Sutherland, R.J., 2011. Chronic stress prior to hippocampal stroke enhances post-stroke spatial deficits in the ziggurat task. Neurobiol. Learn. Mem. 95, 335–345.

Feibel, J.H., Hardy, P.M., Campbell, R.G., Goldstein, M.N., Joynt, R.J., 1977. Prognostic value of the stress response following stroke. JAMA 238, 1374–1376.

Gong, S., Miao, Y.L., Jiao, G.Z., Sun, M.J., Li, H., Lin, J., Luo, M.J., Tan, J.H., 2015. Dynamics and correlation of serum cortisol and corticosterone under different physiological or stressful conditions in mice. PLoS One 10, e0117503.

Gourley, S.L., Kiraly, D.D., Howell, J.L., Olausson, P., Taylor, J.R., 2008a. Acute hippocampal brain-derived neurotrophic factor restores motivational and forced swim performance after corticosterone. Biol. Psychiat. 64, 884–890.

Gourley, S.L., Kiraly, D.D., Taylor, J.R., 2006. Modeling the persistent, depressive-like state in rodents: Long-lasting effects of prior chronic corticosterone. Biol. Psychiat. 59, 6s.

Gourley, S.L., Taylor, J.R., 2009. Recapitulation and reversal of a persistent depression-like syndrome in rodents. Curr. Protoc. Neurosci. Chapter 9, Unit 9 32.

Gourley, S.L., Wu, F.J., Taylor, J.R., 2008b. Corticosterone regulates pERK1/2 map kinase in a chronic depression model. Ann. N. Y. Acad. Sci. 1148, 509–514.

Hilari, K., Northcott, S., Roy, P., Marshall, J., Wiggins, R.D., Chataway, J., Ames, D., 2010. Psychological distress after stroke and aphasia: the first six months. Clin. Rehabil. 24, 181–190.

Jin, Z., Wu, J., Oh, S.Y., Kim, K.W., Shin, B.S., 2010. The effect of stress on stroke recovery in a photothrombotic stroke animal model. Brain Res. 1363, 191–197.

Joels, M., de Kloet, E.R., 1992. Control of neuronal excitability by corticosteroid hormones. Trends Neurosci. 15, 25–30.

Jones, K.A., Zouikr, I., Patience, M., Clarkson, A.N., Isgaard, J., Johnson, S.J., Spratt, N., Nilsson, M., Walker, F.R., 2015. Chronic stress exacerbates neuronal loss associated with secondary neurodegeneration and suppresses microglial-like cells following focal motor cortex ischemia in the mouse. Brain Behav. Immun.

Karten, Y.J.G., Nair, S.M., van Essen, L., Sibug, R., Joels, M., 1999. Long-term exposure to high corticosterone levels attenuates serotonin responses in rat hippocampal CA1 neurons. Proc. Natl. Acad. Sci. U.S.A. 96, 13456–13461.

Kirkland, S.W., Coma, A.K., Colwell, K.L., Metz, G.A., 2008. Delayed recovery and exaggerated infarct size by post-lesion stress in a rat model of focal cerebral stroke. Brain Res. 1201, 151–160.

Kongsui, R., Johnson, S.J., Graham, B.A., Nilsson, M., Walker, F.R., 2015. A combined cumulative threshold spectra and digital reconstruction analysis reveal structural alterations of microglia within the prefrontal cortex following low-dose LPS administration. Neuroscience 310, 629–640.

Labat-gest, V., Tomasi, S., 2013. Photothrombotic ischemia: a minimally invasive and reproducible photochemical cortical lesion model for mouse stroke studies. J. Vis. Exp.

Lyon, B.L., 2002. Psychological stress and coping: framework for poststroke psychosocial care. Top. Stroke Rehabil. 9, 1–15.

Malisch, J.L., Saltzman, W., Gomes, F.R., Rezende, E.L., Jeske, D.R., Garland Jr., T., 2007. Baseline and stress-induced plasma corticosterone concentrations of mice selectively bred for high voluntary wheel running. Physiol. Biochem. Zool. 80, 146–156.

Myers, R., Manjil, L.G., Frackowiak, R.S., Cremer, J.E., 1991. [3H]PK 11195 and the localisation of secondary thalamic lesions following focal ischaemia in rat motor cortex. Neurosci. Lett. 133, 20–24.

Nacher, J., Pham, K., Gil-Fernandez, V., McEwen, B.S., 2004. Chronic restraint stress and chronic corticosterone treatment modulate differentially the expression of molecules related to structural plasticity in the adult rat piriform cortex. Neuroscience 126, 503–509.

Olausson, P., Kiraly, D.D., Gourley, S.L., Taylor, J.R., 2013. Persistent effects of prior chronic exposure to corticosterone on reward-related learning and motivation in rodents. Psychopharmacology 225, 569–577.

Ong, L.K., Zhao, Z., Kluge, M., TeBay, C., Zalewska, K., Dickson, P.W., Johnson, S.J., Nilsson, M., Walker, F.R., 2017. Reconsidering the role of glial cells in chronic stress-induced dopaminergic neurons loss within the substantia nigra? Friend or foe? Brain Behav. Immun. 60, 117–125.

Ong, L.K., Zhao, Z., Kluge, M., Walker, F.R., Nilsson, M., 2016. Chronic stress exposure following photothrombotic stroke is associated with increased levels of Amyloid beta accumulation and altered oligomerisation at sites of thalamic secondary neurodegeneration in mice. J. Cereb. Blood Flow Metab.

Padgett, D.A., Marucha, P.T., Sheridan, J.F., 1998. Restraint stress slows cutaneous wound healing in mice. Brain Behav. Immun. 12, 64–73.

Pappata, S., Levasseur, M., Gunn, R.N., Myers, R., Crouzel, C., Syrota, A., Jones, T., Kreutzberg, G.W., Banati, R.B., 2000. Thalamic microglial activation in ischemic stroke detected in vivo by PET and [C-11]PK11195. Neurology 55, 1052–1054.

Patel, A.R., Ritzel, R., McCullough, L.D., Liu, F., 2013. Microglia and ischemic stroke: a double-edged sword. Int. J. Physiol. Pathophysiol. Pharmacol. 5, 73–90.

Patience, M.J., Zouikr, I., Jones, K., Clarkson, A.N., Isgaard, J., Johnson, S.J., Walker, F. R., Nilsson, M., 2015. Photothrombotic stroke induces persistent ipsilateral and contralateral astrogliosis in key cognitive control nuclei. Neurochem. Res. 40, 362–371.

Paxinos, G., Franklin, K.B.J., 2004. The Mouse Brain in Stereotaxic Coordinates. Academic, Oxford.

Pietrogrande, G., Mabotuwana, N., Zhao, Z., Mahmoud, A., Johnson, S.J., Nilsson, M., Walker, F.R., 2017. Chronic stress induced disturbances in Laminin: a significant contributor to modulating microglial pro-inflammatory tone? Brain Behav. Immun.

Ramamoorthy, S., Cidlowski, J.A., 2016. Corticosteroids: mechanisms of action in health and disease. Rheum. Dis. Clin. North Am. 42, 15–31.

Schaar, K.L., Brenneman, M.M., Savitz, S.I., 2010. Functional assessments in the rodent stroke model. Exp. Transl. Stroke Med. 2, 13.

Sugama, S., Takenouchi, T., Kitani, H., Fujita, M., Hashimoto, M., 2009. Microglial activation is inhibited by corticosterone in dopaminergic neurodegeneration. J. Neuroimmunol. 208.

Tynan, R.J., Naicker, S., Hinwood, M., Nalivaiko, E., Buller, K.M., Pow, D.V., Day, T.A., Walker, F.R., 2010. Chronic stress alters the density and morphology of microglia in a subset of stress-responsive brain regions. Brain Behav. Immun. 24, 1058–1068.

Tyson, J.M., 1995. On being a stroke patient. J. Adv. Nurs. 21, 412–414.

Walker, F.R., Jones, K.A., Patience, M.J., Zhao, Z.D., Nilsson, M., 2014. Stress as necessary component of realistic recovery in animal models of experimental stroke. J. Cereb. Blood Flow Metab. 34, 208–214.

Zalewska, K., Ong, L.K., Johnson, S.J., Nilsson, M., Walker, F.R., 2017. Oral administration of corticosterone at stress-like levels drives microglial but not vascular disturbances post-stroke. Neuroscience.

Zhang, H.Y., Zhao, Y.N., Wang, Z.L., 2015a. Chronic corticosterone exposure reduces hippocampal astrocyte structural plasticity and induces hippocampal atrophy in mice. Neurosci. Lett. 592, 76–81.

Zhang, H.Y., Zhao, Y.N., Wang, Z.L., Huang, Y.F., 2015b. Chronic corticosterone exposure reduces hippocampal glycogen level and induces depression-like behavior in mice. J. Zhejiang Univ. Sci. B 16, 62–69.

Zhao, Z., Ong, L.K., Johnson, S., Nilsson, M., Walker, F.R., 2017. Chronic stress induced disruption of the peri-infarct neurovascular unit following experimentally induced photothrombotic stroke. J. Cereb. Blood. Flow. Metab. https://doi.org/10.1177/0271678X17696100.

`

Appendix 2

Copyright permission

I, Giovanni Pietrogrande, warrant that I have obtained, permission from the copyright owners to use any third party copyright material reproduced in the thesis and those of my own published work in which the copyright is held by another party.

As an author, copyright permission is not required for the right to include a publication in a thesis or dissertation from the following publications and publishers: Brain, Behaviour and Immunity (Elsevier) and Scientific Reports.

SPRINGER NATURE LICENSE
TERMS AND CONDITIONS

Dec 12, 2018

This Agreement between Mr. giovanni pietrogrande ("You") and Springer Nature ("Springer Nature") consists of your license details and the terms and conditions provided by Springer Nature and Copyright Clearance Center.

License Number	4486360292777
License date	Dec 12, 2018
Licensed Content Publisher	Springer Nature
Licensed Content Publication	Nature Reviews Neuroscience
Licensed Content Title	Pathophysiology of the brain extracellular matrix: a new target for remyelination
Licensed Content Author	Lorraine W. Lau, Rowena Cua, Michael B. Keough, Sarah Haylock-Jacobs, V. Wee Yong
Licensed Content Date	Aug 29, 2013
Licensed Content Volume	14
Licensed Content Issue	10
Type of Use	Thesis/Dissertation
Requestor type	academic/university or research institute
Format	print and electronic
Portion	figures/tables/illustrations
Number of figures/tables/illustrations	1
High-res required	no
Will you be translating?	no
Circulation/distribution	<501
Author of this Springer Nature content	no
Title	INVOLVEMENT OF MICROGLIA ACTIVATION IN THE DEVELOPMENT OF CNS DISEASES
Institution name	university of newcastle
Expected presentation date	Dec 2018
Portions	Figure 1
Requestor Location	Mr. giovanni pietrogrande edmondstone st 9 brisbane, queensland 4101 Australia Attn: Mr. giovanni pietrogrande
Billing Type	Invoice
Billing Address	Mr. giovanni pietrogrande edmondstone st 9 brisbane, Australia 4101 Attn: Mr. giovanni pietrogrande
Total	0.00 AUD

Terms and Conditions

Springer Nature Terms and Conditions for RightsLink Permissions

Springer Nature Customer Service Centre GmbH (the Licensor) hereby grants you a non-exclusive, world-wide licence to reproduce the material and for the purpose and requirements specified in the attached copy of your order form, and for no other use, subject to the conditions below:

1. The Licensor warrants that it has, to the best of its knowledge, the rights to license reuse of this material. However, you should ensure that the material you are requesting is original to the Licensor and does not carry the copyright of another entity (as credited in the published version).

   If the credit line on any part of the material you have requested indicates that it was reprinted or adapted with permission from another source, then you should also seek permission from that source to reuse the material.

2. Where **print only** permission has been granted for a fee, separate permission must be obtained for any additional electronic re-use.

3. Permission granted **free of charge** for material in print is also usually granted for any electronic version of that work, provided that the material is incidental to your work as a whole and that the electronic version is essentially equivalent to, or substitutes for, the print version.

4. A licence for 'post on a website' is valid for 12 months from the licence date. This licence does not cover use of full text articles on websites.

5. Where **'reuse in a dissertation/thesis'** has been selected the following terms apply: Print rights of the final author's accepted manuscript (for clarity, NOT the published version) for up to 100 copies, electronic rights for use only on a personal website or institutional repository as defined by the Sherpa guideline (www.sherpa.ac.uk/romeo/).

6. Permission granted for books and journals is granted for the lifetime of the first edition and does not apply to second and subsequent editions (except where the first edition permission was granted free of charge or for signatories to the STM Permissions Guidelines http://www.stm-assoc.org/copyright-legal-affairs/permissions/permissions-guidelines/), and does not apply for editions in other languages unless additional translation rights have been granted separately in the licence.

7. Rights for additional components such as custom editions and derivatives require additional permission and may be subject to an additional fee. Please apply to Journalpermissions@springernature.com/bookpermissions@springernature.com for these rights.

8. The Licensor's permission must be acknowledged next to the licensed material in print. In electronic form, this acknowledgement must be visible at the same time as the figures/tables/illustrations or abstract, and must be hyperlinked to the journal/book's homepage. Our required acknowledgement format is in the Appendix below.

9. Use of the material for incidental promotional use, minor editing privileges (this does not include cropping, adapting, omitting material or any other changes that affect the meaning, intention or moral rights of the author) and copies for the disabled are permitted under this licence.

10. Minor adaptations of single figures (changes of format, colour and style) do not require the Licensor's approval. However, the adaptation should be credited as shown in Appendix below.

Appendix — Acknowledgements:

For Journal Content:
Reprinted by permission from **[the Licensor]**: **[Journal Publisher** (e.g. Nature/Springer/Palgrave)] **[JOURNAL NAME] [REFERENCE CITATION** (Article name, Author(s) Name), **[COPYRIGHT]** (year of publication)

For **Advance Online Publication papers:**
Reprinted by permission from [**the Licensor**]: [**Journal Publisher** (e.g. Nature/Springer/Palgrave)] [**JOURNAL NAME**] [**REFERENCE CITATION** (Article name, Author(s) Name), [**COPYRIGHT**] (year of publication), advance online publication, day month year (doi: 10.1038/sj.[JOURNAL ACRONYM].)

For Adaptations/Translations:
Adapted/Translated by permission from [**the Licensor**]: [**Journal Publisher** (e.g. Nature/Springer/Palgrave)] [**JOURNAL NAME**] [**REFERENCE CITATION** (Article name, Author(s) Name), [**COPYRIGHT**] (year of publication)

Note: For any republication from the British Journal of Cancer, the following credit line style applies:

Reprinted/adapted/translated by permission from [**the Licensor**]: on behalf of Cancer Research UK: : [**Journal Publisher** (e.g. Nature/Springer/Palgrave)] [**JOURNAL NAME**] [**REFERENCE CITATION** (Article name, Author(s) Name), [**COPYRIGHT**] (year of publication)

For **Advance Online Publication** papers:
Reprinted by permission from The [**the Licensor**]: on behalf of Cancer Research UK: [**Journal Publisher** (e.g. Nature/Springer/Palgrave)] [**JOURNAL NAME**] [**REFERENCE CITATION** (Article name, Author(s) Name), [**COPYRIGHT**] (year of publication), advance online publication, day month year (doi: 10.1038/sj.[JOURNAL ACRONYM])

For Book content:
Reprinted/adapted by permission from [**the Licensor**]: [**Book Publisher** (e.g. Palgrave Macmillan, Springer etc) [**Book Title**] by [**Book author**(s)] [**COPYRIGHT**] (year of publication)

Other Conditions:

Version 1.1

SPRINGER NATURE LICENSE
TERMS AND CONDITIONS

Dec 12, 2018

This Agreement between Mr. giovanni pietrogrande ("You") and Springer Nature ("Springer Nature") consists of your license details and the terms and conditions provided by Springer Nature and Copyright Clearance Center.

License Number	4486830420789
License date	Dec 12, 2018
Licensed Content Publisher	Springer Nature
Licensed Content Publication	Translational Stroke Research
Licensed Content Title	Low Oxygen Post Conditioning as an Efficient Non-pharmacological Strategy to Promote Motor Function After Stroke
Licensed Content Author	Giovanni Pietrogrande, Katarzyna Zalewska, Zidan Zhao et al
Licensed Content Date	Jan 1, 2018
Type of Use	Thesis/Dissertation
Requestor type	academic/university or research institute
Format	print and electronic
Portion	full article/chapter
Will you be translating?	no
Circulation/distribution	<501
Author of this Springer Nature content	yes
Title	INVOLVEMENT OF MICROGLIA ACTIVATION IN THE DEVELOPMENT OF CNS DISEASES
Institution name	university of newcastle
Expected presentation date	Dec 2018
Requestor Location	Mr. giovanni pietrogrande edmondstone st 9 brisbane, queensland 4101 Australia Attn: Mr. giovanni pietrogrande
Billing Type	Invoice
Billing Address	Mr. giovanni pietrogrande edmondstone st 9 brisbane, Australia 4101 Attn: Mr. giovanni pietrogrande
Total	0.00 AUD
Terms and Conditions	

Springer Nature Terms and Conditions for RightsLink Permissions

Springer Nature Customer Service Centre GmbH (the Licensor) hereby grants you a non-exclusive, world-wide licence to reproduce the material and for the purpose and requirements specified in the attached copy of your order form, and for no other use, subject to the conditions below:

1. The Licensor warrants that it has, to the best of its knowledge, the rights to license reuse of this material. However, you should ensure that the material you are requesting is original to the Licensor and does not carry the copyright of another entity (as credited in the published version).

   If the credit line on any part of the material you have requested indicates that it was reprinted or adapted with permission from another source, then you should also seek permission from that source to reuse the material.

2. Where **print only** permission has been granted for a fee, separate permission must be obtained for any additional electronic re-use.

3. Permission granted **free of charge** for material in print is also usually granted for any electronic version of that work, provided that the material is incidental to your work as a whole and that the electronic version is essentially equivalent to, or substitutes for, the print version.

4. A licence for 'post on a website' is valid for 12 months from the licence date. This licence does not cover use of full text articles on websites.

5. Where **'reuse in a dissertation/thesis'** has been selected the following terms apply: Print rights of the final author's accepted manuscript (for clarity, NOT the published version) for up to 100 copies, electronic rights for use only on a personal website or institutional repository as defined by the Sherpa guideline (www.sherpa.ac.uk/romeo/).

6. Permission granted for books and journals is granted for the lifetime of the first edition and does not apply to second and subsequent editions (except where the first edition permission was granted free of charge or for signatories to the STM Permissions Guidelines http://www.stm-assoc.org/copyright-legal-affairs/permissions/permissions-guidelines/), and does not apply for editions in other languages unless additional translation rights have been granted separately in the licence.

7. Rights for additional components such as custom editions and derivatives require additional permission and may be subject to an additional fee. Please apply to Journalpermissions@springernature.com/bookpermissions@springernature.com for these rights.

8. The Licensor's permission must be acknowledged next to the licensed material in print. In electronic form, this acknowledgement must be visible at the same time as the figures/tables/illustrations or abstract, and must be hyperlinked to the journal/book's homepage. Our required acknowledgement format is in the Appendix below.

9. Use of the material for incidental promotional use, minor editing privileges (this does not include cropping, adapting, omitting material or any other changes that affect the meaning, intention or moral rights of the author) and copies for the disabled are permitted under this licence.

10. Minor adaptations of single figures (changes of format, colour and style) do not require the Licensor's approval. However, the adaptation should be credited as shown in Appendix below.

Appendix — Acknowledgements:

For Journal Content:
Reprinted by permission from **[the Licensor]**: **[Journal Publisher** (e.g. Nature/Springer/Palgrave)] **[JOURNAL NAME] [REFERENCE CITATION** (Article name, Author(s) Name), **[COPYRIGHT]** (year of publication)

For **Advance Online Publication papers:**
Reprinted by permission from **[the Licensor]**: **[Journal Publisher** (e.g. Nature/Springer/Palgrave)] **[JOURNAL NAME] [REFERENCE CITATION** (Article name, Author(s) Name), **[COPYRIGHT]** (year of publication), advance online publication, day month year (doi: 10.1038/sj.[JOURNAL ACRONYM].)

`

For Adaptations/Translations:
Adapted/Translated by permission from [**the Licensor**]: [**Journal Publisher** (e.g. Nature/Springer/Palgrave)] [**JOURNAL NAME**] [**REFERENCE CITATION** (Article name, Author(s) Name), [**COPYRIGHT**] (year of publication)

Note: For any republication from the British Journal of Cancer, the following credit line style applies:

Reprinted/adapted/translated by permission from [**the Licensor**]: on behalf of Cancer Research UK: : [**Journal Publisher** (e.g. Nature/Springer/Palgrave)] [**JOURNAL NAME**] [**REFERENCE CITATION** (Article name, Author(s) Name), [**COPYRIGHT**] (year of publication)

For **Advance Online Publication** papers:
Reprinted by permission from The [**the Licensor**]: on behalf of Cancer Research UK: [**Journal Publisher** (e.g. Nature/Springer/Palgrave)] [**JOURNAL NAME**] [**REFERENCE CITATION** (Article name, Author(s) Name), [**COPYRIGHT**] (year of publication), advance online publication, day month year (doi: 10.1038/sj. [JOURNAL ACRONYM])

For Book content:
Reprinted/adapted by permission from [**the Licensor**]: [**Book Publisher** (e.g. Palgrave Macmillan, Springer etc) [**Book Title**] by [**Book author**(s)] [**COPYRIGHT**] (year of publication)

Other Conditions:

Version 1.1